

INVESTIGATIONS INTO THE DESIGN OF POWER SYSTEM STABILIZERS

**A Thesis Submitted
In Partial Fulfilment of the Requirements
for the Degree of
DOCTOR OF PHILOSOPHY**

**by
ANWARUDDIN ANWAR**

**to the
DEPARTMENT OF ELECTRICAL ENGINEERING
INDIAN INSTITUTE OF TECHNOLOGY KANPUR
SEPTEMBER, 1985**

17 DEC 1987

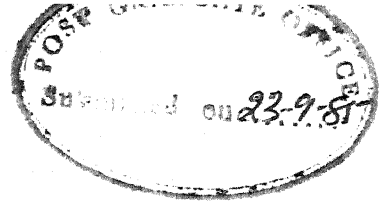
CENTRAL LIBRARY

Acc. No. **A** 99150

EE-1985-D-ANW-INV

Dedicated to

my parents



CERTIFICATE

Certified that this work, 'INVESTIGATIONS INTO THE DESIGN OF POWER SYSTEM STABILIZERS' by A. Anwar has been carried out under our supervision and that this work has not been submitted elsewhere for a degree.

S. S. Prabhu
(S.S. Prabhu)

Professor

Department of Electrical Engineering
Indian Institute of Technology
Kanpur 208016, INDIA.

K. R. Padiyar
(K.R. Padiyar)
Professor

ACKNOWLEDGEMENTS

With profound sense of gratitude, I express my indebtedness and sincere thanks to my supervisors Professor K.R. Padiyar and Professor S.S. Prabhu for initiating the problem and providing invaluable and unfailing guidance throughout the course of this work.

I am highly thankful to Professor L.P. Singh and Professor R.P. Aggarwal for their advice and encouragement at various stages during my stay here.

I thank my senior colleagues Dr. M.L. Chanana, Dr. C. Radhakrishna, Dr. P. Rajashekharam and Dr. R.S. Shanbhag for fruitful discussions during the course of my work. Association with Dr. P.C. Sharma, Dr. S.N. Tiwari and Dr. Sachchidanand has been a rich experience in itself and has made my stay here a memorable event.

It gives me pleasure to acknowledge the splendid company and moral support of my fellow research scholars especially Dr. K.V. Desikachar, Dr. H.S.Y. Shastri and M/s K.K. Ghosh, H.K. Patel, T.L. Jose, A.G. Kothari, R.K. Verma and V.N. Rajurkar. I express my sincere thanks to M/s J. Senthil, P.N. Sridhara, M. Muneer, V. Jain and B.H. Khan who helped me throughout the preparation of this thesis.

My thanks are due to Mr. C.M. Abraham for his patient and skilful typing and M/s T. Tewari and Gangaram for the efficient cyclostyling. Thanks are also due to Mr. R.K. Bajpai for good drawing.

And of course, no list is complete without a word of appreciation to my wife Qudsia for her patience and sincere cooperation and my children Tariq and Arif for their forbearance.

A. Anwar

CONTENTS

Page

LIST OF FIGURES

LIST OF TABLES

LIST OF PRINCIPAL SYMBOLS

SYNOPSIS

CHAPTER 1	INTRODUCTION	1
	1.1 General	2
	1.2 Design of Power System Stabilizers : State of the Art	3
	1.2.1 Design Objective	3
	1.2.2 Power System Model	4
	1.2.3 Selection of PSS Location	7
	1.2.4 Choice of Control Signals	8
	1.2.5 Design Procedure	9
	1.3 Controller Design	14
	1.4 Objective and Scope of the Thesis	19
	1.5 Summary of the Work	20
CHAPTER 2	DYNAMIC COMPENSATOR DESIGN FOR POWER SYSTEM STABILIZATION	25
	2.1 Introduction	25
	2.2 Problem of Power System Stabilization	27
	2.2.1 General	27
	2.2.2 Development of System Model	29
	2.2.3 Power System Stabilizer	35
	2.3 Design of Dynamic Compensator	39
	2.3.1 Pole Assignment with Partial State Feedback Compensator	40
	2.3.2 Pole Assignment with Output Feed- back Compensator	46
	2.3.3 Design of Optimal Compensator for Output Feedback Systems	49
	2.3.4 Comparison of Methods	51

2.4	Numerical Example	52
2.4.1	Design of PSS with Partial State Feedback	53
2.4.2	Design of PSS with Output Feedback	55
2.4.3	Design of PSS with Parameter Optimization	59
2.4.4	Design of PSS with Classical Control Theory	62
2.4.5	Discussion of Results	67
2.5	Conclusions	68
CHAPTER 3	INFLUENCE OF GENERATOR MODELLING ON PSS DESIGN	70
3.1	Introduction	70
3.2	Formulation of System Model	71
3.3	Eigenvalue Analysis	77
3.3.1	Numerical Example	77
3.3.2	Discussion of Results	82
3.4	PSS Design	83
3.4.1	Discussion of Results	89
3.5	Adequacy of Lower Order Representation of Machine	90
3.5.1	Discussion of Results	90
3.6	Conclusions	94
CHAPTER 4	INVESTIGATION OF CONTROL SIGNALS	96
4.1	Introduction	96
4.2	Single Machine Infinite Bus System	99
4.2.1	Design of PSS	99
4.2.2	Determination of Stable P-Q Region	102
4.2.3	Discussion of Results	109

4.3	Generating Plant Infinite Bus System	112
4.3.1	Development of System Model	112
4.3.2	Numerical Example	128
4.3.3	Discussion of Results	135
4.4	Conclusions	137
CHAPTER 5	MODELLING OF MULTIMACHINE SYSTEM AND CHOICE OF PSS LOCATION	139
5.1	Introduction	139
5.2	Development of System Model	142
5.2.1	Generating Units	143
5.2.2	Network Representation	146
5.2.3	Load Representation	146
5.2.4	State-Space Model of Overall System	147
5.3	Choice of PSS Location	150
5.4	Numerical Example	152
5.4.1	Eigenvalue Analysis	153
5.4.2	Choice of PSS Location	155
5.4.3	Discussion of Results	161
5.5	Conclusions	168
CHAPTER 6	APPLICATION OF DECENTRALIZED CONTROL FOR THE DESIGN OF PSS IN MULTIMACHINE POWER SYSTEMS	170
6.1	Introduction	170
6.2	PSS Design Based on Eigenvalue Assignment	172
6.2.1	Formulation of the Control Problem	172
6.2.2	Design Algorithm	180
6.3	PSS Design Based on Minimization of Performance Index	181
6.3.1	Formulation of the Control Problem	182
6.4	Numerical Examples	185
6.4.1	A Three Machine Power System	185
6.4.2	A Thirteen Machine Power System	202
6.4.3	Discussions	208
6.5	Conclusions	217

CHAPTER 7	CONCLUSION	218
	7.1 General	218
	7.2 Objectives and Techniques for PSS Design	218
	7.3 Choice of Machine Model and Effectiveness of Control Signals	221
	7.4 PSS Design in Multimachine System	223
	7.5 Suggestion for Further Work	224
REFERENCES		225
APPENDIX A	COMPENSATOR TRANSFER FUNCTION	233
APPENDIX B	POLE ASSIGNMENT WITH OUTPUT FEEDBACK	238
APPENDIX C	DESIGN OF OPTIMAL CONTROLLER FOR OUTPUT FEEDBACK SYSTEMS	244
APPENDIX D	SYNCHRONOUS MACHINE EQUATIONS AND EXCITATION SYSTEM	248
APPENDIX E	PSS DESIGN BASED ON CLASSICAL TECHNIQUE	269
APPENDIX F	ANALYSIS OF RESULT OF CHAPTER 4	275
APPENDIX G	NETWORK REPRESENTATION	277
APPENDIX H	JUSTIFICATION OF CRITERIA USED FOR CHOICE OF PSS LOCATION	279
APPENDIX I	13-MACHINE 71-BUS POWER SYSTEM	282
APPENDIX J	3-MACHINE 9-BUS POWER SYSTEM	293
CURRICULUM VITAE		

LIST OF FIGURES

Fig No.	Contents	Page
2.1	Single Machine Infinite Bus System	28
2.2	Single Phase Equivalent Circuit of the Model	28
2.3	Block Diagram of Excitation System	28
2.4	Block Diagram of a Practical PSS	37
2.5	Block Diagram of Alternator with Two-Input Controller	57
2.6	Response of $\Delta\delta$ for $\Delta V_{ref} = 1.0$ p.u.	64
2.7	Response of ΔP_e for $\Delta V_{ref} = 1.0$ p.u.	65
2.8	Response of $\Delta\omega$ for $\Delta V_{ref} = 1.0$ p.u.	66
3.1	Single Phase Equivalent Circuit of the Model given in Fig. 2.1	73
3.2	Loci of Open-Loop Eigenvalues Corresponding to Rotor Oscillation	81
3.3	Frequency Plot of PSS Transfer Function for Variation in Machine Loading	86
3.4	Frequency Plot of PSS Transfer Function for Variation in Inertia Constant	87
3.5	Frequency Plot of PSS Transfer Function for Variation in Voltage Regulator Gain	88
3.6	Response of $\Delta\delta$ and $\Delta\omega$ at Full Load for $\Delta V_{ref} = 1.0$ p.u.	92
3.7	Response of $\Delta\delta$ and $\Delta\omega$ at Half Full Load for $\Delta V_{ref} = 1.0$ p.u.	93

4.1	Frequency Response of PSS Transfer Function	103
4.2	Stable P-Q Region for Single M/c Case at $X_T = 0.2$ p.u.	104
4.3	Stable P-Q Region for Single M/c Case at $X_T = 0.4$ p.u.	105
4.4	Stable P-Q Region for Single M/c Case at $X_T = 0.6$ p.u.	106
4.5	Stable P-Q Region for Single M/c Case at $X_T = 0.8$ p.u.	107
4.6	Stable P-Q Region with Speed Signal for Single M/c System (Comparison with Classical Design)	108
4.7	Generating Plant with n Machines Connected to Infinite Bus	113
4.8	Equivalent Circuit of System given in Fig. 4.7	113
4.9	Circuit Model of a Synchronous Machine	114
4.10	Stable P-Q Region with Speed (Individual) Signal for Single and Two Machine System	130
4.11	Stable P-Q Region with Speed (Average) Signal for Single and Two Machine System	131
4.12	Stable P-Q Region with Individual and Average Speed Signals for Two Machine System	132
4.13	Stable P-Q Region with Power Signal for Single and Two Machine System	133
4.14	Stable P-Q Region with Frequency Signal for Single and Two Machine System	134
5.1	Loci of Eigenvalues for Variation in Controller Gain (Machines on Control : 1,2 and 3)	164
5.2	Loci of Eigenvalues for Variation in Controller Gain (Machines on Control: 4,5,6 and 7)	165
5.3	Loci of Eigenvalues for Variation in Controller Gain (Machines on Control: 8,9 and 10)	166
5.4	Loci of Eigenvalues for Variation in Controller Gain (Machines on Control: 11,12 and 13)	167

6.1	Sector for Pole-Assignment	189
6.2	Fluctuations in Power Output of Generators in p.u. Case 1 : for $\Delta V_{\text{ref}} = 1.0$ p.u. of Machine 1	196
6.3	Response of Relative Rotor Angle of Generators in rad. Case 1 : for $\Delta V_{\text{ref}} = 1.0$ p.u. of Machine 1	197
6.4	Fluctuations in Power Output of Generators in p.u. Case 2 : for $\Delta V_{\text{ref}} = 1.0$ p.u. of Machine 2	198
6.5	Response of Relative Rotor Angle of Generators in rad. Case 2 : for $\Delta V_{\text{ref}} = 1.0$ p.u. of Machine 2	199
6.6	Fluctuations in Power Output of Generators in p.u. Case 3 : for $\Delta V_{\text{ref}} = 1.0$ p.u. of Machine 3	200
6.7	Response of Relative Rotor Angle of Generators in rad. Case 3 : for $\Delta V_{\text{ref}} = 1.0$ p.u. of Machine 3	201
6.8	Fluctuations in Power Output of Generators in p.u. Case 1 : for $\Delta V_{\text{ref}} = 1.0$ p.u. of Machine 1	209
6.9	Response of Relative Rotor Angle of Generators in rad. Case 1 : for $\Delta V_{\text{ref}} = 1.0$ p.u. of Machine 1	210
6.10	Fluctuations in Power Output of Generators in p.u. Case 2 : for $\Delta V_{\text{ref}} = 1.0$ p.u. of Machine 7	211
6.11	Response of Relative Rotor Angle of Generators in rad. Case 2 : for $\Delta V_{\text{ref}} = 1.0$ p.u. of Machine 7	212
6.12	Fluctuations in Power Output of Generators in p.u. Case 3 : for $\Delta V_{\text{ref}} = 1.0$ p.u. of Machine 11	213
6.13	Response of Relative Rotor Angle of Generators in rad. Case 3 : for $\Delta V_{\text{ref}} = 1.0$ p.u. of Machine 11	214
D.1	Circuit Model of the Synchronous Machine	249
D.2	Synchronous Machine with Three Damper Windings	249
D.3	Phasor Diagram	258
D.4	Steady State Equivalent Circuit for Armature	258
D.5	Phasor Diagram of Synchronous Machine	260
D.6	IEEE Type 1 Excitation System	267

E.1	System Block Diagram with PSS	273
E.2	Compensated Phase for Various Lead/Lag Settings	274
E.3	Loci of Closed-Loop Eigenvalues for Variation in PSS Gain K_s	274
I.1	Single-Line Diagram of a 13-Machine System	292
J.1	Single-Line Diagram of a Nine-Bus, Three-Machine Power System	295
J.2	Load-Flow Diagram of the Nine-Bus, Three-Machine Power System	295

LIST OF TABLES

Table No.	Contents	Page
2.1	Open-Loop Eigenvalues of the System	35
2.2	Closed-Loop Eigenvalues of the System	54
2.3	Eigenvalues of the System with Two Input Compensator	58
2.4	Closed-Loop Eigenvalues of the System	62
3.1	Open-Loop Real Eigenvalues for Variation in Machine Loading	79
3.2	Open-Loop Real Eigenvalues for Variation in Inertia Constant	80
3.3	Open-Loop Real Eigenvalues for Variation in Voltage Regulator Gain	80
3.4	PSS Parameters for Variation in Machine Loading	84
3.5	PSS Parameters for Variation in Inertia Constant	85
3.6	PSS Parameters for Variation in Voltage Regulator Gain	85
3.7	Closed-Loop Eigenvalues with Detailed Representation of Machine	91
4.1	Open-Loop Eigenvalues	100
4.2	Closed-Loop Eigenvalues	101
4.3	Parameters of PGS	102
5.1	Open-Loop Eigenvalues for the 13-Machine System	154
5.2	Magnitude of Scalar Product $\langle W_j, b_i \rangle$ for Different Locations of PSS	156
5.3	Eigenvalue Sensitivity for Different Locations of PSS	158
5.4	Ranking of Different Locations of PSS	160
5.5	Effective Locations of PSS in 13-Machine System	168

6.1	Open-Loop Eigenvalues of the 3-Machine System	187
6.2	Eigenvalues of the 3-Machine System at $r = 0$	188
6.3	PSS Parameters for the 3-Machine System at $r = 0$	190
6.4	PSS Parameters for the 3-Machine System at $r = 1$	191
6.5	Closed-Loop Eigenvalues of the 3-Machine System	192
6.6	PSS Parameters for the 3-Machine System Obtained from Parameter Optimization Technique	194
6.7	Eigenvalues of the 3-Machine System with PSS of Table 6.6	194
6.8	Eigenvalues of the Selected Machines in the 13-Machine System at $r = 0$	203
6.9	PSS Parameters for the Selected Machines in the 13-Machine System at $r = 0$	204
6.10	PSS Parameters for the Selected Machines in the 13-Machine System at $r = 1$	204
6.11	Closed-Loop Eigenvalues of the 13-Machine System	205
6.12	PSS Parameters for the Selected Machines in the 13-Machine System Obtained from Parameter Optimization Technique	207
6.13	Eigenvalues of the 13-Machine System with PSS of Table 6.12	207
I.1	Bus Data and Load Flow Result	282
I.2	Generator Data	286
I.3	Line and Transformer Data	287
I.4	Shunt Capacitor Data	291
J.1	Line and Transformer Data for the 3-Machine System	293
J.2	Generator Data for the 3-Machine System	294

LIST OF PRINCIPAL SYMBOLS

p	differential operator d/dt
Δ	prefix to denote small changes about the operating point
o	subscript to denote the value of the operating point
t	time in seconds
ω_o	synchronous angular velocity in radians per second
ω	instantaneous angular velocity of machines in radians per second
δ	rotor angle with respect to system reference (radians)
E	generator internal voltage magnitude (p.u.)
V_t	generator terminal voltage magnitude (p.u.)
θ	generator terminal voltage phase angle (radians)
v_d, v_q	d and q axes components of V_t
i_d, i_q	d and q axes components of the armature current
x_d, x_q	d and q axes synchronous reactances (p.u.)
x'_d, x'_q	d and q axes transient reactances (p.u.)
x''_d, x''_q	d and q axes subtransient reactances (p.u.)
T'_{do}, T'_{qo}	d and q axes transient open circuit time constant
T''_{do}, T''_{qo}	d and q axes subtransient open circuit time constant
H	inertia constant in seconds
M	$(2H/\omega_o)$
K_D	damping coefficients

V_{fd}	generator field voltage (p.u.)
Ψ	flux linkages
T_e	electrical torque developed (p.u.)
T_m	mechanical torque input (p.u.)
R_T	resistance of transmission line in p.u.
X_T	reactance of transmission line in p.u.
K_R	voltage regulator gain
T_R	voltage regulator time constant

Other symbols used in the text are explained as and when they are introduced.

SYNOPSIS

INVESTIGATION INTO THE DESIGN OF POWER SYSTEM STABILIZERS

With increasing size and complexity of modern power systems, stability investigations are assuming greater significance in system planning, design and operation. Transient stability of power systems is improved by incorporating fast acting and high gain excitation systems with synchronous generators. However, such excitation systems introduce negative damping in the system impairing dynamic stability. Oscillations of small magnitude and low frequency, in the range of 0.2 to 2.0 Hz, can persist for long periods of time and in some cases present limitations to the power transfer capability. Power System Stabilizers (PSS) are developed to damp-out these oscillations. PSS are dynamic compensators which receive a feedback signal from rotor speed, angular position, frequency or electrical power and provide a corrective input to the excitation system.

The basis for the design of PSS is explained in the classic paper by deMello and Concordia [1]. The PSS is designed as a dynamic compensator, using input derived from

local control signal, with the objective of increasing the damping torque while maintaining the synchronizing torque. The model given in [1] is a simplified one where the power system is represented by a single generator feeding an infinite bus through a transmission line. The synchronous machine is represented by a third order model neglecting damper windings. This simplified model of the power system permits application of classical control theory for the design of PSS.

Since then, there has been much work on power system stabilization reported in the literature using classical and modern control theory. In the latter approach the PSS design is based on the objective of assignment of closed-loop poles or minimizing a performance index. In spite of the extensive literature on PSS there are still some gaps which are described below. :

(1) It is observed that a simple model of a power system (that of single machine connected to infinite bus) is not adequate in many situations and coordinated application of PSS using multimachine system model is essential [2]. The design based on the concept of damping torque, utilizing classical control theory is not adequate here. However the direct application of modern control theory is also not feasible due to the practical constraint of having to use only local control

signals. While some theoretical work on decentralized control in large systems has been carried out, its application for design of PSS in a large power system is not reported.

If PSS are to be equipped on the generators that are already installed in a system for the purpose of improving dynamic stability, there arises the question of selecting appropriate locations for PSS in order to provide an effective control. This question has not also been satisfactorily answered.

(2) The objective of PSS design given in [1] is to increase the damping torque in the generators. It can be shown that this is equivalent to shifting the complex pair of eigenvalues, corresponding to electromechanical oscillations, to the left in the complex plane [3]. This indicates that pole assignment is a suitable objective for PSS design. However, the design freedom (in the selection of parameters) is not fully utilized in the work reported in this area; for example, with a second order dynamic compensator, using a single input, it is possible to assign upto five closed-loop poles to their desired locations. With more complex compensators (multi-input) it may be possible to assign more closed-loop poles.

Generally, for the purpose of stabilization, it is adequate to specify the region in the complex-plane where closed-loop poles should lie, rather than specifying exact locations.

However, unique compensators cannot be obtained unless exact locations are specified. This problem can be avoided if a suitable performance index is chosen as an objective in conjunction with the application of optimal control theory.

(3) While there is some work reported on the choice of control signals [4], a detailed study comparing their relative merits is not available. The comparison should be based on satisfactory performance of the controller under varying conditions of operating point and system strength.

Interaction between two or more parallel connected generators in a power station complicates the choice of control signals for PSS. A detailed analysis is not available in the literature.

(4) Third order synchronous machine model is widely used for PSS design. Adequacy of this model needs to be tested.

The work reported in this thesis is directed at trying to fill the gaps mentioned above. The major contributions are as follows :

(1) Study of decentralized control for the design of PSS in large power systems by considering application to a particular large power system.

(2) Determination of effective PSS locations in a large multi-machine system through eigenvalue sensitivity analysis and validation of the results.

- (3) A detailed investigation on the effectiveness of various feedback control signals (viz. rotor speed, electrical power and bus frequency), for PSS design, including consideration of interaction between adjacent machines in the choice of signal.
- (4) Application of modern control theory for the design of dynamic compensators (to be used as PSS) utilizing full design freedom. Comparison of the performance of PSS designed using pole assignment techniques, parameter optimization technique and classical control method.
- (5) Verification of the adequacy of using simplified model of synchronous machine in PSS design.

An outline of the work reported in the thesis is given below :

- (1) Chapter 1 introduces various aspects of dynamic stability and design of PSS in large multimachine power systems and reviews the literature in this area.
- (2) Chapter 2 deals with design techniques for PSS. The techniques developed here are general enough to be applied to multimachine systems. Pole-assignment in closed-loop system is a well accepted design objective for PSS and is used in the first two techniques presented. In the first technique, modal control theory is utilized for PSS design. Only accessible states are used as feedback signals to PSS. Pole assignment technique given by Munro and Hirbod [5], with dynamic output feedback, is

utilized for PSS design in the second techniques.

Electromechanical oscillations of machine rotors with respect to one another cause power surges between machines and limit power transfer capabilities, particularly in systems having long transmission lines. Damping of these oscillations can be achieved by minimization of power fluctuations in generator output. The third design technique is based on parameter optimization with the objective to minimize power fluctuations in generator outputs due to disturbances. The three design techniques presented in this chapter are compared with the classical design technique used in the power industry.

(3) The main study in chapter 3 is concerned with the adequacy of simplified machine models, neglecting the effect of damper circuits, for the design of PSS. This is done by employing the PSS designed for lower order machine model to the the machine represented in detail, considering the effect of damper circuits. Comparison between the performances of the stabilizers designed using simplified and detailed models of the machine is presented based on time-domain analysis of the closed-loop systems.

(4) Chapter 4 presents a case study on the evaluation of the effectiveness of various feedback signals that can be used for PSS design. Three control signals, namely, rotor speed,

electrical power output and terminal bus frequency are considered. PSS for the three control signals are designed and the effectiveness of signals is judged by determining stable regions in the P-Q domain. The influence of ac system strength on the design of PSS utilizing the three control signals, is studied. Analysis of interaction between two generating units equipped with PSS, in a power plant is also carried out. The results indicate the importance of using average rotor speed instead of individual speeds as control signal.

(5) Chapter 5 deals with the development of a state-space model for large power systems, suitable for dynamic stability analysis and the selection of proper locations of PSS. The system model of the multimachine system is obtained systematically by developing the models of various machines and their interconnections through the network. The network is represented by its Jacobian matrix.

Two analytical techniques are presented for the choice of effective locations of PSS. A case study of a 13-machine system is presented for the selection of PSS locations. Loci of eigenvalues are obtained to validate the results obtained through the analytical techniques.

(6) Chapter 6 presents the application of two design techniques for PSS in a multimachine system using decentralized feedback control. The first technique is based on the

algorithm given in [6]. PSS for the selected machines are designed, neglecting the interconnection between machines, to assign closed-loop eigenvalues. Parameters of the stabilizers are then updated by introducing the interconnections in discrete increments, keeping the closed-loop eigenvalues unchanged. The algorithm is found to be not suitable when the constraint of providing PSS on limited number of machines is considered.

In the second technique a performance index, based on minimization of fluctuations in the power outputs of relevant generators, is used to design PSS using parameter optimization technique.

Two examples of power systems, one with 3 machines and the other with 13 machines, are considered to illustrate the techniques.

(7) The concluding chapter summarizes the research results and indicates possibilities for future work.

References

- [1] F.P. deMello and C. Concordia, 'Concepts of Synchronous Machine Stability as Affected by Excitation Control', IEEE Trans. Power App. Sys., Vol. PAS-88, pp 316-329, April 1969.
- [2] F.P. deMello, P.J. Nolan, T.F. Laskowski and J.M. Undrill, 'Coordinated Application of Stabilizers in Multimachine Power Systems', IEEE Trans. Power App. and Sys., Vol. PAS-99, pp 892-901, May/June 1980.

- [3] K. Gomathi, 'Pole Assignment Techniques for Power System Stabilization', Ph.D. Thesis, Electrical Engg. Dept., IIT Kanpur, 1979.
- [4] E.V. Larsen and D.A. Swann, 'Applying Power System Stabilizers, Part I : General Concepts, Part II : Performance Objectives and Tuning Concepts, Part III : Practical Considerations', IEEE Trans., Power App.Sys., Vol.PAS-100, pp 3017-3046, June 1981.
- [5] N. Munro and S.N. Hirbod, 'Pole Assignment using Full Rank Output Feedback Compensator', Int. J. Sys.Sci., Vol.10, pp 285-306, 1979.
- [6] S. Lefebure, D.P. Carrol and R.A. De Carlo, 'Decentralized Power Modulation of Multiterminal HVDC Systems', IEEE Trans., Power App.Sys., Vol.PAS-100, pp 3331-3339, July 1981.

CHAPTER 1

INTRODUCTION

1.1 GENERAL

One of the important considerations in the planning, design and operation of a power system is the stability of the system. Stability of a power system is usually classified as 'transient stability' and 'dynamic stability'. The former refers to the stability of the system under large disturbance such as fault on a heavily loaded line which requires opening of the line or the tripping of a loaded generator or an abrupt drop in a large load. The latter refers to the stability of the system under small perturbations such as random change in loading conditions of the system. Transient stability of a power system is improved by the use of high speed protection gear and by incorporating fast acting and high gain excitation systems with the synchronous machines. Although the use of such an excitation system improves transient stability, it also introduces negative damping in the system, impairing dynamic stability. Another reason for an increasing tendency towards dynamic instability is decrease in the transmission strength of the system relative to the size of generating stations. Low frequency oscillations of a sustained or growing nature have been reported in the literature by power utilities [1-5]. These oscillations typically occur in the frequency

range of approximately 0.2 to 2.0 Hz and insufficient damping of these oscillations may limit the power transfer capability in the system. These oscillations in power can be related to oscillations of rotors of synchronous machines in the system relative to one another. Power system stabilizers (PSS) have been developed to provide damping of these electro-mechanical oscillations.

Power system stabilizers are auxiliary controllers which receive feedback signal from rotor speed, angular position, electrical power output or bus frequency and provide a supplementary stabilizing signal to the excitation system of synchronous machines.

Design of PSS has received much attention in the power industry. Industrial PSS design is primarily based on the work of de Mello and Concordia [6]. The work reported in [6] provided an insight into the nature of damping and synchronizing torques which is utilized in PSS design. They used a simplified power system model consisting of a synchronous machine connected to an infinite bus through a transmission line. This model enables use of classical control theory for the design of PSS. It should, however, be noted that this representation of power system is not adequate in general and coordinated application of PSS using multimachine system model is necessary [17]. Classical control theory is not

adequate in such cases. Modern multivariable system control theory has to be used for PSS design in multimachine systems. Two approaches would be useful for PSS design, in multimachine systems, namely those based on optimal control theory and pole assignment.

The main theme of this thesis is to investigate into the design procedures of PSS for single and multimachine systems using modern control theory. Before discussing the work reported here, a brief literature survey on the design of PSS will be undertaken.

1.2 DESIGN OF POWER SYSTEM STABILIZERS : STATE OF THE ART

1.2.1 Design Objective

The different methods available for PSS design can be broadly classified as :

- (1) Improvement of damping torque. This objective of PSS design is used by most of the power industries. A single machine infinite bus equivalent of the actual system is considered and usually Heffron-Phillips model [7] is obtained to apply the frequency domain classical design procedure given by de Mello and Concordia [6].

- (2) Minimization of a performance index. Not much work has been done to develop design methodology based on this approach and its application is not adopted by the power industry yet. Lack of feel for performance index is another reason for its poor acceptance.
- (3) Assignment of closed-loop eigenvalues. This objective of PSS design is slowly being adopted by power engineers particularly where it is difficult to represent the system by single-machine infinite bus model and coordinated design of PSS is essential.

1.2.2 Power System Model

In most of the literature on PSS design, a single-machine infinite-bus equivalent of power system is considered [1-7]. In deriving the system model, the effect of turbine and governor dynamics is usually ignored because of the large time constants associated with them. Damper circuits are also neglected because their effect is considered to be small. Also, since damper circuits provide some damping of rotor oscillations, neglecting them, leads to a conservative design. Another assumption which is usually made is that the network is in steady-state. Dynamical equations of machine and excitation system are described as a set of first order differential equations. Although, the system is nonlinear, for the purpose of PSS design, dynamical equations are linearized around an

operating point, to get the system model in the linearized state-space form as

$$p \underline{X} = [A] \underline{X} + [B] \underline{u} \quad (1.1)$$

where \underline{X} and \underline{u} are state and input variables. 'A' is known as the coefficient or system matrix. The single-machine infinite-bus equivalent model can be justified when designing PSS on a generator connected to a load centre by a long transmission line. Even in this case it may be inaccurate to neglect the interaction between adjacent generators in a power station. Baker et al. [8] investigated the excitation system interaction in a two unit plant feeding an infinite bus. Their investigation reveals that dynamic behaviour of machines in isolation is much different from that when they are operating in parallel.

When a single-machine infinite-bus equivalent model is not adequate, it is necessary to consider a detailed system model including the dynamics of all the relevant machines. The linearized model of a multimachine system can still be obtained in the general state-space form given in eqn. (1.1). To simplify the model it may be sufficient to represent the generators, on which PSS is not being designed, by classical models, neglecting flux decay.

The above equation is general enough to consider any degree of detail in representing the machine, exciter and turbine-governor systems (if desired). The excitation system used on modern generators have been compiled into standard categories [9].

The formulation of system matrix is rather involved and recently many papers have been published on this [10-16]. Laughton [10] obtained the system matrix from the algebraic and differential equations representing the entire power system by employing matrix reductions and inversions. Van Ness and Goddard [11] and Undrill [12] have given methods of building up the system matrix from submatrices representing individual components. Methods of forming the system matrix which do not involve matrix inversion are suggested in Refs. [14-16]. In all the formulations given in Refs. [10-15], the power system network is reduced by treating loads as constant impedances. Padiyar et al. [16] have suggested a systematic method for the formulation of system model for large AC/DC power systems. The system model is obtained by developing the models of various components and subsystems (such as machines, excitation and governor systems) and their interconnection through the network which is represented by its Jacobian. The effect of any nonlinear voltage dependent loads can be obtained by modifying the corresponding diagonal blocks in the Jacobian.

1.2.3 Selection of PSS Location

In a large multimachine system there are many modes of rotor oscillations, some of which can pose problem in terms of the dynamic stability. This can be solved by providing PSS on selected generators.

The choice of generators on which PSS is to be equipped is complicated by the fact that not all machines are effective in damping a particular mode of oscillation. Furthermore, PSS on an arbitrarily chosen machine can introduce negative damping on some modes while damping other modes. The selection of PSS location can be done by trial and error, but this is very time consuming. Some recent papers have addressed the question of fast analytical methods to determine the best location of PSS to a particular mode [17-20]. de Mello et al. [17] used eigenvectors to develop the criteria for optimum location. But this is not the best approach. Recently a technique based on eigenvalue sensitivity has been given for the selection of PSS location [18,19]. This is a fast technique as it avoids simulation, at the same time it can reveal the conflicts in the design of PSS (e.g., whether PSS can undamp some modes). Reference [20] also gives a similar idea but the selection of PSS is based on simulation.

It is to be noted that case studies on large systems have not been reported in the application of the techniques given in [17-20].

1.2.4 Choice of Control Signal

As the objective of PSS design is to produce a component of electrical torque in phase with rotor velocity [6], it is natural to use rotor speed as feedback signal to PSS. Accelerating power and frequency deviation are directly related to the rotor speed and, therefore, these three signals are widely used for the design of PSS [21-27]. Conceptually other signals can also be used as input to PSS. Signals such as armature current, field current and reactive power were investigated [21] and it was found that the signals derived from rotor speed are more effective than these signals. It was observed [4,22] that speed input stabilizers can contribute to negative damping of shaft torsional oscillation mode. The use of accelerating power as control signal has received considerable attention [23,24] due to its inherent low level of torsional interaction. Rapidly fluctuating loads in the vicinity of generating plants restrict the use of frequency signal [25]. Larsen and Swann [26] in their three part paper have presented an investigation into the effectiveness of three control signals, namely, rotor speed, electrical power and frequency. They recommend that stabilizers using frequency signal should be tuned for weak systems and those using speed and power signals should be tuned for strong systems. Both speed and electrical power signals are used for PSS design given in Ref. [27]. They claim that the resulting PSS removes the inherent limitations of speed stabilizers.

Schleif et al. [25] suggested that in case of a two-unit plant, average speed signal cancels any component of swings between units (local mode). They further suggest that such a signal is suitable when rapidly fluctuating loads (like arc furnace) are close to generating plants. Concordia in a discussion of Ref. [26] suggested that the use of average power signal is advisable in comparison with individual power signal.

1.2.5 Design Procedure

1.2.5.1 Design Based on Classical Control Theory

The problem of undamped oscillations in power systems was analysed by de Mello and Concordia [6] through the concept of synchronizing and damping torques produced in the system at the oscillation frequencies. A design method for stabilizers using frequency response techniques was suggested with the objective of improving damping torque without reducing the synchronizing torque. This led to the choice of speed signal and provision of a phase lead compensator in the feedback path. Bollinger et al. [28] used the root-locus method for design. Multi-variable frequency response plots were used by Hamdan and Hughes [29] for the analysis and design of PSS. A good analysis of damping and synchronizing torques has been presented by Alden and Shaltout [30]. Larsen and Swann [26] used the concept of 'plant' characteristic for the design of PSS. They suggest a tuning procedure for a practical PSS used in the industry. The

above methods are applicable mainly to single machine equivalent models of the system.

Coordinated design of PSS in multimachine systems have received much attention recently. de Mello et al. [17] were the first to present the need for coordinated design of PSS in multimachine systems. Crenshaw et al. [31] used the procedure given in [26] for the design of PSS in a two unit plant. Rudnick et al. [32] extended the concepts of synchronizing and damping torques for the analysis of dynamic stability in multimachine systems. However, this was not utilized for PSS design. Gooi et al. [33] presented an iterative technique for the 'optimal' setting of PSS parameters, by solving nonlinear algebraic equations, in multimachine system. Their technique is based on the computation of damping and synchronizing torque coefficients with the help of signal flow graph. The technique is restricted to smaller systems.

Classical design of PSS based on damping torque analysis is devised mainly for single-machine infinite-bus equivalent model of the power system. Although, there have been some efforts to extend this technique to multimachine system, this is not easy and application for large systems is not reported in the literature.

1.2.5.2 Design Based on Minimization of Performance Index

A distinct departure from the classical control techniques is found in the application of modern control theory to the PSS design. Design methods based on optimal regulator theory have been suggested by many authors[34-38]. By this, the stabilizer is designed as an optimal, state feedback controller which minimizes a quadratic performance index. Yu, Vongsuria and Wedman [34] were the first to apply optimal regulator theory to power system problems. Optimal controllers were designed for excitation and governor control. Anderson [35] presented design of an optimal controller for a wide range of operating conditions. Moussa and Yu [36,37] proposed methods where the weighting matrix in performance index is obtained in terms of shift of dominant eigenvalues to the left in the complex plane. A slight departure from the conventional optimal regulator theory is found in the method proposed by Kumar and Richards [38]. Optimal linear feedback law is obtained to achieve pre-assigned eigenvalues for a closed-loop system with much smaller computational effort. The resulting controllers obtained in Refs. [34-38] improve the closed-loop system response. However, inaccessibility of all the states for feedback poses problems in practical situations.

Yu and Siggers [39] developed suboptimal controllers with the system represented by lower order models with measurable states as state variables. Davison and Rau [40] developed a design method for PSS using output feedback by minimizing an average performance index as proposed by Levine and Athans [53]. De Sarkar and Rao [41] designed excitation control for stabilizing a synchronous machine through output feedback by first considering the state feedback obtained through the application of optimal control theory and then getting a minimum norm sub-optimal control for output feedback.

Recently use of Kalman filter to counteract the noise in the control signal output due to random fluctuation of load is given in [42]. Doraiswami et al. [43] presented the design of decentralized controllers for multimachine system using feedback signals from terminal voltage, rotor speed and power.

Industry acceptance of optimal regulator theory is poor because the choice of a suitable performance index is difficult to make. It is not easy to judge good system performance through a performance index. Another reason is that direct application of full state feedback optimal regulator theory is not possible for large multimachine systems because of the decentralized structure of PSS. Moreover, the design of optimal dynamic output feedback controllers is not reported.

1.2.5.3 Design Based on Pole Assignment

Improvement of damping torque is equivalent to the shifting of eigenvalues corresponding to rotor oscillations [44]. Thus, pole assignment techniques give better understanding of the system damping. State or output feedback can be used for pole assignment, however, output feedback is more practical. Constant gain feedback or dynamic feedback are two alternatives for pole assignment. From system response point of view dynamic feedback is attractive. Most of the literature available have considered PSS design as that of dynamic output feedback compensator [45-50]. The number of poles that can be assigned depends upon the order of PSS. Usually a second order PSS is designed to assign dominant eigenvalues of the system.

Padiyar et al. [45] have presented three methods for the design of PSS by pole assignment with output feedback. The first method is based on modal control theory. The second and third methods involve static optimization for exact assignment of poles and assignment into a sector. Arcidiacono et al. [46] proposed a technique for PSS design which utilizes the residues of open-loop transfer function to get a specified set of closed-loop eigenvalues. Fleming et al. [47] proposed a sequential algorithm for tuning the parameters of PSS with fixed poles in multimachine power systems. A similar procedure is given in [20]. Sequential addition of stabilizers disturbs previously assigned eigenvalues and hence is not

satisfactory. An algorithm for simultaneously tuning the PSS in a multimachine system is proposed by Lefebvre [48]. Abe and Doi [49,50] developed a design technique by combining the frequency response method and the pole assignment method.

1.2.5.4 Design Utilizing Adaptive Control

In all the methods discussed so far, PSS are designed at a particular operating point to provide adequate damping to the system. However, the operating point is not fixed, but keeps changing and the performance of stabilizers, under changed conditions, may not be satisfactory. The need for adaptation has been felt since long. The availability of low cost microprocessors has made it possible to design adaptive PSS. The use of digital adaptive regulators, called self tuning regulators, for power system stabilization has been reported recently in the literature [51,52].

1.3 CONTROLLER DESIGN

As the techniques for PSS design presented in this thesis are based on modern control theory, a brief survey of the relevant design techniques is presented in this section.

Although the techniques based on optimal regulator theory are well known, mention of a few points will help in the use of these techniques in subsequent chapters. The solution of an optimal output feedback regulator problem depends on the initial values of state variables (x_0) of the system. This poses

problems in controller realization. Levine and Athans [53] were first to eliminate this dependence by assuming x_0 as a random variable uniformly distributed on the unit sphere. They presented a design technique for optimal gain controller using output feedback in which solution of nonlinear simultaneous matrix equations is required. Later, Hole [54] and Horisberger and Belanger [55] modified the technique to avoid solution of simultaneous matrix equations. Design of optimal dynamic output feedback controller is, however, not available in the literature.

Controller design based on pole assignment techniques is of later origin. Much work has been reported in this area [56-64]. Pole assignment can be achieved either by state or output feedback, using gain controller or dynamic controller. Wang and Davison [60] have shown that $\min(n, m+r-1)$ closed-loop poles can be assigned with a gain output feedback, for a completely controllable and observable system, where n, m and r are respectively the number of state, input and output variables. Brasch and Pearson [61] and Ahmari and Vacroux [62] have shown that for a completely controllable and observable system defined by plant, input and output matrices A, B and C respectively, a p th order controller can be designed to assign $\max(\alpha+p, \beta+p)$ closed-loop poles to desired locations where α and β are given by

$$\alpha = \text{Rank}[B \quad AB \quad A^2B \quad \dots \quad A^pB]$$

$$\beta = \text{Rank}[C^t \quad A^t C^t \quad (A^t)^2 C^t \dots \quad (A^t)^p C^t]$$

Techniques given in Refs. [57-64] suffer from the drawback that the resulting feedback matrix is dyadic. Due to the rank deficiency of the feedback controller, the resulting closed-loop system has poor disturbance rejection properties [65]. Munro and Hirbod [66] presented a systematic design of full rank output feedback controllers which allow arbitrary pole assignment in the closed-loop system. Youla et al. [67] presented a necessary and sufficient condition for the stabilization of a dynamical plant described by the transfer function matrix $P(s)$. The plant $P(s)$ can be stabilized by an asymptotically stable controller $C(s)$ iff real poles and zeros of $P(s)$ in the right half of complex plane, have the interlacing property (i.e., poles and zeros of $P(s)$ in the right-half of complex plane should lie alternatively).

Very often, it is uneconomical and impractical to globally (centrally) control a large, geographically dispersed, interconnected physical system. Control problems associated with large-scale systems led to the area of decentralized control [68-78]. The system is divided into various subsystems with local control stations. At each station, the controller observes only local system outputs and controls only local inputs. All the controllers are, however, involved in controlling

the same large system. A brief review on decentralized control is presented here.

Wang and Davison [68] introduced the fixed mode concept. Fixed modes cannot be assigned using 'local' dynamic controllers. The remaining modes can be so assigned. Corfmat and Morse [69] gave a more complete characterization of the conditions for stabilization of large systems. Sacks [70] used a decoupled model known as component connection model (CCM) to show that the fixed modes of the composite system [68] and the set of fixed modes of the individual components coincide in CCM. Basically this paper shows that, within the CCM framework, there exist local output dynamic controllers which will assign a prescribed eigenvalue spectrum provided each component or subsystem is controllable and observable. A good bibliography on decentralized control is given in a survey paper by Sandell et al. [71]. Wang and Davison [72] presented a design of local feedback controller when all the fixed modes are not stable. It is shown that by limited exchange of information between local stations, it is possible to stabilize the entire system. Sezer and Huseyin [73] have given sufficient conditions based on graph theoretic concept for an interconnected system to be stabilizable using only local state feedback. Xingolas et al. [74] presented a two-level hierarchical computational scheme for the determination of decentralized gains. At lower level, two Liapunov equations are solved and at higher level a predictive

corrective routine is used. Ramakrishna and Viswanadham [75] have developed sufficient conditions for the decentralized stabilization of a class of large systems with dynamic interconnections between subsystems. These conditions are given in terms of the subsystem coefficient matrices. It is shown that if interactive subsystems are stable with mild restriction on the subsystems, then the large system can be stabilized with decentralized feedback. Viswanadham and Ramakrishna [76] have presented the synthesis of decentralized observer based on local measurements to generate maximum possible linear combination of local states for the stabilization of the interconnected system.

Basically the above papers provide existence theorems for a system to be stabilizable with decentralized control. No clear cut methodology is available for the design of such a controller. Lefebvre et al. [77] have given an algorithm to assign closed-loop poles by dynamic decentralized output feedback. Two-level design is presented. In the first level closed-loop poles are assigned by local outputs neglecting the interconnection between subsystems. Interconnection is then introduced in discrete steps to update the parameters of local controllers with the objective to retain the closed-loop eigenvalues at their specified location.

1.4 OBJECTIVE AND SCOPE OF THE THESIS

The design of PSS can be based on pole assignment or minimization of a performance index provided the index is properly chosen. Although much work has been reported on the use of these techniques for PSS design, the following points have not been properly considered :

- (1) In pole assignment techniques full design freedom has not been utilized in the selection of PSS parameters.
- (2) Design of dynamic optimal output feedback compensator has not been reported. Moreover, use of parameter optimization technique to large systems taking into account the decentralized nature of controller is not reported.
- (3) Although methods are available for the selection of PSS location in multimachine systems, their application to large systems is not available in the literature.
- (4) Though some work has been reported on the choice of feedback control signals, a detailed study is not available, particularly for plants having two or more units operating in parallel.
- (5) A third order synchronous machine model is widely used in the design of PSS. Adequacy of the model has not been investigated.

The work reported in this thesis is directed at removing some of the gaps in the aspects of PSS design mentioned above.

The major emphasis is on evolving design procedures in large multimachine power systems subject to the practical constraints of using decentralized dynamic compensators. The design objectives are chosen as either pole assignment or minimization of a performance index in the framework of optimal control theory.

As adaptive control is yet to be introduced in power system, scope of the thesis is limited to the application of deterministic control.

1.5 SUMMARY OF THE WORK

A chapterwise summary of the work done in the thesis is given below.

Chapter 2 discusses the problem of dynamic stability of present day power systems and the need for its improvement through the use of power system stabilizers. Different techniques based on modern control theory are developed for PSS design. The techniques developed here have better methodology and are general enough to be applied to multimachine systems. Two design objectives are used. Pole assignment is used in the first two techniques presented. Modal control theory is applied in the first design technique. Only accessible states are used as feedback signals to PSS. The PSS dynamics is chosen in such a way that zeros of PSS transfer function are specified. Pole assignment technique developed by Munro and Mirbod [66] with dynamic output feedback is utilized for PSS

design in the second technique. This technique puts no restriction on the parameters of PSS and their values are directly obtained in terms of the desired locations of closed-loop eigenvalues. For complete pole assignment a two-input dynamic compensator is designed. In the techniques developed, PSS parameters are directly computed, unlike trial and error method used in classical design.

Minimization of a performance index is another objective which is used in PSS design. Electromechanical oscillations of machine rotors with respect to one another cause fluctuations in power output of machines and limit power transfer capabilities of the systems. This effect is of great concern in systems having long transmission lines. Damping of these oscillations can be achieved by minimizing the fluctuations in power output of generators. The third technique is based on parameter optimization using output feedback with the objective to minimize power fluctuations in generator outputs following a disturbance. These techniques are used to design PSS for a single-machine infinite-bus system. Comparison is made of the performance of these PSS with the PSS designed using the classical technique used in the power industry.

Chapter 3 presents a detailed investigation into the effect of synchronous machine modelling on the design of PSS. Two different models are considered for the investigation. The simplified or the lower order model considers only the

effect of field flux decay in addition to the equation of mechanical motion. Effect of amortisseur windings are neglected in this representation. The detailed or higher order model considers the damper circuits in addition to the lower order representation [78]. PSS are designed, for both representations of synchronous machine, at different machine loading, inertia constant and voltage regulator gain, to determine the effect of machine representation on PSS parameters. Adequacy of the simplified model for PSS design is analysed by incorporating PSS, designed for lower order model, to the machine represented in detail. Performances of the stabilizers, designed for both representations of machine, are compared by eigenvalue and time-domain analyses.

Chapter 4 presents a detailed analysis on the effectiveness of different feedback control signals that can be used for PSS design. Rotor speed, electrical power output and terminal bus frequency signals are considered. A generating plant, having a number of generating units, connected to a large power system is considered for the analysis. First, the effectiveness of control signals is studied for a plant having one machine. Then, the interaction between machines present in the plant on the effectiveness of control signals is investigated by considering another machine operating in parallel with the existing machine. Effectiveness of a PSS utilizing a particular feedback signal is judged by determining the stable P-Q region for the machine equipped with that

PSS. The influence of ac system strength on the design of PSS utilizing the three control signals is studied. The suitability of average speed and average power signals is also presented in the case of plant with more than one machine.

Chapter 5 presents the development of a state-space model for large power systems, suitable for dynamic stability analysis, and the investigation into the selection of effective locations of PSS in such a system. The development of the system model proceeds systematically by developing the models of various machines and their interconnection through the network model. The network is represented by its Jacobian matrix. In the development of system model it is not necessary to eliminate the non-generator buses and the identity of each bus of the system is retained. Changes in the system matrix caused by the changes in the system configuration can be easily accommodated.

A proper choice of PSS location is essential for the coordinated operation of multimachine systems. Two analytical techniques are presented for the choice of effective locations of PSS. The first technique is independent of controller structure and the second is based on eigenvalue sensitivity. A case study of a 13-machine system is presented for the selection of PSS locations. The results obtained through analytical techniques are validated from the loci of eigenvalues.

Chapter 6 presents the application of decentralized control with output feedback for the design of PSS in multi-machine power systems. Techniques based on eigenvalue assignment and minimization of a performance index are presented for the design of PSS.

The technique based on eigenvalue assignment utilizes the algorithm given in Ref. [77]. PSS for the selected machines are designed, neglecting the interconnections between machines, to assign closed-loop eigenvalues. Parameters of the stabilizers are then updated by introducing the interconnections, in steps, keeping the closed-loop eigenvalues unchanged. The advantage of this iterative method is that stabilizers are designed for smaller subsystems, easy to handle in comparison with the design of stabilizers for the entire system considered together. In the second technique a performance index, based on minimization of power fluctuations in the output of relevant generators, is used to design PSS. Steepest descent method is used to update the parameters of stabilizers in the optimization routine. A three machine and a thirteen machine examples are considered to illustrate the proposed techniques and to compare the results obtained.

A brief review of the major contributions of this thesis and possibilities for further work are given in the concluding chapter.

CHAPTER 2

DYNAMIC COMPENSATOR DESIGN FOR POWER SYSTEM STABILIZATION

2.1 INTRODUCTION

Since early 1960, most of the new generating units added to electric utility systems have been equipped with continuously acting voltage regulators. As these units increased in number, it became apparent that the voltage regulator action had a detrimental effect on the dynamic stability of power systems. Oscillations of small magnitude and low frequency often persisted for long periods of time and in some cases presented limitations on power transfer capability [1,2]. Damping of these oscillations can be achieved by the use of power system stabilizers (PSS). PSS are auxiliary feedback controllers which receive signal from rotor speed, electrical power output or terminal bus frequency and superimpose a corrective signal on the voltage error signal of the normal voltage regulators.

Design of PSS has been conventionally carried out using classical control theory [6,26]. This approach has its limitation in that it is restricted to systems which can be represented as a single machine connected to an infinite bus. This model of power system is not adequate in many situations and coordinated application of PSS using multimachine system model is essential [17]. Thus, it is possible that PSS designed on

the basis of single machine infinite bus system may introduce negative damping for some modes of oscillations while damping some others [17].

Modern control theory provides a better tool for the design of PSS in large multimachine power systems [34-48] than classical control theory. Modern approach to PSS design is based either on pole assignment techniques [44-48] or on optimal regulator theory [34-41]. Pole assignment can be achieved via state feedback, but inaccessibility of state variables necessitates the use of output feedback. Industry application of optimal regulator theory is somewhat poor because of lack of feel for performance index. Pole assignment techniques, on the other hand, give better understanding of system damping. It is to be noted, however, that in the works reported, design freedom has not been fully utilized.

The basic aim of this chapter is to provide techniques, with better methodology, for the design of PSS as a dynamic compensator, fully utilizing the freedom available in the choice of its parameters. Three design techniques are presented based on pole assignment and minimization of a performance index. The first technique utilizes partial state feedback and is based on modal control [56] to assign dominant eigenvalues corresponding to rotor oscillations. The second technique utilizes output feedback and follows the algorithm of Munro and Hirbod [66] with the objective of assigning closed-loop poles.

Design objective in the third technique is minimization of fluctuations in power output of generators. The technique is based on the works reported in Refs. [53,54].

Although the PSS design techniques presented can be applied to multimachine power systems, their application is restricted to single machine infinite bus system in this chapter. Chapter 6 deals with their application to multimachine power systems.

2.2 PROBLEM OF POWER SYSTEM STABILIZATION

2.2.1 General

The problem of power system stabilization can be explained with the help of a single-machine infinite-bus system, shown in Fig. 2.1. This representation of power systems has been considered by many authors [1-7] for the design of PSS. As discussed in Chapter 1, for the purpose of dynamic stability analysis, linearized state space model of the system is used.

In this section a state space model of the system given in Fig. 2.1 is developed and with the help of eigenvalue analysis, dynamic behaviour of the system is analysed. The need of a PSS to stabilize the system and the objective of its design is discussed in terms of the concepts used by power engineers.

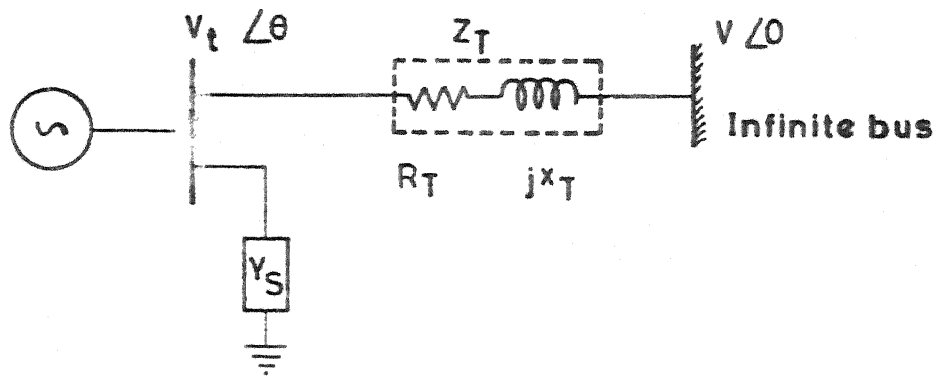


FIG. 2.1 SINGLE MACHINE INFINITE BUS SYSTEM.

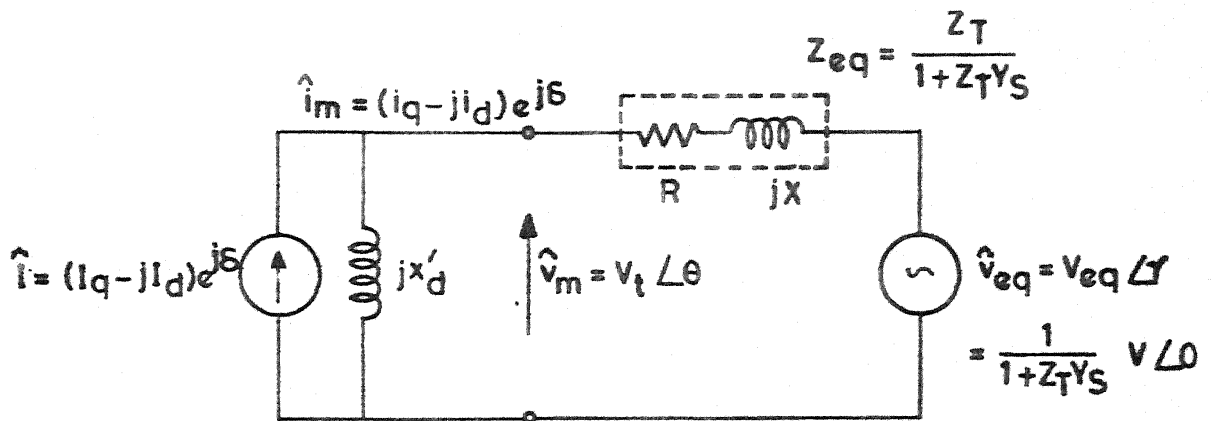


FIG. 2.2 SINGLE-PHASE EQUIVALENT CIRCUIT OF THE MODEL.

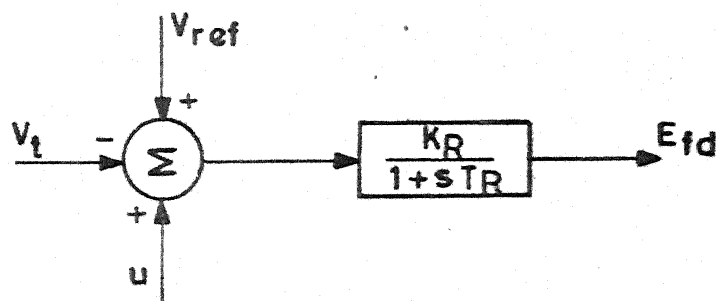


FIG. 2.3 BLOCK DIAGRAM OF EXCITATION SYSTEM.

2.2.2 Development of System Model

The following assumptions are made for developing the state-space model of the system given in Fig. 2.1 :

1. The synchronous machine has no amortisseur windings.
2. Governor and turbine dynamics can be ignored.
3. The machine stator and the external network are in quasi-steady state.

2.2.2.1 Machine Model

A three winding model of the machine is considered. Stator of the machine is represented by a dependent current source in conjunction with a constant impedance [78]. Derivation of the machine model is given in Appendix D. The system dynamical equations are as follows :

$$p\omega = \frac{1}{M} (T_m - T_e) - \frac{K_D}{M} (\omega - \omega_o) \quad (2.1)$$

$$p\delta = (\omega - \omega_o) \quad (2.2)$$

and

$$pI_d = \frac{1}{L'_d T'_{do}} [E_{fd} - L'_d I_d - (L_d - L'_d) i_d] \quad (2.3)$$

where

$$M = \frac{2H}{\omega_o}$$

$$T_e = L'_d (I_d i_q - I_q i_d) \quad (2.4)$$

$$I_q = \xi i_q \quad (2.5)$$

$$\xi = \frac{L_d - L'_d}{L'_d}$$

The non-state variables i_d , i_q and I_q in eqns. (2.1) to (2.4) are eliminated by representing them in terms of the state variables I_d and δ as given below. Figure 2.2 represents the single phase equivalent circuit of the power system shown in Fig. 2.1. From Fig. 2.2, the armature current phasor \hat{i}_m can be written as :

$$\hat{i}_m = \frac{j x'_d}{Z_{eq} + j x'_d} \hat{I} - \frac{1}{Z_{eq} + j x'_d} \hat{V}_{eq}$$

Substituting the values of \hat{I} , Z_{eq} and \hat{V}_{eq} , we get

$$(i_q - j i_d) e^{j\delta} = (a_1 + j a_2)(I_q - j I_d) e^{j\delta} - (b_1 + j b_2) V_{eq} \quad (2.6)$$

where

$$a_1 + j a_2 \triangleq \frac{j x'_d}{R + j(X + x'_d)}$$

and

$$b_1 + j b_2 \triangleq \frac{\cos \gamma + j \sin \gamma}{R + j(X + x'_d)}$$

Substituting the value of I_q from eqn. (2.5) into eqn. (2.6) and equating the real and imaginary parts, we get

$$i_q = \frac{a_2}{1 - a_1 \xi} I_d - \frac{V_{eq}}{1 - a_1 \xi} (b_1 \cos \delta + b_2 \sin \delta) \quad (2.7)$$

and

$$i_d = a_1 I_d - \frac{a_2 \xi}{1 - a_1 \xi} [a_2 I_d - V_{eq} (b_1 \cos \delta + b_2 \sin \delta)] + V_{eq} (b_2 \cos \delta - b_1 \sin \delta) \quad (2.8)$$

2.2.2.2 Excitation System Model

A single time-constant excitation system, IEEE Type IS [9], is considered. Figure 2.3 gives the block diagram representation of the excitation system. The state equation of the excitation system as obtained from Fig. 2.3 is

$$p E_{fd} = -\frac{1}{T_R} E_{fd} + \frac{K_R}{T_R} (V_{ref} - V_t + u') \quad (2.9)$$

where $V_t = (v_d^2 + v_q^2)^{1/2}$

The Park's components of terminal voltage, v_d and v_q are obtained from the equivalent circuit of Fig. 2.2 as :

$$\hat{V}_m = (v_q - jv_d) e^{j\delta} = jx_d' [I_q - jI_d - (i_q - ji_d)] e^{j\delta}$$

Equating the real and imaginary parts, we get

$$v_d = x_d' (1 - \xi) i_q$$

and

$$v_q = x_d' (I_d - i_d)$$

2.2.2.3 Linearized Model

The linearized state space model is derived by linearizing eqns. (2.1) to (2.3) and (2.9). The non-state variables Δi_d and Δi_q are eliminated using the following expressions obtained by linearizing eqns. (2.7) and (2.8).

$$\Delta i_q = K_1 \Delta I_d + K_2 \Delta \delta \quad (2.10)$$

$$\Delta i_d = K_3 \Delta I_d + K_4 \Delta \delta$$

where $K_1 \triangleq \frac{a_2}{1-a_1\xi}$

$$K_2 \triangleq \frac{V_{eq}}{1-a_1\xi} (b_1 \sin \delta_o - b_2 \cos \delta_o)$$

$$K_3 \triangleq a_1 - \frac{a_2^2\xi}{1-a_1\xi}$$

and $K_4 \triangleq V_{eq} [-(b_2 + b_1 \frac{a_2\xi}{1-a_1\xi}) \sin \delta_o -$
 $(b_1 - b_2 \frac{a_2\xi}{1-a_1\xi}) \cos \delta_o]$

The resulting fourth order model of the system is described by the state equation

$$p \underline{x} = [A] \underline{x} + \underline{b} u \quad (2.11)$$

where

$$\underline{x} \triangleq [\Delta\omega \quad \Delta\delta \quad \Delta I_d \quad \Delta E_{fd}]$$

$$u \triangleq \Delta u'$$

$$[A] = \begin{bmatrix} a_{11} & a_{12} & a_{13} & 0 \\ 1 & 0 & 0 & 0 \\ 0 & a_{32} & a_{33} & a_{34} \\ 0 & a_{42} & a_{43} & a_{44} \end{bmatrix}$$

$$\underline{b} = [0 \quad 0 \quad 0 \quad b_4]^t$$

$$a_{11} = -K_D/M$$

$$a_{12} = \frac{x'_d}{M} [\xi i_{q0} K_4 - (I_{d0} - \xi i_{d0}) K_2]$$

$$a_{13} = \frac{x'_d}{M} [(\xi K_3 - 1) i_{q0} + (\xi i_{d0} - I_{d0}) K_1]$$

$$a_{32} = - \frac{(x_d - x'_d) K_4}{x'_d T'_{d0}}$$

$$a_{33} = - \frac{x'_d + (x_d - x'_d) K_3}{x'_d T'_{d0}}$$

$$a_{34} = 1/(x'_d T'_{d0})$$

$$a_{42} = \frac{K_R x'_d}{T_R v_{to}} [v_{q0} K_4 - v_{d0}(1-\xi) K_2]$$

$$a_{43} = \frac{K_R x'_d}{T_R v_{to}} [v_{q0}(K_3-1) - v_{d0}(1-\xi) K_1]$$

$$a_{44} = -1/T_R$$

$$b_4 = K_R/T_R$$

2.2.2.4 Numerical Example

A single-machine infinite-bus system as shown in Fig. 2.1 is considered. The following system data, given in Ref. [13],

are taken for the study. The machine and transmission line parameters are given in per unit on machine base.

Generator parameters : $x_d = 1.72$; $x'_d = 0.45$; $x_q = 1.63$
 $T'_{do} = 6.3$ sec ; $H = 4.0$ sec.
 $\omega_o = 314$ rad/sec.

Transmission Line parameters : $R_T = 0.024$; $X_T = 0.6$
 $G_S = 0$; $B_S = 0.066$

Voltage Regulator parameters : $K_R = 50.$; $T_R = 0.02$ sec.

Operating data : Generated power = 1.0 p.u. at 0.9 power factor lagging

Infinite bus voltage = 1.0 $\angle 0^\circ$

The matrices A and b of the system at the operating point are as follows :

$$[A] = \begin{bmatrix} 0 & -35.95933 & -15.84320 & 0 \\ 1 & 0 & 0 & 0 \\ 0 & -0.38083 & -0.34625 & 0.35273 \\ 0 & 240.33139 & -544.65348 & -50 \end{bmatrix}$$

and

$$\underline{b} = [0 \quad 0 \quad 0 \quad 2500]^t$$

Open-loop eigenvalues of the system matrix A are given in Table 2.1. The complex pair of eigenvalues, shown in Table 2.1, corresponds to the rotor oscillation mode. As the real part of

this eigenvalue is positive, the system will be dynamically unstable and there is a need to stabilize the system by employing a PSS.

Table 2.1 Open-Loop Eigenvalues

$0.20788 \pm j6.11383$
-5.00647
-45.75554

2.2.3 Power System Stabilizer

The concepts used by power engineers for the design of PSS can be explained with the help of the pioneering work of de Mello and Concordia [6]. Stability analysis given in [6] is based on the concept of synchronizing and damping torques. Synchronizing torque is defined as the component of electrical torque which is in phase with the rotor angle phasor. Damping torque is represented by the out of phase component, namely, the component in phase with rotor velocity. Synchronizing torques are basically provided by the electrical ties between machines and are functions of machine operating conditions and network characteristics. Damping torques are provided from different sources : machine damper windings, field windings, excitation system (AVR controller) and speed governors [32]. Damping torques produced by first two sources are positive while

contributions of AVR controllers and speed governors may be negative. According to stability criteria given in [6], both the damping and synchronizing torques should be positive for the system to be stable. It is shown in [6] that excitation system has conflicting effects on the synchronizing and damping torques. Under heavy loading conditions the effect of excitation system is to increase the synchronizing torque in the system and reduce the damping torque. The reduction in damping torques, particularly in systems with long transmission lines, results in extremely oscillatory behaviour of the system. The problem is solved by providing a torque component, through external means, in phase with rotor velocity such that the reduction in damping torque is compensated. This forms the basis for the design of PSS and is widely used in power industry.

It can be shown [44] that the damping and synchronizing torques are approximately related to real and imaginary parts of the eigenvalues corresponding to rotor oscillations. The design objective of PSS given in [6] can, therefore, be translated into that of shifting the real parts of the dominant eigenvalues corresponding to rotor oscillations. Thus, the design of PSS can be treated as a problem of pole-assignment.

Before discussing the design techniques for PSS, the functions of various components of a practical PSS using speed signal is explained with the help of the block diagram given in Fig. 2.4.

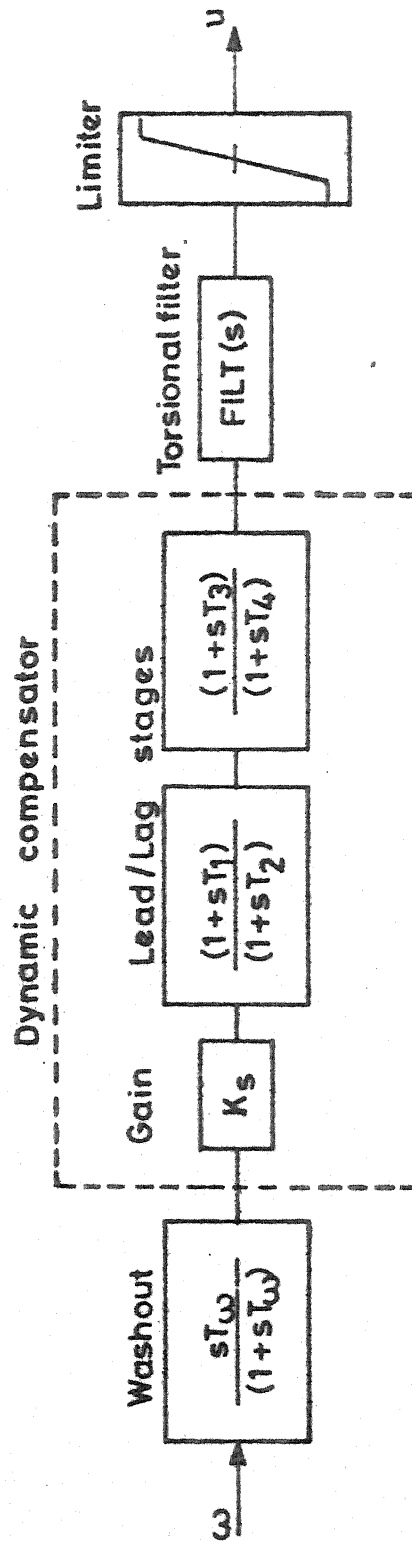


FIG.2.4 BLOCK DIAGRAM OF A PRACTICAL PSS.

Washout Stage

The washout stage is provided to prevent offsets in terminal voltage for the steady-state change in system frequency. The washout time constant T_w should be large enough to pass signals at the required stability frequencies relatively unchanged.

Gain

The amount of damping associated with rotor oscillations depends on stabilizer gain K_s . The damping increases with increase in K_s upto a certain value, beyond which, further increase in gain results in a decrease in damping. The stabilizer gain should be set at the value corresponding to the maximum damping of the rotor oscillations.

Lead/Lag Stages

To provide damping torque for oscillation of the machine with respect to the power system, it is necessary to develop an electrical torque which is in phase with speed changes. With speed as input signal, it is necessary to provide a phase lead to compensate for lags between regulator input and the resulting electrical torque. The function of this stage is to provide the required phase lead over the desired range of frequencies.

Torsional Filter

Torsional filter is used to attenuate the stabilizer gain at high frequencies to limit the impact of noise and to minimize torsional interaction between generator and turbine.

Stabilizer Limit

To allow maximum contribution of the stabilizer, a large positive limit of about 0.2 p.u. is used. On the negative side, a limit of 0.05 to 0.1 p.u. is used to allow sufficient control range and to reduce the probability of a unit trip for failure of a stabilizer component.

As the influence of washout, filter and limiter stages is very small in the range of rotor oscillation frequencies, the design of a practical PSS can be considered as the determination of gain and time constants of lead/lag stages. In general, the design of PSS can be viewed as the design of a dynamic compensator for stabilization of the system.

2.3 DESIGN OF DYNAMIC COMPENSATOR

As discussed in the previous section, power system stabilizers are basically dynamic compensators of a fixed order. The control signals to the PSS are appropriate measurable outputs of the system such as rotor speed, electrical power output or bus frequency. Thus, the design of PSS can be considered as the design of output feedback dynamic compensator. The aim

of this section is to develop various techniques, based on modern control theory, for the design of dynamic compensators. These techniques will be subsequently used for the PSS design.

The first technique utilizes modal control [56] with partial state feedback to assign closed-loop eigenvalues. Compensator dynamics and control law are assumed in such a way that the zeros of compensator transfer function are fixed. Thus, gain and poles of the compensator are to be determined. The second technique utilizes the algorithm suggested by Munro and Hirsbod [66]. The design objective is to assign closed-loop eigenvalues with output feedback. Compensator structure is fixed and the parameters of the compensator, namely, gain, poles and zeros are obtained to meet the design objective. The third technique is based on parameter optimization to minimize a performance index using output feedback [53,54].

2.3.1 Pole Assignment with Partial State Feedback Compensator

2.3.1.1 Formulation of Control Problem

Consider the single input linear time invariant system

$$\dot{\underline{x}} = [\underline{A}] \underline{x} + \underline{b} u \quad (2.12)$$

where $\underline{x} \in R^n$ and $u \in R^1$. Let \underline{x}' represent the vector of accessible state variables, then

$$\underline{x}' = [\underline{C}] \underline{x} \quad (2.13)$$

where $\underline{x}' \in \mathbb{R}^r$, $r \leq n$, and C is an $r \times n$ matrix. Without loss of generality C can be considered to be of the form

$$[C] = [C \mid I_r] \quad (2.14)$$

where I_r is an $r \times r$ identity matrix and C represents an $r \times (n-r)$ null matrix.

Consider a k th order dynamic controller and the control law of the form

$$p \underline{z} = [D] \underline{z} + \underline{e} u \quad (2.15)$$

and

$$u = \underline{K}_1^t \underline{x}' + \underline{K}_2^t \underline{z} \quad (2.16)$$

where $[D] = \text{diag} [d_1 \ d_2 \ \dots \ d_k]$

and $\underline{e} = [1 \ 1 \ \dots \ 1]^t$

The structure of D and e fixes zeros of the controller at d_1, d_2, \dots and d_k (Appendix A). K_1 and K_2 are respectively $r \times 1$ and $k \times 1$ matrices, representing feedback gains. Combining eqns. (2.12) and (2.15) and substituting for x' from eqn. (2.13) into eqn. (2.16), we get

$$p \hat{\underline{x}} = [\hat{A}] \hat{\underline{x}} + \hat{\underline{b}} u \quad (2.17)$$

and

$$u = \underline{K}_m^t \hat{\underline{x}} \quad (2.18)$$

where

$$[\hat{A}] = \begin{bmatrix} A & O \\ O & D \end{bmatrix} ; \quad \hat{\underline{b}} = \begin{bmatrix} b \\ e \end{bmatrix} ; \quad \hat{\underline{x}} = \begin{bmatrix} x \\ z \end{bmatrix}$$

and

$$\underline{K}_m^t = \begin{bmatrix} 0 & \vdots & K_1^t & \vdots & K_2^t \end{bmatrix} \quad (2.19)$$

Eqn. (2.17) represents the dynamical equations of the composite system of order n_1 , where $n_1 = (n+k)$. \underline{K}_m in eqn. (2.18) is an $n_1 \times 1$ matrix of state feedback gain which from modal control theory [56] can be obtained as

$$\underline{K}_m = [W] \underline{\alpha} \quad (2.20)$$

where W is $n_1 \times n_1$ matrix formed by the reciprocal eigenvectors of matrix \hat{A} corresponding to the open-loop eigenvalues $\lambda_1, \lambda_2, \dots, \lambda_{n_1}$. The expression for the j th element of $\underline{\alpha}$ is given as [56]

$$\alpha_j = \beta_j \sum_{i=1}^{n_1} \frac{\pi}{\lambda_j - \rho_i} \quad (2.21)$$

where

$$\beta_j = -1 / \left[\sum_{\substack{i=1 \\ i \neq j}}^{n_1} \frac{\pi}{\lambda_j - \lambda_i} \right]$$

and $\rho_1, \rho_2, \dots, \rho_{n_1}$ are the desired locations of the closed-loop eigenvalues. From eqns. (2.19) and (2.20), it is clear that entries of $\underline{\alpha}$ should be such that first $(n-r)$ elements of \underline{K}_m are equal to zero. Now, as the elements of α are functions of open-loop and closed-loop eigenvalues and as they have to satisfy the above constraint, all the closed-loop eigenvalues cannot be assigned arbitrarily. In other words, if some of

the closed-loop eigenvalues are to be assigned to specified locations, there is no control on the location of remaining closed-loop eigenvalues. Let n_2 eigenvalues be assigned and $t = (n_1 - n_2)$ eigenvalues are allowed to assume arbitrary locations. Expanding eqn. (2.21)

$$\alpha_j = \beta_j [(\lambda_j - \rho_1)(\lambda_j - \rho_2) \dots (\lambda_j - \rho_t)(\lambda_j - \rho_{t+1})(\lambda_j - \rho_{t+2}) \dots \dots (\lambda_j - \rho_{n_1})]$$

$\begin{matrix} 1 & 2 & \dots & t & 1 & 2 \end{matrix}$

$\rho_1, \rho_2, \dots, \rho_t$ are unknown while $\rho_{t+1}, \rho_{t+2}, \dots, \rho_{n_1}$ are specified. α_j can be written as

$$\alpha_j = \beta_j^t (\lambda_j^t + q_1 \lambda_j^{t-1} + q_2 \lambda_j^{t-2} + \dots + q_t) \quad (2.22)$$

where $\beta_j^t = \beta_j (\lambda_j - \rho_{t+1})(\lambda_j - \rho_{t+2}) \dots (\lambda_j - \rho_{n_1})$

and q_1, q_2, \dots, q_t are coefficients of polynomial in λ_j and functions of $\rho_1, \rho_2, \dots, \rho_t$. In vector matrix notation eqn. (2.22) can be written as

$$\underline{\alpha} = [P] \underline{q} \quad (2.23)$$

where

$$[P] = \begin{bmatrix} \beta_1^t & \bigcirc & & \\ & \beta_2^t & \bigcirc & \\ & & \ddots & \\ \bigcirc & & & \beta_{n_1}^t \end{bmatrix} \begin{bmatrix} \lambda_1^t & \lambda_1^{t-1} & \dots & 1 \\ \lambda_2^t & \lambda_2^{t-1} & \dots & 1 \\ \vdots & & \ddots & \vdots \\ \lambda_{n_1}^t & \lambda_{n_1}^{t-1} & \dots & 1 \end{bmatrix}$$

$$\underline{q} = [1 \quad q_1 \quad q_2 \quad \dots \quad q_t]^t$$

and

$$\underline{\alpha} = [\alpha_1 \quad \alpha_2 \quad \dots \quad \alpha_{n_1}]^t$$

Substituting the value of α from eqn. (2.23) into eqn. (2.20)

$$\underline{K}_m = [S] \underline{q} \quad (2.24)$$

where

$$[S] = [W] [P]$$

Partitioning of eqn. (2.24) results in

$$\begin{bmatrix} 0 \\ K_1 \\ K_2 \end{bmatrix} = \begin{bmatrix} S_0 \\ S_1 \\ S_2 \end{bmatrix} \underline{q} \quad (2.25)$$

considering the first set of $(n-r)$ equations in eqn. (2.25), the order of the submatrix. S_0 will be $(n-r) \times (t+1)$. These equations can be rearranged as

$$\underline{s}'_0 = [S'_0] \underline{q}' \quad (2.26)$$

where

$$\underline{s}'_0 = -\underline{s}_{01}$$

$$[S'_0] = [\underline{s}_{02} \quad \underline{s}_{03} \quad \dots \quad \underline{s}_{0t+1}]$$

$$\underline{q}' = [q_1 \quad q_2 \quad \dots \quad q_t]^t$$

and $s_{01}, s_{02}, \dots, s_{0t+1}$ are columns of the submatrix S_0 . Eqn. (2.26) is a set of $(n-r)$ simultaneous linear equations in t

unknowns which can be solved for $q_1 \ q_2 \dots q_t$ and in turn for $\rho_1, \rho_2, \dots, \rho_t$, the unassigned closed-loop eigenvalues. The necessary and sufficient condition for the existence of the solution of eqn. (2.26) is [66].

$$\text{Rank } [s'_0] = \text{Rank } [s'_0, s'_0] \quad (2.27)$$

Substitution of the solution vector q in eqn. (2.24) gives the feedback gain vector K_m . The parameters of the compensator can be obtained in terms of K_m and matrix D (see Appendix A).

2.3.1.2 Algorithm

Parameters of the compensator of a fixed order can be obtained as follows :

- Step 1 : Select zeros of the compensator by defining the matrix D in eqn. (2.15) and augment the system equations as given in eqn. (2.17).
- Step 2 : Construct matrix s of eqn. (2.24) for different values of t and from the condition given in eqn. (2.27) find out minimum value of t , the number of unassigned closed-loop poles.
- Step 3 : Solve eqn. (2.26) for q (i.e., $q_1 \ q_2 \dots q_t$) and find out the locations of unassigned closed-loop poles.
- Step 4 : From eqn. (2.24) evaluate the feedback gain vector K_m
- Step 5 : Calculate the parameters of dynamic compensator: gain and poles in terms of K_m and D as given in eqn. (A.9) of Appendix A.

has a desired set of poles. The k th order compensator has the form

$$F(s) = \frac{1}{\Delta_c(s)} [M_1(s) \dots M_r(s)] \quad (2.33)$$

where $M_i(s)$, $i = 1, \dots, r$ are polynomials of degree k and $\Delta_c(s)$ is the characteristic polynomial of $F(s)$.

If $\Delta_d(s)$ is the closed-loop characteristic polynomial with the desired set of poles, then the basic equation which relates the parameters of compensator (i.e., coefficients of $\Delta_c(s)$ and $M_i(s)$, $i = 1, \dots, r$) and the desired locations of closed-loop poles is [66]

$$\Delta_d(s) = \Delta_o(s) \Delta_c(s) + \sum_{i=1}^r N_i(s) M_i(s) \quad (2.34)$$

If q is the number of specified closed-loop poles with $0 < q \leq n+k$ and $t = (n+k-q)$ is the number of unspecified poles, then $\Delta_d(s)$ can be expressed as

$$\Delta_d(s) = (s^q + d_1 s^{q-1} + \dots + d_q)(s^t + e_1 s^{t-1} + \dots + e_t) \quad (2.35)$$

where d_i , $i = 1, \dots, q$ are known and e_i , $i = 1, \dots, t$ are unknown. Equating the coefficients of like power of s in eqns. (2.34) and (2.35), we get

$$[X_k^i] p_k^i = \delta_k^i \quad (2.36)$$

where X_k^i , p_k^i and δ_k^i are defined in eqn. (B.23) of Appendix B.

Eqn. (2.36) is a set of $(n+k)$ equations in $[r(k+1) + k+t]$ unknowns. Vector p_k^i contains the parameters of $F(s)$ and the coefficients of the polynomial of unassigned closed-loop poles. The solution of eqn. (2.36) gives the desired compensator and the location of unassigned closed-loop poles. Two questions can be asked at this stage.

- (1) For the system defined by eqns. (2.28) and (2.29), what should be the minimum order of the compensator (i.e., the minimum value of k), which assigns all closed-loop poles (i.e., $q = n+k$)?
- (2) For a given value of k , how many poles can be assigned?

The answer to these questions can be obtained from the necessary and sufficient condition given in eqn. (B.15), Appendix B, for existence of solution to the pole assignment problem, whether it is partial or full assignment :

$$\text{Rank}[X_k^i] = \text{Rank}[X_k^i, \delta_k^i] \quad (2.37)$$

2.3.2.2 Algorithm

The following steps are to be followed for the design of output feedback compensator to assign closed-loop poles.

Step 1 : Construct the $(r \times 1)$ open-loop transfer function matrix $G(s)$

Step 2 : If k is specified, determine the maximum value of q for which eqn. (2.37) is satisfied by defining d_1, d_2, \dots, d_q in eqn. (2.39).

Step 3 : If q is specified, determine minimum value of k for which eqn. (2.37) is satisfied.

Step 4 : Solve eqn. (2.36) for p'_k to get the parameters of $F(s)$ and locations of unassigned closed-loop poles.

2.3.3 Design of Optimal Controller for Output Feedback Systems

2.3.3.1 Formulation of Control Problem

Consider the linear, time-invariant, controllable and observable systems

$$p \underline{x} = [A] \underline{x} + [B] \underline{u} \quad (2.38)$$

and
$$\underline{y} = [C] \underline{x} \quad (2.39)$$

where $\underline{x} \in R^n$, $\underline{u} \in R^m$ and $\underline{y} \in R^r$ are respectively vectors of state input and output variables. The problem is to design a controller using output feedback with control law of the form

$$\underline{u} = -[K] \underline{y} \quad (2.40)$$

such that a quadratic cost function

$$J = \int_0^{\infty} (\underline{x}^t Q \underline{x} + \underline{u}^t R \underline{u}) dt \quad (2.41)$$

is minimized, where Q is a constant $n \times n$ positive semi-definite matrix and R is a constant $m \times m$ positive definite matrix. From eqns. (2.38) to (2.40), the closed-loop system and the cost function can be expressed as

$$p \underline{x} = [A_c] \underline{x} \quad (2.42)$$

and

$$J = \int_0^{\infty} \underline{x}^t (Q + C^t K^t R K C) \underline{x} dt \quad (2.43)$$

where

$$A_c = A - BKC$$

As the solution of eqn. (2.42) depends on the initial state $x(0)$, the cost function J given by eqn. (2.43) is a function of $x(0)$. The dependence of cost on $x(0)$ can be eliminated by assuming the initial state to be a random variable uniformly distributed on the surface of n -dimensional unit sphere [53]. With this assumption, the problem is reduced to the determination of the optimal feedback matrix K which minimizes the cost function

$$J = \text{trace } [S] \quad (2.44)$$

where S is the cost matrix and is the unique positive definite solution of Liapunov equation

$$A_c^t S + S A_c + (Q + C^t K^t R K C) = 0 \quad (2.45)$$

Derivation of eqns. (2.44) and (2.45) is given in Appendix C. Defining the Hamiltonian [54] corresponding to eqns. (2.44) and (2.45) as

$$H = \text{trace } [S] + \text{trace}[P^t(A_c^t S + S A_c + Q + C^t K^t R K C)] \quad (2.46)$$

the following necessary conditions are obtained for minimum value of J [54] :

(1) Eqn. (2.45)

$$(2) \quad P A_c^t + A_c P + I = 0 \quad (2.47)$$

$$(3) \quad \frac{\partial H}{\partial K} = 2(RKPC^t - D^t SPC^t) = 0 \quad (2.48)$$

Appendix C gives an iterative procedure, utilising the above necessary conditions for optimality, to determine the optimal feedback matrix K.

2.3.4 Comparison of Methods

The design objective in the first two techniques presented here is the same : to assign poles of the closed-loop system. In both techniques, relationship between compensator parameters and closed-loop poles is used to obtain compensator parameters. No trial and error method is to be applied as in the case of classical control theory.

In the first technique zeros of the compensators are specified. For a second order single input compensator, (i.e. with one accessible state), three parameters, namely, gain and two poles of the compensator are to be obtained. Since zeros of compensator are specified apriori, the design does not utilize full freedom and is therefore restricted.

In the second technique no restriction is placed on the parameters of compensator. For a second order single input compensator all the five parameters - gain, poles and zeros are to be determined. This results in a less restrictive design and more closed-loop poles can be assigned in comparison with the first technique.

The third technique is based on parameter optimization where parameters of compensator are determined to minimize a quadratic performance index. The selection of proper locations of closed-loop poles, which is a difficult task in a practical system, is not required here. Closed-loop poles are assigned to stable locations in the process of optimization. If it is desired to define a sector for closed-loop poles, then the technique can be modified to solve the constrained optimization problem.

2.4 NUMERICAL EXAMPLE

The example of a single-machine connected to an infinite bus, given in Sec. 2.2.2.4, is considered. PSS are designed for this system with the three techniques suggested in Sec. 2.3. Neglecting the washout and filter stage in Fig. 2.4, the transfer function of a practical PSS used in power industry can be given as :

$$F(s) = K_s \frac{(1+sT_1)(1+sT_3)}{(1+sT_2)(1+sT_4)} \quad (2.49)$$

which is equivalent to

$$F(s) = \frac{\theta_0 s^2 + \theta_1 s + \theta_2}{s^2 + \gamma_1 s + \gamma_2} \quad (2.50)$$

where

$$\theta_o = K_s \frac{T_1 T_3}{T_2 T_4}$$

$$\theta_1 = K_s \frac{(T_1 + T_3)}{T_2 T_4}$$

$$\theta_2 = \frac{K_s}{T_2 T_4}$$

$$\gamma_1 = \frac{T_2 + T_4}{T_2 T_4}$$

and

$$\gamma_2 = \frac{1}{T_2 T_4}$$

The corresponding output feedback matrix for the augmented system (machine and PSS) can be given as (see Appendix A).

$$[K] = \begin{bmatrix} \theta_o & \theta_2' & \theta_1' \\ 0 & 0 & 1 \\ 1 & -\gamma_2 & -\gamma_1 \end{bmatrix}$$

where $\theta_1' = \theta_1 - \theta_o \gamma_1$

and $\theta_2' = \theta_2 - \theta_o \gamma_2$

2.4.1 Design of PSS with Partial State Feedback

Change in rotor speed $\Delta\omega$, which is one of the state variables of the system is used as feedback signal. Zeros of

the PSS transfer function are specified as -1.5 and -2.5. A maximum of three closed-loop eigenvalues can be assigned by this technique to satisfy the condition given in eqn. (2.27). The desired locations of these three poles are selected as $-1 \pm j7.0$ and -2.0 . The feedback matrices K_1 and K_2 and the corresponding PSS transfer function are obtained as

$$[K_1^t \mid K_2^t] = [0.09146 \mid -2.37908 \quad -2.10896]$$

$$F(s) = \frac{0.09146 s^2 + 0.36584 s + 0.34298}{s^2 + 8.48804 s + 12.86115}$$

The remaining three closed-loop eigenvalues alongwith the assigned three are given in the first column of Table 2.2.

Table 2.2 Closed-Loop Eigenvalues of the System

	With Partial State Feedback	With Output Feedback	
		$q = 5$	$q = 3$
Desired Location of Eigenvalues	$-1 \pm j7.0$ -2.0	$-1 \pm j7.00$ -2.0 -1.0 -6.0	$-1.0 \pm j7.0$ -2.0
Location of Remaining Eigenvalues	$-4.18011 \pm j2.49997$ -46.47408	-46.26379	$-4.18012 \pm j2.49997$ -46.47409

2.4.2 Design of PSS with Output Feedback

2.4.2.1 Single Input Compensator

Change in rotor speed is used as output feedback signal. It can be seen from the condition of eqn. (2.37) that, with a second order PSS, at the most five closed-loop eigenvalues can be assigned. If zeros of PSS are specified as in Sec. 2.4.1, then a maximum of three closed-loop eigenvalues can be assigned. The following two cases are considered here :

- (a) Five closed-loop eigenvalues are assigned at $-1 \pm j7.0$, -1.0 , -2.0 and -6.0 and no restriction is placed on the zeros of PSS.
- (b) Zeros of PSS are specified at -1.5 and -2.5 as in Sec. 2.4.1 and three closed-loop eigenvalues are assigned at $-1.0 \pm j7.0$ and -2.0 .

The transfer function of PSS and the output feedback matrix for the above two cases are obtained as follows :

Case (a)

$$F(s) = \frac{0.06501 s^2 + 0.17175s - 1.22898}{s^2 + 6.91754 s + 3.23809}$$

$$[K] = \begin{bmatrix} 0.06501 & -1.43940 & -0.27798 \\ 0 & 0 & 1 \\ 1 & -3.23809 & -6.91754 \end{bmatrix}$$

Case (b)

$$F(s) = \frac{0.09146 s^2 + 0.36584 s + 0.34293}{s^2 + 8.48806 s + 12.86118}$$

$$[K] = \begin{bmatrix} 0.09146 & -0.83332 & -0.41048 \\ 0 & 0 & 1 \\ 1 & -12.86118 & -8.48806 \end{bmatrix}$$

The remaining closed-loop eigenvalues alongwith assigned closed-loop eigenvalues for the above two cases are respectively given in the second and third columns of Table 2.2.

2.4.2.2 Two Input Compensator

In the previous section it was observed that all the six closed-loop eigenvalues cannot be assigned with a single input second order PSS. At the most, five eigenvalues can be assigned and there is no control on the location of the remaining eigenvalue. All the eigenvalues of the system can be assigned either by using a compensator of higher order or by using a two input compensator. In order to avoid the complexities of increasing the size of closed-loop system, two input compensator is designed. Rotor speed was used as the control signal for PSS design in the previous sections. The second signal for the two input compensator is selected as the terminal voltage of the generator. The block diagram of the system with two input compensator is shown in Fig. 2.5.

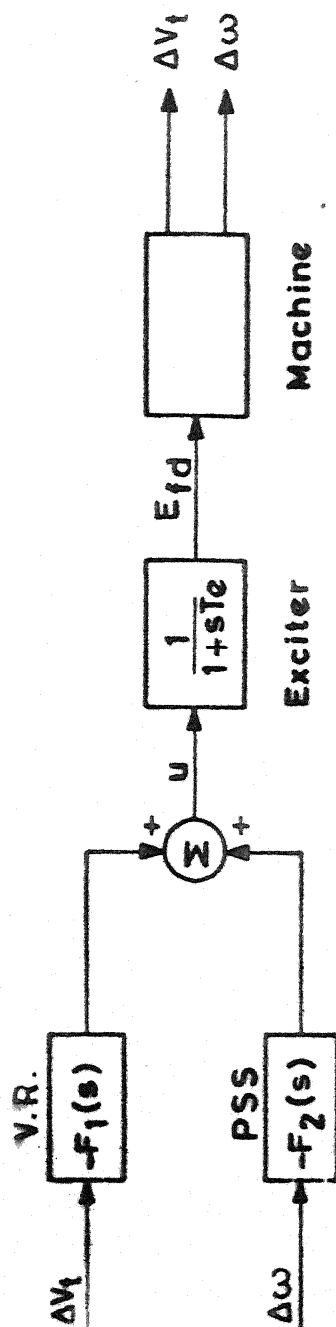


FIG. 2.5 BLOCK DIAGRAM OF ALTERNATOR WITH TWO INPUT CONTROLLER.

Synchronous machine is represented by the model discussed in Sec. 2.2.2. The excitation system used here is shown in Fig. 2.5 with the value of T_e as 0.005 sec. Machine and line parameters and system operating conditions are the same as in the previous section. The matrices A,B and C obtained are as follows :

$$[A] = \begin{bmatrix} 0 & -35.36912 & -26.43598 & 0 \\ 1 & 0 & 0 & 0 \\ 0 & -0.13571 & -0.35072 & 0.15873 \\ 0 & 0 & 0 & 200.0 \end{bmatrix}$$

$$b = [0 \quad 0 \quad 0 \quad 200.0]^t$$

$$[C] = \begin{bmatrix} 0 & 0.20863 & -0.54971 & 0 \\ 1 & 0 & 0 & 0 \end{bmatrix}$$

The open-loop eigenvalues of the system are given in the first column of Table 2.3. The desired locations of closed-loop eigenvalues are given in the second column of Table 2.3.

Table 2.3 Eigenvalues of the System with Two Input Compensator

Open-loop Eigenvalues	Closed-loop eigenvalues
$-0.05063 \pm j5.94486$	$-1.05 \pm j5.945$
-0.249466	-1.25
-200.00	-200.00
	-5.00
	-10.00

The two input compensator is designed using the technique given in Sec. 2.3.2 with $r = 2$. The parameters of the two input compensator to be determined are : $\theta_{10}, \theta_{11}, \theta_{12}, \theta_{20}, \theta_{21}, \theta_{22}, \gamma_1$ and γ_2 . In this case eqn. (2.36) is a set of six equations in eight unknown parameters of the compensator. To satisfy the condition given in eqn. (2.41), two parameters are to be specified. Let both the poles of the compensator be placed at -10. The transfer functions of the two input compensator are obtained as

$$F_1(s) = \frac{0.95406 s^2 + 197.9891 s + 394.4889}{s^2 + 20.0 s + 100}$$

$$F_2(s) = \frac{0.05621 s^2 + 20.28683 s + 277.2835}{s^2 + 20.0 s + 100.0}$$

The results are discussed in Sec. 2.4.5.

2.4.3 Design of PSS with Parameter Optimization

Low frequency electromechanical oscillations have detrimental effect on the dynamic stability of power systems, particularly in systems having long transmission lines. This is due to the continuous variation of rotor angles which in turn results in fluctuations in power output of the generators leading to fluctuation of power in transmission lines. Thus, damping of rotor oscillations which is the basic function of a PSS can be viewed as the minimization of fluctuation in power output of machine.

PSS of the form given in eqn. (2.50) is designed using the parameter optimization technique given in Sec. 2.3.3.

2.4.3.1 Representation of Fluctuation in Power Output of Generator

The electrical power output of machine in per unit can be obtained from eqn. (2.4) as

$$P_e = x'_d (I_d - \xi i_d) i_q \quad (2.51)$$

Linearizing eqn. (2.51) and substituting the values of Δi_q and Δi_d from eqn. (2.10), we get

$$\Delta P_e = K_5 \Delta I_d + K_6 \Delta \delta \quad (2.52)$$

where

$$K_5 = x'_d [i_{q0} + K_1(I_{d0} - \xi i_{d0}) - K_3 \xi i_{q0}]$$

and

$$K_6 = x'_d [K_2(I_{d0} - \xi i_{d0}) - K_4 \xi i_{q0}]$$

Eqn. (2.52) can also be written as

$$\Delta P_e = [T] \underline{x} \quad (2.53)$$

where $[T] = [0 \quad K_6 \quad K_5 \quad 0]$

For the example considered matrix T is given as

$$T = [0 \quad 0.91570 \quad 0.40344 \quad 0]$$

The cost function, defined by eqn. (2.41) will take the form as

$$J = \int_0^{\infty} \Delta P_e^2 dt \quad (2.54)$$

or

$$J = \int_0^{\infty} \underline{x}^t Q \underline{x} dt$$

where

$$Q = [T]^t [T]$$

To start the optimization routine, PSS obtained in Sec. 2.4.2.1 case (a) is selected. The value of performance index obtained with this PSS is 0.88535. The optimum value of performance index is obtained as 0.26852 and the corresponding PSS transfer function and feedback gain matrix are obtained as :

$$F(s) = \frac{0.25648 s^2 + 0.67334 s + 0.48338}{s^2 + 6.81412 s + 3.23453}$$

$$[K] = \begin{bmatrix} 0.25648 & -0.34571 & -1.07434 \\ 0 & 0 & 1 \\ 1 & -3.23453 & -6.81412 \end{bmatrix}$$

The eigenvalues of the closed-loop system with the above PSS are given in the first column of Table 2.4.

Table 2.4 Closed-Loop Eigenvalues of the System

With Parameter Optimization Technique	With Classical Control Theory
-0.48070	-3.20609
-2.02667 \pm j9.90360	-3.57405 \pm j12.64363
-2.43789 \pm j2.37399	-1.42775 \pm j3.05105
-47.65056	-49.13654

2.4.4 Design of PSS with Classical Control Theory

The performance of the stabilizers designed in Secs. 2.4.1 to 2.4.3 and the stabilizer used in power industry is compared by designing PSS using classical control approach of Larsen and Swann[26]. As per recommendations given in [26], PSS utilizing speed signal should be designed at full load conditions and for strong systems (i.e., with low value of transmission line reactance). Thus, $X_T = 0.2$ p.u. is considered.

The design of PSS involves determination of gain and time constants of two lead/lag stages in Fig. 2.4. Usually two identical lead/lag stages are used with $T_3 = T_1$ and $T_4 = T_2$. The ratio $n_t = T_1/T_2$, known as band spread, varies from 2 to 10 depending upon the requirement of phase compensation. Thus, PSS design reduces to the determination of gain

K_s , band spread n_t and the time constant T_1 . The values of these parameters are (see Appendix E) :

$$n_t = 3$$

$$T_1 = 0.5 \text{ sec.}$$

$$K_s = 0.05$$

and the corresponding PSS transfer function is

$$F(s) = \frac{0.45 s^2 + 1.8 s + 1.8}{s^2 + 12.0 s + 36.0}$$

Eigenvalues of the closed-loop system with this PSS are given in the second column of Table 2.4.

To compare the performance of stabilizers, time response of $\Delta\delta$, ΔP_e and $\Delta\omega$ are obtained for unit step change in the reference voltage when machine is equipped with the following stabilizers :

- (1) PSS-1, obtained in Sec. 2.4.1
- (2) PSS-2, obtained in Sec. 2.4.2.1 case (a)
- (3) PSS-3, obtained in Sec. 2.4.3, and
- (4) PSS-4, obtained in Sec. 2.4.4.

The responses are obtained for full load and half full load conditions at 0.9 power factor lagging and are given in Figs. 2.6 to 2.8.

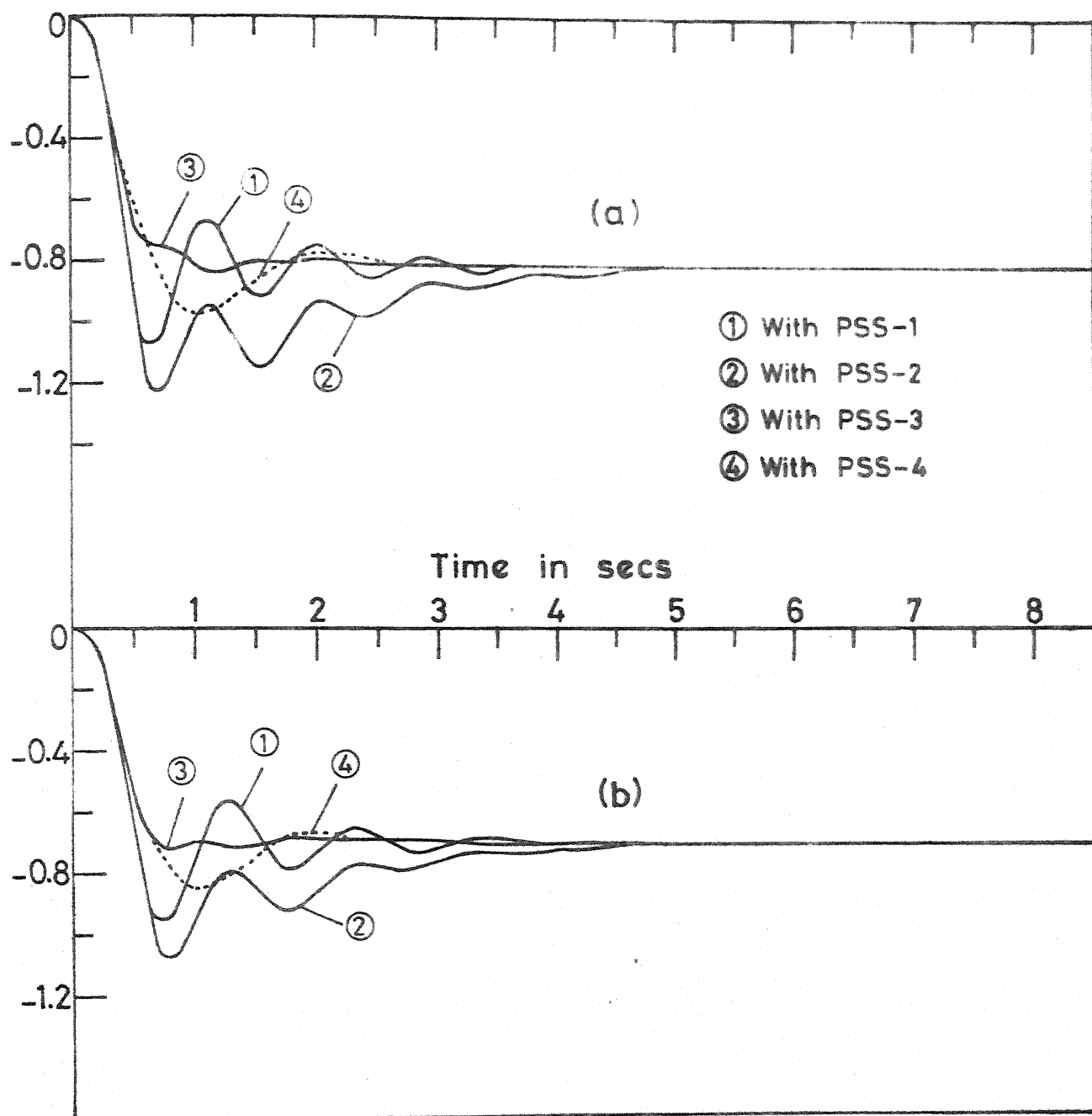


FIG. 2.6 RESPONSE OF $\Delta\delta$ FOR $\Delta V_{ref} = 1.0$ p.u.
(a) AT FULL LOAD (b) AT HALF FULL LOAD.

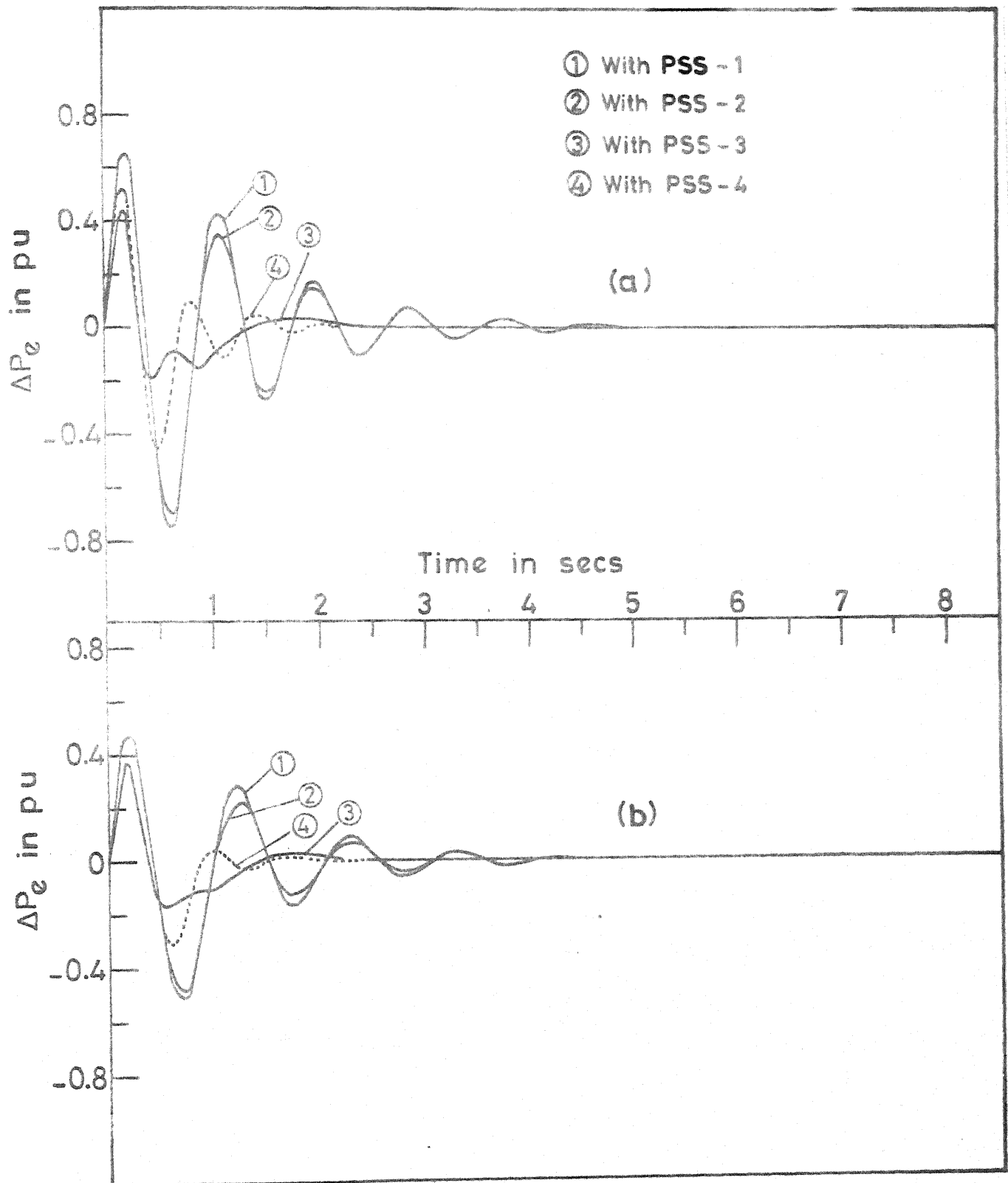


FIG. 2.7 RESPONSE OF ΔP_e FOR $\Delta V_{ref} = 1.0$ pu
(a) AT FULL LOAD (b) AT HALF FULL LOAD.

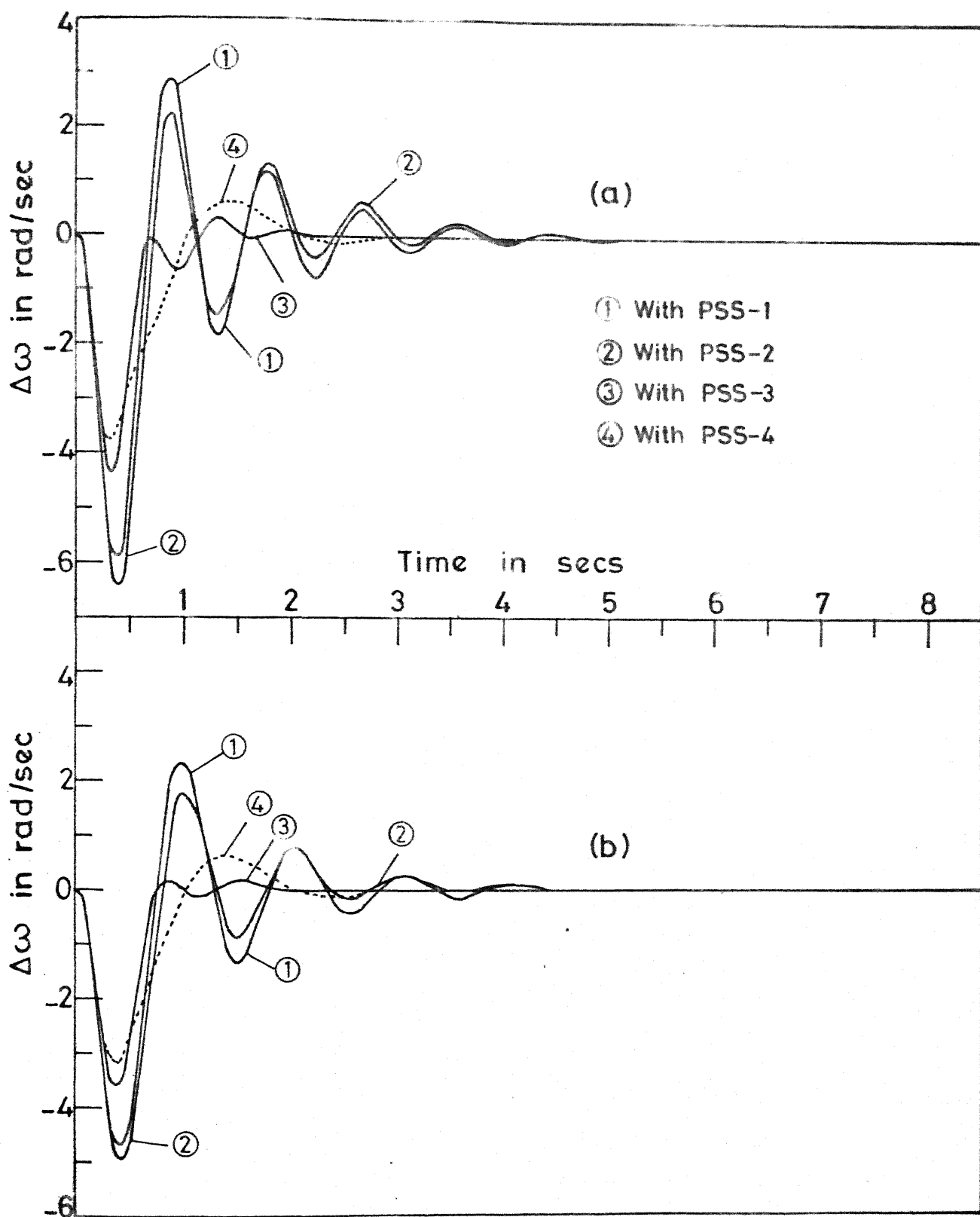


FIG.2.8 RESPONSE OF $\Delta\omega$ FOR $\Delta V_{ref} = 1.0$ pu
(a) AT FULL LOAD (b) AT HALF FULL LOAD.

2.4.5 Discussion of Results

The first design technique, based on modal control theory with partial state feedback is restricted, since PSS zeros have to be specified apriori and consequently full design freedom is not utilized. However, the technique is able to assign the dominant modes of rotor oscillation without significant shift of non-dominant eigenvalues.

The second technique with output feedback is less restrictive as the number of closed-loop poles that can be assigned is more in comparison with the first design technique. If zeros of PSS are specified, the same results are obtained (see first and third columns of Table 2.2 and PSS transfer functions given in Secs. 2.4.1 and 2.4.2.1 case (b)). With two input compensator it is possible to assign all closed-loop eigenvalues.

The third technique, based on parameter optimization, minimizes the fluctuations in power output of the generator. Responses of ΔP_e , $\Delta \delta$ and $\Delta \omega$ of the power system, with the various PSS designed, are shown in Figs. 2.6 to 2.8. It should be noted that there is no justification for comparing the responses to judge the superiority of any one design over the others, since the design objective is different in different cases. However, we wish to draw attention to the appropriateness of PSS-3, if the main concern is reduction of

power fluctuations following system disturbance, as is clear from the responses of ΔP_e shown in the figures.

Responses of ΔP_e , $\Delta \delta$ and $\Delta \omega$ with PSS-4 is better than those obtained with PSS-1 and PSS-2. But this does not reflect the superiority of the PSS designed using classical control theory over PSS designed using pole assignment techniques, because one can always assign poles to the same locations by first two techniques as obtained with PSS-4. The result shows the importance of selecting proper locations of closed-loop poles.

2.5 CONCLUSIONS

In this chapter a basic system model, in the state-space form, of a single machine infinite bus power system, is developed for the design of PSS. Three techniques for dynamic compensator design are presented. These techniques are successfully applied to a single machine infinite bus system example and the relevant numerical results are presented. Pole assignment is directly related to the design objective, of providing damping torque, used in power industries [6]. However, it may sometimes be difficult to choose proper pole locations which result in satisfactory system performance. The technique based on parameter optimization to minimize a given performance index has the advantage that it permits

minimization of power fluctuations at the output of the generator, following system disturbance. The method, thus, provides direct control on an important aspect of system performance. Indeed, the problem of power system dynamic stability is associated primarily with swinging of machine rotors and the consequent power fluctuations at the output of generators.

CHAPTER 3

INFLUENCE OF GENERATOR MODELLING ON PSS DESIGN

3.1 INTRODUCTION

In the previous chapter, a simplified model of the synchronous machine, neglecting the effect of amortisseur circuits, was considered for the design of PSS. Most of the literature available on the design of PSS utilizes the simplified model of synchronous machine neglecting the effect of damper windings. A detailed study on the adequacy of this simplified representation of synchronous machine, however, is not reported. The main objective of this chapter is to investigate the adequacy of the simplified machine model.

A single machine infinite bus system is considered to analyse the effect of the machine modelling on the design of power system stabilizers. A sixth order model of synchronous machine [73], with three amortisseur circuits, is considered for the detailed representation of machine. A comparison of simplified and detailed representation of synchronous machine is made by evaluating the effect of modelling details on (a) open-loop system behaviour and (b) characteristics of PSS designed for both representations of the machine. Adequacy of the simplified representation of machine is analysed by employing PSS, designed for lower order model, to the machine

represented in detail. Eigenvalue and time-domain analysis of the closed-loop system are carried out for this purpose.

3.2 FORMULATION OF SYSTEM MODEL

The single-machine infinite-bus system of Fig. 2.1 is considered. For detailed representation of synchronous machine, three amortisseur windings, as shown in Fig. D.2, are considered. The current source model of Ref. [78] with some modification, discussed in Appendix D, is utilized for the representation of synchronous machine. A single time constant excitation system of Fig. 2.3 is considered. Turbine and governor dynamics are ignored and it is assumed that the machine stator and the external network are in quasi-steady state. Dynamical equations of machine and excitation system (whose derivation is given in Appendix D) are as follows :

$$p\omega = \frac{1}{M} (T_m - T_e) - \frac{K_D}{M} (\omega - \omega_0) \quad (3.1)$$

$$p\delta = (\omega - \omega_0) \quad (3.2)$$

$$pI_d = C_1 I_d + C_3 \Psi_f + C_{11} i_d + C_9 E_{fd} \quad (3.3)$$

$$pI_q = C_2 I_q + C_4 \Psi_k + C_{12} i_q \quad (3.4)$$

$$p\Psi_f = C_5 I_d + C_7 \Psi_f + C_{13} i_d + C_{10} E_{fd} \quad (3.5)$$

$$p\Psi_k = C_6 I_q + C_8 \Psi_k + C_{14} i_q \quad (3.6)$$

$$pE_{fd} = -\frac{1}{T_R} E_{fd} + \frac{K_R}{T_R} (V_{ref} - V_t + u') \quad (3.7)$$

where C_1, C_2, \dots, C_{14} are functions of machine inductances and resistances; and are defined in Appendix D. Electrical torque, T_e , is given as

$$T_e = L_d'' (I_d i_q - I_q' i_d) \quad (3.8)$$

where

$$I_q' = I_q + \xi i_q \quad (3.9)$$

$$\xi \triangleq 1 - L_q''/L_d''$$

Eqn. (3.9) represents subtransient saliency. The equivalent circuit of the system is shown in Fig. 3.1. The non-state variables i_d, i_q and V_t in eqns. (3.1) to (3.8) are eliminated by representing them in terms of state variables.

From Fig. 3.1, the armature current phasor \hat{i}_m can be expressed as

$$\hat{i}_m = \frac{j x_d''}{Z_{eq} + j x_d''} \hat{I} - \frac{1}{Z_{eq} + j x_d''} \hat{V}_{eq} \quad (3.10)$$

Substituting the values of \hat{I} , \hat{V}_{eq} and Z_{eq} from Fig. 3.1 in eqn. (3.10) and separating real and imaginary parts, we get

$$i_q = \frac{1}{1-\xi a_1} [a_1 I_q + a_2 I_d - V_{eq} (b_1 \cos \delta + b_2 \sin \delta)] \quad (3.11)$$

$$i_d = (a_1 - \frac{a_2^2 \xi}{1-\xi a_1}) I_d - \frac{a_2}{1-a_1 \xi} I_q + \frac{\xi a_2}{1-a_1 \xi} V_{eq} (b_1 \cos \delta + b_2 \sin \delta) \\ + V_{eq} (b_2 \cos \delta - b_1 \sin \delta) \quad (3.12)$$

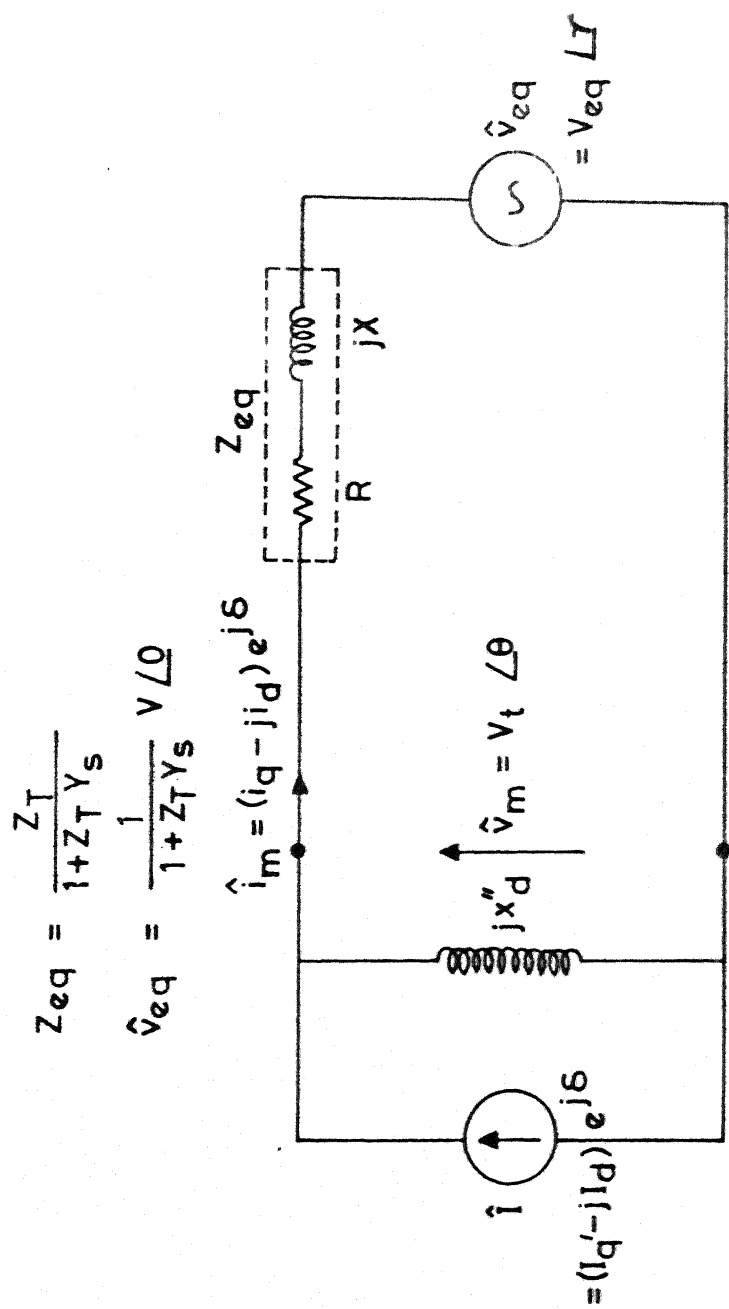


FIG.3.1 SINGLE PHASE EQUIVALENT CIRCUIT OF THE SYSTEM GIVEN IN FIG.2.1 .

where

$$a_1 + ja_2 \triangleq \frac{jx_d''}{R + j(X + x_d'')}$$

$$b_1 + jb_2 \triangleq \frac{\cos\gamma + js\sin\gamma}{R + j(X + x_d'')}$$

The terminal voltage V_t can be expressed as :

$$V_t = (v_d^2 + v_q^2)^{1/2} \quad (3.13)$$

Park's components of terminal voltage can be obtained from the equivalent circuit of Fig. 3.1 as :

$$v_q = x_d''(I_d - i_d) \quad (3.14)$$

$$v_d = -x_d''[I_q + (\xi - 1)i_q] \quad (3.15)$$

The state-space model is derived by linearizing eqns.(3.1) to (3.8). The non-state variables Δi_d , Δi_q and ΔV_t are eliminated using the following expressions which are obtained by linearizing eqns. (3.11), (3.12) and (3.13)

$$\Delta i_q = K_1 \Delta I_d + K_2 \Delta I_q + K_3 \Delta \delta$$

$$\Delta i_d = K_4 \Delta I_d + K_5 \Delta I_q + K_6 \Delta \delta$$

$$\Delta V_t = K_7 \Delta I_d + K_8 \Delta I_q + K_9 \Delta \delta$$

where

$$K_1 \triangleq \frac{a_2}{1 - a_1 \xi}, \quad K_2 \triangleq \frac{a_1}{1 - a_1 \xi}, \quad K_3 \triangleq \frac{V_{eq}}{1 - a_1 \xi} (b_1 \sin \delta_o - b_2 \cos \delta_o)$$

$$K_4 \triangleq (a_1 - \frac{a_2^2 \xi}{1-a_1 \xi}), \quad K_5 \triangleq -\frac{a_2}{1-a_1 \xi}$$

$$K_6 \triangleq V_{eq} [-(b_2 + b_1 \frac{a_2 \xi}{1-a_1 \xi}) \sin \delta_o - (b_1 - b_2 \frac{a_2 \xi}{1-a_1 \xi}) \cos \delta_o]$$

$$K_7 \triangleq \frac{x_d''}{V_{to}} [v_{do} K_1 (1 - \xi) + v_{qo} (1 - K_4)]$$

$$K_8 \triangleq \frac{x_d''}{V_{to}} [v_{do} \{K_2 (1 - \xi) - 1\} - v_{qo} K_5]$$

and

$$K_9 \triangleq \frac{x_d''}{V_{to}} [v_{do} K_3 (1 - \xi) - v_{qo} K_6]$$

The resulting seventh order model of the system is described by the state equations

$$p \underline{x} = [A] \underline{x} + \underline{b} u \quad (3.16)$$

where

$$\underline{x} \triangleq [\Delta \omega \quad \Delta \delta \quad \Delta I_d \quad \Delta I_q \quad \Delta \Psi_f \quad \Delta \Psi_k \quad \Delta E_{fd}]^t$$

and

$$u \triangleq \Delta u'$$

The matrix A and the vector b are as follows

$$[A] = \begin{bmatrix} a_{11} & a_{12} & a_{13} & a_{14} & 0 & 0 & 0 \\ 1 & 0 & 0 & 0 & 0 & 0 & 0 \\ 0 & a_{32} & a_{33} & a_{34} & a_{35} & 0 & a_{37} \\ 0 & a_{42} & a_{43} & a_{44} & 0 & a_{46} & 0 \\ 0 & a_{52} & a_{53} & a_{54} & a_{55} & 0 & a_{57} \\ 0 & a_{62} & a_{63} & a_{64} & 0 & a_{66} & 0 \\ 0 & a_{72} & a_{73} & a_{74} & 0 & 0 & a_{77} \end{bmatrix}$$

$$\underline{b} = [0 \quad 0 \quad 0 \quad 0 \quad 0 \quad 0 \quad b_7]^t$$

where

$$a_{11} = -K_D/M$$

$$a_{12} = \frac{x_d''}{M} (K_6 I'_{q0} - K_3 I_{d0} + K_3 \xi i_{d0})$$

$$a_{13} = \frac{x_d''}{M} (-i_{q0} + K_4 I'_{q0} - K_1 I_{d0} + K_1 \xi i_{d0})$$

$$a_{14} = \frac{x_d''}{M} (i_{d0} + K_5 I'_{q0} - K_2 I_{d0} + K_2 \xi i_{d0})$$

$$a_{32} = K_6 C_{11} ; \quad a_{33} = C_1 + K_4 C_{11} ; \quad a_{34} = K_5 C_{11}$$

$$a_{35} = C_3 ; \quad a_{37} = C_9$$

$$a_{42} = K_3 C_{12} ; \quad a_{43} = K_1 C_{12} ; \quad a_{44} = C_2 + K_2 C_{12} ; \quad a_{46} = C_4$$

$$a_{52} = K_6 C_{13} ; \quad a_{53} = C_5 + K_4 C_{13} ; \quad a_{54} = K_5 C_{13}$$

$$a_{55} = C_7 ; \quad a_{57} = C_{10}$$

$$a_{62} = K_3 C_{14} ; \quad a_{63} = K_1 C_{14} ; \quad a_{64} = C_6 + K_2 C_{14} ; \quad a_{66} = C_8$$

$$a_{72} = -\frac{K_R}{T_R} K_9 ; \quad a_{73} = -\frac{K_R}{T_R} K_7$$

$$a_{74} = -\frac{K_R}{T_R} K_8 ; \quad a_{77} = -\frac{1}{T_R}$$

$$b_7 = \frac{K_R}{T_R}$$

3.3 EIGENVALUE ANALYSIS

In order to investigate the effect of modelling details on dynamic stability, eigenvalues of system matrix are calculated when the machine is represented by (i) a simplified model and (ii) a detailed model. The simplified model is obtained by neglecting amortisseur windings. This results in a third order machine model as developed in Chapter 2. The detailed model considers three amortisseur windings and results in a sixth order model as discussed in previous section. For both models a single time constant excitation system, as shown in Fig. 2.3, is considered.

3.3. 1 Numerical Example

The single machine infinite bus system example of Chapter 2 is considered for analysis. Machine parameters, with usual notations in per unit on machine base, for the detailed representation are as follows :

$$x_d = 1.72 \quad ; \quad x'_d = 0.45 \quad ; \quad x''_d = 0.33$$

$$x_q = 1.68 \quad ; \quad x'_q = 0.59 \quad ; \quad x''_q = 0.33$$

$$x_c = 0.33$$

$$T'_{do} = 6.3 \text{ sec.} \quad ; \quad T''_{do} = 0.033 \text{ sec.}$$

$$T'_{qo} = 0.43 \text{ sec.} \quad ; \quad T''_{qo} = 0.033 \text{ sec.}$$

$$H = 4.0 \text{ sec.}$$

x_c is the armature leakage reactance.

Excitation System Parameters : $K_R = 50$; $T_R = 0.02$ sec.

System Parameters and Operating Data (in p.u.) :

Transmission line (Fig. 2.1) : $R_T = 0.024$; $X_T = 0.6$.
(on machine base)

$G_S = 0.$; $B_S = 0.066$

Infinite bus voltage = $1.0 \angle 0^\circ$

Generation = 1.0 p.u. at 0.9 lagging power factor (i.e.

$$S_t = 0.9 + j0.43589).$$

Data of Equivalent Circuit : $R = 0.02602$; $X = 0.62470$

$$V_{eq} = 1.04123 \angle -0.0945^\circ$$

Eigenvalues of the system matrix, for both lower and higher order models, are computed for variation in the following three parameters of the system :

- (1) Machine Loading - Machine loading is varied from 0.25 p.u. to 1.0 p.u. at constant power factor of 0.9 lagging.
- (2) Inertia constant - Following three values of H are taken :
(a) 2.0 sec., (b) 4.0 sec. (nominal value) and (c) 6.0 sec.
- (3) Voltage regulator - Following three values of K_R are taken:
gain
(a) 25, (b) 50 (nominal value) and
(c) 100.

. Loci of the complex eigenvalue corresponding to the rotor oscillation mode are given in Fig. 3.2. Remaining eigenvalues of the system are given in Tables 3.1 to 3.3 for variations in the machine loading, inertia constant and the voltage regulator gain.

Table 3.1 Open-Loop Real Eigenvalues for Variation in Machine Loading

S_t (p.u.) M/c Model	1.00	0.75	0.50	0.25
Lower	-5.00647	-4.90288	-4.89002	-5.26300
	-45.75554	-45.52209	-45.25670	-44.97106
Higher	-2.73754	-2.48687	-2.27434	-2.08560
	-6.60439	-6.55367	-6.53043	-6.54077
	-24.73196	-24.26378	-23.71774	-23.10618
	-47.04315	-47.00341	-46.96310	-46.92039
	-55.75159	-55.97981	-56.22590	-56.48232

Table 3.2 Open-loop Real Eigenvalues for Variation in Inertia Constant

$H.(\text{sec.})$ M/c Model	2.0	4.0	6.0
Lower	-5.11354 -45.74099	-5.00647 -45.75554	-4.93739 -45.76051
Higher	-2.69351 -7.03917 -24.42457 -46.98191 -55.77214	-2.73754 -6.60439 -24.73196 -47.04315 -55.75159	-2.77947 -6.35397 -24.83933 -47.06425 -55.74454

Table 3.3 Open-loop Real Eigenvalues for Variation in Voltage Regulator Gain

K_R M/c Model	25	50	100
Lower	-2.56222 -47.97734	-5.00647 -45.75554	-10.49709 -40.35721
Higher	-2.11701 -4.01728 -29.94829 -47.03204 -53.38993	-2.73754 -6.60439 -24.73196 -47.04315 -55.75159	-2.91418 (-13.90742 $\pm j7.95523$) -47.05051 -59.24737

- Simplified model
- Detailed model

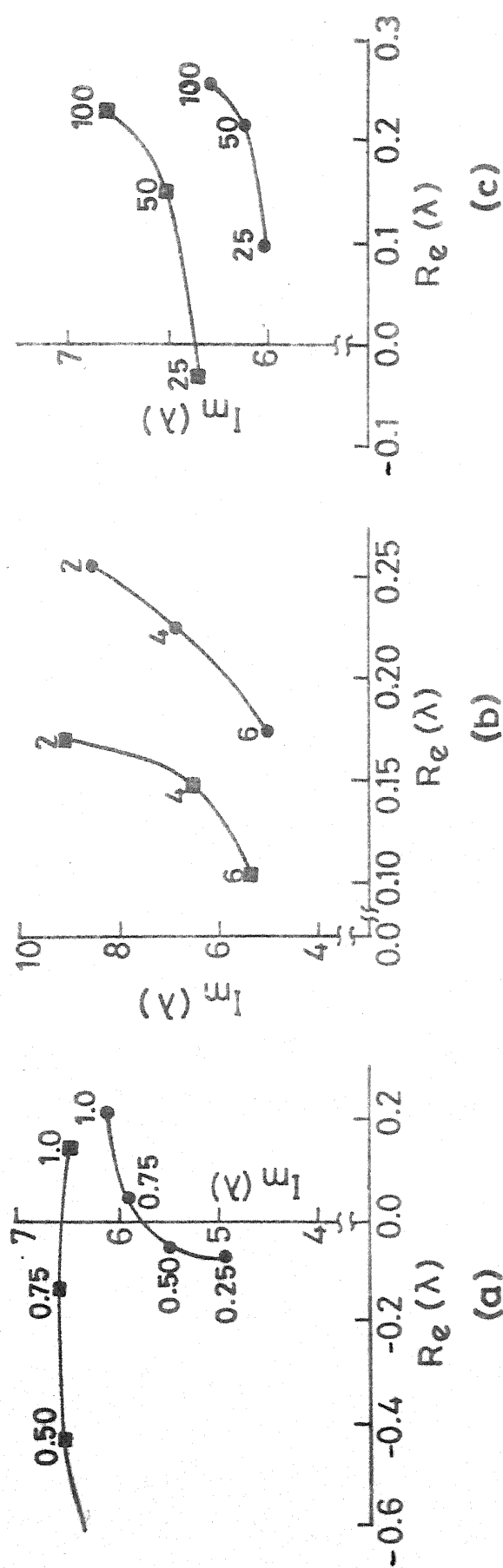


FIG. 3.2 LOCI OF OPEN-LOOP EIGENVALUE CORRESPONDING TO ROTOR OSCILLATION.

(a) Variation in machine loading.

(b) Variation in inertia constant.

(c) Variation in voltage regulator gain.

3.3.2 Discussion of Results

Inspection of Fig. 3.2 shows that the nature of eigenvalue loci is same in both representations of the machine for the variations in the parameters considered. More damping of rotor oscillation mode is observed in the detailed representation. This is to be expected because of the inclusion of amortisseur windings in the detailed model.

The effect of increasing the machine loading is to reduce the damping of the rotor oscillation mode. Reducing the inertia of the machine or increasing the voltage regulator gain have similar effects.

The frequency of the rotor oscillation mode is related to the synchronizing torque coefficient and the inertia, the frequency increases with reduction of inertia. Increasing the voltage regulator gain has the effect of increasing the synchronizing torque coefficient thereby increasing the frequency particularly at higher values of gain [6]. Increasing the loading on the machine has not much effect on the synchronizing torque coefficient because the increase in the internal voltage of the generator counteracts the effect of rotor angle. It is observed that the synchronizing torque coefficient is less with the simplified model. This is because of the fact that the synchronizing torque contributed by the amortisseur windings is neglected. This contribution is seemed to be significant particularly at light loads.

Non-oscillatory modes are not of much concern as long as they are sufficiently away in the left half of the complex plane and their variations are, therefore, not important. However, an inspection of Tables 3.1 to 3.3 shows that they are not affected much, in both representations, by load variation and variation in inertia constant. They vary with the variation in the voltage regulator gain as shown in Table 3.3. High voltage regulator gain in the detailed representation of machine shows an additional oscillatory mode. As this mode is highly damped, it will not effect much the stability of the system.

3.4 PSS DESIGN

To investigate the effect of modelling detail on the PSS characteristics, PSS are designed for both the representations of machine. Pole assignment technique, given in Sec. 2.4.2.1, is used for the design of PSS utilizing rotor speed as feedback signal. Variations in the following three parameters of the system are considered for PSS design :

- (1) Machine Loading - 1.0, 0.5 and 0.25p.u. loading at
0.9 lagging power factor
- (2) Inertia constant - 2.0, 4.0 and 6.0 sec.
- (3) Voltage regulator- 25, 50 and 100.
gain

A second order PSS with transfer function of the form

$$F(s) = \frac{\theta_o(s+z_1)(s+z_2)}{(s+p_1)(s+p_2)}$$

is designed for both representations of machine. The objective is same for each PSS design, namely, to assign five closed-loop poles to the specified locations. These are $-1.0 \pm j7.0$, -1.0 , -2.0 and -6.0 .

PSS parameters obtained for different machine loadings and for different values of inertia constant and voltage regulator gain are given respectively in Tables 3.4, 3.5 and 3.6. Frequency plots of the PSS transfer function for each case are given in Figs. 3.3 to 3.5.

Table 3.4 PSS Parameters for Variation in Machine Loading

Machine Loading	Model Order	θ_o	z_1	z_2	p_1	p_2
1.0	Lower	0.06501	-5.86475	3.22300	-6.41258	-0.50496
	Higher	0.11148	-7.67585	3.17181	-21.02139	-0.65124
0.50	Lower	0.11286	-6.06547	0.47719	-5.80205	-0.69254
	Higher	0.05374	-6.21340	1.45426	-7.91252	-0.78866
0.25	Lower	0.22691	-6.10750	-0.61723	-5.46609	-0.87463
	Higher	0.13097	-10.71719	-1.57561	-20.02707	-1.06966

Table 3.5 PSS Parameters for Variation in Inertia Constant

Inertia constant	Model Order	θ_o	z_1	z_2	p_1	p_2
2.0	Lower	0.03197	-11.27945	-6.18399	-5.77025	-0.27530
	Higher	-0.05000	-7.99723	-3.49388	-4.36127	-0.40832
4.0	Lower	0.06501	-5.86475	3.22300	-6.41258	-0.50496
	Higher	0.11148	-7.67585	3.17181	-21.02139	-0.65124
6.0	Lower	0.15799	-5.88597	-0.15379	-6.41940	-0.76093
	Higher	0.17414	-6.38861	-0.09334	-11.02523	-0.81156

Table 3.6 PSS Parameters for Variation in Voltage Regulator Gain

V.R. Gain	Model Order	θ_o	z_1	z_2	p_1	p_2
25	Lower	0.18051	-3.25016	0.65649	-8.50293	-0.77156
	Higher	0.16373	-2.34043	1.51371	-10.53550	-0.82940
50	Lower	0.06501	-5.86475	3.22300	-6.41258	-0.50496
	Higher	0.11148	-7.67585	3.17181	-21.02139	-0.65124
100	Lower	0.04863	-0.21972	$\pm j1.97548$	-1.03975	$\pm j0.62952$
	Higher	0.01952	-7.97605	9.07333	-6.82988	-0.52706

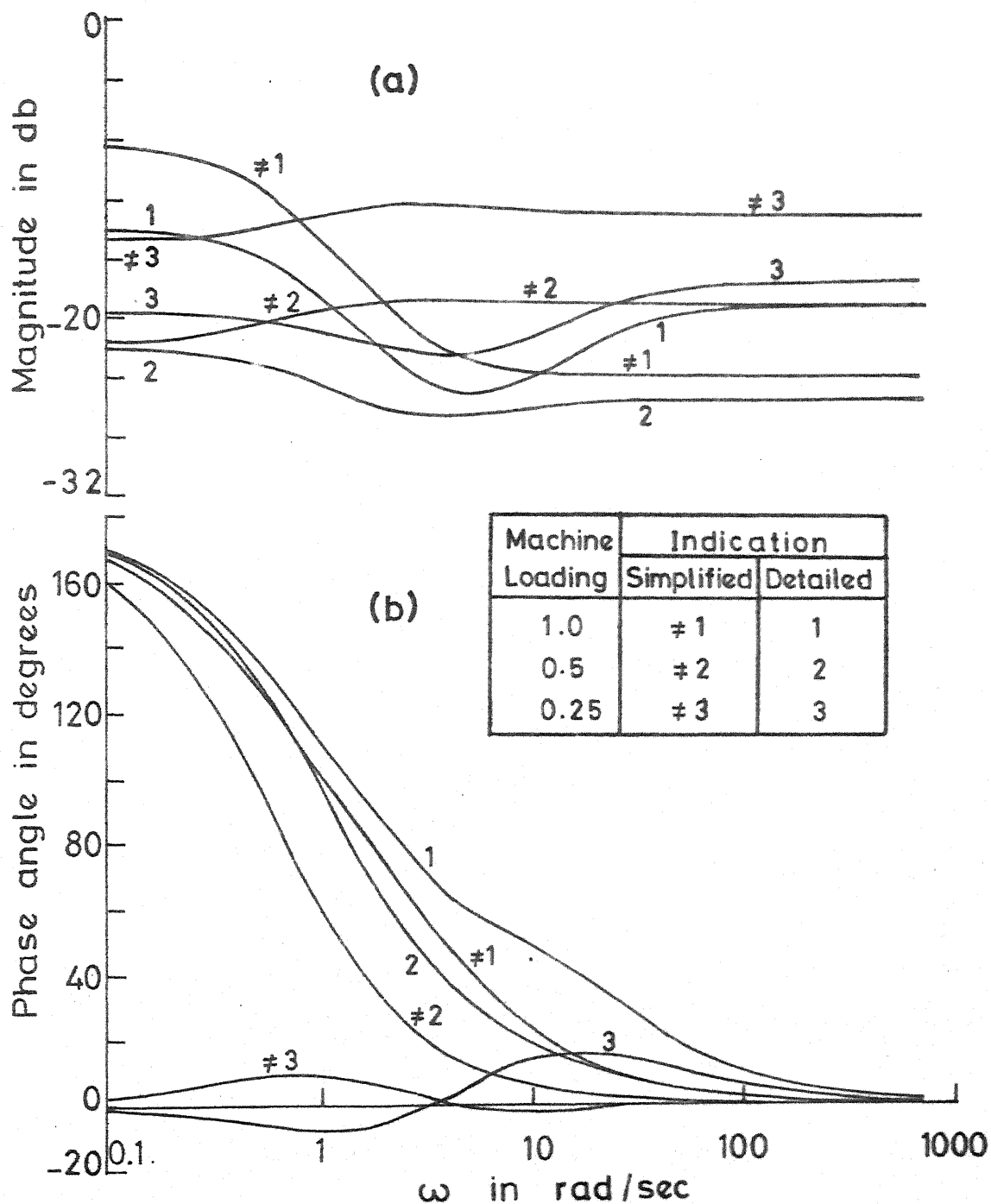


FIG.3.3 FREQUENCY PLOT OF PSS TRANSFER FUNCTION FOR VARIATION IN MACHINE LOADING
(a) MAGNITUDE (b) PHASE ANGLE

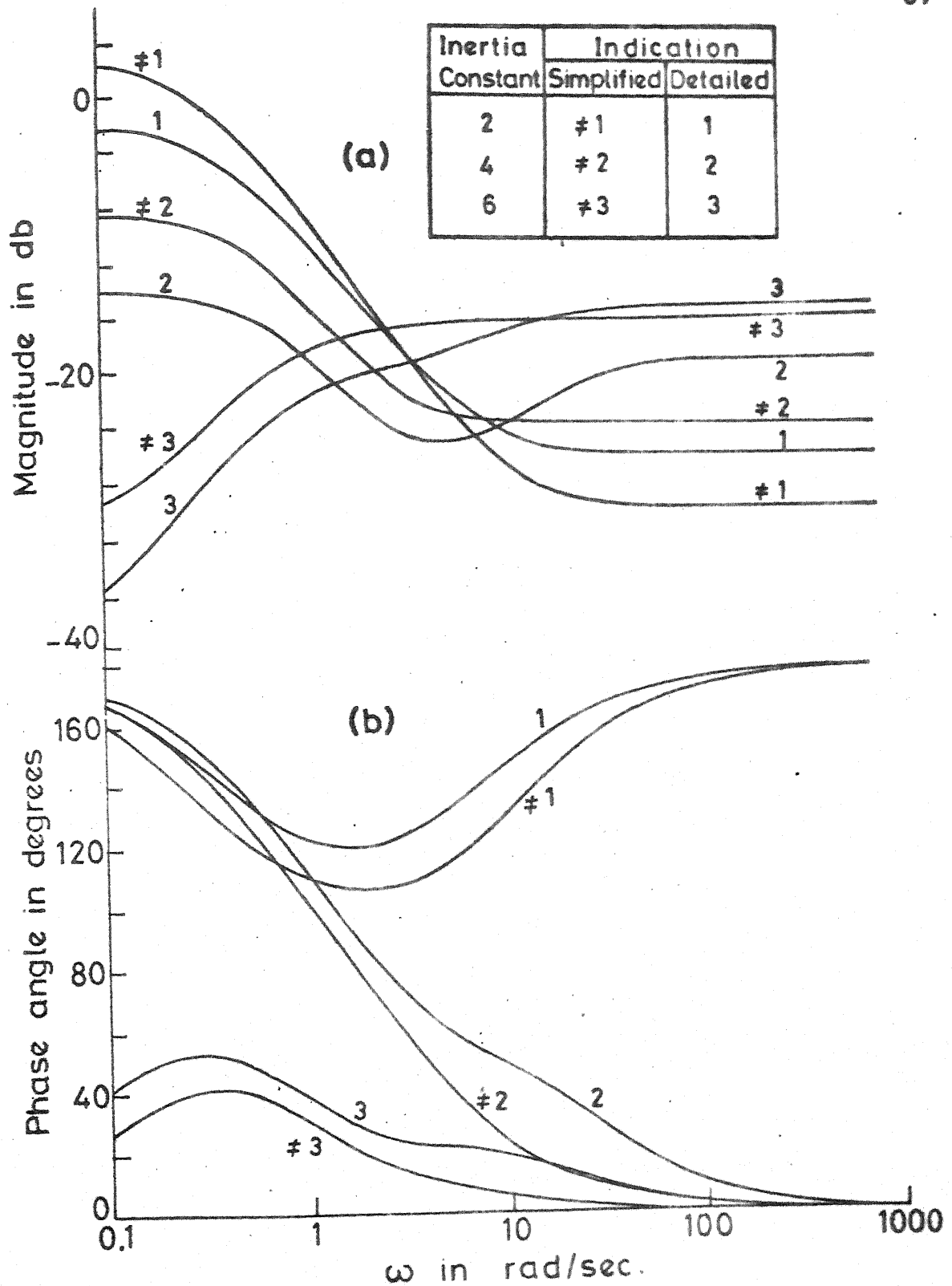


FIG. 3.4 FREQUENCY PLOT OF PSS TRANSFER FUNCTION FOR VARIATION IN INERTIA CONSTANT.
(a) MAGNITUDE (b) PHASE ANGLE

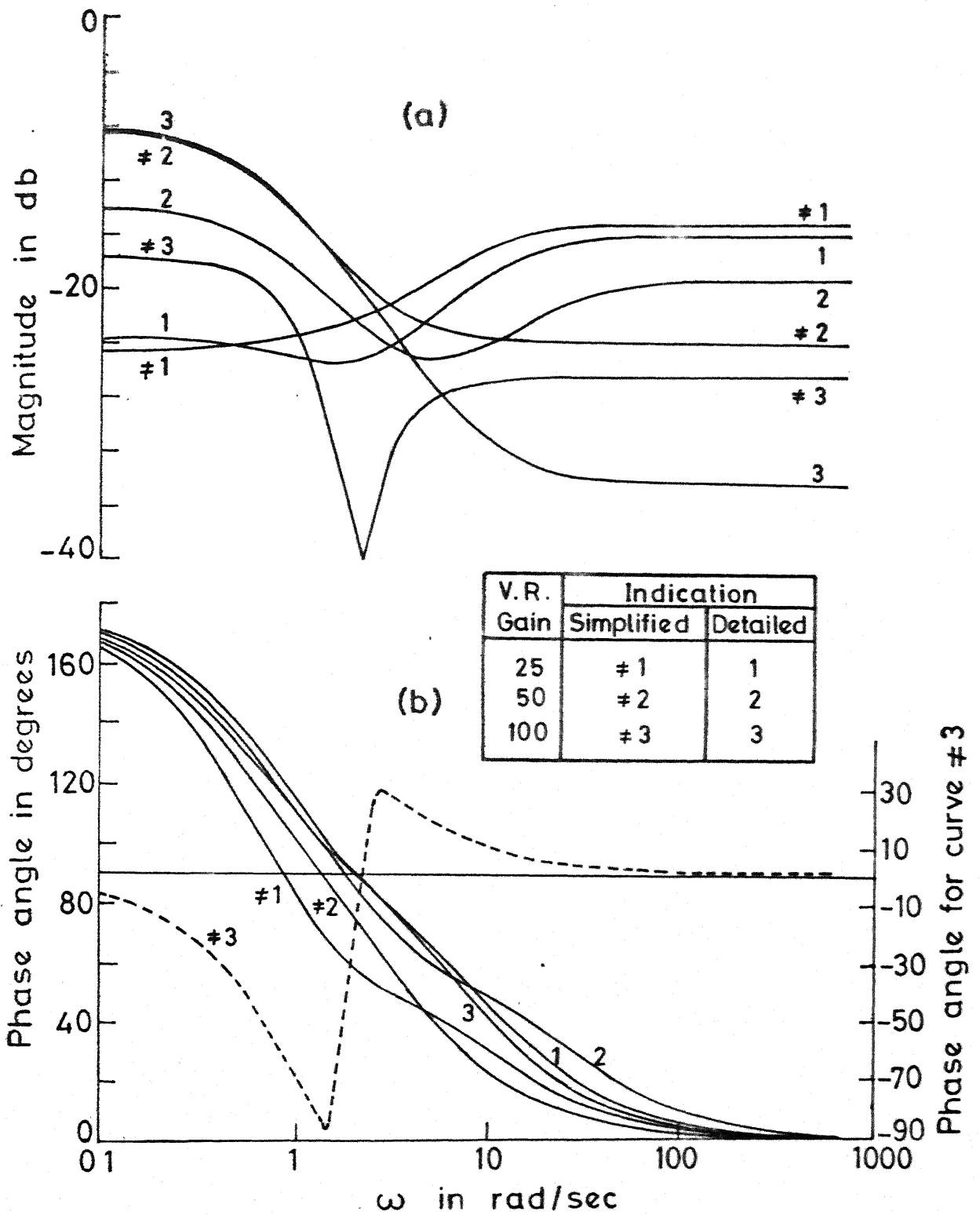


FIG.3.5 FREQUENCY PLOT OF PSS TRANSFER FUNCTION FOR VARIATION IN VOLTAGE REGULATOR GAIN.
(a) MAGNITUDE (b) PHASE ANGLE

3.4.1 Discussion of Results

An inspection of the gain and phase characteristics of stabilizers, given in Figs. 3.2 to 3.5, shows that in most of the cases they are similar for the simplified and the detailed representations of machine except for the case when the voltage regulator gain is equal to 100. The typical gain and phase characteristics of PSS transfer function for $K_R = 100$, with the simplified machine model, shown in Fig. 3.5, is due to the presence of a complex pair of zeros with the oscillation frequency of about 2 rad./sec.

It is interesting to observe that the PSS characteristic vary widely for the different cases considered. This is due to the fact that no limitations regarding the locations of zeros and poles of the PSS are imposed in the design, in contrast with the classical design of PSS where only lead compensators are considered. This does not provide full freedom that can be utilized to assign as many closed-loop poles as possible. There is no need to restrict the locations of zeros and poles, except for the requirement that the poles be in the left half plane. In all the cases of PSS design given here, poles of the PSS are in the left half plane.

Bode plots of PSS transfer function, given in Figs. 3.3 to 3.5, show that in most of the cases, the stabilizer has non-minimum phase characteristics. This is a desirable feature which reduces the effect of torsional interaction [26].

3.5 ADEQUACY OF LOWER ORDER REPRESENTATION OF MACHINE

Adequacy of lower order representation of machine for PSS design is analysed in this section. This is carried out by designing PSS for both the representations of machine, with the same objective of placing the five closed-loop eigenvalues at $-1.0 \pm j7.0$, -1.0 , -2.0 and -6.0 . PSS_l and PSS_h are respectively the stabilizers obtained for the lower and the higher order representation of machine. Closed-loop eigenvalues of the system, with detailed representation of the machine, is then obtained with PSS_h and PSS_l . The analysis is carried out for three different loading conditions, namely, 1.0, 0.5 and 0.25 per unit at 0.9 lagging power factor. Eigenvalues of the closed-loop system, for each case, are given in Table 3.7.

The performances of the two stabilizers PSS_h and PSS_l , designed for full load conditions, are compared by observing the responses of δ and ω for unit step change in the reference voltage. The responses at full load and at half full load are shown in Figs. 3.6 and 3.7.

3.5.1 Discussion of Results

An inspection of Table 3.7 reveals that the damping of rotor oscillation mode, obtained with stabilizer designed for simplified machine model (PSS_l) is comparable with that obtained with PSS designed for higher order machine model (PSS_h).

Table 3.7 Closed-loop Eigenvalues with Detailed Representation of Machine

Machine Loading	1.00 (p.u.)	0.50 (p.u.)	0.25 (p.u.)
	$-1.0 \pm j7.0$ -1.0 -2.0 -6.0 -14.023724 -31.380179 -47.080218 -54.760952	$-1.0 \pm j7.0$ -1.0 -2.0 -6.0 -6.806135 -28.797788 -41.306949 -56.005314	$-1.0 \pm j7.0$ -1.0 -2.0 -6.0 -16.827955 -26.791239 -46.949659 -56.100309
	$-0.687814 \pm j7.628617$ $-1.140974 \pm j0.314649$ -5.050309 -5.552861 -26.822258 -47.055388 -55.351604	$-0.718301 \pm j8.130632$ $-1.081705 \pm j0.304101$ -4.547683 -6.111549 -26.035408 -46.980672 -55.791721	$-0.716801 \pm j8.395452$ $-1.100936 \pm j0.181090$ -4.273976 -6.183122 -29.911529 -46.959130 -55.949948

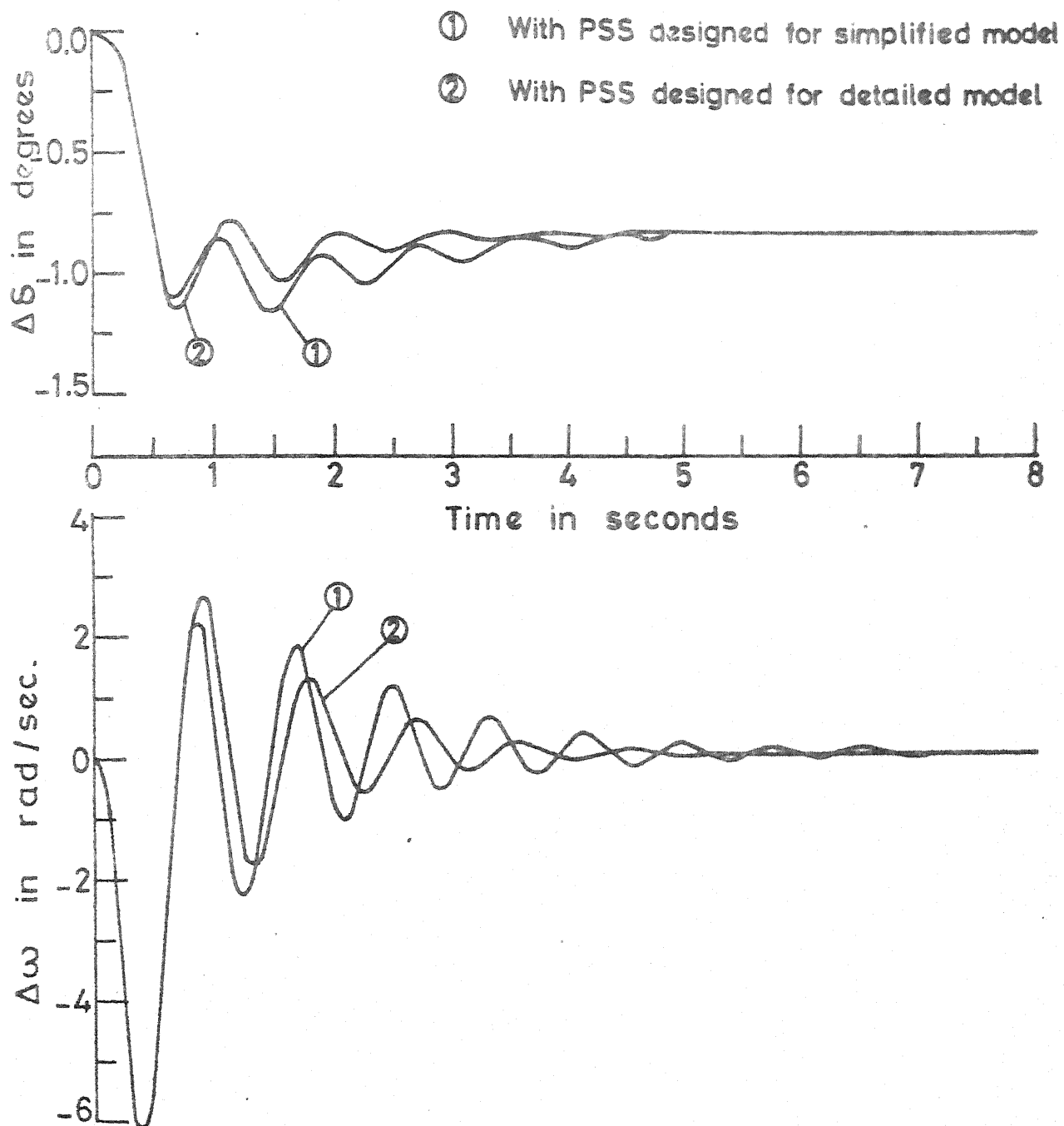


FIG. 3.6 RESPONSE OF $\Delta\delta$ AND $\Delta\omega$ AT FULL LOAD
FOR $\Delta V_{ref} = 1.0$ p.u.

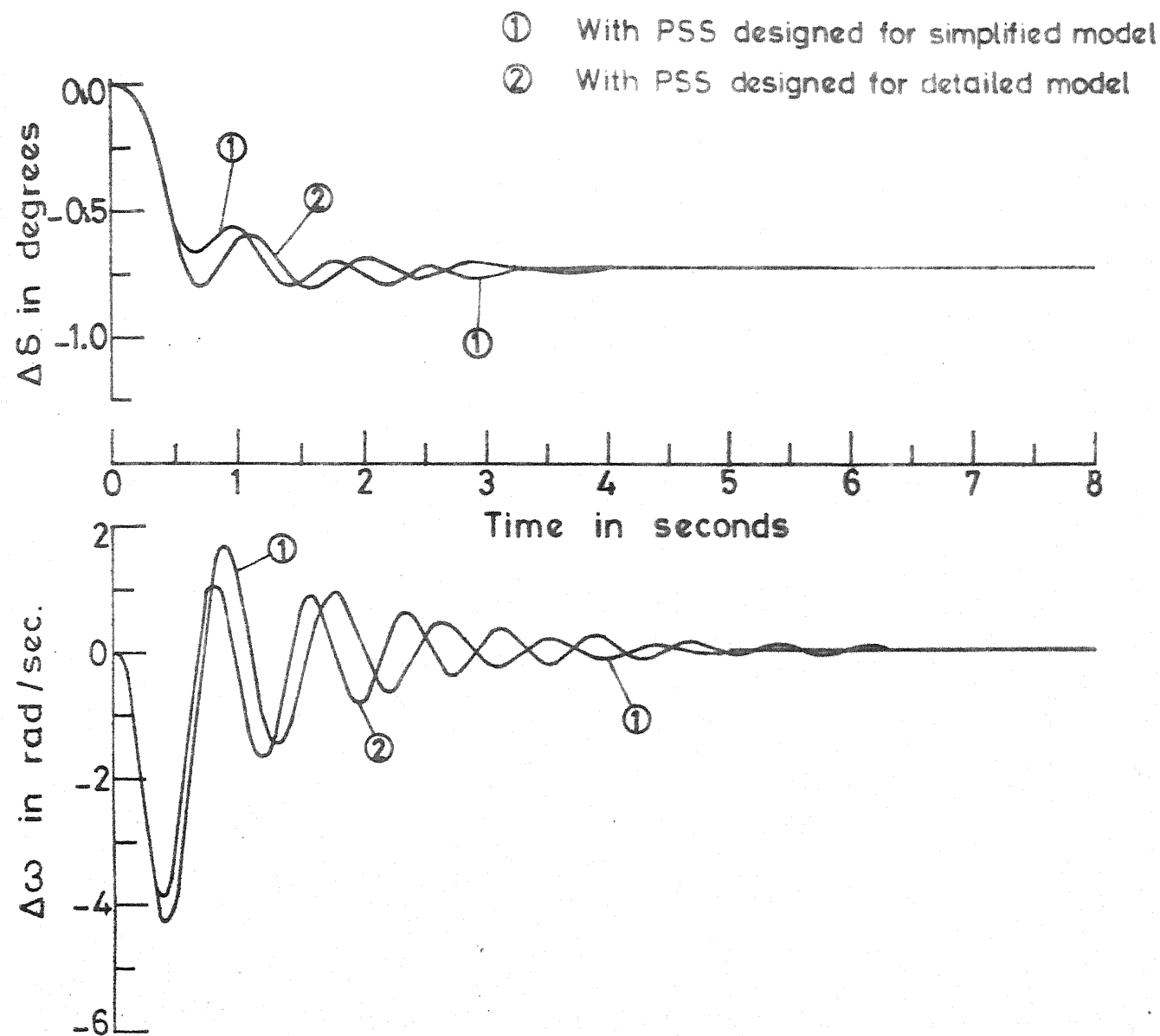


FIG.3.7 RESPONSE OF $\Delta\delta$ AND $\Delta\omega$ AT HALF FULL LOAD FOR $\Delta V_{ref} = 1.0$ p.u.

This is true for all the three loading conditions considered. It is observed that with the application of PSS_l , another oscillatory mode of low frequency and high damping ratio is introduced which will not affect much the stability of the system.

Responses given in Figs. 3.6 and 3.7 show that, for the disturbance considered, performances, of the closed-loop system, when machine is equipped with PSS_h and PSS_l , are comparable. The initial peak and settling time obtained with PSS_h are less than that obtained with PSS_l , however, the difference is not significant.

Thus from eigenvalue analysis of the closed-loop system and time responses given in Figs. 3.6 and 3.7, it can be concluded that simplified representation of machine for PSS design is adequate.

3.6 CONCLUSIONS

A detailed investigation into the effect of generator modelling on PSS design has been presented in this chapter. A sixth order machine model including representation of amortisseur circuits is compared to the third order machine model, described in Chapter 2, in terms of the system behaviour and the characteristics of PSS.

The results from a numerical example indicate that the open-loop system behaviour is predicted from the simplified and detailed machine models are similar. The characteristics of the PSS designed with the same objective are also similar in most of the cases.

Adequacy of the simplified machine model is analysed by incorporating stabilizer, designed for simplified model to the machine represented in detail. Eigenvalue and time-domain analyses of the closed-loop system are used to demonstrate the validity of using simplified machine model in PSS design.

CHAPTER 4

INVESTIGATION OF CONTROL SIGNALS

4.1 INTRODUCTION

For improving dynamic stability through PSS, it is important to select a proper feedback signal. Since the purpose of the stabilizing signal is to damp-out electro-mechanical oscillation; rotor speed, electrical power and frequency deviation have been considered as input signals to PSS [6, 21-27]. Other control signals derived from terminal voltage, armature current, active and reactive powers and field current were investigated [21] and it was found that none of these signals is as effective as signal derived from generator speed. Larsen and Swann [26], in their three part paper, analysed the effectiveness and tuning of stabilizers using speed, power and frequency signals. The analysis presented in Ref.[26] is based on gain and phase characteristics of the transfer function of the plant consisting of the generator, the excitation system and the power system. The plant transfer function is strongly influenced by voltage regulator gain, generator power level and ac system strength. They recommended that speed and power stabilizers should be tuned for strong ac systems and stabilizers using frequency signal should be tuned for weak ac systems. These

recommendations are based on classical design of PSS. The design approach in this thesis is based on modern control theory as given in Chapter 2, where complete design freedom is utilized. The validity of the recommendations given in [26] for PSS design in general needs to be examined.

Interaction between two or more parallel connected generators in a generating plant [25,31] makes the choice of control signal difficult. A detailed study in this regard is not available in the literature.

The principal aim of this chapter is to present a case study on the effectiveness of various feedback control signals that can be used to design PSS for improvement of dynamic stability. Three signals, namely, rotor speed, electrical power output and terminal bus frequency are considered. A generating plant, having a number of generating units, connected to a large power system is considered for analysis. First, the effectiveness of control signals is obtained for a plant having one machine, that is, for the single machine infinite bus system described in Chapter 2. Influence of interactions between machines present in the plant on the effectiveness of control signals is then investigated by considering another machine operating in parallel with the existing machine. A general multi-machine system model is developed for this purpose in which dynamics of the generators are described by linearized state

equations and the network is represented by the reduced admittance matrix which retains only internal buses of the generators. The non-state variables in the system model are eliminated by the use of power flow equations. The important feature of this formulation is that the elements of system matrices are directly evaluated from the knowledge of generator loading and reduced bus admittance matrix. Although the system model developed here is applied to a simple system of a generating plant, having a number of machines, connected to a large power system, it can be used for any multimachine power system where the network is represented by the reduced admittance matrix retaining generator internal buses.

PSS are provided to achieve increased damping of electro-mechanical oscillations. This enables enhancement of the dynamic stability limit. It is necessary to evolve a criterion to judge the effectiveness of PSS, designed for different feedback signals. A convenient criterion is to base the judgement on the stable region of operation in the P-Q plane for the machine equipped with the PSS. The chapter also includes study of the influence of system strength on the design and performance of PSS. The suitability of average speed and average power signals has also been studied in the case of plant with more than one machine.

4.2 SINGLE MACHINE INFINITE BUS SYSTEM

The single machine infinite-bus system of Chapter 2 is considered. For simplicity, transient saliency of generators, resistance and line charging of transmission line are neglected, that is, it is assumed that $x_q = x_d'$, $R_T = 0$ and $Y_S = 0$. Other parameters of machine and excitation system are the same as given in Chapter 2.

4.2.1 Design of PSS

Effectiveness of the three control signals, namely, rotor speed, electrical power output and bus frequency are obtained with the designed PSS. Stabilizers are designed for full load conditions, that is, machine delivering rated power at 0.9 power factor lagging ($P+jQ = 0.9000+j0.4359$ p.u.). The following three cases of system strength are considered in the design of PSS for each control signal :

- (1) $X_T = 0.4$ p.u. (Strong system),
- (2) $X_T = 0.6$ p.u. (System of moderate strength), and
- (3) $X_T = 0.8$ p.u. (Weak system).

System matrices obtained for $X_T = 0.6$ p.u. are given below :

$$[A] = \begin{bmatrix} 0 & -35.36908 & -11.89618 & 0 \\ 1 & 0 & 0 & 0 \\ 0 & -0.30157 & -0.35072 & 0.35273 \\ 0 & 521.57320 & -618.42114 & -50.0000 \end{bmatrix}$$

$$\underline{b} = [0 \quad 0 \quad 0 \quad 2500]^t$$

$$\underline{c} = [1 \quad 0 \quad 0 \quad 0] \quad \text{for speed signal}$$

$$= [0 \quad 0.90067 \quad 0.30293 \quad 0] \quad \text{for power signal}$$

$$= [0.66252 \quad -0.01909 \quad -0.02220 \quad 0.02233] \quad \text{for frequency signal}$$

Open-loop eigenvalues for the above three cases are given in Table 4.1.

Table 4.1 Open-loop Eigenvalues

$X_T = 0.4 \text{ p.u.}$	$X_T = 0.6 \text{ p.u.}$	$X_T = 0.8 \text{ p.u.}$
$0.26105 + j7.21497$	$0.35281 + j6.19653$	$0.46974 + j5.06393$
-4.86833	-5.95422	-6.79143
-46.04967	-45.10213	-44.46803

Eigenvalue assignment with output feedback as given in Section 2.4.2.1 is used to design stabilizers with each of the three control signals and for each case of system strength. As discussed in Chapter 2, with a second order PSS, at the most five closed-loop eigenvalues can be assigned. The location of the remaining closed-loop eigenvalue is obtained alongwith the parameters of PSS. The desired locations of

closed-loop eigenvalues and location of the remaining eigenvalue obtained for each case are given in Table 4.2. The parameters of PSS with transfer function of the form

$$F(s) = \frac{\theta_o(s+z_1)(s+z_2)}{(s+p_1)(s+p_2)}$$

are obtained using each of the three control signals and are given in Table 4.3, where z_1 and z_2 are the zeros and p_1 and p_2 are the poles of PSS.

Frequency response of PSS transfer function, designed at $X_T = 0.6$ p.u. is given in Fig. 4.1

Table 4.2 Closed-Loop Eigenvalues

Signal		$X_T=0.4$ p.u.	$X_T=0.6$ p.u.	$X_T = 0.8$ p.u.
Desired Location		- 2.14359	- 1.87564	- 1.60770
		$\pm j8.00000$	$\pm j7.00000$	$\pm j6.00000$
		- 4.86833	- 5.95422	- 6.79143
		- 1.00000	- 1.00000	- 1.00000
		- 2.00000	- 2.00000	- 2.00000
Remaining Eigen- values	Speed	-46.90553	-45.89207	-45.21988
	Power	-42.02226	-41.65311	-41.86691
	Freq.	-35.87726	-35.99440	-35.44419

Table 4.3 Parameters of PSS

Signal	X_T	θ_o	z_1	z_2	p_1	p_2
Speed	0.4	0.12954	7.83588	-4.86832	-8.34385	-0.32131
	0.6	0.12084	5.25912	-5.95422	-7.89546	-0.35140
	0.8	0.11513	2.78286	-6.79144	-7.50228	-0.40442
Power	0.4	-0.69783	-5.91149	-4.86835	-2.97439	-0.80750
	0.6	-0.59832	-6.43534	-5.95450	-3.22773	-0.78017
	0.8	-0.45801	-8.18041	-6.79142	-3.81797	-0.73576
Frequency	0.4	0.16589	9.08061	-4.86833	-4.95754	-0.41363
	0.6	0.13263	6.00710	-5.95423	-5.34637	-0.40702
	0.8	0.11228	3.22053	-6.79141	-5.51648	-0.43110

4.2.2 Determination of Stable P-Q Region

With each PSS of Table 4.3, stable P-Q region is obtained by varying the active power output in steps and determining the limiting values of reactive power output for closed-loop system stability. To study the effect of ac system strength on the performance of stabilizers, stable P-Q regions are obtained with each PSS of Table 4.3, using appropriate signal, at different values of transmission line reactances, that is, at X_T equal to 0.2, 0.4, 0.6 and 0.8 p.u. These regions are shown in Figs. 4.2 to 4.5. The stable P-Q region in these figures is the region above the appropriate boundary lines.

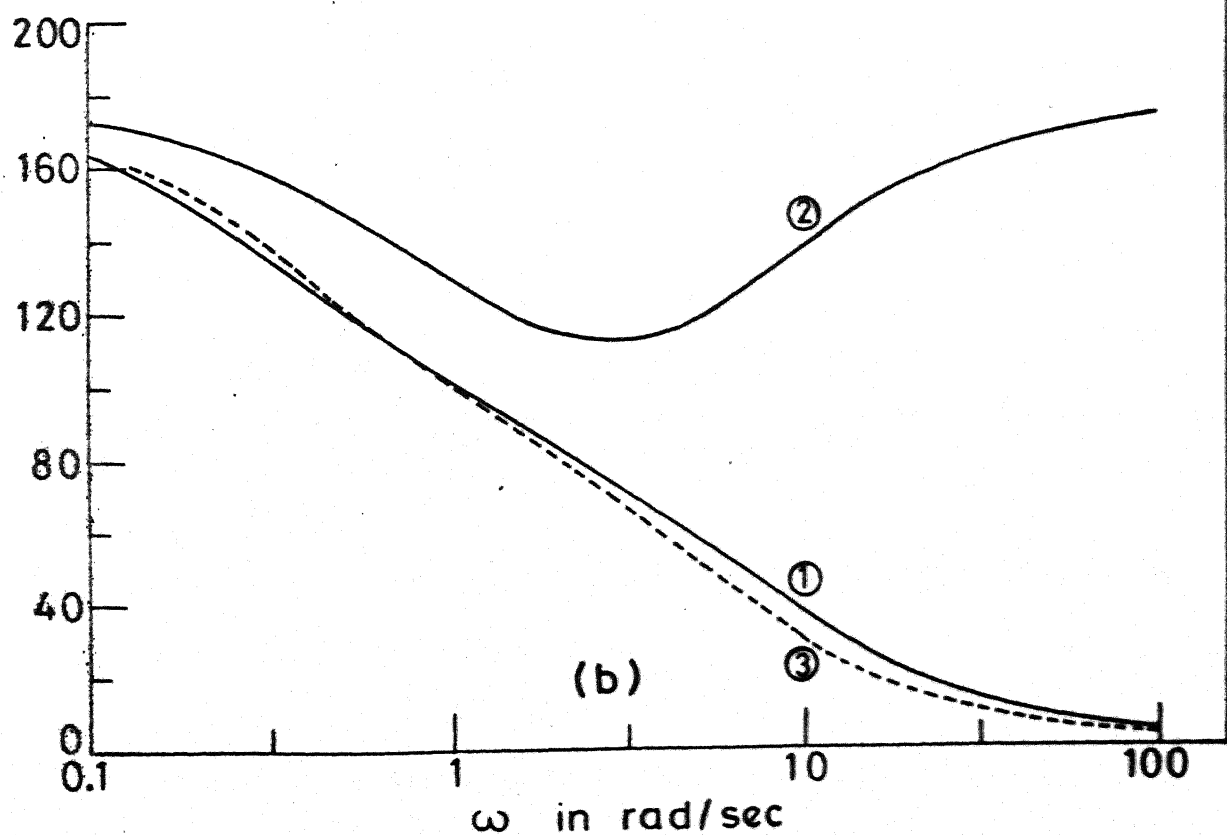
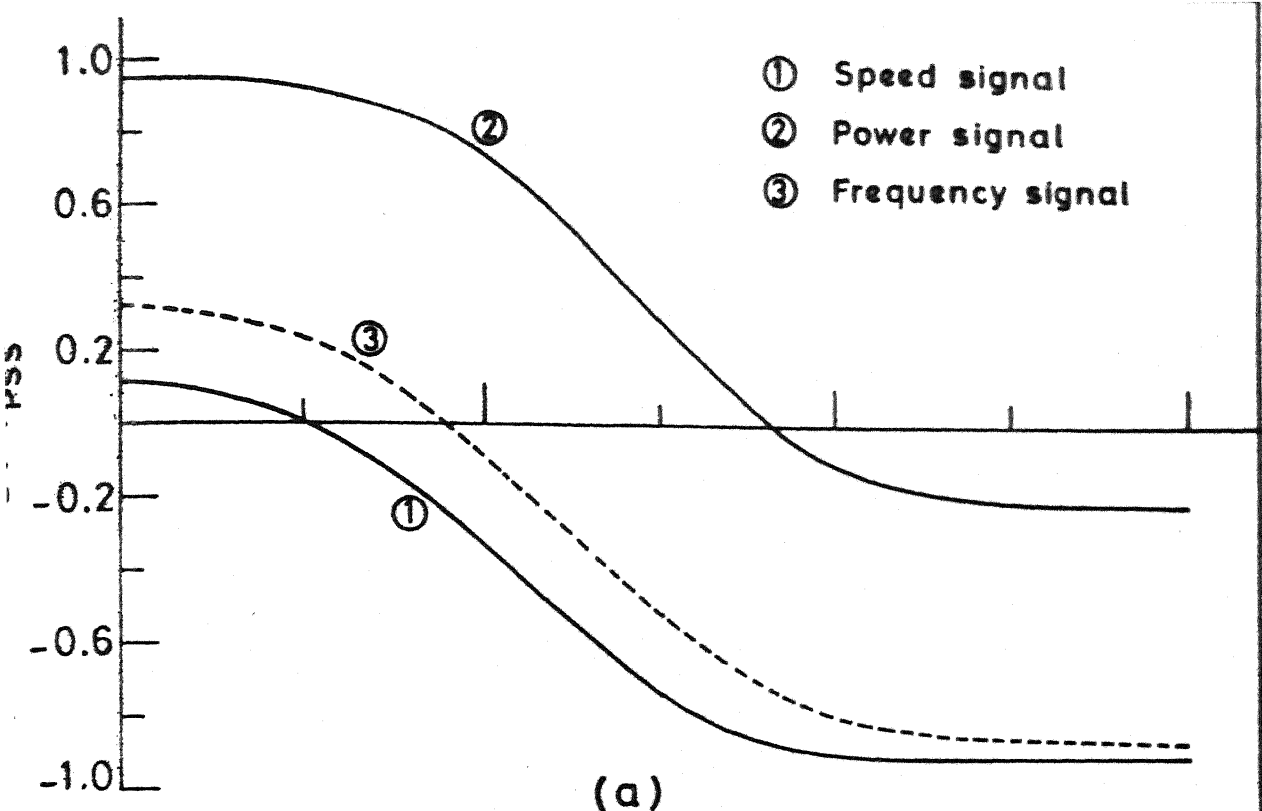


FIG. 4.1 FREQUENCY RESPONSE OF PSS TRANSFER FUNCTION.
(a) MAGNITUDE Vs. ω , (b) PHASE ANGLE Vs. ω .

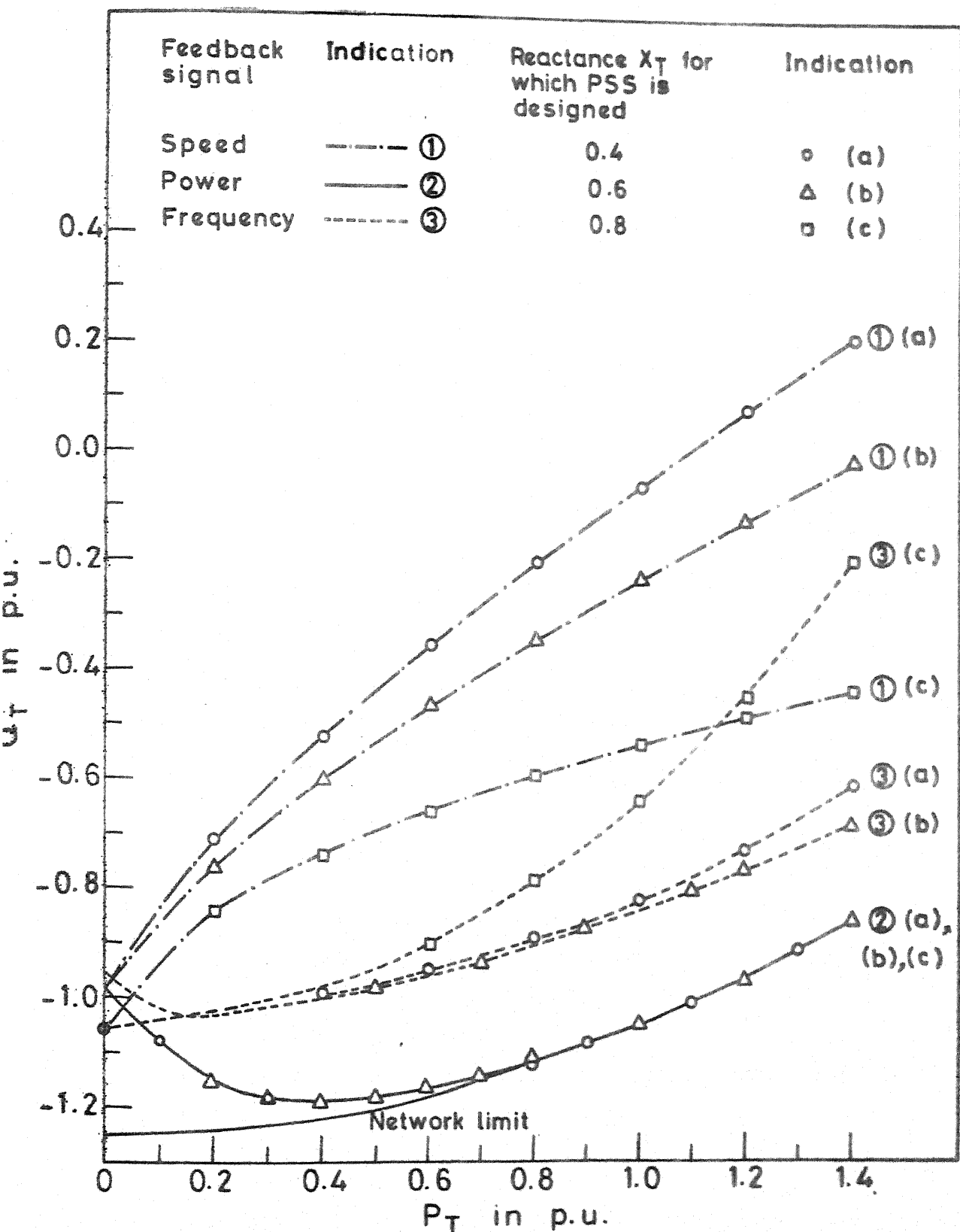
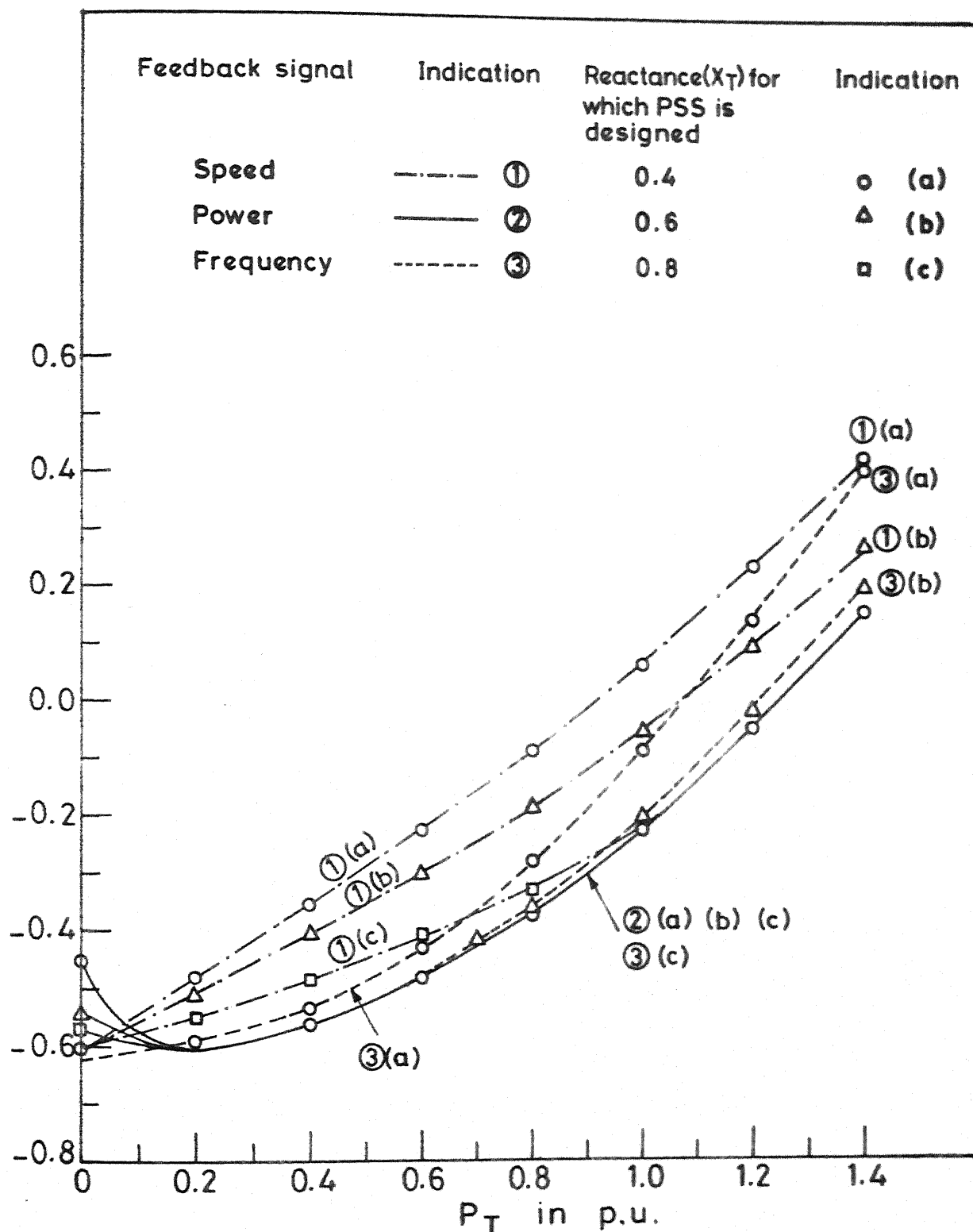


FIG. 4.2 STABLE P-Q REGION FOR SINGLE M/C SYSTEM AT $X_T = 0.2$ p.u.



**FIG. 4.3 STABLE P-Q REGION FOR SINGLE M/C SYSTEM
AT $X_T = 0.4$ p.u.**

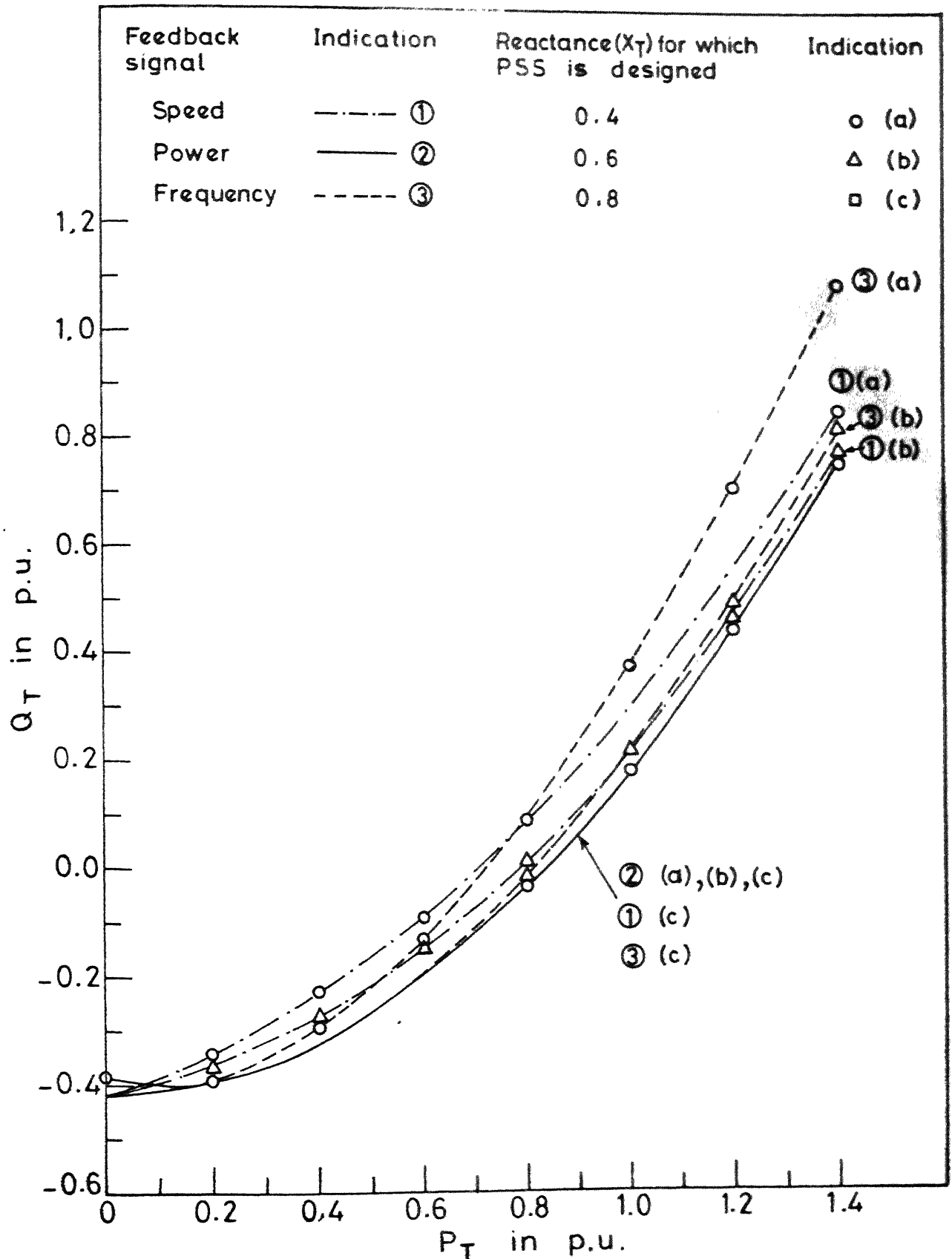
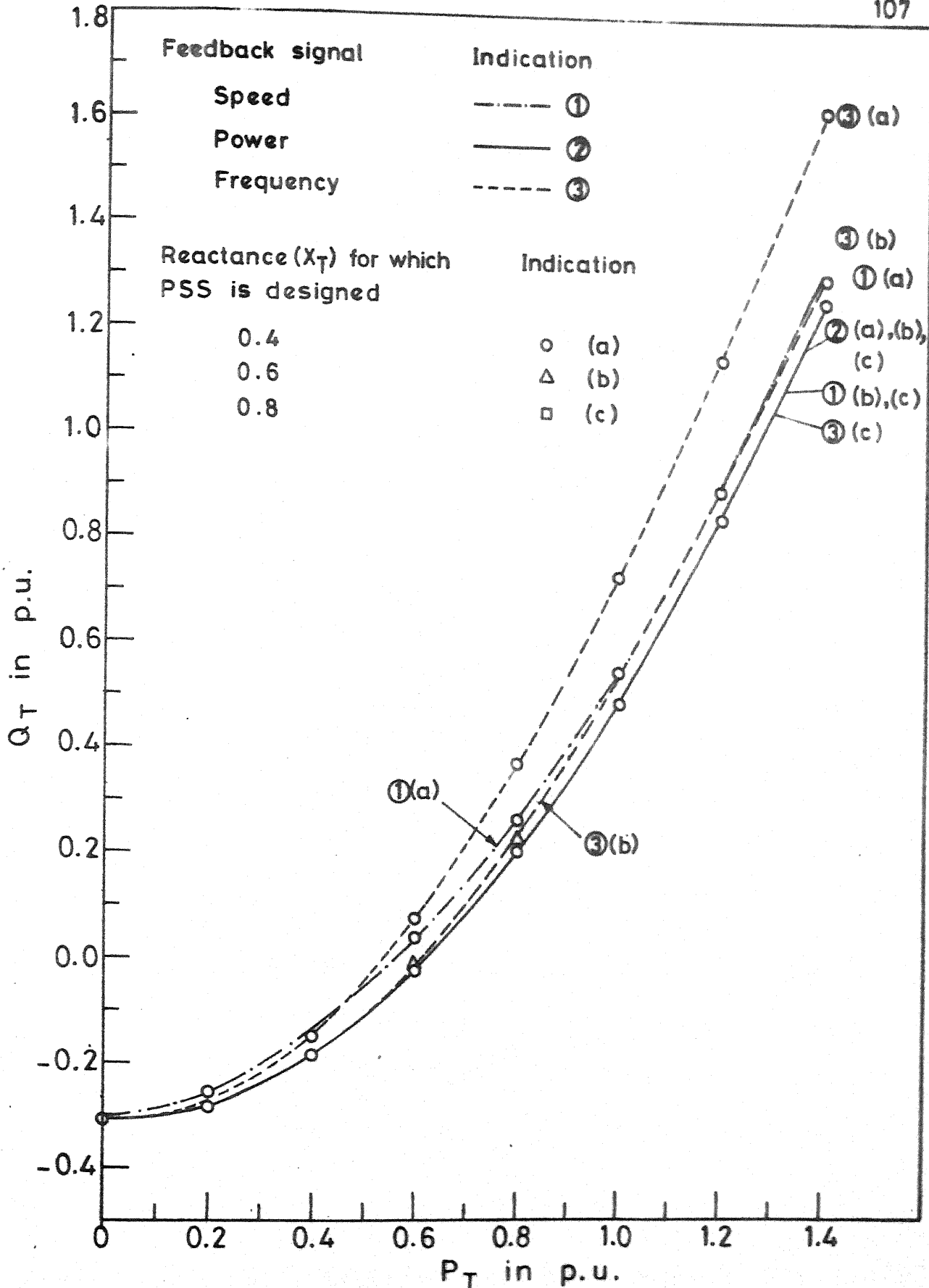


FIG.4.4 STABLE P-Q REGION FOR SINGLE M/C SYSTEM AT $X_T = 0.6$ p.u.



**FIG.4.5 STABLE P-Q REGION FOR SINGLE M/C SYSTEM .
AT $X_T = 0.8$ p.u.**

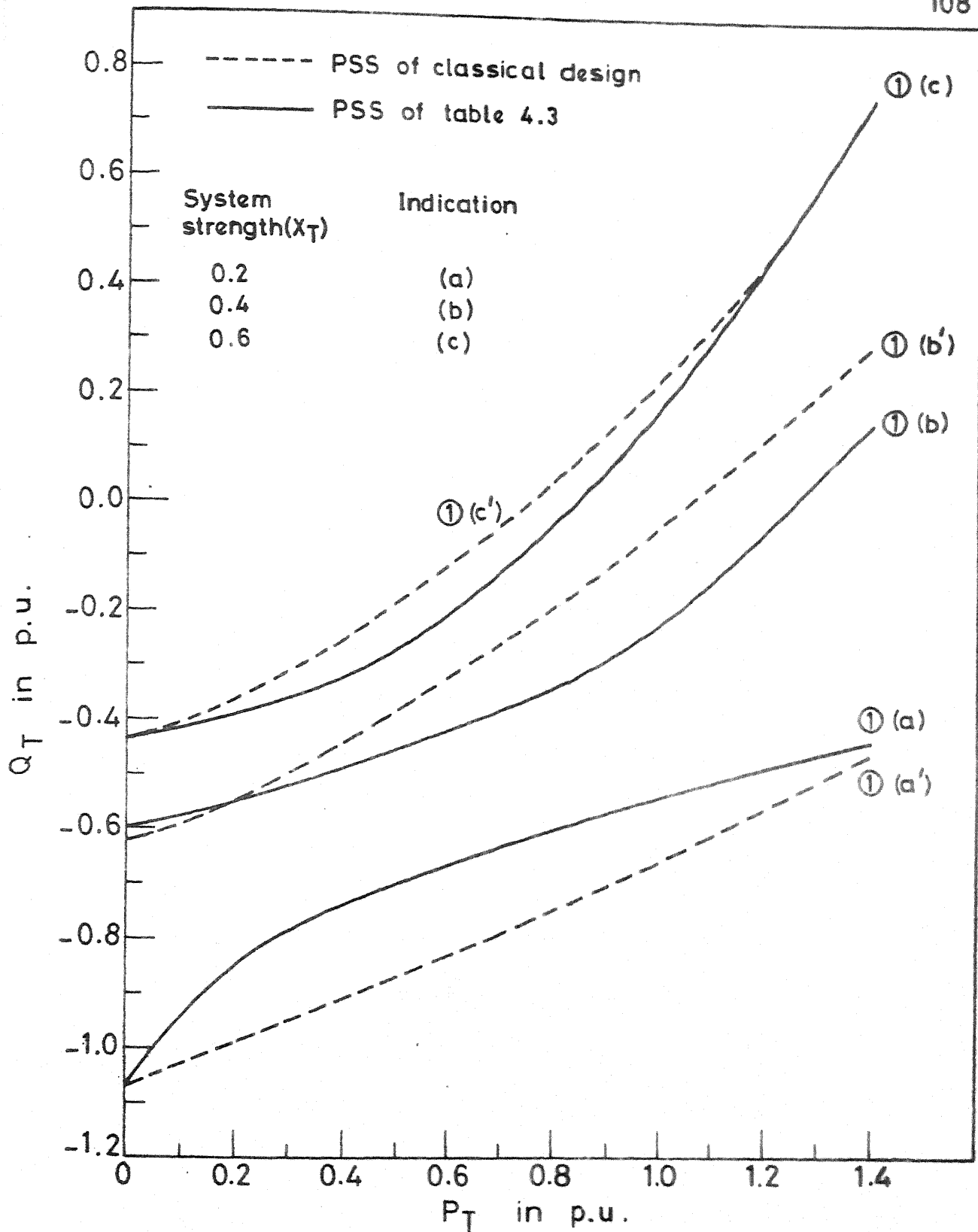


FIG. 4.6 STABLE P-Q REGION WITH SPEED SIGNAL FOR SINGLE M/C SYSTEM (COMPARISON WITH PSS OF CLASSICAL DESIGN).

Figure 4.6 compares the stable P-Q regions, for speed signal feedback, obtained with PSS designed using classical control theory (sec 2.4.4) and that obtained with PSS of Table 4.3, at different ac system strengths (i.e. at X_T equal to 0.2, 0.4 and 0.6 p.u.). In case of PSS of Table 4.3, the PSS which gives maximum P-Q region at a particular ac system strength is chosen for comparison.

4.2.3 Discussion of Results

From Fig. 4.1 it is clear that the gain required with power signal is higher than those for speed and frequency signals. Speed signal requires minimum gain. In the frequency response plot it is seen that gain requirement reduces with increase in frequency for all the three signals. Phase characteristics of speed and frequency signals are the same. Phase requirement reduces to zero for higher frequencies in case of speed and frequency signals. For power signal the minimum phase is required at 0.5 Hz.

System Strength for PSS Design

Speed Signal :

From Figs. 4.2 to 4.5, it is evident that PSS utilizing speed signal should be designed for weak system as the stable P-Q region obtained is maximum with such a PSS designed at $X_T = 0.8$ p.u. Difference in stable P-Q regions obtained is

significant for strong system, (see curves 1(a), 1(b) and 1(c) of Fig. 4.2). The difference reduces with the reduction in system strength, (see curves 1(a), 1(b) and 1(c) of Figs. 4.3 to 4.5).

power Signal :

Curves 2(a), 2(b) and 2(c) of Figs. 4.2 to 4.5 show that the stable P-Q regions obtained utilizing power signal, with PSS designed at X_T equal to 0.4, 0.6 and 0.8 p.u. coincide, suggesting that PSS can be designed for either weak or strong system.

Frequency Signal :

In case of frequency signal the following typical behaviour is observed in curves 3(a), 3(b) and 3(c) of Fig. 4.2 : for strong system, i.e., at $X_T = 0.2$ p.u. stable P-Q region obtained with PSS designed at $X_T = 0.6$ p.u. is more than that obtained with PSS designed at $X_T = 0.4$ p.u. but again it reduces with PSS designed at $X_T = 0.8$ p.u. For system of moderate strength and for weak system, stable P-Q region obtained with PSS designed at $X_T = 0.8$ p.u. is maximum, curves 3(a), 3(b) and 3(c) of Figs. 4.3 to 4.5. Thus, for system of moderate strength and for weak system, it appears that PSS utilizing frequency signal should be designed for weak system.

Comparison of Signals

From Figs. 4.2 to 4.5 it is clear that stabilizers utilizing power signal give maximum stable P-Q region in comparison with PSS utilizing speed or frequency signal for all cases, irrespective of the system strength at which it is designed and irrespective of the system strength at which it is operating. In fact, with power signal, network limit is reached first for all values of X_T except for $X_T = 0.2$ p.u. where instability is observed before network limit. Even for this case, $X_T = 0.2$ p.u., the stable P-Q region is very close to network limit as shown in Fig. 4.2. For stronger system, $X_T = 0.2$ and 0.4 p.u., the difference in stable P-Q region obtained with power signal and that obtained with speed or frequency signal is significant. The difference reduces with the reduction in system strength. Figure 4.2 shows that speed signal is most inefficient for strong systems for all loading conditions. Figures 4.4 and 4.5 show that for weak systems and at higher loading condition speed signal gives more stable P-Q region than frequency signal but the difference is not significant.

From Fig. 4.6 it is observed that PSS designed by classical control theory utilizing speed signal gives larger stable P-Q region than that obtained by PSS of Table 4.3 for strong system, curves 1(a) and 1(a'). For weak system it is vice-versa (see curves 1(b), 1(c), 1(b') and 1(c')).

4.3 GENERATING PLANT INFINITE BUS SYSTEM

In order to investigate the interaction of other machines present in the plant, on the suitability of control signals, another machine is considered operating in parallel with the existing machine of section 4.2. A general system model is developed as follows :

4.3.1 Development of System Model

Consider a generating plant having n number of generating units supplying power to an infinite bus through a transmission line of impedance Z_T as shown in Fig. 4.7. Y_S represents line charging and local loads of the generating plant, if any. Fig. 4.8 is the equivalent circuit of the system shown in Fig. 4.7, where Z_{eq} and $V_{eq} \angle \gamma$ are the Thevenin's equivalent of the transmission system and can be expressed as

$$Z_{eq} = \frac{Z_T}{(1 + Y_S Z_T)} \quad (4.1)$$

$$V_{eq} \angle \gamma = \frac{1}{(1 + Y_S Z_T)} V_{\infty} \quad (4.2)$$

$E_i \angle \delta_i$ for $i = 1, 2, \dots, n$ are the voltages of internal buses of alternators.

4.3.1.1 Development of Dynamical Equation

The following assumptions are made in the development of system model.

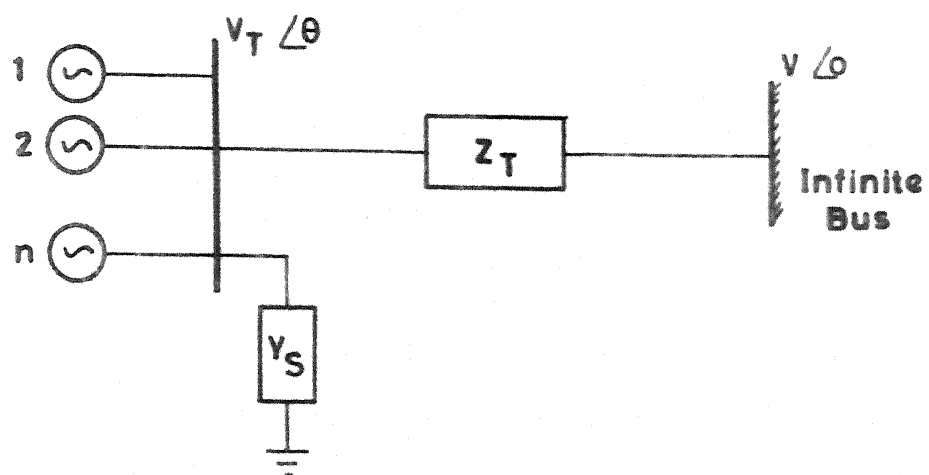


FIG.4.7 GENERATING PLANT WITH n MACHINES CONNECTED TO INFINITE BUS.

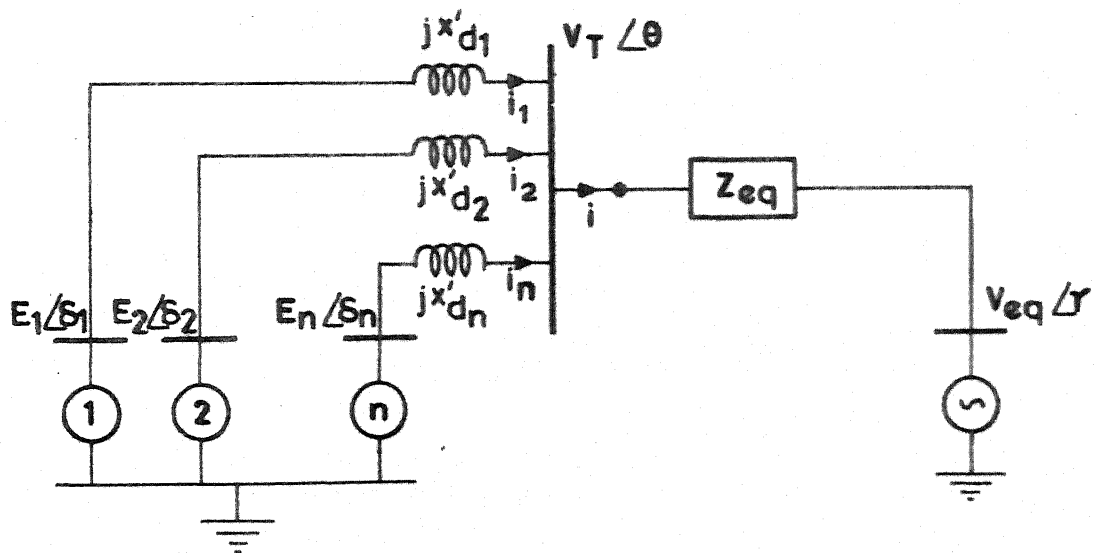


FIG.4.8 EQUIVALENT CIRCUIT OF SYSTEM GIVEN IN FIG. 4.7.

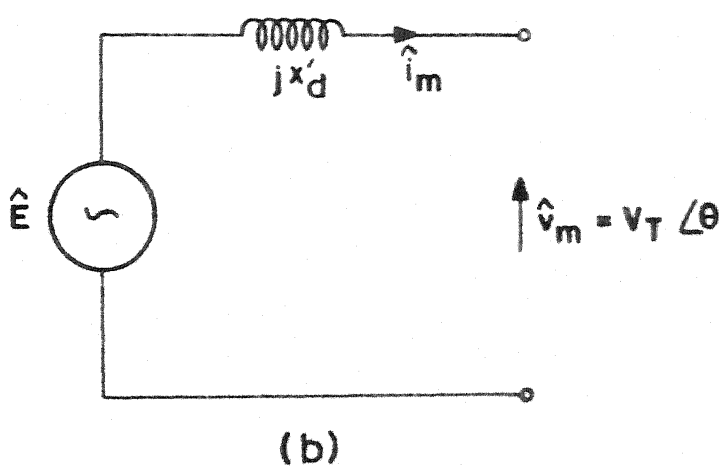
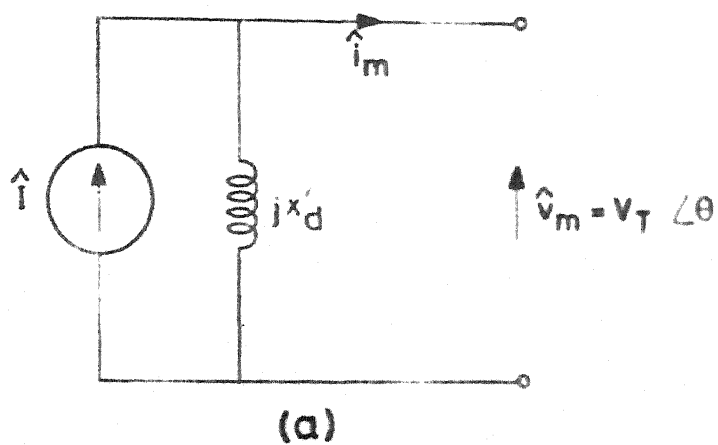


FIG. 4.9 CIRCUIT MODEL OF A SYNCHRONOUS MACHINE.

(a) CURRENT SOURCE MODEL.

(b) VOLTAGE SOURCE MODEL.

- (1) Synchronous machines have no amortisseur winding
- (2) Transient saliency is ignored for all machines
- (3) Governor and Prime Mover dynamics are ignored for all machines.

The system model is developed by combining machine and network models. The network is represented by linear algebraic equations utilizing the reduced bus admittance matrix which retains only the internal buses of machines. Each machine of the plant is represented by the circuit model given in Fig. 4.9 (Appendix D). Parks components of variables shown in Fig. 4.9 can be given from Eqn. (D.16) of Appendix D as

$$\begin{aligned}\hat{I} &= (I'_q - jI'_d) e^{j\delta} \\ \hat{E} &= (E'_q - jE'_d) e^{j\delta} \\ \hat{i}_m &= (i_q - ji_d) e^{j\delta} \\ \hat{v}_m &= (v_q - jv_d) e^{j\delta}\end{aligned}$$

where δ represents the angular displacement of machine q -axis with respect to reference frame (infinite bus). From Figs. 4.9(a) and 4.9(b) we have

$$\hat{E} = jx'_d \hat{I} \quad (4.3)$$

Separating real and imaginary parts, we get

$$\begin{aligned}E'_q &= x'_d I'_d \\ E'_d &= x'_d I'_q\end{aligned}$$

Since transient saliency is neglected, I'_q will be zero as $I'_q = \xi i_q$ (Appendix D) when $\xi = 1 - x_q/x'_d$. Thus, there will be no voltage source resulting from I'_q and the voltage source \hat{E} will be given as

$$\hat{E} = E'_q e^{j\delta} \quad (4.4)$$

From Eqn. (4.4) and Fig. 4.8, the voltage of internal bus of i th machine can be expressed as

$$E'_{qi} e^{j\delta_i} = E_i \angle \delta_i \quad (4.5)$$

The linearized dynamical equations of the i th machine and the excitation system can be given as

$$p \Delta \omega_i = \frac{1}{M_i} [-\Delta P_{ei} - K \Delta \omega_i] \quad (4.6)$$

$$p \Delta \delta_i = \Delta \omega_i \quad (4.7)$$

$$p \Delta E_i = \frac{1}{T'_{doi}} [\Delta E_{fdi} - \Delta E_i - (x_{di} - x'_{di}) \Delta i_{di}] \quad (4.8)$$

$$p \Delta E_{fdi} = \frac{1}{T_{Ri}} [K_R (\Delta V_{ref_i} - \Delta V_{Ti} + u_i) - \Delta E_{fdi}] \quad (4.9)$$

The non-state variables ΔP_{ei} , Δi_{di} and ΔV_{Ti} in eqns. (4.6) to (4.9) can be eliminated by expressing them in terms of state variables as follows.

Representation of ΔP_e

The active and reactive power output of the machines at their internal buses, Fig. 4.8, can be expressed as

$$P_i = E_i \sum_{j=1}^{n+1} E_j C_{ij} \quad (4.10)$$

$$Q_i = E_i \sum_{j=1}^{n+1} E_j D_{ij} \quad (4.11)$$

for $i = 1, 2, \dots, n$.

where

$$C_{ij} = G_{ij} \cos(\delta_i - \delta_j) + B_{ij} \sin(\delta_i - \delta_j)$$

$$D_{ij} = G_{ij} \sin(\delta_i - \delta_j) - B_{ij} \cos(\delta_i - \delta_j)$$

$$Y_{ij} \triangleq G_{ij} + jB_{ij}$$

and

$$E_{n+1} \angle \delta_{n+1} \triangleq V_{eq} \angle \gamma$$

Y_{ij} is the ij th element of reduced bus admittance matrix and can be expressed as follows. The star point at the terminal bus, Fig. 4.8, is eliminated by converting the star into an equivalent delta from the relation

$$Z_{ij} = Z_i Z_j \sum_{K=1}^{n+1} \frac{1}{Z_K} \quad (4.12)$$

for i and $j = 1, 2, \dots, n+1$. Z_i in Eqn. (4.12) is the impedance of i th machine, Z_{n+1} is equal to Z_{eq} and $\sum \frac{1}{Z_K}$ is the sum of reciprocals of all impedances connected to the terminal bus including Z_{eq} . The element Y_{ij} of the reduced bus admittance matrix is then obtained as

$$Y_{ij} = \frac{1}{Z_{ij}} \quad \text{for } i \neq j$$

and

$$Y_{ii} = \sum \frac{1}{Z_{iK}}$$

where subscript K represents the bus numbers connected to ith bus. Linearizing eqns. (4.10) and (4.11), we get

$$\begin{aligned} \Delta P_i = & -(Q_{io} + B_{ii} E_{io}^2) \Delta \delta_i + (P_{io} + G_{ii} E_{io}^2) \frac{1}{E_{io}} \Delta E_i \\ & + E_{io} \sum_{\substack{j=1 \\ j \neq i}}^n (E_{jo} D_{ij} \Delta \delta_j + C_{ij} \Delta E_j) \end{aligned} \quad (4.13)$$

and

$$\begin{aligned} \Delta Q_i = & (P_{io} - G_{ii} E_{io}^2) \Delta \delta_i + (Q_{io} - B_{ii} E_{io}^2) \frac{1}{E_{io}} \Delta E_i \\ & + E_{io} \sum_{\substack{j=1 \\ j \neq i}}^n (-E_{jo} C_{ij} \Delta \delta_j + D_{ij} \Delta E_j) \end{aligned} \quad (4.14)$$

Representation of Δi_d

Referring to Fig. 4.9(b), power output at the internal bus of ith machine can be given as

$$S_i = P_i + jQ_i = \hat{E}_i \cdot \hat{i}_m^* \quad (4.15)$$

Separating real and imaginary parts from eqn. (4.15) and rearranging, we get

$$i_{di} = \frac{Q_i}{E_i} \quad (4.16)$$

and

$$i_{qi} = \frac{P_i}{E_i}$$

Linearizing eqn. (4.16) and substituting the value of ΔP_i and ΔQ_i from eqns. (4.13) and (4.14), we get

$$\begin{aligned} \Delta i_{di} &= (P_{i0} - G_{ii} E_{i0}^2) \frac{1}{E_{i0}} \Delta \delta_i - B_{ii} \Delta E_i \\ &+ \sum_{\substack{j=1 \\ j \neq i}}^n (-E_{j0} C_{ij} \Delta \delta_j + D_{ij} \Delta E_j) \end{aligned} \quad (4.17)$$

and

$$\begin{aligned} \Delta i_{qi} &= -(Q_{i0} + B_{ii} E_{i0}^2) \frac{1}{E_{i0}} \Delta \delta_i + G_{ii} \Delta E_i \\ &+ \sum_{\substack{j=1 \\ j \neq i}}^n (E_{j0} D_{ij} \Delta \delta_j + C_{ij} \Delta E_j) \end{aligned} \quad (4.18)$$

Representation of ΔV_T

The magnitude of terminal voltage V_{Ti} can be expressed as

$$V_{Ti} = (v_{di}^2 + v_{qi}^2)^{1/2} \quad (4.19)$$

Linearizing eqn. (4.19), we get

$$\Delta V_{Ti} = \frac{1}{V_{Tio}} (v_{dio} \Delta v_{di} + v_{qio} \Delta v_{qi}) \quad (4.20)$$

Now, from Fig. 4.9(b), the Park's component of terminal voltage can be expressed as

$$v_{di} = x'_{di} i_{qi} \quad (4.21)$$

and

$$v_{qi} = E_i - x'_{di} i_{di} \quad (4.22)$$

Linearizing eqns. (4.21) and (4.22) and substituting Δi_{di} and Δi_{qi} from eqns. (4.17) and (4.18), we get

$$\begin{aligned} \Delta v_{di} = & -\frac{x'_{di}}{E_{io}} (Q_{io} + B_{ii} E_{io}^2) \Delta \delta_i + x'_{di} G_{ii} \Delta E_i \\ & + x'_{di} \sum_{\substack{j=1 \\ j \neq i}}^n (E_{jo} D_{ij} \Delta \delta_j + C_{ij} \Delta E_j) \end{aligned} \quad (4.23)$$

and

$$\begin{aligned} \Delta v_{qi} = & -\frac{x'_{di}}{E_{io}} (P_{io} - G_{ii} E_{io}^2) \Delta \delta_i + (1 + x'_{di} B_{ii}) \Delta E_i \\ & + x'_{di} \sum_{\substack{j=1 \\ j \neq i}}^n (E_{jo} C_{ij} \Delta \delta_j - D_{ij} \Delta E_j) \end{aligned} \quad (4.24)$$

From eqns. (4.20) to (4.24), we get

$$\Delta V_{Ti} = \beta_1^{ii} \Delta \delta_i + \beta_2^{ii} \Delta E_i + \sum_{\substack{j=1 \\ j \neq i}}^n (\beta_1^{ij} \Delta \delta_j + \beta_2^{ij} \Delta E_j) \quad (4.25)$$

where

$$\beta_1^{ii} = -\frac{x'_{di}}{V_{Tio}} [x'_{di} (P_{io} B_{ii} + Q_{io} G_{ii}) + (P_{io} - G_{ii} E_{io}^2)]$$

$$\beta_2^{ii} = \frac{1}{V_{Tio}} \left[\frac{x'_{di}}{E_{io}} \{x'_{di} (P_{io} G_{ii} - Q_{io} B_{ii}) - Q_{io}\} + E_{io} (1 + x'_{di} B_{ii}) \right]$$

$$\beta_1^{ij} \Big|_{j \neq i} = \frac{E_{io} E_{jo}}{V_{Tio}} \left[\frac{x'^2_{di}}{E_{io}^2} (P_{io} D_{ij} - Q_{io} C_{ij}) + x'_{di} C_{ij} \right]$$

and

$$\beta_2^{ij} \Big|_{j \neq i} = \frac{E_{io}}{V_{Tio}} \left\{ \frac{x'^2_{di}}{E_{io}^2} (P_{io} C_{ij} + Q_{io} D_{ij}) - x'_{di} D_{ij} \right\}$$

Final Machine Equations Eliminating Non-State Variables

Substituting the values of ΔP_e , Δi_d and ΔV_T respectively from eqns. (4.13), (4.17) and (4.25) in eqns. (4.6) to (4.9), the dynamical equation of i th machine can be expressed as

$$p \underline{x}_i = [A_{ii}] \underline{x}_i + \sum_{\substack{j=1 \\ j \neq i}}^n [A_{ij}] \underline{x}_j + b_i u_i \quad (4.26)$$

where \underline{x}_i is the vector of state variables

$$\underline{x}_i \triangleq [\Delta \omega_i \quad \Delta \delta_i \quad \Delta E_i \quad \Delta E_{fdi}]^t$$

and the matrices A_{ii} , A_{ij} and b_i are as follows :

$$[A_{ii}] = \begin{bmatrix} a_{11}^{ii} & a_{12}^{ii} & a_{13}^{ii} & 0 \\ 1 & 0 & 0 & 0 \\ 0 & a_{32}^{ii} & a_{33}^{ii} & a_{34}^{ii} \\ 0 & a_{42}^{ii} & a_{43}^{ii} & a_{44}^{ii} \end{bmatrix}$$

$$[A_{ij}] = \begin{bmatrix} 0 & a_{12}^{ij} & a_{13}^{ij} & 0 \\ 0 & 0 & 0 & 0 \\ 0 & a_{32}^{ij} & a_{33}^{ij} & 0 \\ 0 & a_{42}^{ij} & a_{43}^{ij} & 0 \end{bmatrix}$$

and

$$\underline{b}_i = [0 \ 0 \ 0 \ b_4]^t$$

where

$$a_{11}^{ii} = -K_{Di}/M_i$$

$$a_{12}^{ii} = (Q_{io} + B_{ii} E_{io}^2)/M_i$$

$$a_{13}^{ii} = -(P_{io} + G_{ii} E_{io}^2)/(M_i E_{io})$$

$$a_{32}^{ii} = -(x_{di} - x'_{di})(P_{io} - G_{ii} E_{io}^2)/(T'_{doi} E_{io})$$

$$a_{33}^{ii} = [(x_{di} - x'_{di}) B_{ii} - 1]/T'_{doi}$$

$$a_{34}^{ii} = 1/T'_{doi}$$

$$a_{42}^{ii} = K_{Ri} [x_{di}'^2 (P_{io} B_{ii} + Q_{io} G_{ii}) + x'_{di} (P_{io} - G_{ii} E_{io}^2)] / (T_{Ri} V_{Tio})$$

$$a_{43}^{ii} = -K_{Ri} [x'_{di} \{ x'_{di} (P_{io} G_{ii} - Q_{io} B_{ii}) - Q_{io} \} / E_{io} + E_{io} (1 + x'_{di} B_{ii})] / (T_{Ri} V_{Tio})$$

$$a_{44}^{ii} = -1/T_{Ri}$$

for $j \neq i$

$$a_{12}^{ij} = -E_{io} E_{jo} D_{ij} / M_i$$

$$a_{13}^{ij} = -E_{io} C_{ij} / M_i$$

$$a_{32}^{ij} = (x_{di} - x'_{di}) E_{jo} C_{ij} / T'_{doi}$$

$$a_{33}^{ij} = (x_{di} - x'_{di}) D_{ij} / T'_{dio}$$

$$a_{42}^{ij} = -K_{Ri} E_{io} E_{jo} [x'_{di}{}^2 (P_{io} D_{ij} - Q_{io} C_{ij}) / E_{io}^2 + x'_{di} C_{ij}] / (T_{Ri} V_{Tio})$$

$$a_{43}^{ij} = -K_{Ri} E_{io} [x'_{di}{}^2 (P_{io} C_{ij} + Q_{io} D_{ij}) / E_{io}^2 - x'_{di} D_{ij}] / (T_{Ri} V_{Tio})$$

and

$$b_4 = K_{Ri} / T_{Ri}$$

4.3.1.2 Development of Output Equation

The output equation, in general, can be written as

$$y = [C] \underline{x}$$

where the elements of matrix C depend upon the output signal. Here, three signals are considered, namely, speed, power and frequency and matrix C is defined for each case. In case of speed and power signals, individual value for each machine and average value of all machines are considered.

Speed Signal

Change in rotor speed of machines is utilized as control signal and can be expressed as

(a) Individual Speed

$$y = \begin{bmatrix} \Delta \omega_1 \\ \Delta \omega_2 \\ \vdots \\ \Delta \omega_n \end{bmatrix} = \begin{bmatrix} C_1 & & & \\ & \bigcirc & & \\ & & C_2 & \\ & & & \ddots \\ \bigcirc & & & & C_n \end{bmatrix} \begin{bmatrix} x_1 \\ x_2 \\ \vdots \\ x_n \end{bmatrix} \quad (4.27)$$

where $\underline{C}_i = [1 \ 0 \ 0 \ 0]$

and $\underline{x}_i = [\Delta\omega_i \ \Delta\delta_i \ \Delta E_i \ \Delta E_{fdi}]^t$

(b) Average Speed :

$$y = \frac{1}{n} \sum_{i=1}^n \Delta\omega_i$$

$$= [C_1 \ C_2 \ \dots \ C_n] \begin{bmatrix} x_1 \\ x_2 \\ \vdots \\ x_n \end{bmatrix}$$

where $\underline{C}_i = [\frac{1}{n} \ 0 \ 0 \ 0]$

Power Signal

As the armature resistance of machines are neglected, active power available at the terminal bus of a generator will be same as the active power developed by the generator at its internal bus and is given by eqn. (4.13) as shown below.

(a) Individual Power

$$y = [\Delta P_1 \ \Delta P_2 \ \dots \ \Delta P_n]^t$$

where

$$\Delta P_i = C_{ii} x_i + \sum_{\substack{j=1 \\ j \neq i}}^n C_{ij} x_j \quad (4.28)$$

$$C_{ii} = [0 \mid -(Q_{i0} + B_{ii} E_{i0}^2) \mid (P_{i0} + G_{ii} E_{i0}^2) / E_{i0} \mid 0]$$

and

$$C_{ij} \Big|_{j \neq i} = [0 \mid (E_{i0} E_{j0} D_{ij}) \mid (E_{i0} C_{ij}) \mid 0]$$

(b) Average Power

Feedback signal for each machine will be

$$y = \frac{1}{n} \sum_{i=1}^n \Delta P_i$$

Frequency Signal

Frequency signal can be derived from the voltage the terminal bus as

$$\Delta f_i = p \Delta \theta_i$$

The voltage angle θ_i can be expressed as (Appendix D)

$$\theta_i = \delta_i - \beta_i$$

where $\beta_i = \tan^{-1} \left(\frac{v_{di}}{v_{qi}} \right)$

Linearizing eqn. (4.30) and substituting the values of v_{di} , v_{qi} , Δv_{di} and Δv_{qi} respectively from eqn. (4.21), (4.22), (4.23) and (4.24), we get

$$\Delta \theta_i = \eta_1^{ii} \Delta \delta_i + \eta_2^{ii} \Delta E_i + \sum_{\substack{j=1 \\ j \neq i}}^n (\eta_1^{ij} \Delta \delta_j + \eta_2^{ij} \Delta E_j) \quad (4.31)$$

where

$$\eta_1^{ii} = \frac{1}{V_{Tio}^2} [V_{Tio}^2 - x'_{di} \{ \frac{x'_{di}}{E_{io}} (P_{io}^2 + Q_{io}^2) + x'_{di} (P_{io} G_{ii} - Q_{io} B_{ii}) + Q_{io} + B_{ii} E_{io}^2 \}]$$

$$\eta_2^{ii} = \frac{x'_{di}}{V_{Tio}^2 E_{io}} [x'_{di} (P_{io} B_{ii} + Q_{io} G_{ii}) + (P_{io} - G_{ii} E_{io}^2)]$$

$$\eta_1^{ij} \Big|_{j \neq i} = \frac{E_{i0} E_{j0}}{V_{Tio}^2} \left[\frac{x_{di}'^2}{E_{i0}^2} (P_{i0} C_{ij} + Q_{i0} D_{ij}) - x_{di}' D_{ij} \right]$$

and

$$\eta_2^{ij} \Big|_{j \neq i} = \frac{E_{i0}}{V_{Tio}^2} \left[\frac{x_{di}'^2}{E_{i0}^2} (Q_{i0} C_{ij} - P_{i0} D_{ij}) - x_{di}' C_{ij} \right]$$

Substituting the value of $\Delta \theta_i$ from eqn. (4.31) in eqn. (4.29).

we get

$$\Delta f_i = \sum_{i=1}^n C_i x_i \quad (4.32)$$

where C_i is a row-vector and can be expressed as

$$C_i = \left[\eta_1^{ii} \mid \sum_{j=1}^n \eta_2^{ij} a_{32}^{ij} \mid \sum_{j=1}^n \eta_2^{ij} a_{33}^{ij} \mid \eta_2^{ii} a_{34}^{ii} \right]$$

4.3.1.3 Calculation of Operating Point

The development of system model presented in the previous section is general and can be applied to any multimachine system where the network is represented by reduced admittance matrix retaining generator internal buses. Elements of system matrix can be directly evaluated, as shown, from the knowledge of active and reactive powers and voltages at the internal buses of generators. For any multimachine system this information can be obtained from load flow analysis. For the system considered, Fig. 4.7, bus quantities, i.e., P, Q, E and δ at the internal buses of generators can be obtained as follows.

For a given plant output and fixed infinite bus voltage, first the magnitude and angle of terminal bus voltage are obtained and then from the knowledge of load distribution factor, internal bus quantities are obtained. From Fig. 4.8, plant output can be expressed as

$$P_T + jQ_T = V_T \angle \theta \cdot i^* \quad (4.33)$$

where

$$i = \frac{1}{Z_{eq}} [V_T \angle \theta - V_{eq} \angle \gamma] \quad (4.34)$$

Substituting the values of i , Z_{eq} and $V_{eq} \angle \gamma$ respectively from eqns. (4.34), (4.19) and (4.2) in eqn. (4.33) and separating the real and imaginary parts, we get

$$V_T V \cos \theta = V_T^2 a - u \quad (4.35)$$

$$V_T V \sin \theta = V_T^2 b - v \quad (4.36)$$

where

$$u + jv = (P_T + jQ_T) Z_T^*$$

and

$$a + jb = (1 + Z_T Y_S)^*$$

Solving eqns. (4.35) and (4.36) for V_T and θ , as

$$V_T = \left[\frac{1}{2a_1} (-b_1 + \sqrt{b_1^2 - 4a_1c_1}) \right]^{1/2} \quad (4.37)$$

and

$$\theta = \tan^{-1} \left(\frac{V_T^2 b - v}{V_T^2 a - u} \right) \quad (4.38)$$

where

$$a_1 = a^2 + b^2$$

$$b_1 = -(V^2 + 2ua + 2vb)$$

$$c_1 = u^2 + v^2$$

Consider the load distribution among various units of the plant as

$$P_{Ti} = \alpha_i^p P_T$$

$$Q_{Ti} = \alpha_i^q Q_T$$

α_i^p and α_i^q are distribution factors such that $\sum \alpha_i^p = 1$ and $\sum \alpha_i^q = 1$. Current supplied by the i th unit will be

$$i_i = \left(\frac{P_{Ti} + jQ_{Ti}}{V_T \angle \theta} \right)^* \quad (4.39)$$

and the internal bus voltage, from Fig. 4.8, will be

$$E_i \angle \delta_i = V_T \angle \theta + jx'_{di} i_i \quad (4.40)$$

Power developed at the internal bus of the generator can be expressed as

$$P_i + jQ_i = E_i \angle \delta_i \cdot i_i^* \quad (4.41)$$

4.3.2 Numerical Example

The system described in Section 4.2 is considered for the analysis. In order to investigate the effect of interaction between machines in the plant, an identical machine is

considered to operate in parallel with the existing machine of the plant. PSS of Table 4.3, designed at $X_T = 0.6$ p.u., is employed on both the machines with appropriate signals. Stable P-Q regions are then obtained for different system transmission strengths, i.e., for values of X_T of 0.2, 0.4, 0.6 and 0.8 p.u. In obtaining the stable P-Q regions it is assumed that both the machines are equally loaded. Figures 4.10 to 4.14 represent the stable P-Q regions obtained in the two machine case. P_T and Q_T in these figures represent the per unit plant output.

Speed Signal

Figures 4.10 and 4.11 compare the stable P-Q regions obtained with speed signal in case of single machine and two machine systems. In Fig. 4.10 stable P-Q regions for two machine system are obtained using individual speed signals while in Fig. 4.11 the regions are obtained using the average speed signal. Figure 4.12 compares the effectiveness of individual and average speed signals for the two machine case.

Power Signal

Figure 4.13 represents the stable P-Q regions obtained with power signal in case of single and two machine systems. In the two machine case, individual and average power signals give same stable P-Q regions. Curves with bold lines represent the network limits.

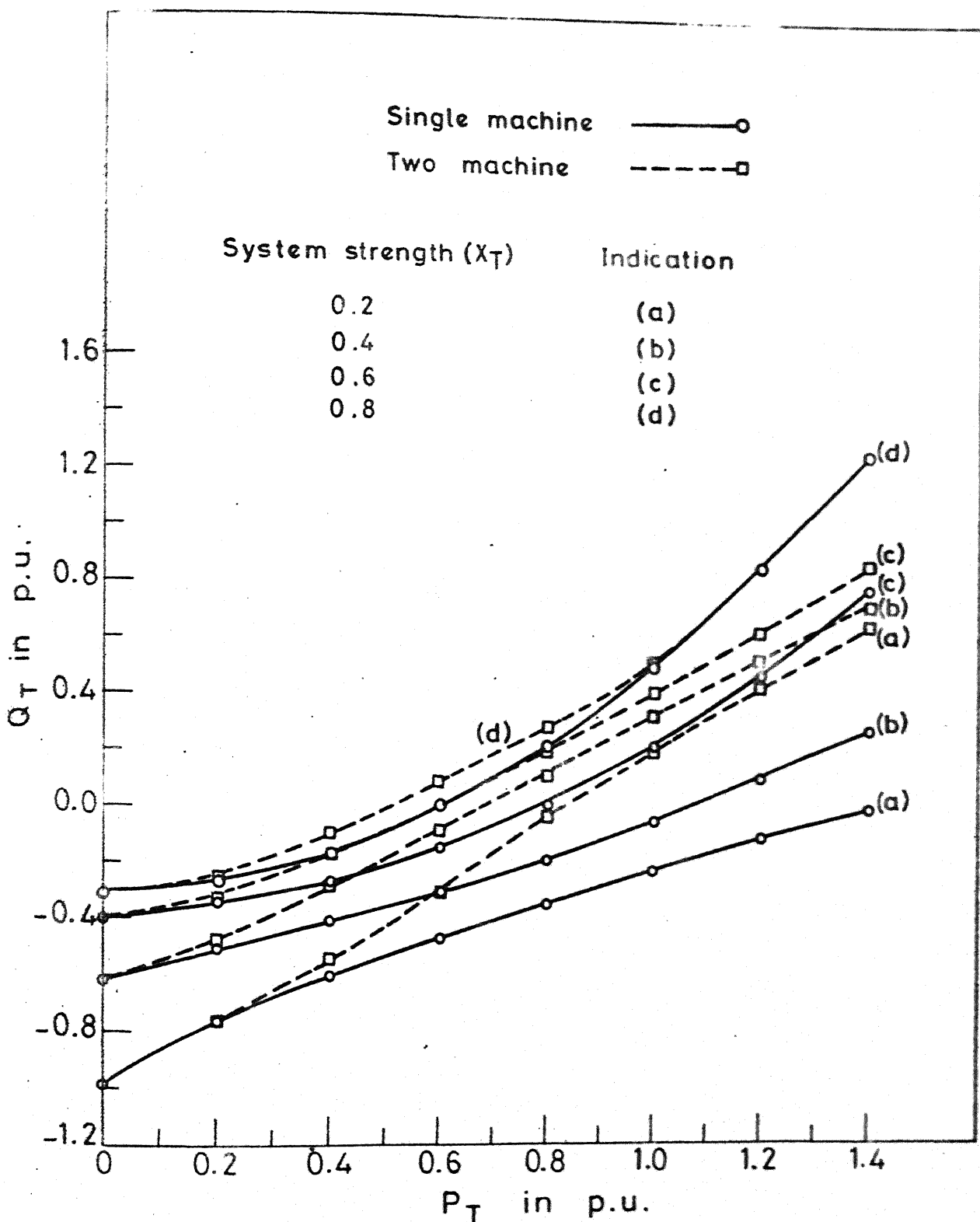


FIG. 4.10 STABLE P-Q REGION WITH SPEED (INDIVIDUAL) SIGNAL FOR SINGLE AND TWO MACHINE SYSTEM.

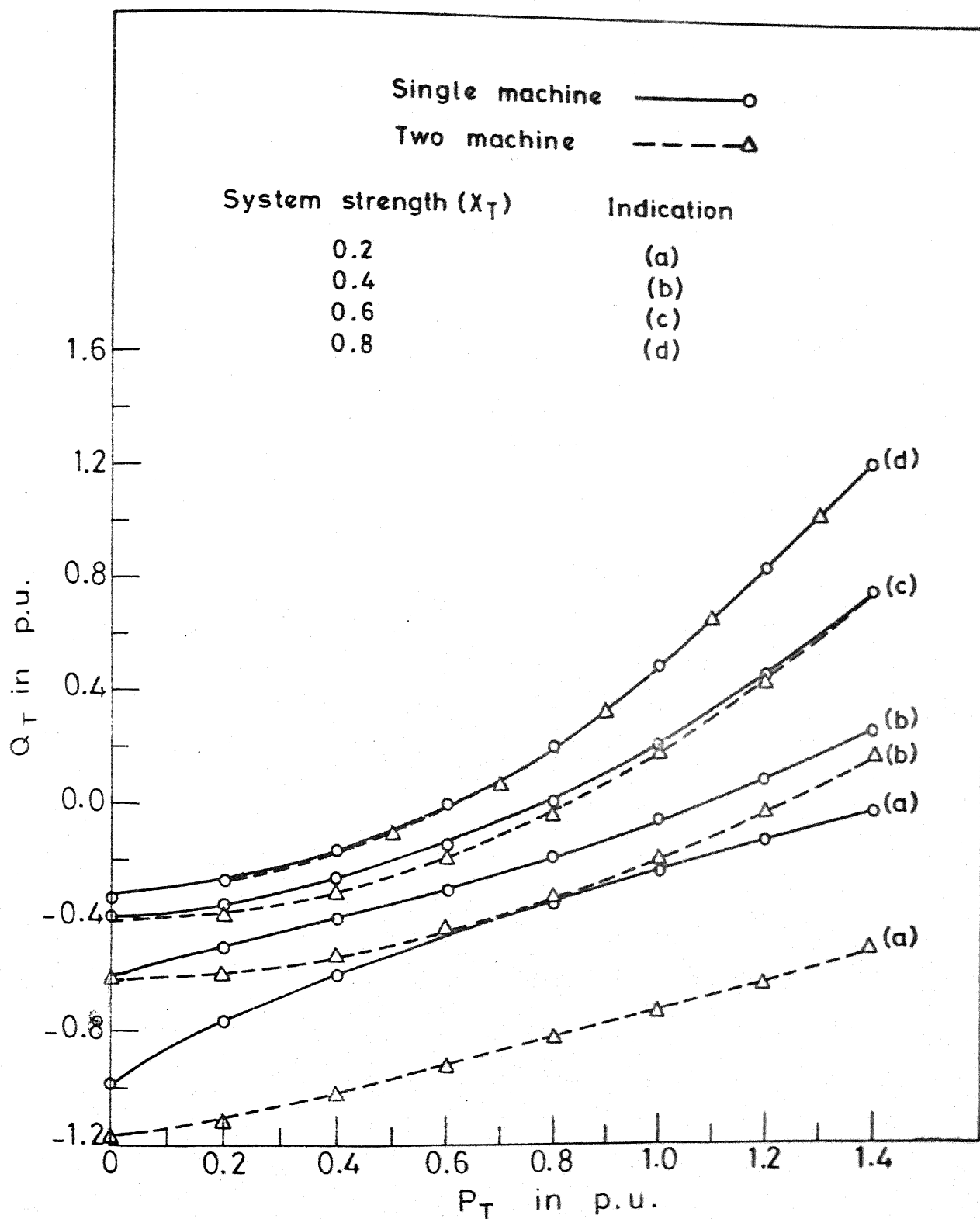


FIG. 4.11 STABLE P-Q REGION WITH SPEED (AVERAGE) SIGNAL FOR SINGLE AND TWO MACHINE SYSTEM.

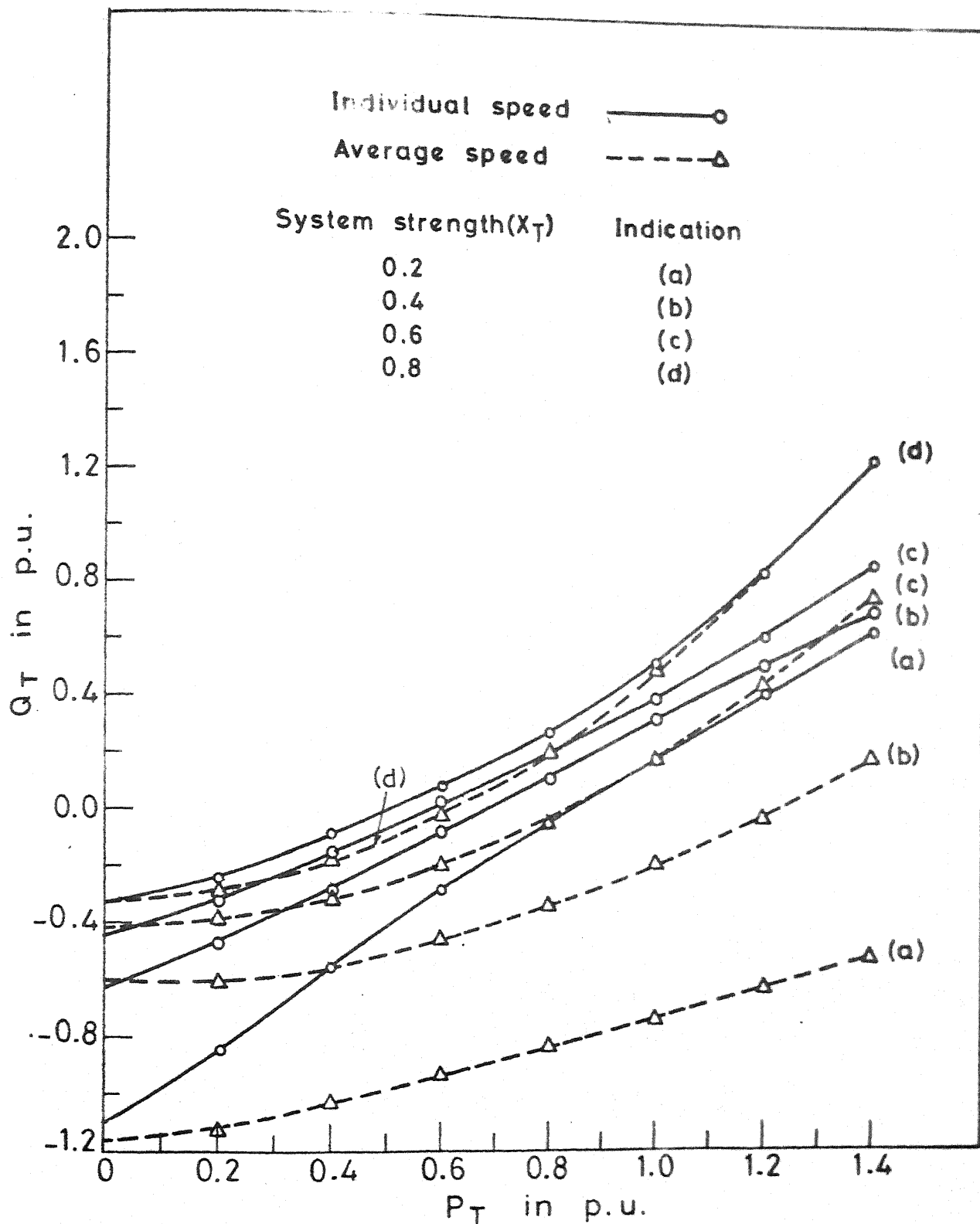


FIG. 4.12 STABLE P-Q REGION WITH INDIVIDUAL AND AVERAGE SPEED SIGNAL FOR TWO M/C SYSTEM.

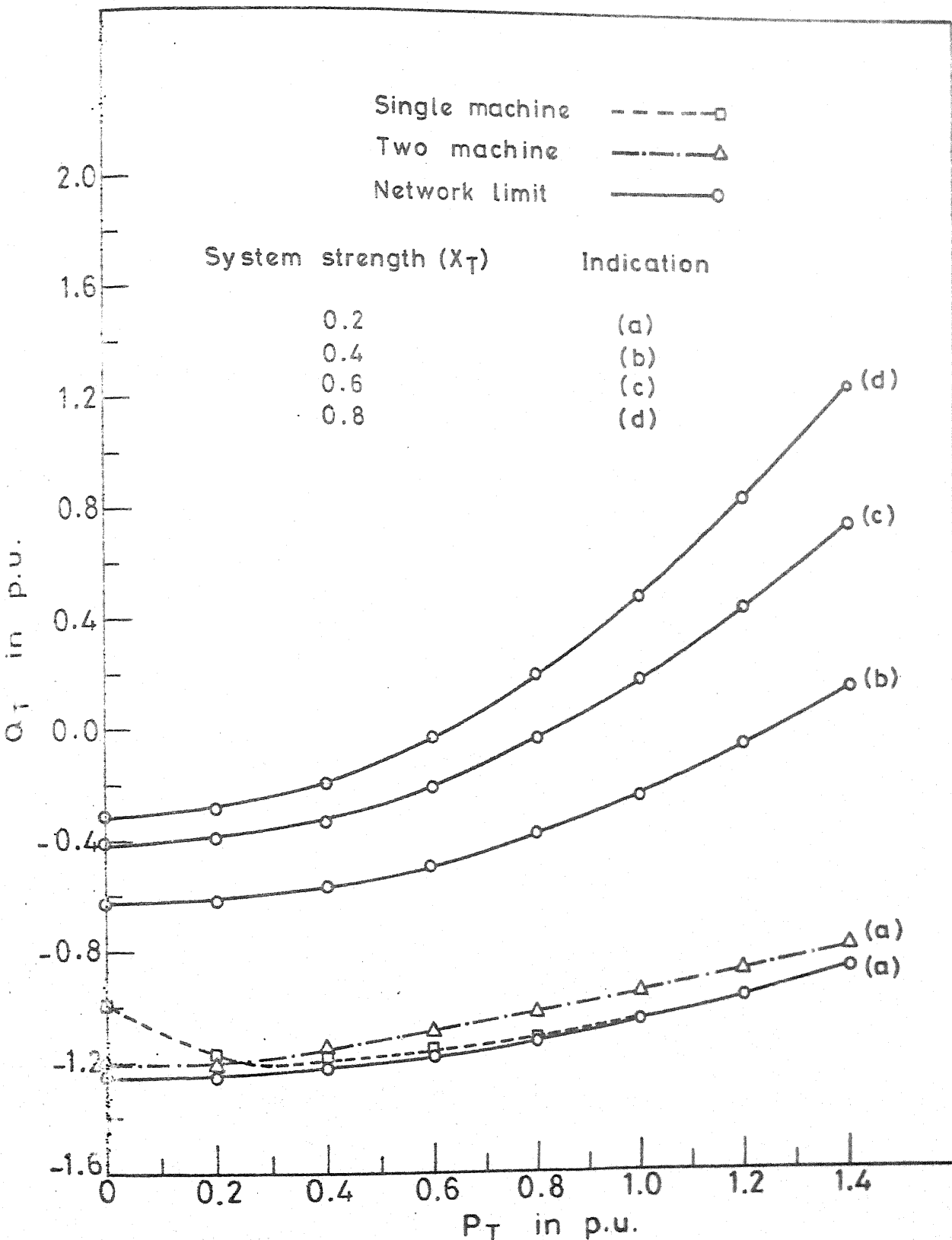


FIG. 4.13 STABLE P-Q REGION WITH POWER SIGNAL FOR SINGLE AND TWO MACHINE SYSTEM.

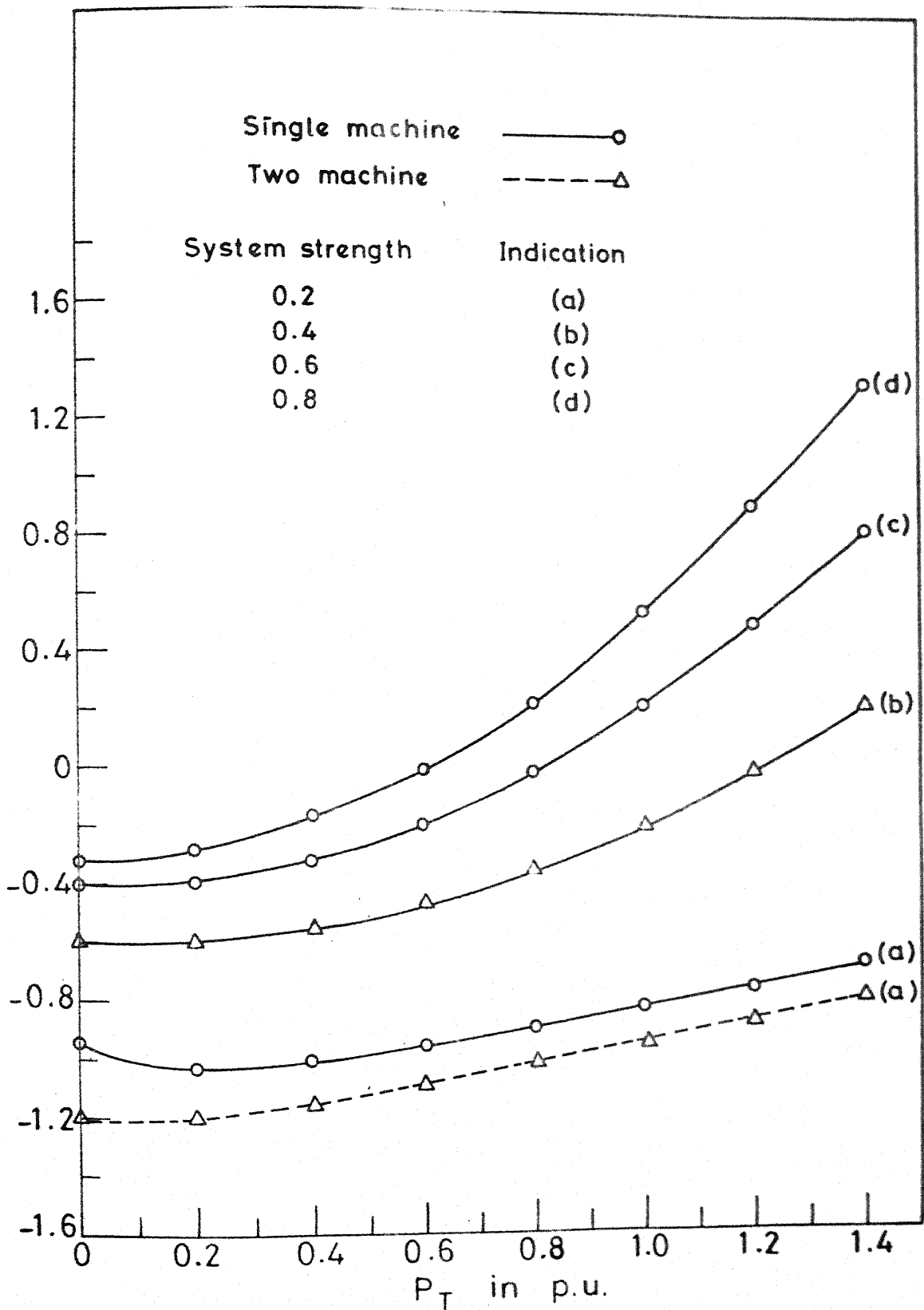


FIG. 4.14 STABLE P-Q REGION WITH FREQUENCY SIGNAL FOR SINGLE AND TWO M/C SYSTEM.

Frequency Signal

Figure 4.14 represents the stable P-Q regions obtained with frequency signal in case of single and two machine systems.

4.3.3 Discussion of Results

Speed Signal

Figure 4.10 shows that stable P-Q region obtained in the case of the single machine system is larger than that obtained in the two machine system, for all values of X_T , when the signal fed to PSS is the individual machine speed. The difference in the stable P-Q regions is significant for stronger system and reduces with the reduction in system strength. This shows that the presence of other machines in the generating plant reduces the effectiveness of PSS utilizing individual speed signals. If, instead of individual speed signal, average speed signal is used in the two machine system, the stable P-Q region obtained is larger than that obtained in single machine system as shown in Fig. 4.11. Again, the difference in stable P-Q region is significant for stronger systems. Thus, in case of plants having more than one machine, average speed signal increases the effectiveness of PSS.

Power Signal

As in the case of single machine system with power signal, the network limit is reached before the stability limit for individual and average power signals, except for $X_T = 0.2$ p.u. Curves with full lines in Fig. 4.13 represent network limit. For $X_T = 0.2$ p.u. the stable P-Q region in the two machine system is the same for individual and average power signals. The stable P-Q region for $X_T = 0.2$ p.u. in the two machine system is less than that obtained in the single machine system as shown in Fig. 4.13. This shows that effectiveness of PSS utilizing power signal reduces with the presence of other machines in the plant.

Frequency Signal

Figure 4.14 shows that stable P-Q regions obtained with frequency signal for the single machine and two machine systems coincide for all values of X_T except for $X_T = 0.2$ p.u. For $X_T = 0.2$ p.u. the stable P-Q region obtained in two machine system is more than that obtained in single machine system. Thus, presence of other machines in the generating plant improves the performance of PSS utilizing frequency signal.

An inspection of closed-loop eigenvalues (which are not reproduced here) at the stability boundary reveals that instability in every case is due to the shifting of exciter

mode to the right half of the complex plane. Eigenvalues corresponding to the rotor oscillation mode remain in the left half of the complex plane.

In the two machine system, with speed and power signals, where individual or average signal can be used, average speed signal is more effective than individual speed signal as shown in Fig. 4.12. But individual power and average power signals give the same P-Q region and are thus equally effective.

In two machine case with plant signals, that is, average speed, average power and bus frequency signal, it is found that (with identical machines and with equal loading) six of the closed-loop eigenvalues are unaffected even though PSS is provided on both the machines. This suggests that the system is not fully controllable. This situation is analysed as given in Appendix F and proof is obtained in the support of these results.

4.4 CONCLUSIONS

A case study on the effectiveness of the various feedback control signals that can be used in the design of PSS for the improvement of dynamic stability has been presented. Rotor speed, electrical power output and bus frequency are the three signals considered for the study. The effectiveness of signals is judged from the stable P-Q regions obtained using the above signals as input to PSS. A comparison of the effectiveness of

PSS designed using classical control theory and pole assignment technique has been made. The effect of the presence of other machines in a generating plant on the system performance with different PSS is studied.

From the results it can be concluded that PSS utilizing speed and frequency signals should be designed for weak systems. In case of power signal the results show that it is immaterial what value of ac system strength the PSS is designed for, in terms of stable P-Q domains.

Power signal is most effective for all operating conditions in comparison with speed and frequency signals. Effectiveness is more significant for strong systems. For strong systems speed signal is most inefficient. For weak systems and higher loading conditions speed signal is better than frequency signal, however the difference in stable P-Q regions is small.

In the example considered it is observed that with speed and frequency signals, effectiveness of PSS increases with the presence of other machines in the generating plant. But with power signal effectiveness decreases with the presence of other machines. For the two machine case average speed signal is better than individual speed signals but individual and average power signals are equally efficient.

CHAPTER 5

MODELLING OF MULTIMACHINE SYSTEM AND CHOICE OF PSS LOCATION

5.1 INTRODUCTION

In the previous chapter, development of system model is presented for a generating plant having n number of machines, connected to a large power system. The formulation is general enough to be applied to any multimachine system with the condition that (a) the network is represented by reduced admittance matrix which retains only the internal buses of the machines and (b) the transient saliency of the machines is neglected. The formulation assumes that the loads are represented by constant impedances. It is not always possible to reduce the network to the generator internal buses, particularly when the identity of the loads is to be retained. Moreover, when the saliency of machines is considered, it is not possible to represent the deviations in active and reactive powers as functions of state-variables only, as given in eqns. (4.13) and (4.14). Each machine, alongwith its excitation system in the formulation, is represented by a fourth order model. No freedom is available to increase or decrease the order of machine model. Apart from the method proposed in Chapter 4, a number of methods are available for the formulation of system

matrix in a multimachine power system [10-15]. In all the methods, the power system network is reduced to eliminate the non-generator buses by representing loads as constant impedances.

In this chapter a general formulation, similar to that of Ref. [16], is presented for the development of system model in a multimachine system. In the formulation presented here, the identity of the entire power system network is retained by utilizing the network Jacobian which is calculated during the load-flow analysis by Newton's method. This approach helps in the representation of nonlinear voltage dependent loads which otherwise are represented as constant impedances. Freedom is available for the representation of each machine either by a detailed model or by simplified models as per the requirement. The system model of the multimachine system is obtained systematically by developing the models of various machines and their interconnection through the network Jacobian.

The second aspect which is discussed in this chapter is the choice for proper locations of PSS in a large multimachine system. A proper choice of PSS location is essential to get the maximum benefit from the point of view of improving dynamic stability in an interconnected power system. In a large scale power system the selection of effective locations of PSS is a complex problem and is normally decided by the economical and technical considerations. Incorporation of PSS on all the

machines of a multimachine power system is not essential as it would be uneconomical and also it may not be desirable from the point of view of coordination between various machines in a large system [17]. For satisfactory system damping it is usually sufficient to equip relatively few machines with PSS. The optimal location of PSS has been investigated in various references [17-20]. de Mello et al. [17] suggested a method, based on eigenvalue-eigenvector analyses, for the selection of the machine which is the most effective candidate for stabilization. No conclusive results were given about the effectiveness of the method. Reference [20] presents a sequential procedure for the selection of machines to be equipped with PSS. The selection is based on the sensitivity of critical eigenvalues to the increase in the coefficient of a damping term which is inserted in each equation of motion, in succession.

Two analytical techniques are presented here for the selection of PSS locations in multimachine power systems. The first technique is independent of the feedback controller structure and the second one is based on eigenvalue sensitivity analysis [18]. A case study of a 13-machine system is presented for the selection of PSS. Root-loci of the closed-loop eigenvalues are obtained to validate the results obtained through the proposed techniques.

5.2 DEVELOPMENT OF SYSTEM MODEL

The formulation of system matrices A, B and C in a multi-machine power system is based on identifying the interconnections between various machines through the power system network. Each generating unit comprises of synchronous machine, excitation system, turbine and governor systems. For dynamic stability analysis, dynamics of turbine and governor systems are neglected because of the large time constants associated with them. Network is represented by its Jacobian matrix, J as

$$\Delta \underline{S} = [J] \Delta \underline{Z} \quad (5.1)$$

where

$$\Delta \underline{S} = [\Delta \underline{S}_1^t \quad \Delta \underline{S}_2^t \quad \dots \quad \Delta \underline{S}_N^t]^t$$

$$\Delta \underline{Z} = [\Delta \underline{Z}_1^t \quad \Delta \underline{Z}_2^t \quad \dots \quad \Delta \underline{Z}_N^t]^t$$

and

$$\Delta \underline{S}_i = [\Delta P_i \quad \Delta Q_i]^t$$

$$\Delta \underline{Z}_i = [\Delta \theta_i \quad \Delta V_{ti}]^t$$

The matrix [J] is of (2N, 2N) dimension, where N is the number of buses in the system. The effect of any nonlinear voltage dependent load can be considered by modifying the corresponding diagonal block of J.

In order to utilize the network equations given in the form of eqn. (5.1), the machine model has to be compatible. The linearized machine model is derived in a form such that

ΔP_g and ΔQ_g are the inputs from the network, and the machine terminal quantities $\Delta \theta$ and ΔV_t are expressed in terms of the machine state variables and $\Delta P_g, \Delta Q_g$. A general synchronous machine model [78] is utilized here with some modification where the Park's components of stator currents Δi_d and Δi_q are input variables. Thus, in order to make the machine model compatible with the network model, the stator currents Δi_d and Δi_q are expressed in terms of ΔP_g and ΔQ_g . This representation eliminates the use of transformation of the variables from machine reference frame to the common reference frame because ΔP_g and ΔQ_g remain invariant with change of reference frame. The only assumption made here is that the network is in quasi-steady state, which is well accepted in stability studies.

The development of the system model is based on the formulation of individual machine models and combining them through the network equations given in (5.1).

5.2.1 Generating Units

Synchronous Machine

The general synchronous machine model [78] with some modification (see Appendix D) is used to represent the synchronous machine. The linearized dynamical equations of the machine, (eqn. (D.25)), are given by

$$p \hat{\underline{x}}_m = [A_m] \hat{\underline{x}}_m + [B_{ap}] \Delta \underline{S}_g + b_{me} \Delta E_{fd} + b_{mg} \hat{P}_m \quad (5.2)$$

where $\hat{\underline{x}}_m$ is the vector of state variables. Order of $\hat{\underline{x}}_m$ depends upon the details used in the representation of synchronous machine depending upon the availability of data and the need for suitable accuracy, $\hat{\underline{x}}_m$ usually used in dynamic stability analysis are

$$\text{Detailed representation : } \hat{\underline{x}}_m \triangleq [\Delta \omega \Delta \delta \Delta I_d \Delta I_q \Delta \Psi_f \Delta \Psi_k]^t$$

$$\text{Simplified representation: } \hat{\underline{x}}_m \triangleq [\Delta \omega \Delta \delta \Delta I_d]^t$$

$$\text{Classical representation : } \hat{\underline{x}}_m \triangleq [\Delta \omega \quad \Delta \delta]^t$$

The generator terminal bus voltage phase angle and magnitude are expressed, (eqn. (D.24)), in the form

$$\Delta \underline{Z}_g = [D_s] \hat{\underline{x}}_m + [D_p] \Delta \underline{S}_g \quad (5.3)$$

where

$$\Delta \underline{Z}_g \triangleq [\Delta \theta \quad \Delta V_t]^t$$

The derivation of eqns. (5.2) and (5.3) is given in Appendix D.

Excitation System

The representation of various excitation systems used, is compiled in IEEE Committee Report [9]. The state-space model of the excitation system is represented, (eqn. (D.32)), in the form

$$p \underline{x}_e = [A_e] \underline{x}_e + b_{ev} \Delta V_t + b_{eu} \Delta V_{ref} + b_{eu} \cdot u \quad (5.4)$$

and

$$y_e = \Delta \Xi_{fd} = [C_e] \cdot x_e \quad (5.5)$$

where x_e , u and y_e are respectively the state, input and output variables of the excitation system. ΔV_t can be expressed in terms of state variables of machine and ΔS_g as

$$\Delta V_t = [W_{a5}] \Delta S_g + [W_{a6}] x_m \quad (5.6)$$

where W_{a5} and W_{a6} are submatrices obtained respectively from D_p and \hat{D}_s of eqn. (5.3).

Combined Model of Generating Unit

Combining eqns. (5.2), (5.4), (5.5) and (5.6), the state-space model of the generating unit is obtained as

$$p \underline{x}_m = [A_m] \underline{x}_m + [B_p] \Delta S_g + \underline{b}_g \Delta P_m + \underline{b} \Delta V_{ref} + \underline{b} u \quad (5.7)$$

where

$$\underline{x}_m = [\hat{x}_m^t \ x_e^t]^t$$

$$A_m = \begin{bmatrix} \hat{A}_m & b_{me} \cdot C_e \\ b_{ev} \cdot W_{a6} & A_e \end{bmatrix}; \quad B_p = \begin{bmatrix} B_{ap} \\ b_{ev} \cdot W_{a5} \end{bmatrix}$$

$$\underline{b}_g = [b_{mg}^t \ 0]^t; \quad \underline{b} = [0 \ b_{eu}^t]^t$$

and the terminal condition of the generating unit is given as

$$\Delta Z_g = [D_s] \underline{x}_m + [D_p] \Delta S_g \quad (5.8)$$

where

$$D_s = [D_s \ 0]$$

The values of the various variables, appearing in the elements of A_m , B_p , b_g and b at the operating point are calculated from load-flow results as discussed in Appendix D.

5.2.2 Network Representation

The network is represented by its Jacobian matrix in the polar form as given in eqn. (5.1). For an N-bus power system network, the Jacobian matrix is of $(2N \times 2N)$ dimension. The procedure for evaluating the elements of Jacobian matrix is given in Appendix G. Without loss of generality, it is assumed that the elements of the Jacobian are ordered and arranged in such a form that the first 'n' nodes are generator buses and the last 'm' nodes are load buses. The network eqn. (5.1) can be rearranged as

$$\begin{bmatrix} \Delta S_G \\ \Delta S_L \end{bmatrix} = \begin{bmatrix} J_{GG} & J_{GL} \\ J_{LG} & J_{LL} \end{bmatrix} \begin{bmatrix} \Delta Z_G \\ \Delta Z_L \end{bmatrix} \quad (5.9)$$

where J_{GG} , J_{GL} , J_{LG} and J_{LL} are matrices of order $(2n \times 2n)$, $(2n \times 2m)$, $(2m \times 2n)$ and $(2m \times 2m)$ respectively.

5.2.3 Load Representation

The usual constant power, constant current or constant impedance type loads or any other voltage dependent nonlinear load can be represented in the general form

$$P_{\ell} = K_p V_{\ell}^{n_p} \quad (5.10)$$

$$Q_{\ell} = K_q V_{\ell}^{n_q} \quad (5.11)$$

where the coefficients K_p and K_q and the exponents n_p and n_q depend upon the type of load under consideration. Linearizing eqns. (5.10) and (5.11), we get

$$\Delta \underline{S}_{\ell} = [\underline{A}_{\ell}] \Delta \underline{Z}_{\ell} \quad (5.12)$$

where

$$\Delta \underline{S}_{\ell} \triangleq [\Delta P_{\ell} \ \Delta Q_{\ell}]^t$$

$$\Delta \underline{Z}_{\ell} \triangleq [\Delta \theta_{\ell} \ \Delta V_{\ell}]^t$$

and

$$[\underline{A}_{\ell}] = \begin{bmatrix} 0 & n_p K_p & V_{\ell}^{n_p-1} \\ 0 & n_q K_q & V_{\ell}^{n_q-1} \end{bmatrix}$$

Eqn. (5.12) is used to eliminate $\Delta \underline{S}_{\ell}$ corresponding to the load buses in the network eqn. (5.9). $\Delta \underline{S}_{\ell}$ in eqn. (5.12) represents the change in load power at a load bus and as per convention in load-flow analysis, load power is considered as negative injection. Thus, $\Delta \underline{S}_{\ell}$ in eqn. (5.12) is one of the entries of $\Delta \underline{S}_L$ in eqn. (5.9) with a negative sign.

5.2.4 State-Space Model of the Overall System

For the analysis of large scale power systems consisting of large number of generating units and loads, models of the

individual components are assembled together to get the final state-space model of the entire system. With 'n' number of generator buses and 'm' number of load buses, eqns. (5.7), (5.8) and (5.12) can be written respectively as

$$p \underline{X}_M = [A_M] \underline{X}_M + [B_P] \Delta \underline{S}_G + [B] \Delta \underline{V}_{Ref} + [B] \underline{U} + [B_M] \Delta \underline{T}_M \quad (5.13)$$

$$\Delta \underline{Z}_G = [D_S] \underline{X}_M + [D_P] \Delta \underline{S}_G \quad (5.14)$$

and

$$\Delta \underline{S}_L = -[A_L] \Delta \underline{Z}_L \quad (5.15)$$

where

$$\underline{X}_M = [x_{m1}^t \ x_{m2}^t \ \dots \ x_{mn}^t]^t$$

$$\Delta \underline{S}_G = [\Delta S_{g1}^t \ \Delta S_{g2}^t \ \dots \ \Delta S_{gn}^t]^t$$

$$\Delta \underline{V}_{Ref} = [\Delta V_{ref1} \ \Delta V_{ref2} \ \dots \ \Delta V_{refn}]^t$$

$$\underline{U} = [u_1 \ u_2 \ \dots \ u_n]^t$$

$$\Delta \underline{T}_M = [\Delta T_{m1} \ \Delta T_{m2} \ \dots \ \Delta T_{mn}]^t$$

$$\Delta \underline{Z}_G = [\Delta Z_{g1}^t \ \Delta Z_{g2}^t \ \dots \ \Delta Z_{gn}^t]^t$$

$$\Delta \underline{S}_L = [\Delta S_{l1}^t \ \Delta S_{l2}^t \ \dots \ \Delta S_{lm}^t]^t$$

$$\Delta \underline{Z}_L = [\Delta Z_{l1}^t \ \Delta Z_{l2}^t \ \dots \ \Delta Z_{lm}^t]^t$$

Matrices A_M , B_P , B , B_M , D_S and D_P all have block-diagonal structure with 'n' diagonal blocks as :

$$[A_M] = \text{Block diag. } [A_{m1}, A_{m2}, \dots, A_{mn}]$$

$$[B_p] = \text{Block diag. } [B_{p1}, B_{p2}, \dots, B_{pn}]$$

etc., while A_L is also a block-diagonal matrix with 'm' diagonal blocks. Now, eliminating ΔZ_L from eqns. (5.9) and (5.15), we get

$$\Delta S_G = [J'_{GG}] \Delta Z_G \quad (5.16)$$

where

$$[J'_{GG}] = [J_{GG}] - [J_{GL}] ([J_{LL}] + [A_L])^{-1} [J_{LG}]$$

From eqns. (5.14) and (5.16), ΔZ_G and ΔS_G can be expressed in terms of system state variables as

$$\Delta Z_G = ([I] - [D_p] [J'_{GG}])^{-1} [D_S] \underline{x}_M \quad (5.17)$$

and

$$\Delta S_G = [J'_{GG}] ([I] - [D_p] [J'_{GG}])^{-1} [D_S] \underline{x}_M \quad (5.18)$$

where I is an identity matrix of $(2n \times 2n)$ dimension. Substituting the value of ΔS_G from eqn. (5.18) into eqn. (5.13), the state-space model of the overall system can be expressed as

$$p \underline{x}_M = [A] \underline{x}_M + [B] u + [B] \Delta V_{\text{Ref}} + [B_M] \Delta T_M \quad (5.19)$$

where

$$[A] = [A_M] + [B_p] [J'_{GG}] ([I] - [D_p] [J'_{GG}])^{-1} [D_S]$$

5.3 CHOICE OF PSS LOCATION

It is desired to provide adequate damping to the electro-mechanical oscillations of the rotors of synchronous machines by proper choice of PSS location. For an n machine system, there are in general $(n-1)$ modes of rotor oscillation. For planning studies it is sufficient to use a simplified system model containing only relevant features. Classical model of machines, that is a constant voltage source behind its transient reactance, retains the information regarding electro-mechanical oscillations and is thus considered to be adequate for the development of system model. With this assumption, the system model given in eqn. (5.19) will take the form,

$$p \underline{X} = [A] \underline{X} + [B] \underline{U} \quad (5.20)$$

where $\underline{X} = [x_1^t \ x_2^t \ \dots \ x_n^t]^t$

$$\underline{U} = [u_1 \ u_2 \ \dots \ u_n]^t$$

$$\underline{x}_i \triangleq [\Delta\omega_i \ \Delta\delta_i]^t$$

and

$$u_i \triangleq \Delta E'_{qi}$$

Normally, rotor velocity of the machines is used as feedback control signal for PSS. Thus, the output equation of the entire system is

$$\underline{Y} = [C] \underline{X} \quad (5.21)$$

where the output matrix C has a block diagonal form with the diagonal block

$$C_1^T = [1 \ 0]$$

With the system defined by eqns. (5.20) and (5.21), the problem for the choice of PSS location can be stated as : select the smallest set of locations for PSS, from the n possibilities that exist, such that adequate damping is provided, with economical control effort, to the critical modes of the system

$$p \underline{X} = [A] \underline{X} + \sum_{i=1}^n b_i u_i \quad (5.22)$$

by the incorporation of PSS at these locations.

The two methods presented here are based on two different assumptions given below :

1. The controller structure is not decided apriori,
2. The controller structure is decided in advance.

In the first method, to get the maximum damping to a critical mode λ_j , the scalar products of W_j and b_i are obtained for all values of i , where W_j is the reciprocal eigenvector of the system matrix A corresponding to j th eigenvalue. The value of i for which magnitude of the scalar product, $|\langle W_j, b_i \rangle|$, is maximum decides the PSS location. Justification of this statement is given in Appendix H.

In the second method, the controller structure is decided as :

$$u_i = F_i y_i \quad (5.23)$$

and the eigenvalue sensitivity, $\frac{\partial \lambda_j}{\partial F_i}$, is obtained for all values of i . The value of i for which the real part of $\partial \lambda_j / \partial F_i$ has the maximum magnitude decides the PSS location. Justification of this statement is given in Appendix H. Eigenvalue sensitivity is given as

$$S_{ji} = \partial \lambda_j / \partial F_i = \frac{\langle b_i C_i V_j, W_j \rangle}{\langle V_j, W_j \rangle} \quad (5.24)$$

where C_i is the i th row of output matrix C , V_j and W_j are respectively the eigenvectors of matrices A and A^t corresponding to the j th eigenvalue.

5.4 NUMERICAL EXAMPLE

A case study of a large-scale power system consisting of 13 machines, 71 buses and 94 lines [18] is presented here. It consists of 5 thermal units and 8 hydro units. A single-line diagram of the system alongwith the system data and operating conditions are given in Appendix I. The following assumptions are made in deriving the system model.

1. The loads are represented by constant impedances.
2. For the sake of simplicity, damper circuits and transient saliency of all the machines are ignored. The damping coefficient K_D is considered to be zero for all the machines.

The operating point is obtained from load flow studies and the Jacobian of eqn. (5.9) is constructed as given in Appendix G.

5.4.1 Eigenvalue Analysis

The system matrix 'A' is developed, using the technique presented in Section 5.2, for the following three cases and eigenvalue analysis is carried out in each case.

1. All the machines are represented by second order classical model.
2. All the machines are represented by the third order model by including field flux decay.
3. Machines 1,7 and 11 are represented by a third order model along with a single time constant excitation system (IEEE type 13 -- Appendix D). The gain and time constant of voltage regulator for each machine are respectively selected as 50 and 0.02 sec. Rest of the machines are represented by the classical model.

Eigenvalues are computed for the three cases and are given in Table 5.1.

The first twelve pairs of complex eigenvalues in Table 5.1, for each case, represent the modes corresponding to electromechanical oscillations. In the first case, each machine is represented by the classical model and as damping has been neglected, pure oscillatory modes are obtained.

Table 5.1 Open-Loop Eigenvalues for the 13-Machine System

Case 1	Case 2	Case 3
0.0 ± j14.05998	-0.03030 ± j14.05821	0.02892 ± j14.05587
0.0 ± j12.82911	-0.03661 ± j12.82702	0.04537 ± j12.83184
0.0 ± j11.83387	-0.01742 ± j11.83252	0.00852 ± j11.83472
0.0 ± j10.80104	-0.00729 ± j10.80095	0.00988 ± j10.80273
0.0 ± j10.57432	-0.00962 ± j10.57362	0.00045 ± j10.57437
0.0 ± j10.46123	-0.00645 ± j10.46102	0.00674 ± j10.46237
0.0 ± j10.34287	-0.00512 ± j10.34252	0.01693 ± j10.34604
0.0 ± j10.17931	-0.01298 ± j10.17828	0.01668 ± j10.18523
0.0 ± j 9.40440	-0.00281 ± j 9.40421	0.00640 ± j 9.40696
0.0 ± j 8.83647	-0.01212 ± j 8.83592	0.01546 ± j 8.84131
0.0 ± j 7.87834	-0.01261 ± j 7.87752	0.03302 ± j 7.89500
0.0 ± j 6.11920	-0.03091 ± j 6.11762	0.05525 ± j 6.15929
	-0.23862	-5.78423
	-0.29501	-6.09830
	-0.30725	-6.88359
	-0.33450	-43.87653
	-0.37881	-44.58668
	-0.40155	-44.99036
	-0.41425	0.00000
	-0.42302	
	-0.47232	
	-0.53029	
	-0.65403	
	-0.78346	
	-0.94415	
	0.00000	

Eigenvalues obtained in case 2 indicate that the system is dynamically stable and that the field-windings contribute a small amount of damping. The addition of fast acting excitation systems on the selected machines introduces negative damping to all the modes of rotor oscillation as seen from the eigenvalues obtained in case 3.

5.4.2 Choice of PSS Location

The system model described in eqn. (5.20) is formulated according to the procedure given in Section 5.2, representing each machine by the classical model. Rotor speed is considered as the feedback signal for the calculation of eigenvalue sensitivity in eqn. (5.24). All the machines, taken one at a time, are considered for the location of PSS with the objective to damp the electromechanical oscillations. In the first method, magnitude of the scalar product of the reciprocal eigenvector w_j and the vector b_i is calculated for each pair of the complex eigenvalues, and for different locations of PSS, that is, for all values of i . The scalar products for different locations of PSS are given in Table 5.2. In the second method, eigenvalue sensitivity is calculated from eqn. (5.24) for each pair of the complex eigenvalues and for different locations of PSS. The eigenvalue sensitivities are given in Table 5.3.

Inspection of Tables 5.2 and 5.3 shows that the two methods, suggested for the determination of effective PSS

Table 5.2 Magnitude of Scalar Product $\langle \underline{I}_j, \underline{b}_i \rangle$ for
Different Locations of PSS

PSS Loca- tion (i)	$ \langle \underline{I}_j, \underline{b}_i \rangle $ for $j=1,6$					
	$\omega=14.05998$	12.82911	11.83387	10.80104	10.57432	10.46123
1	0.40381	5.82668	8.71262	12.94110	5.91329	10.77098
2	1.81758	5.58953	20.30348	0.53353	1.62319	2.78022
3	0.12794	0.21663	1.83405	1.13483	2.14868	15.23010
4	0.31270	0.43132	2.37522	0.63677	0.55600	6.81476
5	0.55664	0.69737	2.31093	27.71291	1.13545	1.15367
6	31.80959	32.54492	0.50501	1.25081	1.24167	0.76357
7	26.94005	27.17332	1.46061	0.33290	2.31875	0.29446
8	0.06791	0.59849	0.02936	0.05923	0.21050	0.12716
9	0.11791	1.52749	0.08793	0.12517	0.54344	0.37600
10	1.58906	0.69276	0.19437	1.01525	11.79566	6.64598
11	0.33487	2.05883	0.15234	0.13377	5.86513	3.02008
12	0.10071	0.61253	0.04435	0.03587	0.62803	0.11939
13	0.07338	0.38369	0.05373	0.27381	20.28680	3.28166

Table 5.2 (continued ...)

PSS Loca- tion (i)	$ \langle W_j, b_i \rangle $ for $j = 7, 12$					
	$\omega=10.34287$	10.17931	9.40440	8.83647	7.87834	6.11920
1	1.00089	10.08257	14.54410	12.40288	0.09206	13.17896
2	1.09020	6.68621	6.54314	1.99559	0.41993	14.25188
3	1.17253	3.38395	0.30858	1.74902	0.19675	3.00783
4	0.89402	4.52835	8.57733	16.31328	0.98267	10.64746
5	0.34826	2.79837	3.57630	3.74053	0.11180	4.41189
6	0.66268	3.23808	2.10063	5.14494	0.71179	1.81535
7	0.91773	5.03313	0.58178	5.50522	0.53124	1.56011
8	0.06055	0.69631	11.08748	0.85931	0.58172	0.97262
9	0.10742	1.17678	6.11219	0.93190	12.90535	8.83553
10	4.08828	25.29693	3.72950	8.52706	3.27969	7.38256
11	13.53257	5.09114	4.76912	3.66865	12.60648	13.21448
12	12.99066	2.99232	1.55000	1.21674	3.93132	4.12291
13	0.43437	2.85502	0.30512	0.28569	2.27224	2.99928

Table 5.3 Eigenvalue Sensitivity for Different Locations of PSS

PSS Loca- tion (i)	$R_e(S_{ji})$ for $j = 1$ to 6					
	$\omega=14.05998$	12.82911	11.83387	10.80104	10.57432	10.46123
1	-0.00620	-0.52349	-2.92563	-2.02784	-0.17426	-1.19265
2	-0.01862	-0.50313	-15.49297	-0.00103	-0.01068	-0.05401
3	0.00009	-0.00286	-0.76171	-0.09245	-0.22971	-14.38249
4	0.00011	-0.00278	-0.35346	-0.00615	-0.00355	-0.93463
5	-0.00618	-0.03492	-0.86528	-27.06433	-0.04406	-0.04557
6	-20.69321	-23.04929	-0.00770	-0.05023	-0.02885	-0.01097
7	-20.34194	-17.71073	-0.11821	0.00066	-0.08932	-0.00302
8	0.00111	0.02936	-0.00008	0.00106	-0.00732	-0.00510
9	-0.00026	0.01715	-0.00014	0.00030	-0.00041	-0.00521
10	-0.04659	0.14509	-0.00885	0.00750	-1.78015	-0.72881
11	0.00078	0.02345	-0.00040	-0.00016	-0.56753	-0.18132
12	0.00024	0.00673	-0.00010	-0.00005	-0.03223	-0.00001
13	0.00022	0.00846	-0.00033	0.00021	-19.66322	-0.69768

Table 5.3 (continued)

PSS Loca- tion (i)	$R_e(S_{ji})$ for $j = 7$ to 12					
	$\omega=10.34287$	10.17931	9.40440	8.83647	7.87834	6.11920
1	-0.00429	-1.07824	-0.42762	-3.41157	-0.00008	-1.70626
2	-0.00797	-0.54539	-0.09461	-0.16075	-0.00332	-2.32014
3	-0.07449	-1.06607	-0.00131	-0.34524	-0.00481	-0.71375
4	-0.01442	-0.64578	-0.36242	-10.30540	-0.03856	-2.98398
5	-0.00346	-0.35382	-0.08417	-0.78071	-0.00058	-0.59447
6	-0.00785	-0.36217	-0.01051	-1.02919	-0.01523	-0.03630
7	-0.01520	-0.83706	-0.00377	-1.02836	-0.00876	-0.00031
8	-0.00180	-0.30414	-10.96793	-0.37378	-0.10379	-0.23213
9	-0.00071	-0.10177	-0.37882	-0.13488	-9.82789	-3.98238
10	-0.23157	-15.36443	-0.11936	-1.73276	-0.17001	-1.12578
11	-4.10602	-0.77198	-0.10811	-0.70465	-4.85514	-5.50703
12	-12.23194	-1.01880	-0.04056	-0.25145	-1.54218	-1.74274
13	-0.02385	-0.85541	-0.00030	-0.02246	-0.57739	-1.07597

Table 5.4 Ranking of Different Locations of PSS

Mode of Oscillation		Ranking of Different Location of PSS in Descending Order of Effectiveness												
S.No.	ω	1	2	3	4	5	6	7	8	9	10	11	12	13
1	14.05998	6	7	10	2	1	5	9	3	4	13	12	11	8
2	12.82911	6	7	1	2	5	3	4	12	13	9	11	8	10
3	11.83387	2	1	5	3	4	7	10	6	11	13	9	12	8
4	10.80104	5	1	3	6	4	2	11	12	13	9	7	8	10
5	10.57432	13	10	11	3	1	7	5	12	6	2	8	4	9
6	10.46123	3	1	4	10	13	11	2	5	6	9	8	7	12
7	10.34287	12	11	10	3	13	7	4	2	6	1	5	8	9
8	10.17931	10	1	3	12	13	7	11	4	2	6	5	8	9
9	9.40440	8	1	9	4	10	10	2	5	12	6	7	3	13
10	8.83647	4	1	10	6	7	5	11	8	3	12	2	9	13
11	7.87834	9	11	12	13	10	8	4	6	7	3	2	5	1
12	6.11920	11	9	4	2	12	1	10	13	3	5	8	6	7

locations, give almost similar results. However, the eigenvalue sensitivity method gives additional information regarding the sign of damping provided to any mode.

Table 5.4 shows the ranking, in the descending order of effectiveness, of the PSS location for damping of each mode of rotor oscillation. Table 5.4 is obtained from the eigenvalue sensitivities given in Table 5.3.

5.4.3 Discussion of Results

The two proposed methods for the selection of effective PSS locations give closely agreeing results as shown in Tables 5.2 and 5.3. From the results shown in Table 5.3 it is found that for some of the PSS locations eigenvalue sensitivities are positive. This shows that providing PSS on such machines will result in negative damping of certain modes, while improving damping of other modes. This is expected in large power systems [17]. However, in the example considered, their numerical values are negligibly small in comparison with the sensitivities of other modes for the same PSS location.

An inspection of the elements of the first column of Table 5.4, that is, PSS locations with ranking one, shows that no PSS location occurs twice except location 6. Locations 1 and 7 are not present in this list. This shows that each mode of oscillation can be controlled by equipping PSS

on a different machine. However, the list of PSS locations with ranking two, that is, the second column of Table 5.4, shows that location 1 occurs six times, locations 7 and 11 occur twice. This suggests that equipping machine 1 with PSS will control six modes. In other words, the most effective location of PSS is machine 1. Next in the order of effectiveness are machines 6, 7 and 11. Looking into the numerical values of eigenvalue sensitivities for PSS locations 6 and 7, it is found that both locations provide almost the same damping to first and second modes, suggesting that either location can be chosen for equipping PSS. Thus, by providing PSS on machines 1, 6 (or 7) and 11 all the modes except fifth can be sufficiently damped. The fifth mode can be damped by providing PSS on machine 13. These results are based on the eigenvalue sensitivities obtained at zero feedback gain of controller as V_j and W_j in eqn. (5.24) are eigenvectors of the open-loop system matrix. The sensitivities change with feedback gain. Consequently, the open-loop sensitivity data can be used for a preliminary choice of PSS locations and analysis of the system after incorporation of PSS at these locations will indicate whether any modification in the choice is to be done.

To verify the results of Table 5.4, closed-loop eigenvalues of the system, described by eqn. (5.20), are obtained for variation in the feedback gain F_i using the control law as

$$\Delta E'_{qi} = F_i \Delta \omega_i$$

Figures 5.1 to 5.4 show the loci of closed-loop eigenvalues for variation in feedback gain considering one machine on control at a time.

Inspection of Figs. 5.1 to 5.4 confirms the results obtained from Table 5.4. Loci of eigenvalues show that each PSS location provides large damping to only one of the modes, in accordance with the list of PSS locations with ranking one given in the first column of Table 5.4. However, locations 1,2,4,6,7,9 and 11 provide damping to more than one mode. Locations 6 and 7, both give similar results for first and second modes, but location 7 provides more damping to first mode in comparison with location 6 (see Fig. 5.2). An inspection of Figs. 5.1 to 5.4 shows that by providing PSS on machines 1,7 and 11 all the modes, except fifth and ninth, can be sufficiently damped. Although, location 1 has rank two for the ninth mode in Table 5.4, the mode is unaffected by providing control on machine 1 as seen from Fig. 5.1. This can be explained from the relative values of eigenvalue sensitivities of this mode for locations 1 and 8.

From the foregoing discussions and on the basis of results of Table 5.4 and Figs. 5.1 to 5.4, following recommendations are made, as shown in Table 5.5, for providing PSS in the example considered.

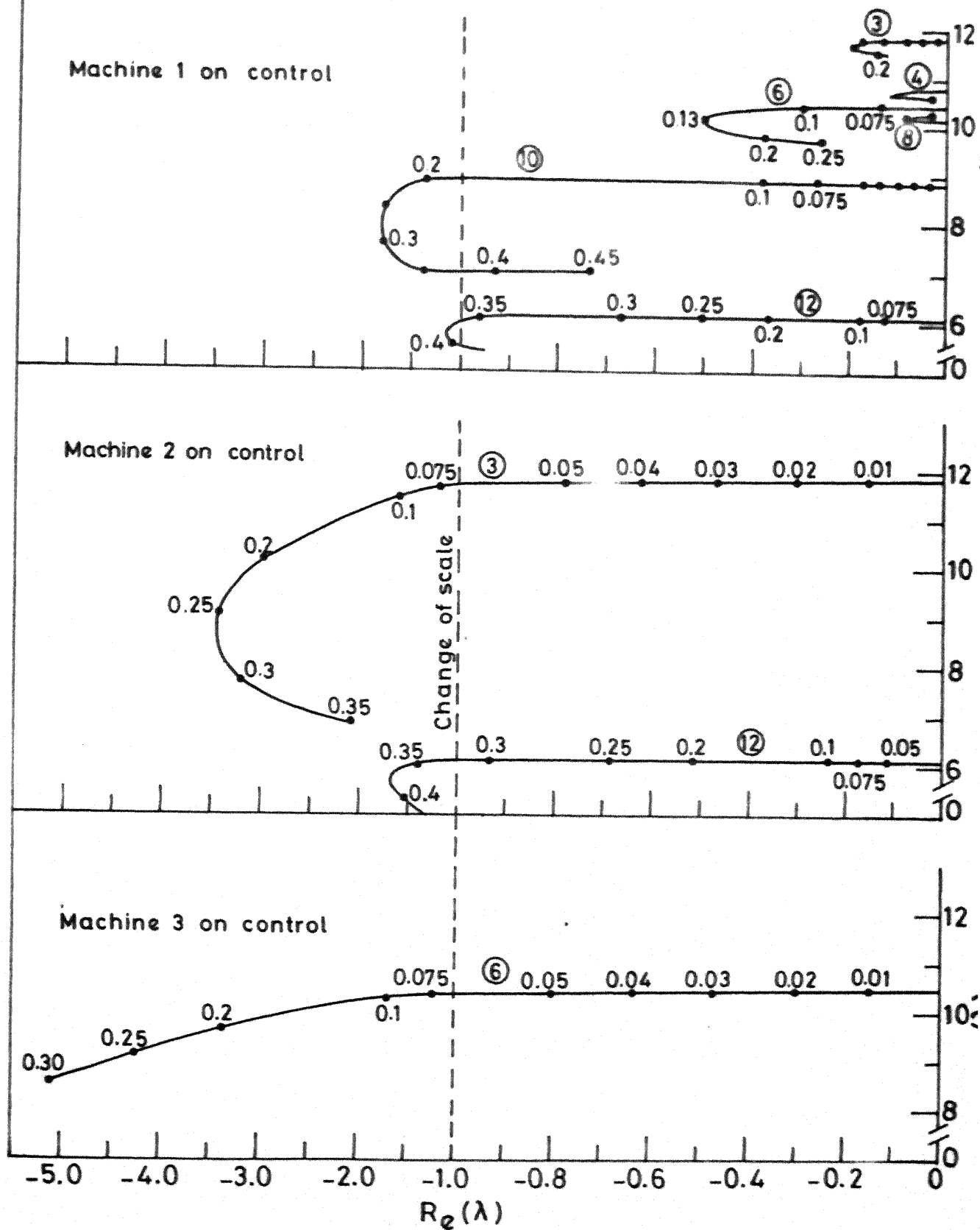


FIG. 5.1 LOCI OF EIGENVALUES FOR VARIATION IN CONTROLLER GAIN (MACHINES ON CONTROL 1, 2 AND 3).

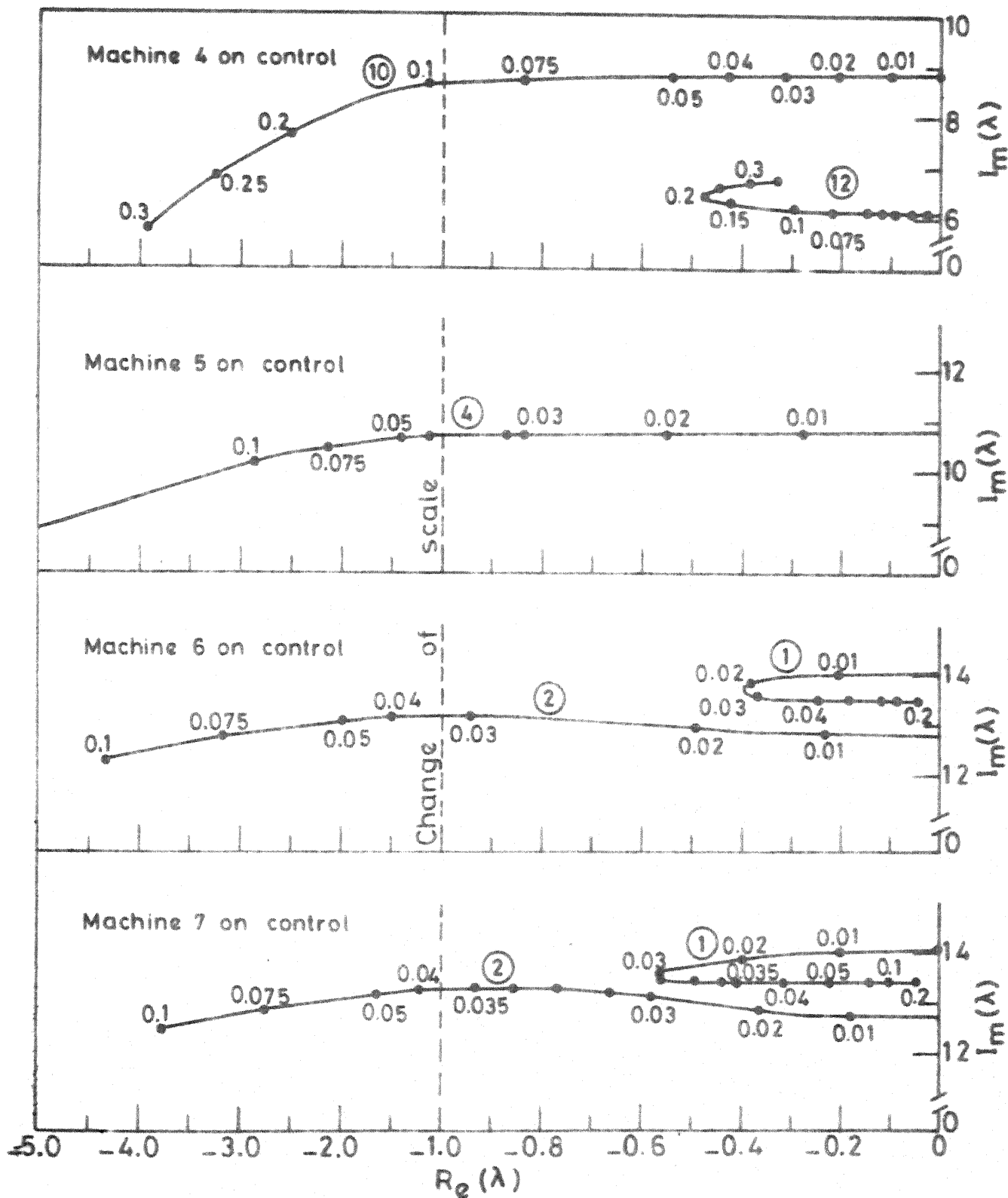


FIG. 5.2 LOCI OF EIGENVALUES FOR VARIATION IN CONTROLLER GAIN (MACHINES ON CONTROL 4, 5, 6 AND 7)

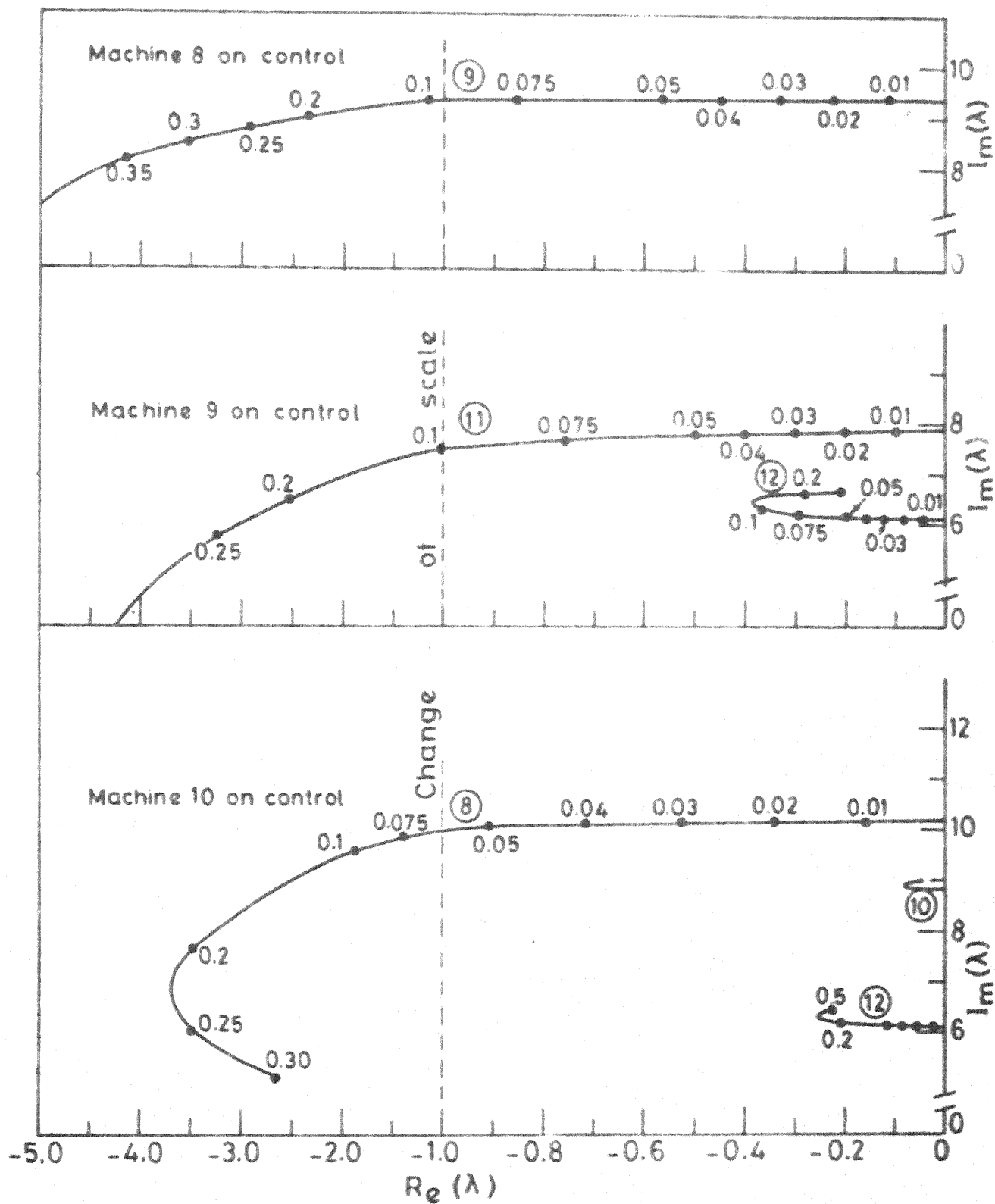


FIG.5.3 LOCI OF EIGENVALUES FOR VARIATION IN CONTROLLER GAIN (MACHINES ON CONTROL 8,9 AND 10).

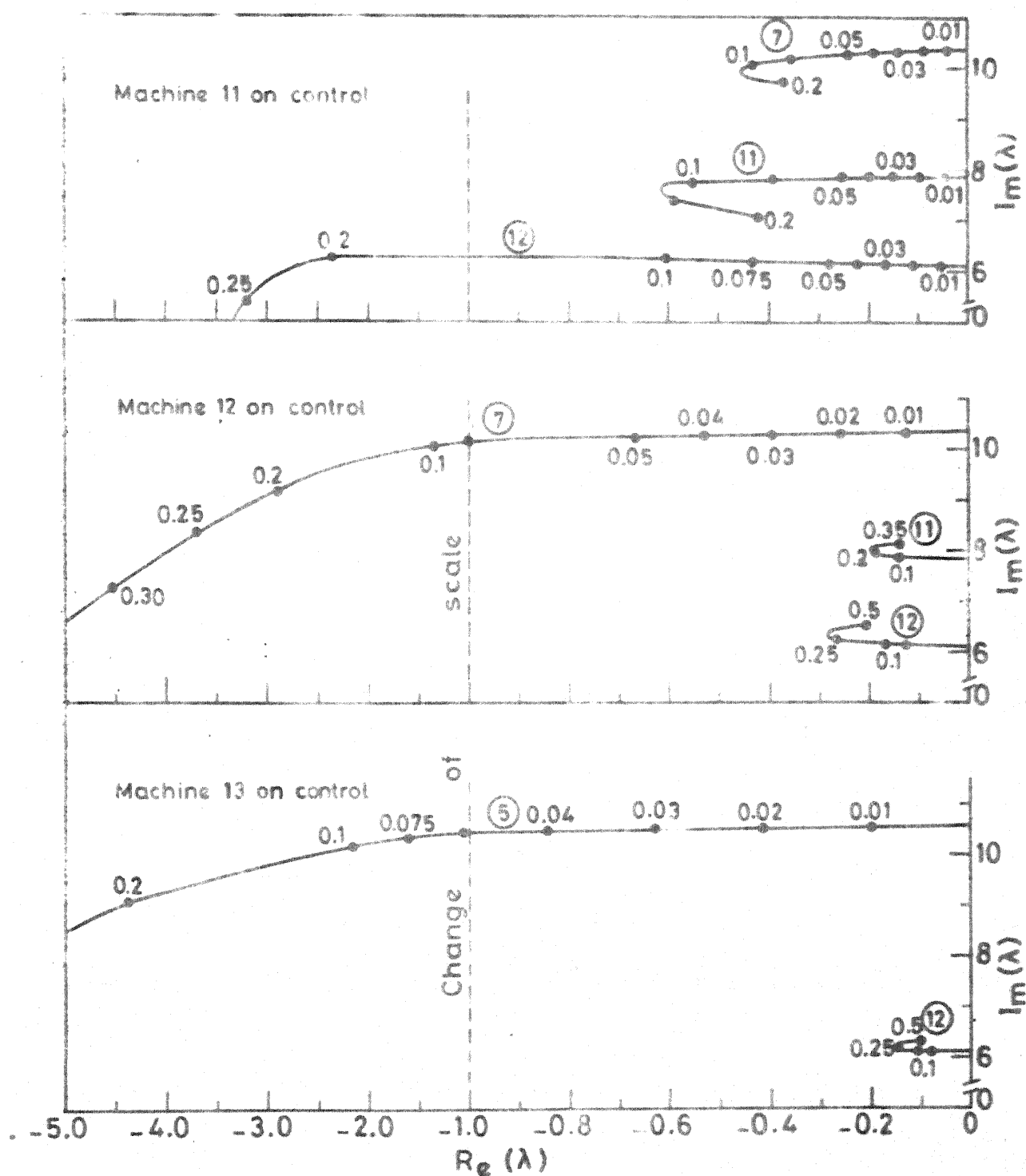


FIG.5.4 LOCI OF EIGENVALUES FOR VARIATION IN CONTROLLER GAIN (MACHINES ON CONTROL 11,12 AND 13).

Table 5.5 Effective Locations of PSS in the 13-Machine System

No. of Machines to be Equipped with PSS	PSS Locations
3	1,7 and 11
4	1,7,8 and 11
5	1,7,8,11 and 13

5.5 CONCLUSIONS

A state space model has been developed in this chapter for large multimachine power systems. The model is based on the linearized machine and network equations around an operating point. Freedom is available to accommodate any degree of detail for machine representation. The model can be used for eigenvalue analysis and design of PSS to improve dynamic stability of systems.

It is found that proper location of PSS is important for the effective damping of rotor oscillations in multimachine systems. Two methods are suggested for this purpose. The first method is independent of the feedback control structure. The second method is based on eigenvalue sensitivity and takes the feedback control structure into account. It is shown that both methods give closely agreeing results.

A case study of a 13-machine system is presented for eigenvalue analysis and for the selection of effective PSS locations. Effective PSS locations are obtained from the suggested methods and validation of results is obtained by the study of loci of eigenvalues. It is found that it is sufficient to equip relatively few machines with PSS for adequate improvement in dynamic stability. At the most five locations are sufficient to damp all the twelve modes of rotor oscillations in the example considered.

CHAPTER 6

APPLICATION OF DECENTRALIZED CONTROL FOR THE DESIGN OF PSS IN MULTIMACHINE POWER SYSTEMS

6.1 INTRODUCTION

Coordinated application and design of power system stabilizers in multimachine power systems have drawn much attention recently [17,20]. In multimachine systems the problem of dynamic stability can be divided into two parts : the selection of generating units to be equipped with PSS and the design/tuning of stabilizers for the selected units such that the entire system is dynamically stable. The selection of PSS locations in a multimachine system has been discussed in Chapter 5. For the selected machines PSS can be designed by any one of the methods discussed in Chapter 2. Direct application of these techniques is not possible for multimachine system, because of the practical problems of information transfer between various machines of the system. These techniques are to be modified to consider the decoupled nature of control for various machines. This leads to the use of decentralized control theory.

In decentralized control, the entire system is divided into various subsystems having local control stations. At

each control station, the controller utilizes only local system outputs and controls only local inputs. However, all the controllers are involved in controlling the same large system. Lefebvre et al. [77] have suggested a technique for the design of such controllers for eigenvalue assignment. In the first stage of this technique the controllers are designed for stabilizing the individual subsystems neglecting the coupling between them. In the second stage, the interconnections are introduced in small increments and the controller parameters are updated to retain the eigenvalues at their preassigned locations. Lefebvre [48] has recently applied this technique for the PSS design in a three machine system with PSS designed on all the machines.

Sequential algorithms have also been suggested for the design of PSS [20,47] using pole-assignment techniques. Unfortunately the sequential addition of stabilizers disturbs previously assigned eigenvalues.

In this chapter, an investigation of PSS design in a large multimachine system is carried out. As described in Chapter 2, PSS design based on (i) eigenvalue assignment and (ii) the minimization of a performance index are considered. In the first case, coordinated design of PSS is carried out using the technique given in [77]. In the second case, the method given in Chapter 2 is modified to consider the

decentralized structure of PSS. Both these methods are compared using the examples of a 3-machine and a 13-machine system. For the 13-machine system, the PSS is designed for a few selected machines determined from the analysis presented in Chapter 5.

6.2 PSS DESIGN BASED ON EIGENVALUE ASSIGNMENT

The objective of eigenvalue assignment by output feedback is used in this section for PSS design. The design problem can be stated as : Design stabilizers for the selected machines in a multimachine system with decentralized output feedback to assign closed-loop eigenvalues to preassigned locations.

6.2.1 Formulation of Control Problem

The state-space model of a multimachine system with n generating units, developed in Sec. 5.2, can be represented as

$$p \underline{X}_M = [A_M] \underline{X}_M + [B_M] \underline{U}_M \quad (6.1)$$

where

$$\underline{X}_M = [x_{m1}^t \ x_{m2}^t \ \dots \ x_{mn}^t]^t$$

and

$$\underline{U}_M = [u_{m1} \ u_{m2} \ \dots \ u_{mn}]^t$$

x_{mi} represents the state variables of i th generating unit and its excitation system. A_M is a full matrix and B_M is a block diagonal matrix as explained in Chapter 5. The dynamical equation of the i th generating unit has the form

$$p \underline{x}_{mi} = [A_{mii}] \underline{x}_{mi} + \sum_{\substack{j=1 \\ j \neq i}}^n [A_{mij}] \underline{x}_{mj} + \underline{b}_{mi} u_{mi} \quad (6.2)$$

where A_{mii} and A_{mij} are submatrices of A_M corresponding to the i th unit and \underline{b}_{mi} is the i th diagonal block of B_M . Similarly the measurable output (viz., rotor speed, electrical power or bus frequency) of the i th unit can be expressed in terms of the state variables of different units as

$$y_{mi} = [C_{mii}] \underline{x}_{mi} + \sum_{\substack{j=1 \\ j \neq i}}^n [C_{mij}] \underline{x}_{mj} \quad (6.3)$$

The summation terms in eqns. (6.2) and (6.3) represent the interconnection of i th generating unit with other units of the system. The interconnections are parameterized, with $0 \leq r \leq 1$ as follows :

$$p \underline{x}_{mi} = [A_{mii}] \underline{x}_{mi} + r \sum_{\substack{j=1 \\ j \neq i}}^n [A_{mij}] \underline{x}_{mj} + \underline{b}_{mi} u_{mi} \quad (6.4)$$

and

$$y_{mi} = [C_{mii}] \underline{x}_{mi} + r \sum_{\substack{j=1 \\ j \neq i}}^n [C_{mij}] \underline{x}_{mj} \quad (6.5)$$

With the introduction of parameter r , the degree of interconnection in eqns. (6.4) and (6.5) can be varied. Clearly at $r = 0$ the system is completely decoupled and at $r = 1$ it is fully connected.

Initially stabilizers for selected machines are designed, neglecting the interconnection, that is, with $r = 0$, with output feedback, using local output variables to assign the closed-loop eigenvalues using any one of the techniques presented in Chapter 2. The interconnection is introduced in steps to update the parameters of PSS in such a way that the closed-loop eigenvalues remain unchanged. Let the dynamical equation and control law for PSS of the i th generating unit be

$$p \underline{z}_i = [S_i] \underline{z}_i + R_i y_{mi} \quad (6.6)$$

and

$$u_{mi} = [Q_i] \underline{z}_i + K_i y_{mi} \quad (6.7)$$

where \underline{z}_i represents the state variables of PSS. Combining eqns. (6.4) to (6.7), the dynamical equation and control law for the augmented system (including PSS dynamics) of the i th unit can be expressed as

$$p \underline{x}_i = [A_{ii}] \underline{x}_i + r \sum_{\substack{j=1 \\ j \neq i}}^n [A_{ij}] \underline{x}_j + [B_i] \underline{u}_i \quad (6.8)$$

$$y_i = [C_{ii}] \underline{x}_i + r \sum_{\substack{j=1 \\ j \neq i}}^n [C_{ij}] \underline{x}_j \quad (6.9)$$

and

$$\underline{u}_i = [K_{di}] y_i \quad (6.10)$$

where

$$\begin{aligned} \underline{x}_i &= [x_{mi}^t \ z_i^t]^t ; & \underline{y}_i &= [y_{mi} \ z_i^t]^t \\ A_{ii} &= \begin{bmatrix} A_{mii} & 0 \\ 0 & 0 \end{bmatrix} ; & A_{ij} &= \begin{bmatrix} A_{mij} & 0 \\ 0 & 0 \end{bmatrix} \\ B_i &= \begin{bmatrix} b_{mi} & 0 \\ 0 & I \end{bmatrix} ; & K_{di} &= \begin{bmatrix} K_i & Q_i \\ R_i & S_i \end{bmatrix} \\ C_{ii} &= \begin{bmatrix} C_{mii} & 0 \\ 0 & I \end{bmatrix} ; & C_{ij} &= \begin{bmatrix} C_{mij} & 0 \\ 0 & 0 \end{bmatrix} \end{aligned}$$

If i th machine has no stabilizer, then $x_i = x_{mi}$, $y_i = y_{mi}$ and matrices A_{ii} , A_{ij} , B_i , C_{ii} and C_{ij} will be equal to matrices, A_{mii} , A_{mij} , b_{mi} , C_{mii} and C_{mij} respectively. K_{di} will be a scalar with zero value.

For the composite power system, eqns. (6.8) to (6.10) will take the form

$$p \underline{X} = [A_D + r A_0] \underline{X} + [B_D] \underline{U} \quad (6.11)$$

$$\underline{Y} = [C_D + r C_0] \underline{X} \quad (6.12)$$

and

$$\underline{U} = [K_D(r)] \underline{Y} \quad (6.13)$$

where A_D = Block Diagonal $[A_{11}, A_{22}, \dots, A_{nn}]$

B_D = Block Diagonal $[B_1, B_2, \dots, B_n]$

C_D = Block Diagonal $[C_{11}, C_{22}, \dots, C_{nn}]$

K_D = Block Diagonal $[K_{d1}, K_{d2}, \dots, K_{dn}]$

and the structure of matrices A_o and C_o are as follows :

$$[A_o] = \begin{bmatrix} 0 & A_{12} & A_{13} & \dots & A_{1n} \\ A_{21} & 0 & A_{23} & \dots & A_{2n} \\ A_{31} & A_{32} & 0 & \dots & A_{3n} \\ \vdots & & & & \vdots \\ A_{n1} & A_{n2} & A_{n3} & \dots & 0 \end{bmatrix} ; [C_o] = \begin{bmatrix} 0 & C_{12} & C_{13} & \dots & C_{1n} \\ C_{21} & 0 & C_{23} & \dots & C_{2n} \\ C_{31} & C_{32} & 0 & \dots & C_{3n} \\ \vdots & & & & \vdots \\ C_{n1} & C_{n2} & C_{n3} & \dots & 0 \end{bmatrix}$$

The objective is to find a decentralized output feedback control law, as given in eqn. (6.13), such that the composite power system depicted by eqn. (6.11), has specified eigenvalues. Using the parameterization introduced in eqns. (6.4) and (6.5) and defining $K_D(r)$ to be the decentralized feedback matrix, the eigenvalues of the composite power system are the eigenvalues of the closed-loop matrix

$$F(r) = A_D + rA_o + B_D K_D(r) (C_D + r C_o)$$

At $r = 0$ the matrix $K_D(0)$, which assigns the specified eigenvalues, is easily computed because the system is decoupled. The idea is to slowly introduce the connections using discrete increments Δr and to modify $K_D(r)$ in such a way that the eigenvalues remain unchanged in presence of the interconnections. The advantage of this approach is that updating $K_D(r)$ to obtain $K_D(r + \Delta r)$ is much easier than trying to directly compute $K_D(1)$, the final answer. $K_D(r + \Delta r)$ is obtained from $K_D(r)$ as follows.

The i th eigenvalue equation of the closed-loop system for any value of r may be written as

$$[\lambda_i(r)I - F(r)] \underline{V}_i(r) = \underline{0} \quad (6.14)$$

where $\underline{V}_i(r)$ is the right eigenvector corresponding to the eigenvalue $\lambda_i(r)$. The system also has a left eigenvector with the properties

$$\underline{W}_j^t(r) [\lambda_j(r)I - F(r)] = \underline{0} \quad (6.15)$$

and

$$\underline{W}_j^*(r) \cdot \underline{V}_i(r) = \begin{cases} 1 & \text{for } j = i \\ 0 & \text{for } j \neq i \end{cases}$$

where $\underline{W}_j^*(r)$ is the conjugate transpose of the left eigenvector $\underline{W}_j(r)$. Differentiating eqn. (6.14) with respect to r and pre-multiplying by $\underline{W}_i^*(r)$, we get

$$\underline{W}_i^*(r) \frac{d}{dr} [\lambda_i(r)I - F(r)] \underline{V}_i(r) + \underline{W}_i^*(r) [\lambda_i(r)I - F(r)] \frac{d}{dr} \underline{V}_i(r) = 0 \quad (6.16)$$

The second term in eqn. (6.16) will vanish as evident from eqn. (6.15). Rearranging eqn. (6.16) and suppressing indication of r -dependence of λ_i , \underline{V}_i , \underline{W}_i and K_D , we get

$$\underline{W}_i^* [B_D \frac{dK_D}{dr} (C_D + rC_o)] \underline{V}_i = \frac{d\lambda_i}{dr} \underline{V}_i - \underline{W}_i^* [A_o + B_D K_D C_o] \underline{V}_i \quad (6.17)$$

In order to make the eigenvalues insensitive to r , $\frac{d\lambda_i}{dr}$ in eqn. (6.17) can be set equal to zero. Then eqn. (6.17) can be

solved for $\frac{dK_D}{dr}$ which is, in turn, utilized for updating K_D as follows :

$$K_D(r + \Delta r) = K_D(r) + \left. \frac{dK_D(r)}{dr} \right|_r \Delta r \quad (6.18)$$

Solution of eqn. (6.17) is obtained by using the tensor product operation. Suppose $M = \{m_{ij}\}$ is a $p \times q$ matrix and L is $r \times s$, then the tensor product of M by L ($M \otimes L$), is defined to be $pr \times qs$ matrix, $M \otimes L = \{m_{ij}L\}$. The 'Vec' operation on the matrix $M = [M_1, M_2, \dots, M_q]$, where M_i is a column of M and defined as

$$\text{Vec}(M) \triangleq \begin{bmatrix} M_1 \\ M_2 \\ \vdots \\ M_q \end{bmatrix}$$

It can be shown [77] that the set of equations (6.17) for $i = 1$ to N , where N is the total number of states in eqn. (6.11), is equivalent to :

$$[\hat{\phi}(r)] \text{Vec} \left[\frac{dK_D(r)}{dr} \right] = \beta(r) \quad (6.19)$$

where the matrix $\hat{\phi}(r)$

$$\hat{\phi}(r) = \begin{bmatrix} [(C_D + rC_o) \underline{V}_1]^t \otimes \underline{W}_1^* B_D \\ [(C_D + rC_o) \underline{V}_2]^t \otimes \underline{W}_2^* B_D \\ \vdots \\ [(C_D + rC_o) \underline{V}_N]^t \otimes \underline{W}_N^* B_D \end{bmatrix}$$

and the vector $\beta(r)$ is

$$\beta(r) = \begin{bmatrix} \frac{d\lambda_1}{dr} - \underline{w}_1^* & [A_o + B_D K_D C_o] & \underline{v}_1 \\ \frac{d\lambda_2}{dr} - \underline{w}_2^* & [A_o + B_D K_D C_o] & \underline{v}_2 \\ \vdots & & \vdots \\ \frac{d\lambda_N}{dr} - \underline{w}_N^* & [A_o + B_D K_D C_o] & \underline{v}_N \end{bmatrix}$$

As K_D is a block-diagonal matrix, columns of $\hat{\varphi}(r)$ corresponding to zero entries of $\text{Vec}(\frac{dK_D}{dr})$ are deleted and eqn. (6.19) can be written as

$$[\varphi(r)] \begin{bmatrix} \text{Vec}(\frac{dK_{d1}}{dr}) \\ \text{Vec}(\frac{dK_{d2}}{dr}) \\ \vdots \\ \text{Vec}(\frac{dK_{dn}}{dr}) \end{bmatrix} = \beta(r) \quad (6.20)$$

Solution for $\text{Vec}(\frac{dK_{di}}{dr})$, $i = 1$ to n can be obtained by computing the pseudo-inverse of the non-square matrix $\varphi(r)$ in eqn.(6.20). Solution of eqn. (6.20) during each iteration provides an update of $\frac{dK_D}{dr}$ which is utilized in eqn. (6.18) to update the gain matrix K_D . The conditions that guarantee the existence of a real solution of eqn. (6.20) are [77] :

- (a) Each subsystem (machine and PSS) is controllable and observable.
- (b) The eigenvalues of each subsystem can be assigned by local dynamic output feedback.
- (c) At most one subsystem has an augmented state space which is of odd order (machine and PSS). This condition guarantees that the feedback gains, that is, matrix K_{di} , are real.
- (d) Matrices B_D and $(C_D + rC_0)$ have full column rank and full row rank respectively.

6.2.2 Design Algorithm

The following algorithm can be used for PSS design in multimachine systems using the procedure under consideration :

- Step 1 : Select the machines to be equipped with PSS.
- Step 2 : Obtain state-space representation of each machine as given in eqns. (6.4) and (6.5).
- Step 3 : Augment state equations of the selected machines to include stabilizer dynamics as given in eqns. (6.8) and (6.9).
- Step 4 : Design feedback matrix $K_{di}(0)$ for each of the selected machines using local output feedback, to assign closed-loop eigenvalues at desired locations, by setting the parameter $r = 0$ in eqns. (6.8) and (6.9).

- Step 5 : Construct eqns. (6.11), (6.12) and (6.13) for the composite power system from eqns. (6.8), (6.9) and (6.10) of individual machines.
- Step 6 : Calculate right and left eigenvectors of closed-loop matrix $F(r)$.
- Step 7 : Calculate elements of $\Psi(r)$ and $\beta(r)$ and solve eqn. (6.20) for $\frac{dK_D}{dr}$.
- Step 8 : Update $K_D(r)$ from eqn. (6.18) by selecting a sufficiently small value of Δr .
- Step 9 : Increase the value of r to $r + \Delta r$.
- Step 10: Go to step 6 if r is less than or equal to unity.

6.3 PSS DESIGN BASED ON MINIMIZATION OF PERFORMANCE INDEX

The objective of PSS design here is to minimize a performance index of the form :

$$J = \int_0^{\infty} \left(\sum_{i=1}^n \alpha_i \Delta P_i^2 \right) dt \quad (6.21)$$

where ΔP_i represents the fluctuation in power output of the i th generator and α_i is the weightage to be attached to ΔP_i .

The technique for PSS design based on the above objective is given in Chapter 2 for a single machine system. This is extended here for a multimachine system. As stated in Chapter 2, this objective is equivalent to minimizing the fluctuations in the power outputs of various machines following a disturbance.

6.3.1 Formulation of the Control Problem

Eqns. (6.11) and (6.12) for the composite power system (including stabilizer dynamics), with interconnections, can be expressed as

$$p \underline{X} = [A] \underline{X} + [B_D] \underline{U} \quad (6.22)$$

$$\underline{Y} = [C] \underline{X} \quad (6.23)$$

where

$$A = A_D + A_O$$

and

$$C = C_D + C_O$$

A and C are full matrices and B_D is a block-diagonal matrix. The decentralized output feedback control law can be defined as

$$\underline{U} = -[K] \underline{Y} \quad (6.24)$$

where K is a block-diagonal feedback matrix and can be expressed in terms of the parameters of stabilizers. The design problem can be stated as : determine the optimum value of K such that the objective defined in eqn. (6.21) is met.

Eqn. (6.21) can also be expressed as

$$J = \int_0^{\infty} \Delta \underline{P}^t [\alpha] \Delta \underline{P} dt \quad (6.25)$$

where

$$\Delta \underline{P} = [\Delta P_1 \quad \Delta P_2 \quad \dots \quad \Delta P_n]^t$$

$$\alpha = \text{Diagonal } [\alpha_i]$$

Incremental change in complex power output of generators, in a multimachine system, can be expressed in terms of the system state variables as given in eqn. (5.18) of Chapter 5.

$$\Delta \underline{S}_G = [T_1] \underline{X}_M \quad (6.26)$$

where

$$T_1 = (I - J'_{GG} D_P)^{-1} J'_{GG} D_S$$

$$\Delta \underline{S}_G = [\Delta S_{g1}^t \Delta S_{g2}^t \dots \Delta S_{gn}^t]^t$$

and

$$\Delta S_{gi} = [\Delta P_i \quad \Delta Q_i]^t$$

Matrices J'_{GG} , D_P and D_S are defined in Chapter 5. ΔP can be obtained from the vector of changes in complex power $\Delta \underline{S}_G$ as

$$\Delta \underline{P} = [T_2] \underline{X}_M \quad (6.27)$$

where matrix T_2 is obtained from the matrix T_1 . System state variables \underline{X}_M can be expressed in terms of the state variables of the composite power system as

$$\underline{X}_M = [T_M] \underline{X} \quad (6.28)$$

From eqns. (6.27) and (6.28), we get

$$\Delta \underline{P} = [T] \underline{X} \quad (6.29)$$

where

$$T = T_2 T_M$$

Substituting the value of ΔP from eqn. (6.29) into eqn. (6.25), the cost function, J can be expressed as

$$J = \int_0^{\infty} (\underline{X}^T \hat{Q} \underline{X}) dt \quad (6.30)$$

where

$$\hat{Q} = [T^t] [\alpha] [T]$$

The optimum value of K that minimizes the performance index is obtained using a slightly modified form of the iterative procedure described in Appendix C. The modification is incorporated, to account for the decentralized control, as indicated below :

In step 5 where K is updated according to

$$K^{(i+1)} = K^{(i)} - \eta^{(i)} \left. \frac{dH}{dK} \right|_{K=K^{(i)}}$$

$K^{(i+1)}$ will be a full matrix even though $K^{(i)}$ is a block diagonal matrix. The block diagonal structure is imposed on $K^{(i+1)}$ by neglecting the elements that do not constitute diagonal blocks.

When the solution for the optimum K is obtained in the final iteration, in the block diagonal form, the parameters of the PSS for the i th machine are obtained from

$$K_{di} = \begin{bmatrix} K_i & Q_i \\ R_i & S_i \end{bmatrix}$$

where K_{di} is the i th diagonal block. The elements of K_{di} define the structure of PSS as given in eqns. (6.6) and (6.7).

6.4 NUMERICAL EXAMPLES

A 3-machine and a 13-machine power system examples are considered to illustrate the techniques, presented in Secs. 6.2 and 6.3, for PSS design.

6.4.1 A Three-Machine Power System

A sample multimachine power system given in Ref. [83], consisting of nine buses and three generators, is considered. The single-line diagram of the system alongwith system data and operating conditions are given in Appendix J. Each machine with its single time constant excitation system is represented by a fourth order model, (see Appendix D). Machine 1 is considered as reference for the measurement of rotor angle. Thus, an eleventh order model, describing the open-loop system, is obtained. Rotor speed is used as feedback signal to design a second order PSS with transfer function of the form

$$F(s) = \frac{\theta_0 s^2 + \theta_1 s + \theta_2}{s^2 + \gamma_1 s + \gamma_2} \quad (6.31)$$

for each machine of the system. Open-loop system matrices are as follows :

$$A_{m11} = \begin{bmatrix} -0.13138 & 0 & 1.83564 \\ -1.20741 & 0 & 0 \\ -134.05135 & 0 & -50. \end{bmatrix};$$

$$A_{m12} = \begin{bmatrix} 0.02351 & 0 & 0.00005 & 0 \\ 0.90183 & 0 & 11.81610 & 0 \\ -21.25201 & 0 & 20.98774 & 0 \end{bmatrix}$$

$$A_{m13} = \begin{bmatrix} 0.03342 & 0 & 0.05088 & 0 \\ 0.85459 & 0 & 7.06217 & 0 \\ -30.96391 & 0 & -36.89218 & 0 \end{bmatrix} ; b_{m1} = [0 \ 0 \ 2500]^t$$

$$; c_{m11} = [0 \ 1 \ 0]$$

$$A_{m22} = \begin{bmatrix} -0.52193 & 0 & -2.64893 & 1.39121 \\ -10.95584 & 0 & -65.97776 & 0 \\ 0 & 1 & 0 & 0 \\ -155.30564 & 0 & -67.39815 & -50 \end{bmatrix}$$

$$A_{m21} = \begin{bmatrix} 0.00700 & 0 & 0 \\ -1.93066 & 0 & 0 \\ 0 & -1 & 0 \\ -69.22754 & 0 & 0 \end{bmatrix}$$

$$A_{m23} = \begin{bmatrix} 0.19452 & 0 & 0.95153 & 0 \\ 2.27457 & 0 & 20.67036 & 0 \\ 0 & 0 & 0 & 0 \\ -79.79709 & 0 & -75.68095 & 0 \end{bmatrix} ; b_{m2} = [0 \ 0 \ 0 \ 2500]^t$$

$$; c_{m22} = [0 \ 1 \ 0 \ 0]$$

$$A_{m33} = \begin{bmatrix} -0.62866 & 0 & -2.18978 & 0.93646 \\ -26.83562 & 0 & -119.75087 & 0 \\ 0 & 1 & 0 & 0 \\ -214.43926 & 0 & -321.13379 & -50 \end{bmatrix}$$

$$A_{m31} = \begin{bmatrix} 0.02403 & 0 & 0 \\ -1.49427 & 0 & 0 \\ 0 & -1 & 0 \\ -74.62402 & 0 & 0 \end{bmatrix}$$

$$A_{m32} = \begin{bmatrix} 0.14140 & 0 & 0.97074 & 0 \\ 5.03265 & 0 & 52.64938 & 0 \\ 0 & 0 & 0 & 0 \\ -54.39683 & 0 & 130.20166 & 0 \end{bmatrix} \quad \begin{aligned} b_{m3} &= [0 \ 0 \ 0 \ 2500]^t \\ c_{m33} &= [0 \ 1 \ 0 \ 0] \end{aligned}$$

$$C_{mij} = 0 \quad \text{for } i \neq j.$$

Table 6.1 shows the open-loop eigenvalues of the system.

Table 6.1 Open-Loop Eigenvalues of the 3-Machine System

$$-0.34411 \pm j \ 8.07210$$

$$-0.81744 \pm j11.61613$$

$$-2.01443$$

$$-3.78028$$

$$-8.36729$$

$$-41.40810$$

$$-46.18024$$

$$-47.20853$$

$$0.0$$

6.4.1.1 Eigenvalue Assignment

In the first stage of design, pole assignment technique based on modal control theory with partial state feedback, as given in Sec. 2.4.1, is used to design stabilizers for each

machine, neglecting interconnections. The technique specifies the zeros of PSS. For the system considered, they are specified as -2.0 and -2.5 for each PSS. Three eigenvalues for each machine can be assigned with this technique.

Table 6.2 shows, at $r = 0$, the open-loop eigenvalues, desired locations of three closed-loop eigenvalues and the remaining closed-loop eigenvalues obtained from the design. The desired locations of the closed-loop eigenvalues are obtained by defining the sector [82] given in Fig. 6.1. This ensures a damping ratio greater than a minimum value, say ξ , where $\xi = \cos\theta$. The values of α and θ chosen are respectively -1 and 75 degrees. The real parts of complex eigenvalues are selected such that they lie on the boundary of the sector and the locations of real eigenvalues are specified inside the sector.

Table 6.2 Eigenvalues of the 3-Machine System at $r = 0$

	Machine 1	Machine 2	Machine 3
Open-loop eigenvalues at $r=0$	0.0 -5.68401 -44.44736	-0.32150 \pm j7.96260 -4.70536 -45.17356	-0.93869 \pm j10.80630 -3.13048 -45.62081
Desired location of 3-closed-loop eigenvalues	-2.0 -3.0, -4.0	-2.14 \pm j8.00 -3.0	-2.94 \pm j11.0 -3.0
Remaining closed-loop eigenvalues	-1.16588 -44.59163	-6.87699 -13.37328 -48.13837	-3.83533 -33.76433 -65.58955

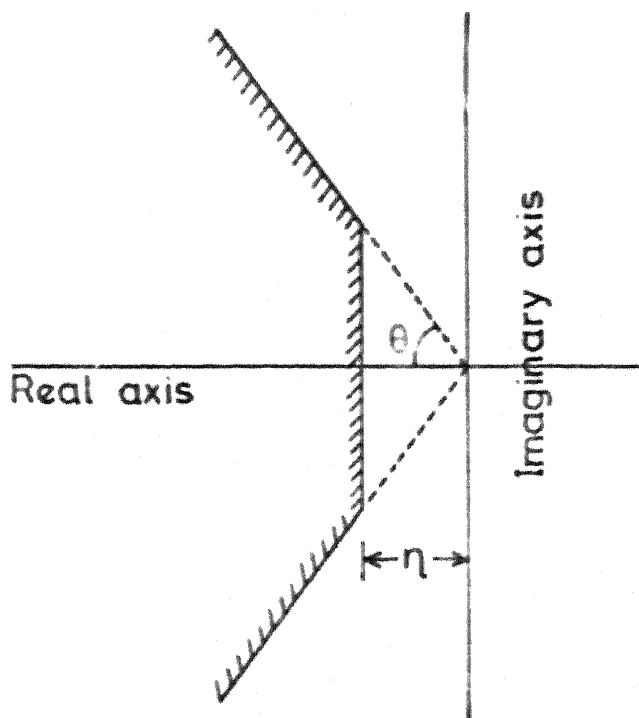


FIG.6.1 SECTOR FOR POLE-ASSIGNMENT.

Table 6.3 shows the parameters of the three stabilizers obtained in the first stage of design.

Table 6.3 PSS Parameters for the 3-Machine System at $r = 0$

Machine	θ_0	θ_1	θ_2	γ_1	γ_2
1	0.04504	0.20267	0.22518	4.62613	5.25227
2	0.09199	0.41397	0.45996	25.14671	67.47599
3	0.15194	0.68372	0.75969	61.44055	196.59640

The feedback gain matrix K_{di} for i th machine can be obtained in terms of PSS parameters, defined in eqn. (6.31) as (Appendix B) :

$$[K_{di}] = \begin{bmatrix} \theta_{10} & \theta'_{2i} & \theta'_{1i} \\ 0 & 0 & 1 \\ 1 & -\gamma_{2i} & -\gamma_{1i} \end{bmatrix}$$

where

$$\theta'_{1i} = \theta_{1i} - \theta_{0i} \gamma_{1i}$$

and

$$\theta'_{2i} = \theta_{2i} - \theta_{0i} \gamma_{2i}$$

In the second stage of design, for updating the decentralized feedback gain matrix K_D , a step of $\Delta r = 0.05$ is chosen to introduce interconnections. Zeros of the stabilizers are

kept fixed, at the specified values in updating K_D . Thus, the number of unknowns in eqn. (6.20) are nine. The order of closed-loop system is seventeen and, therefore, eqn. (6.20) represents a set of seventeen simultaneous linear algebraic equations in nine unknowns. Pseudo-inverse of $\Phi(r)$, a 17×9 matrix, is determined for obtaining a solution of $\frac{dK_D}{dr}$ in eqn. (6.20). Table 6.4 shows the final values of PSS parameters with full interconnection, that is, with $r = 1$. Table 6.5 shows the closed-loop eigenvalues of the system with stabilizers designed in first stage of design and with stabilizers obtained in the second stage, that is, with PSS parameters given in Tables 6.3 and 6.4.

Table 6.4 PSS Parameters for the 3-Machine System
at $r = 1$

Machine	θ_0	θ_1	θ_2	γ_1	γ_2
1	0.05335	0.24005	0.26673	4.58555	5.19168
2	0.09694	0.43624	0.48471	30.56537	148.62700
3	0.15674	0.70533	0.78371	61.20286	188.05422

Table 6.5 Closed-Loop Eigenvalues of the 3-Machine System

Assigned at $r=0$ with PSS of Table 6.3	Obtained with PSS of Table 6.3 at $r = 1$	Obtained with PSS of Table 6.4 at $r = 1$
$-2.14 \pm j 8.00$	$-1.16640 \pm j 8.03543$	$-2.11541 \pm j 7.86407$
$-2.94 \pm j 11.00$	$-2.78779 \pm j 12.41460$	$-2.92745 \pm j 12.25552$
- 1.16588	- 0.09647	- 0.78921
- 2.00000	- 2.00000	- 2.00889
- 3.00000	- 2.04994	- 2.12231
- 3.00000	- 2.69879	- 2.59251
- 3.00000	- 3.05555	- 3.23480
- 3.83530	- 3.45787	- 3.70848
- 4.00000	- 3.70096	- 5.46943
- 6.87702 -13.37271	$-12.62314 \pm j 3.41233$	$-13.95100 \pm j 4.98277$
-33.76433	-33.26061	-32.95496
-44.59163	-44.49973	-44.62495
-48.13835	-48.21465	-48.70835
-65.58957	-65.70617	-65.79412

A comparison of Tables 6.3 and 6.4 shows that the modifications in PSS parameters with interconnections are not significant except for the poles of PSS of machines 2 and 3. The poles of PSS for the second machine have changed significantly by considering the interconnections.

Results shown in Table 6.5 emphasize the need for coordinated design of PSS in multimachine system. The second column of Table 6.5 gives the eigenvalues of the system with PSS designed by neglecting the interconnection. It is seen that one of the real eigenvalue is close to the imaginary axis and the damping of the rotor oscillation modes are reduced.

It is to be noted that eigenvalues given in column 3 are not identical to those given in column 1, although the design algorithm is aimed at maintaining the system eigenvalues at the locations given in column 1 in the presence of interconnections. However, this is not surprising as only nine parameters (of the PSS) are used to control seventeen eigenvalues. Notwithstanding the above, the results are quite encouraging in that the eigenvalues of column 3 are close enough to those of column 1.

6.4.1.2 Minimization of Performance Index

The objective is to minimize the performance index given in eqn. (6.21) with

$$\alpha_i = 1 \quad \text{for } i = 1, 2 \text{ and } 3$$

by designing the PSS for each machine. For convenience, the initial choice of the PSS parameters is made from the results obtained in the previous section, using the eigenvalue assignment technique. The optimal values of PSS parameters are given in Table 6.6. Table 6.7 shows the closed-loop eigenvalues obtained with stabilizers of Table 6.6.

Table 6.6 PSS Parameters for the 3-Machine System
Obtained from Parameter Optimization
Technique

Machine	θ_0	θ_1	θ_2	γ_1	γ_2
1	0.05973	0.25637	0.29749	4.58555	5.19168
2	0.16013	2.33035	9.89180	30.56508	148.62720
3	0.16731	1.33959	2.77806	61.20167	188.05472

Table 6.7 Eigenvalues of the 3-Machine System
with PSS of Table 6.6

-2.41665	$\pm j$	9.30942
-2.45847	$\pm j$	13.68310
-1.00378		
-1.48954		
-1.80292		
-2.12409		
-2.96189		
-3.91836		
-6.45344		
-11.18142		
-15.24140		
-33.53356		
-44.39199		
-49.45159		
-65.85462		

The performance of the stabilizers, obtained from the two design techniques presented, is compared by taking the time-response of fluctuations in power output and relative rotor angle of the machines following a disturbance. Figures 6.2 to 6.7 show the variations in power outputs of the machines and the relative rotor angles for the three cases, namely, for a unit step change in the reference voltage of machines 1,2 and 3.

Response curves shown in Figs. 6.2 to 6.4 indicate the significantly small power fluctuation obtained with PSS of Table 6.6, that is, with stabilizers designed using the parameter optimization technique. The overshoot and settling time of these fluctuations are considerably smaller than those obtained with the stabilizers designed on eigenvalue-assignment basis. This is as expected since the objective of the stabilizer designed in the former case is the minimization of fluctuation in power outputs. It is interesting to observe that the relative rotor angles are well damped (with no oscillations) for the case of stabilizers designed on the basis of minimization of this performance index.

A comparison of Tables 6.4 and 6.6 shows the parameters of the stabilizers designed using the two approaches differ mainly for machines 2 and 3. Even here, the change is mainly in the gain and zeros of the PSS. It was mentioned earlier

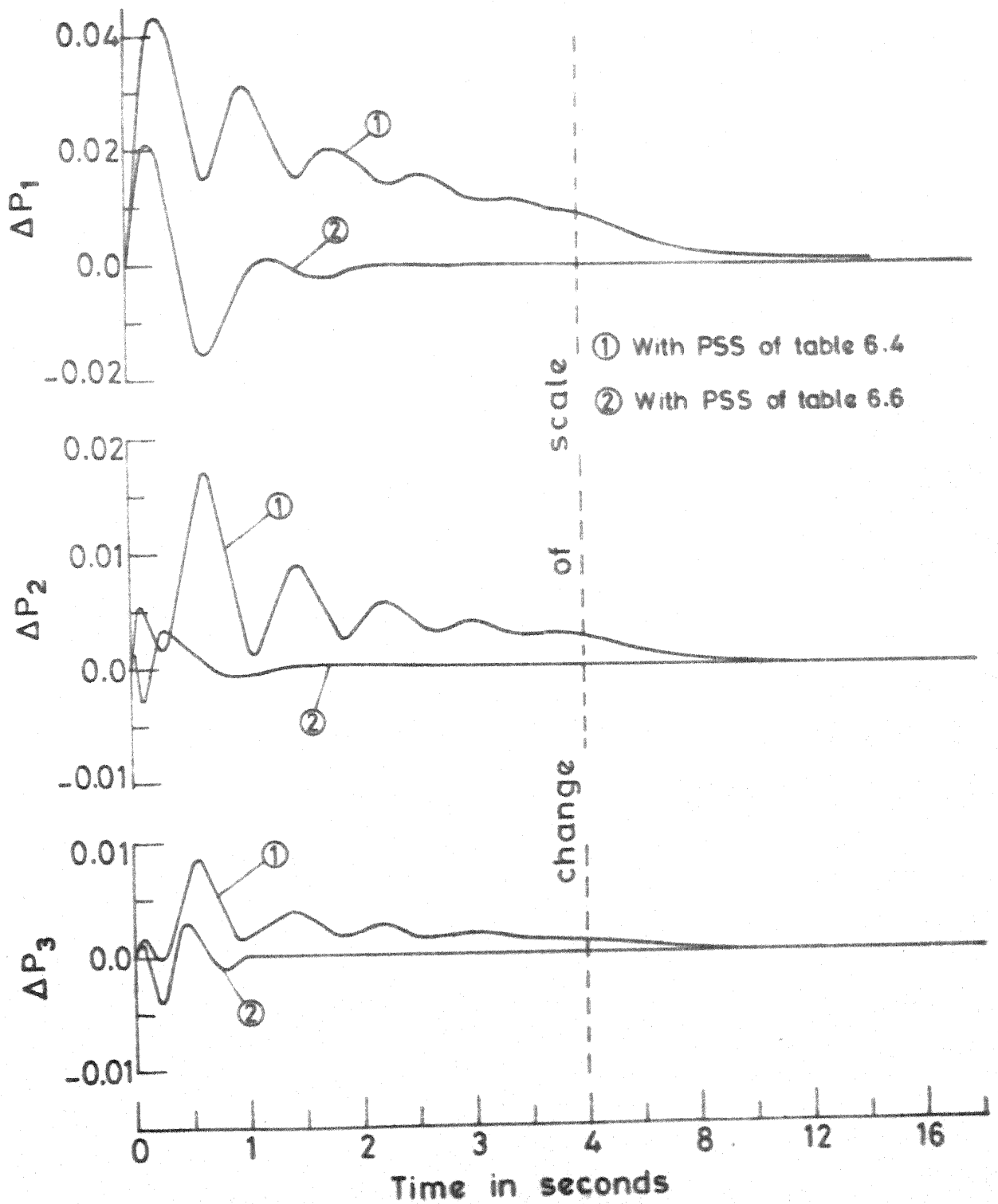


FIG.6.2 FLUCTUATION IN POWER OUTPUT OF GENERATOR IN p.u.

Case 1; for $\Delta V_{ref} = 1.0$ pu of machine 1.

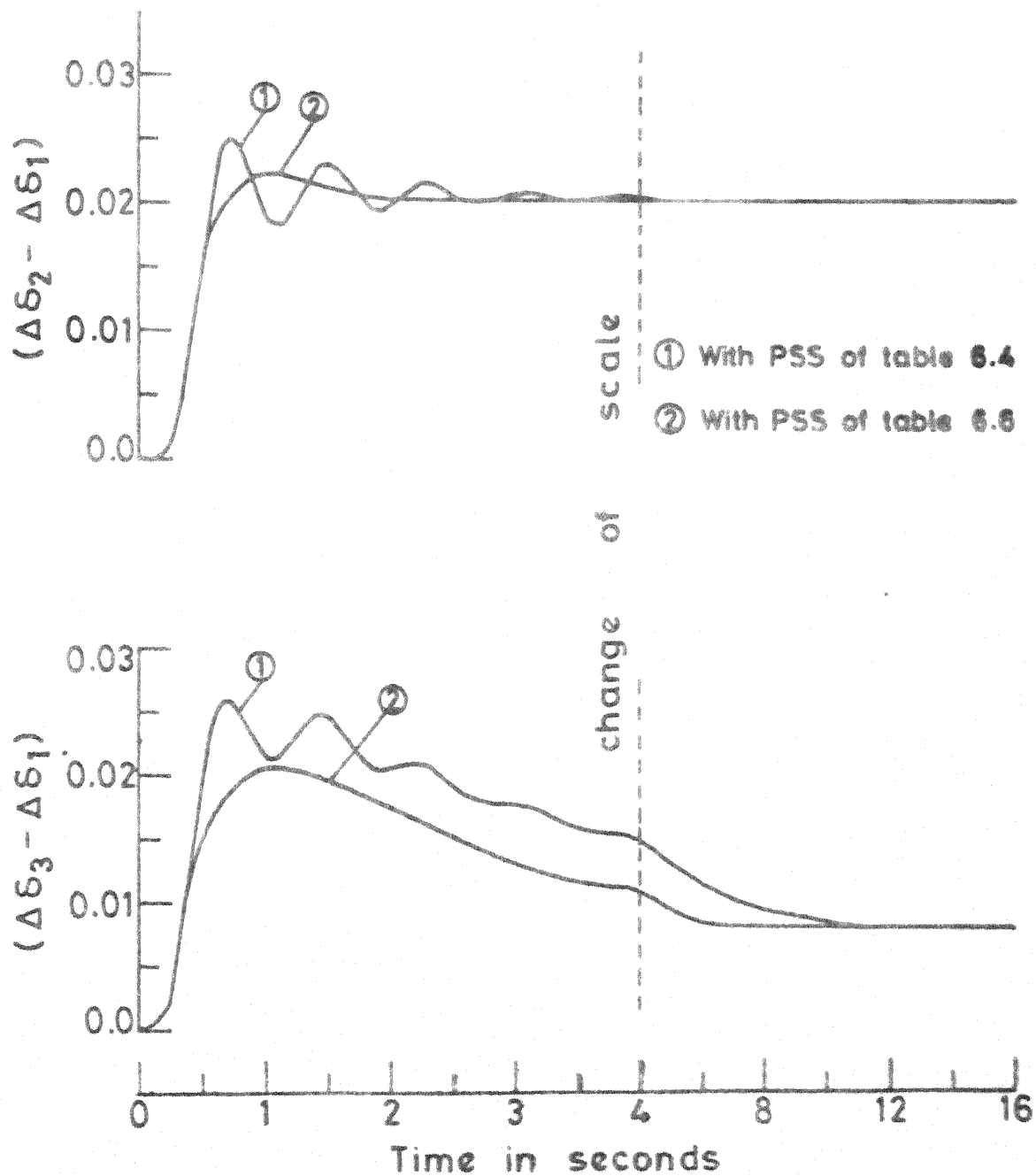


FIG.6.3 RESPONSE OF RELATIVE ROTOR ANGLE OF GENERATORS IN RADIAN.

Case 1: For $\Delta V_{ref} = 1.0$ pu of machine 1.

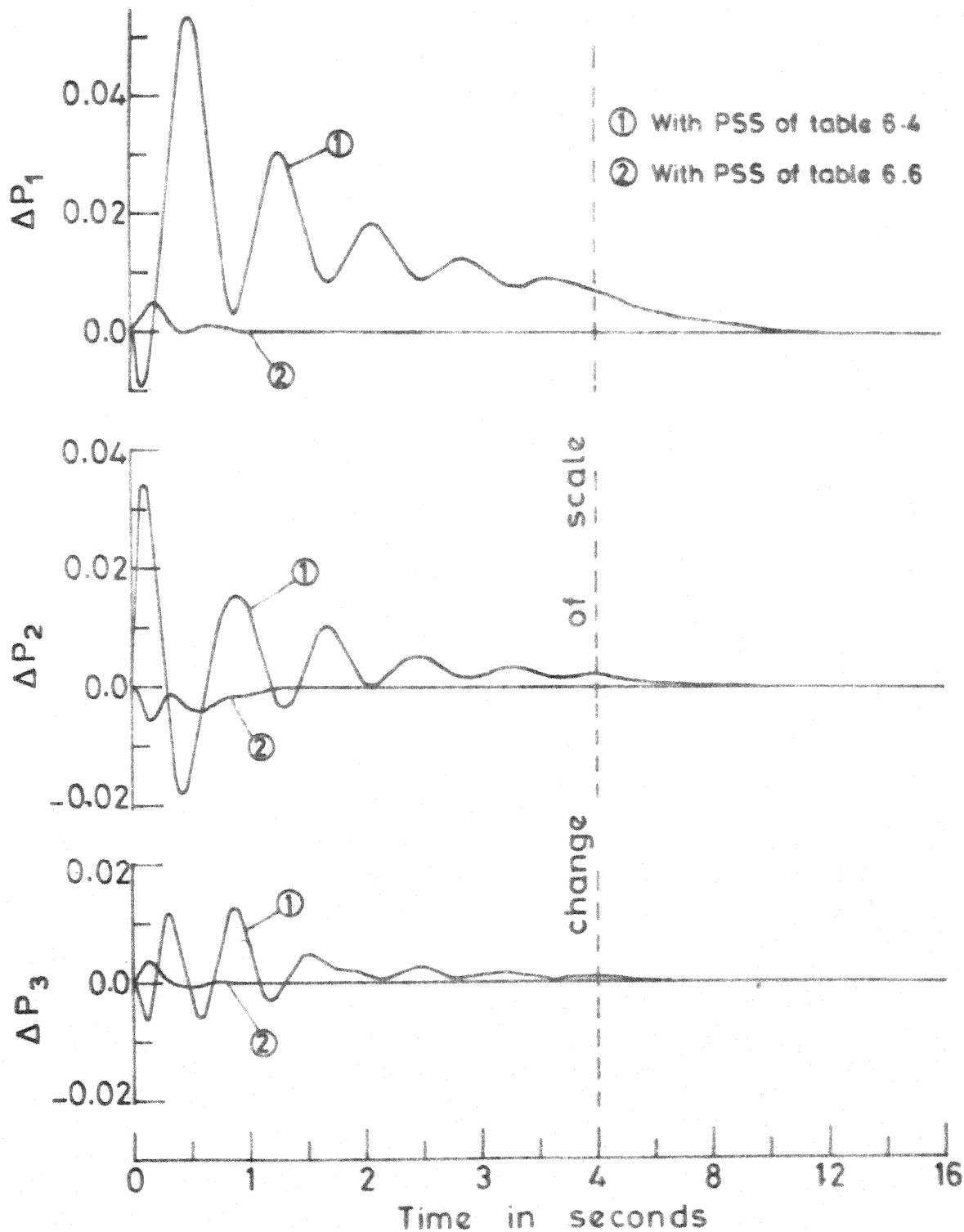


FIG.6.4 FLUCTUATION IN POWER OUTPUT OF GENERATORS IN p.u.

Case 2: for $\Delta V_{ref} = 1.0$ p.u. of machine 2.

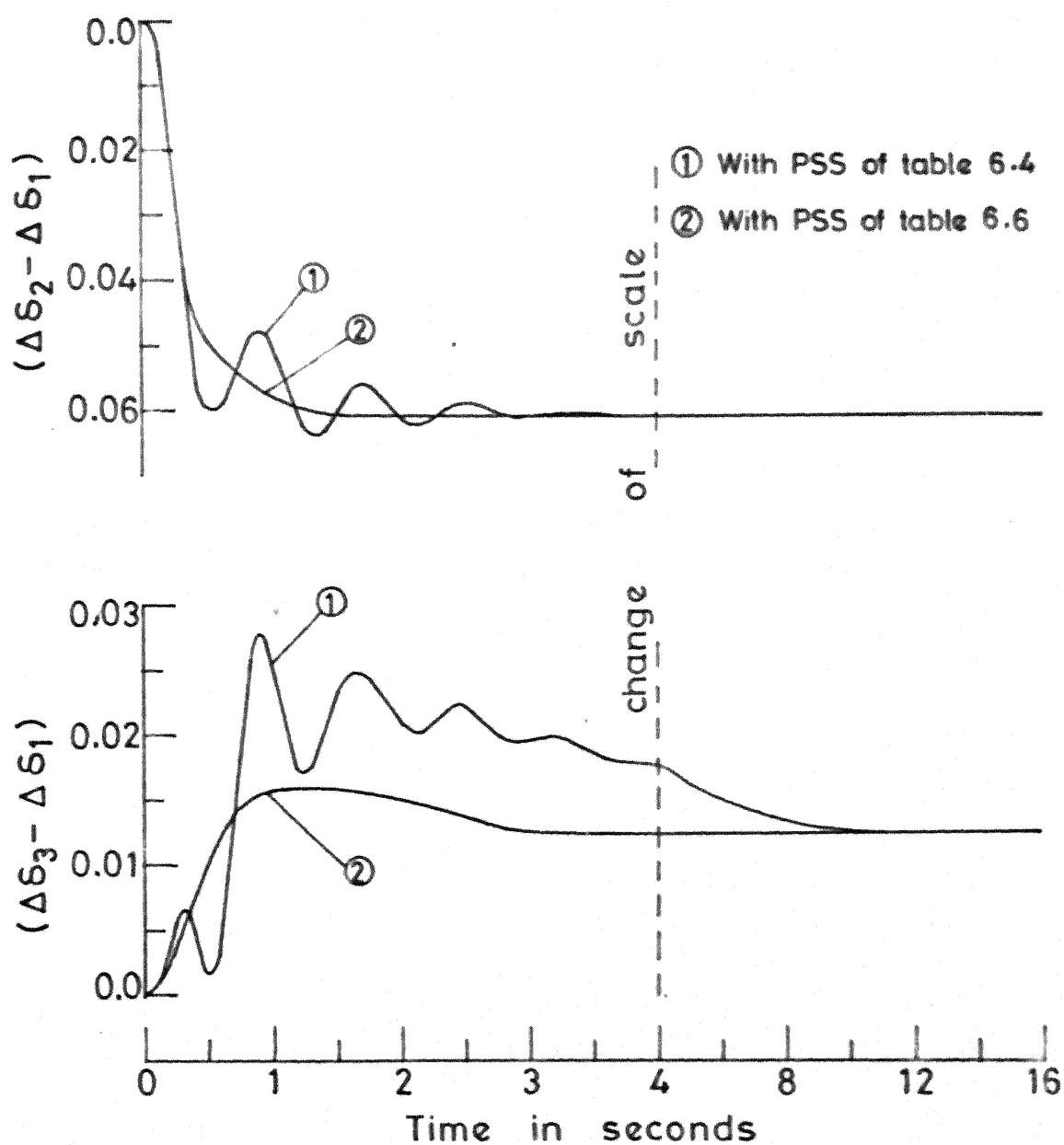


FIG. 6.5 RESPONSE OF RELATIVE ROTOR ANGLE OF GENERATORS IN RADIAN

Case 2: for $\Delta V_{ref} = 1.0$ pu of machine 2.

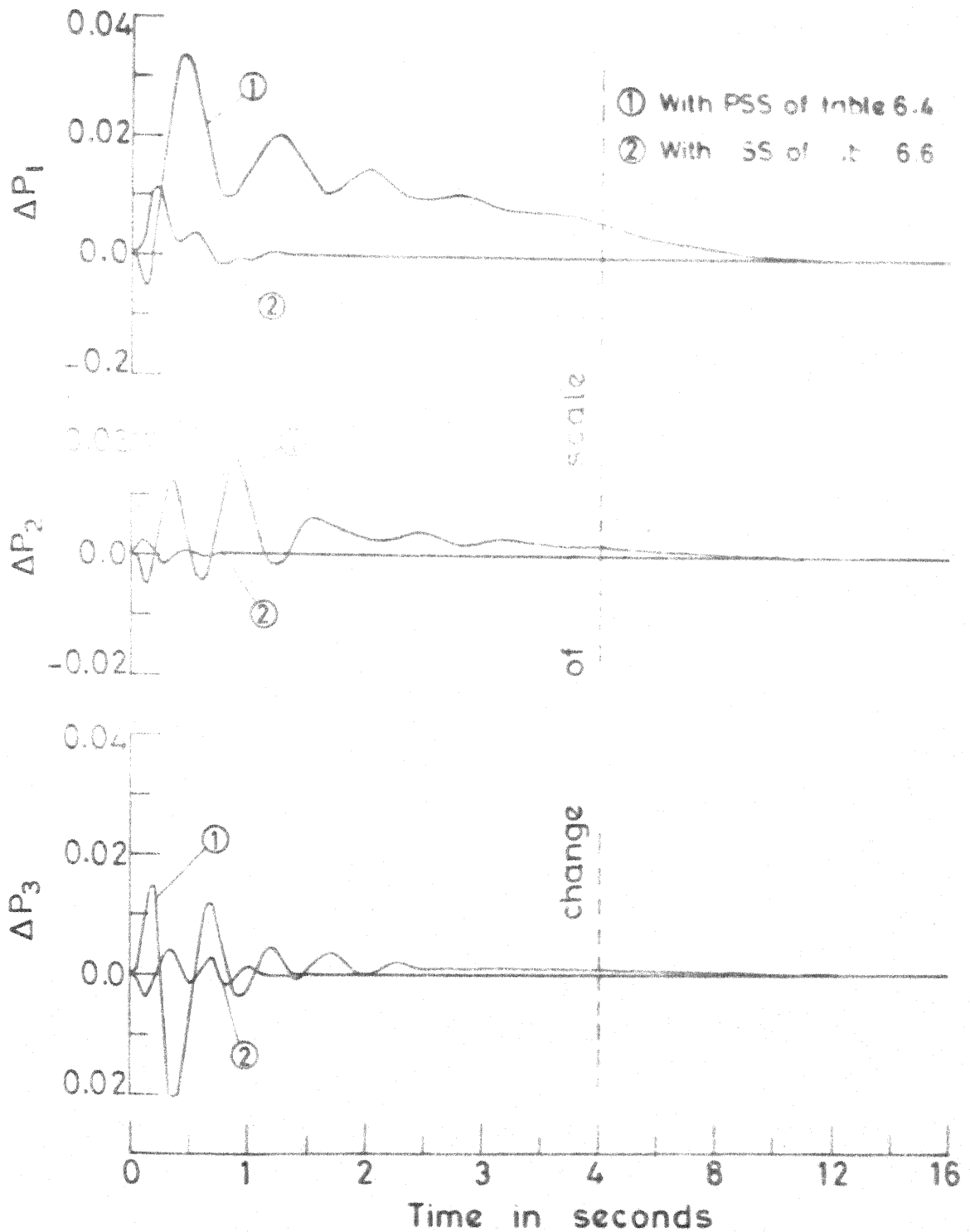


FIG.6.6 FLUCTUATION IN POWER OUTPUT OF GENERATOR IN p.u.

Case 3: For $\Delta V_{ref} = 1.0$ pu of machine 3.

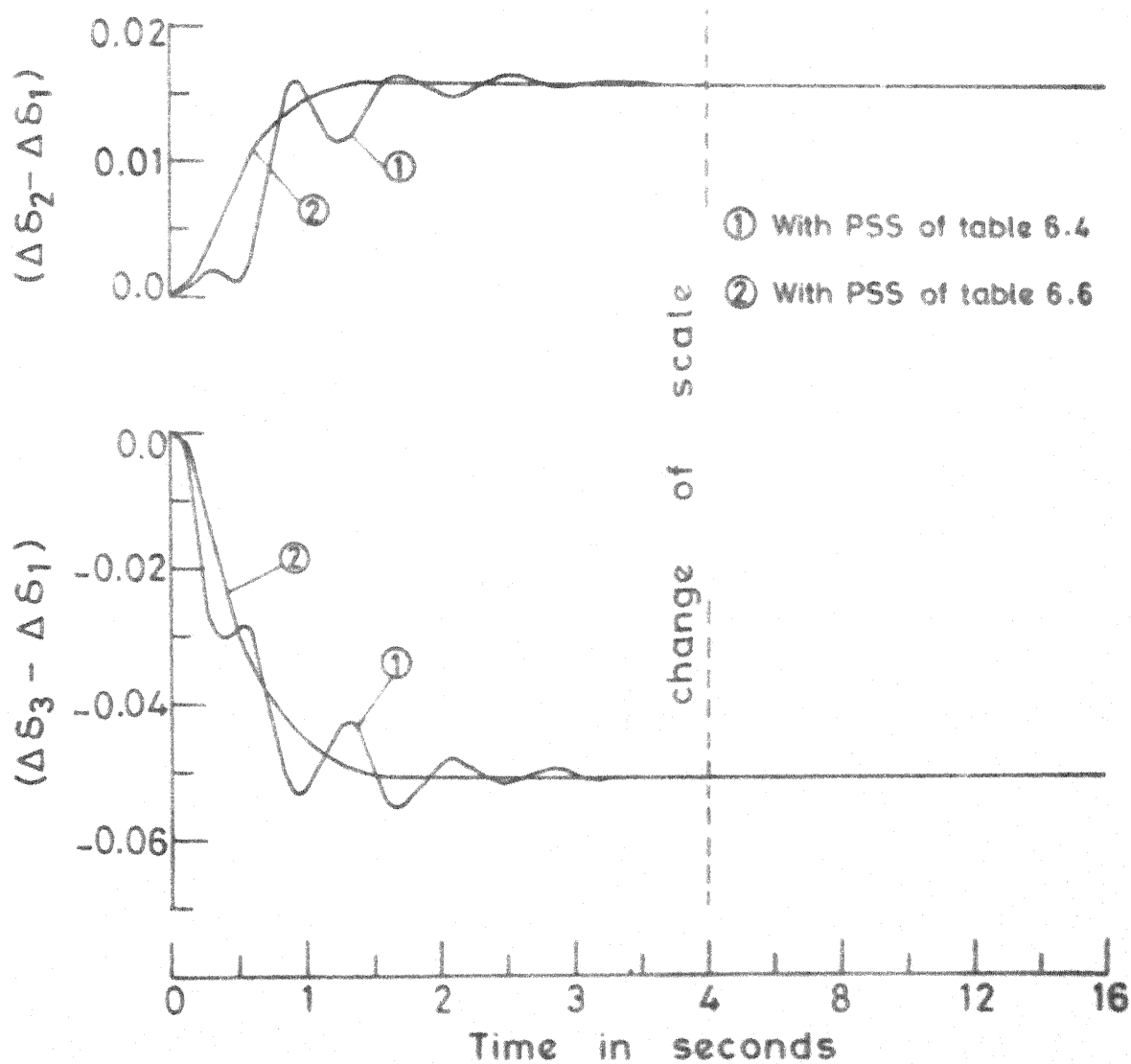


FIG.6.7 RESPONSE OF RELATIVE ROTOR ANGLE OF GENERATORS IN RADIAN

Case 3 : For $\Delta V_{ref} = 1.0$ pu of machine 3.

that parameters of PSS for the machine 1 are not much affected by the interconnection. Thus it would appear that satisfactory design of PSS is required in this system for machines 2 and 3, taking into account the interconnections between machines.

Reference [48] also considers the design of PSS for a three machine system (different than what is given here) based on the technique given in [77]. However, unlike the approach given here (of trying to control all the eigenvalues) the author of [48] has considered the assignment of only six eigenvalues using nine parameters of PSS. The work reported in this chapter was carried out independently and published [79] before the author came to know of the work reported in [48].

6.4.2 A Thirteen Machine Power System

The case study of a 13-machine power system described in Chapter 5 is taken up to illustrate the application of the design techniques, presented in Secs. 6.2 and 6.3, for large scale systems. The analysis presented, in Chapter 5, for the choice of PSS locations suggests that by equipping PSS on three machines, namely, machines 1, 7 and 11, most of the rotor oscillation modes could be adequately damped. Stabilizers are, therefore, designed for machines 1, 7 and 11. These machines are represented by fourth order models. The remaining machines are represented by the classical models. The

order of the open-loop and the closed-loop systems are, respectively, 31 and 37. Eigenvalues of the open-loop system are given in the third column of Table 5.1 in Chapter 5. The system is dynamically unstable without stabilizers.

6.4.2.1 Eigenvalue Assignment

As in case of the 3-machine system, stabilizers are first designed for the selected machines, using the algorithm given in Sec. 2.4.1, by neglecting the interconnections. Zeros of each PSS are specified as -2.0 and -2.5. Table 6.8 shows, at $r = 0$, the open-loop eigenvalues, desired locations of three closed-loop eigenvalues and remaining eigenvalues of the closed-loop system obtained from the design. Parameters of the stabilizers obtained in the first stage of design are given in Table 6.9.

Table 6.8 Eigenvalues of the Selected Machines in the 13-Machine System at $r = 0$

	Machine 1	Machine 7	Machine 11
Open-Loop eigenvalues at $r = 0$	0.08082 ± j9.07955 -5.96516 -44.64544	0.07421 ± j13.16434 -6.65288 -44.40063	0.10407 ± j8.17827 -6.16746 -44.41907
Desired Locations of 3 Closed-Loop Eigenvalue	-2.68 ± j10.00 -3.00	-3.75 ± j14.00 -3.00	-2.41 ± j9.00 -3.00
Remaining Closed-Loop Eigenvalues	-6.77244 ± j4.88345 -47.54431	-12.93100 ± j1.68711 -57.30693	-5.83129 ± j4.90926 -46.55321

Table 6.9 PSS Parameters for the Selected Machines
in the 13-machine System at $r = 0$

Machine	θ_0	θ_1	θ_2	γ_1	γ_2
1	0.29135	1.31110	1.45677	19.00023	48.54020
7	0.34159	1.53715	1.70794	42.76378	119.96623
11	0.18836	0.84761	0.94178	15.65740	38.43923

In the second stage of design, a step of $\Delta r = 0.05$ is considered in updating the gain and the poles of the PSS. Table 6.10 shows the final values of PSS parameters with full interconnection. Table 6.11 shows the closed-loop eigenvalues of the system. First column of Table 6.11 shows the eigenvalues of the decoupled system with PSS parameters of Table 6.9, that is, with stabilizers designed in the first stage of design. Second and third columns of Table 6.11 shows the eigenvalues of the fully connected system obtained with PSS parameters of Tables 6.9 and 6.10 respectively.

Table 6.10 PSS Parameters for the Selected Machines
in the 13-machine System at $r = 1$

Machine	θ_0	θ_1	θ_2	γ_1	γ_2
1	0.28609	1.28739	1.43044	24.94678	119.56568
7	0.32659	1.46966	1.63296	42.51388	119.47225
11	0.17572	0.79076	0.87862	17.17517	51.16386

Table 6.11 Closed-Loop Eigenvalues of the 13-Machine System

Assigned at $r = 0$ with PSS of Table 6.10	Obtained at $r = 1$ with PSS of Table 6.10	Obtained at $r = 1$ with PSS of Table 6.11
$-3.75000 \pm j14.00000$	$-3.08390 \pm j14.12752$	$-2.92632 \pm j14.10790$
$0.0 \pm j13.01410$	$-0.18909 \pm j13.39396$	$-0.18524 \pm j13.37862$
$0.0 \pm j10.50104$	$-0.40267 \pm j11.79312$	$-0.23079 \pm j11.77149$
$0.0 \pm j10.24194$	$-0.40256 \pm j10.86772$	$-0.18680 \pm j10.70338$
$0.0 \pm j10.18118$	$-0.04167 \pm j10.60303$	$-0.06316 \pm j10.56687$
$-2.68000 \pm j10.00000$	$-0.03537 \pm j10.51028$	$-0.06807 \pm j10.50823$
$0.0 \pm j9.86085$	$-0.68569 \pm j10.47898$	$-0.57632 \pm j10.40899$
$0.0 \pm j9.68993$	$-0.03828 \pm j10.27158$	$-0.05326 \pm j10.26468$
$0.0 \pm j9.34472$	$-0.03207 \pm j9.41924$	$-0.02639 \pm j9.41090$
$-2.41000 \pm j9.00000$	$-0.61724 \pm j8.97292$	$-0.43355 \pm j8.77155$
$0.0 \pm j8.13542$	$-0.53791 \pm j8.00539$	$-0.43318 \pm j7.90272$
$0.0 \pm j7.31242$	$-0.65133 \pm j6.43692$	$-0.55035 \pm j6.17615$
0.0000	-0.62008	-0.38637
-3.0000	-2.89078	-2.98356
-3.0000	-2.99349	-3.50351
-3.0000	-3.00116	-4.53175
$-5.83123 \pm j4.90926$	$-6.29856 \pm j5.17551$	$-7.22301 \pm j5.86688$
$-6.77243 \pm j4.88344$	$-9.00956 \pm j7.47702$	$-10.97008 \pm j8.82632$
$-12.93102 \pm j1.68753$	-10.49561	-10.19024
	-13.65274	-15.53490
-46.55321	-46.58312	-46.52583
-47.54433	-47.54057	-47.92226
-57.30651	-57.32446	-56.93663

A comparison of Tables 6.9 and 6.10 shows that the modification in the parameters of PSS are not significant for machine 7. The first column of the Table 6.11 shows that system is critically stable as the real parts of the eigenvalues of the rotor oscillation modes are zero for machines represented by the classical model. If the eigenvalues are to be retained at these locations, as per the objective of the design algorithm, the design will not be acceptable. However, the second and third columns show that the system is stable with the PSS designed for the three selected machines, although the damping of some of the rotor oscillation modes are small.

6.4.2.2 Minimization of Performance Index

As in case of the 3-machine system, parameter optimization technique, of Sec. 6.3, is used to design PSS for the three selected machines, that is machines 1, 7 and 11. The objective is to minimize the performance index given in eqn. (6.21) with the weightage parameter α_i , defined as follows :

$$\alpha_i = \begin{cases} 1 & \text{for } i = 1, 7 \text{ and } 11 \\ 0 & \text{for all other values of } i \end{cases}$$

For the sake of convenience, the initial choice of PSS parameters is made from the results obtained in the previous section. The optimal values of PSS parameters are given in Table 6.12 and the corresponding closed-loop eigenvalues are given in Table 6.13.

Table 6.12 PSS Parameters for the Selected Machines
in the 13-Machine System Obtained from
Parameter Optimization Technique

Machine	θ_0	θ_1	θ_2	γ_1	γ_2
1	0.37164	2.70569	12.05420	25.04285	119.54951
7	0.32432	1.19484	1.45901	42.48807	119.48033
11	0.42671	4.87906	13.83516	17.16288	51.16308

Table 6.13 Eigenvalues of the 13-Machine System with
PSS of Table 6.12

-2.89734 ± j13.80945
-1.61382 ± j13.61650
-0.19060 ± j13.39934
-0.37997 ± j11.79321
-0.35992 ± j10.86744
-0.34208 ± j10.59898
-0.12740 ± j10.51181
-0.53875 ± j10.26825
-0.22389 ± j 9.44422
-0.35956 ± j 9.39171
-0.28609 ± j 8.65416
-0.27365 ± j 6.90138
-10.76684 ± j 9.05954
-1.81087 ± j 2.84426
-12.81823 ± j 2.07492
-2.85494
-3.11521
-5.86962
-7.10297
-48.46174 ± j 0.071491
-56.98209

The effectiveness of stabilizers, designed with the two techniques presented, is compared by taking time response of fluctuations in power output and the relative rotor angle of the selected generators following a disturbance. Three cases are considered :

- (1) a unit step change in reference voltage of machine 1.
- (2) a unit step change in reference voltage of machine 7.
- (3) a unit step change in reference voltage of machine 11.

The variation in the power output and the relative rotor angles for machines 1,7 and 11, for all the three cases are given in Figs. 6.8 to 6.13.

From these figures it is clear that the PSS design based on minimization of performance index results in superior performance particularly in terms of variation in the generator outputs. Not only the magnitudes of oscillations are negligible, but the settling time is also reduced.

A comparison of Tables 6.10 and 6.12 shows that the poles of the stabilizers, designed using the two techniques, remain almost unchanged. The change is mainly in gain and zeros of stabilizers of machine 1 and 11.

6.4.3 Discussions

A comparison of the two approaches for PSS design can be made based on the results of the two examples presented. It is seen that the method based on the minimization of performance

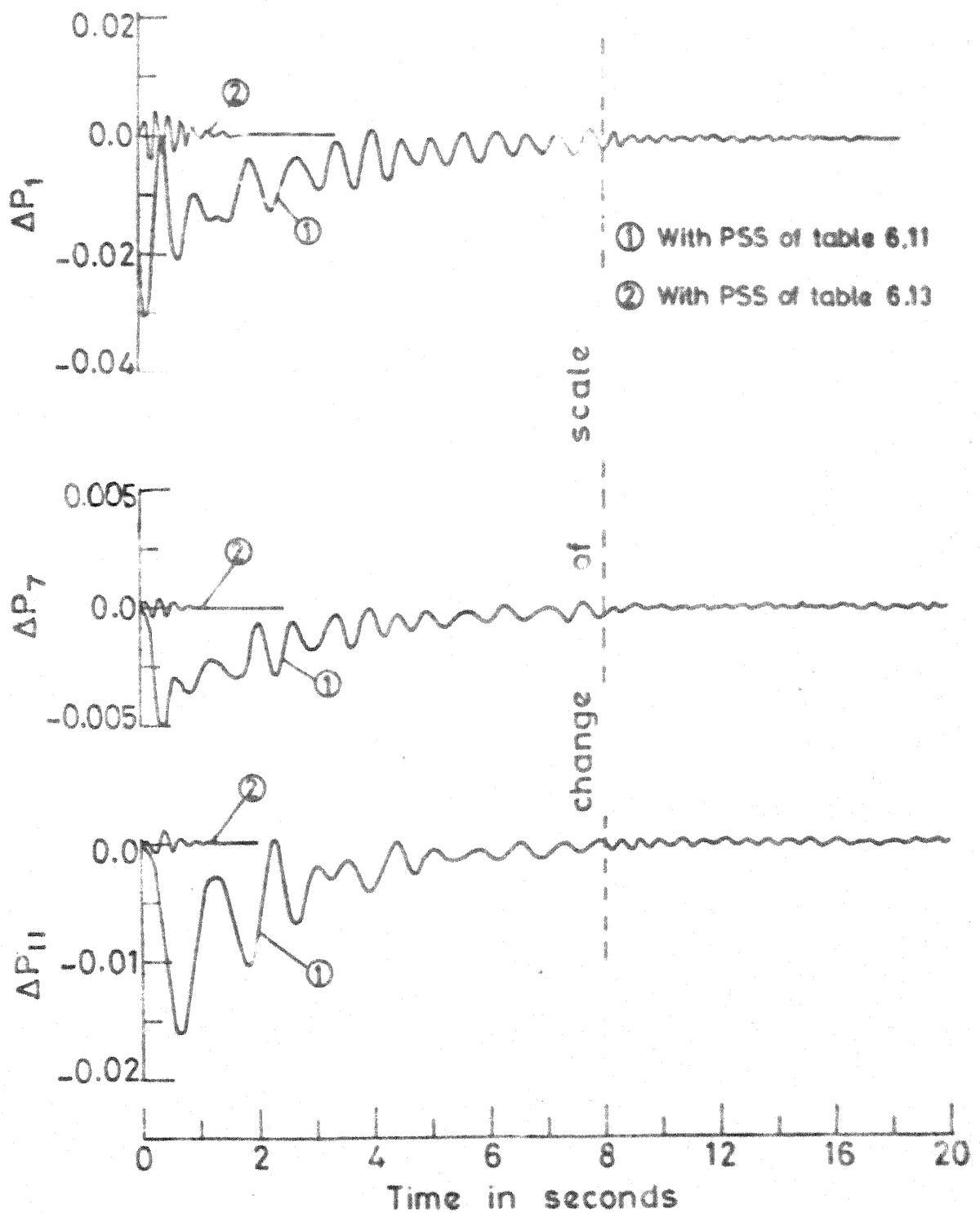


FIG.6.8 FLUCTUATION IN POWER OUTPUT OF GENERATOR IN p.u.

Case 1: for $\Delta V_{ref} = 1.0$ pu of machine 1.

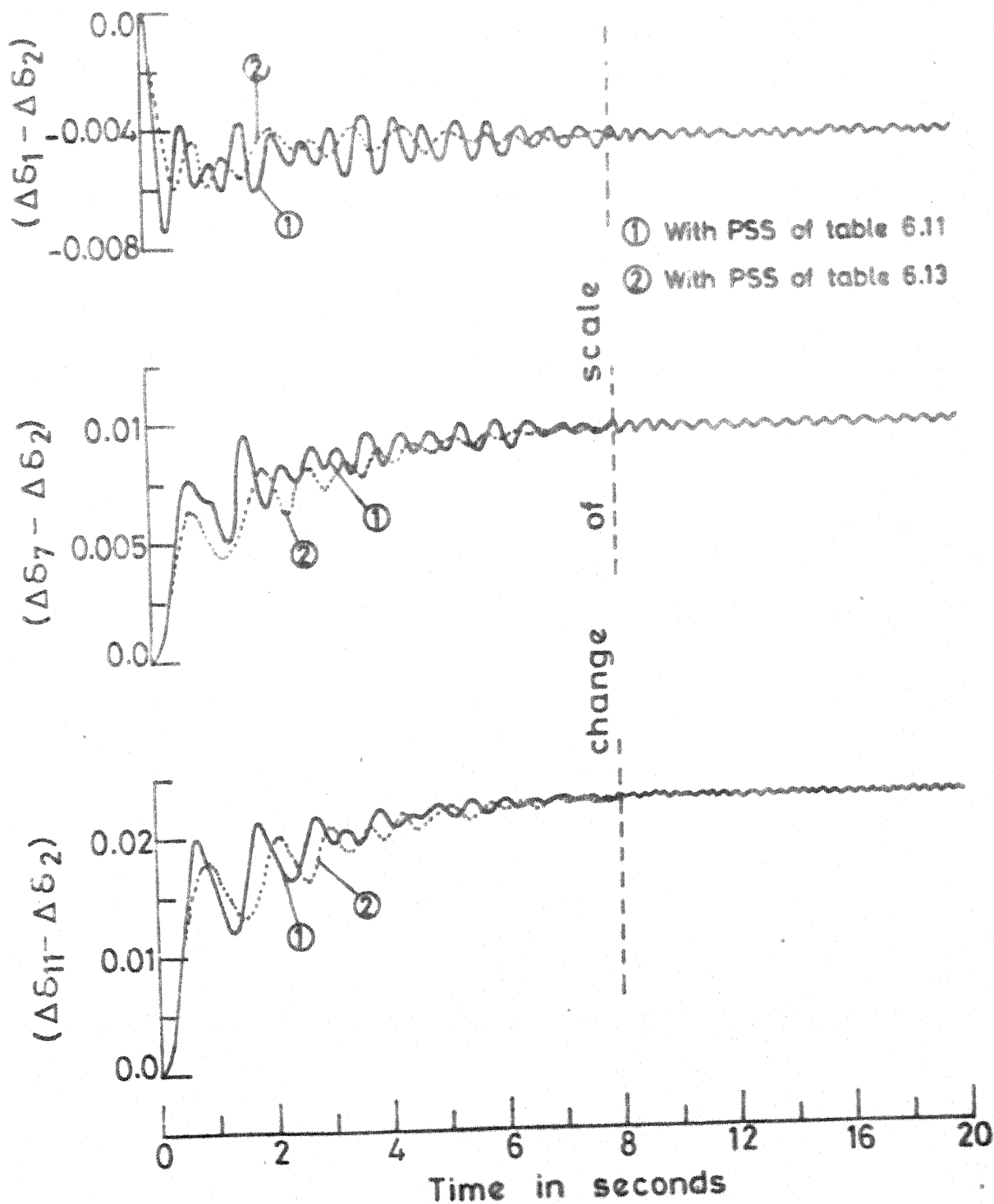


FIG.6.9 RESPONSE OF RELATIVE ROTOR ANGLE OF MACHINE IN RADIAN.

Case 1: for $\Delta V_{ref} = 1.0$ pu of machine 1.

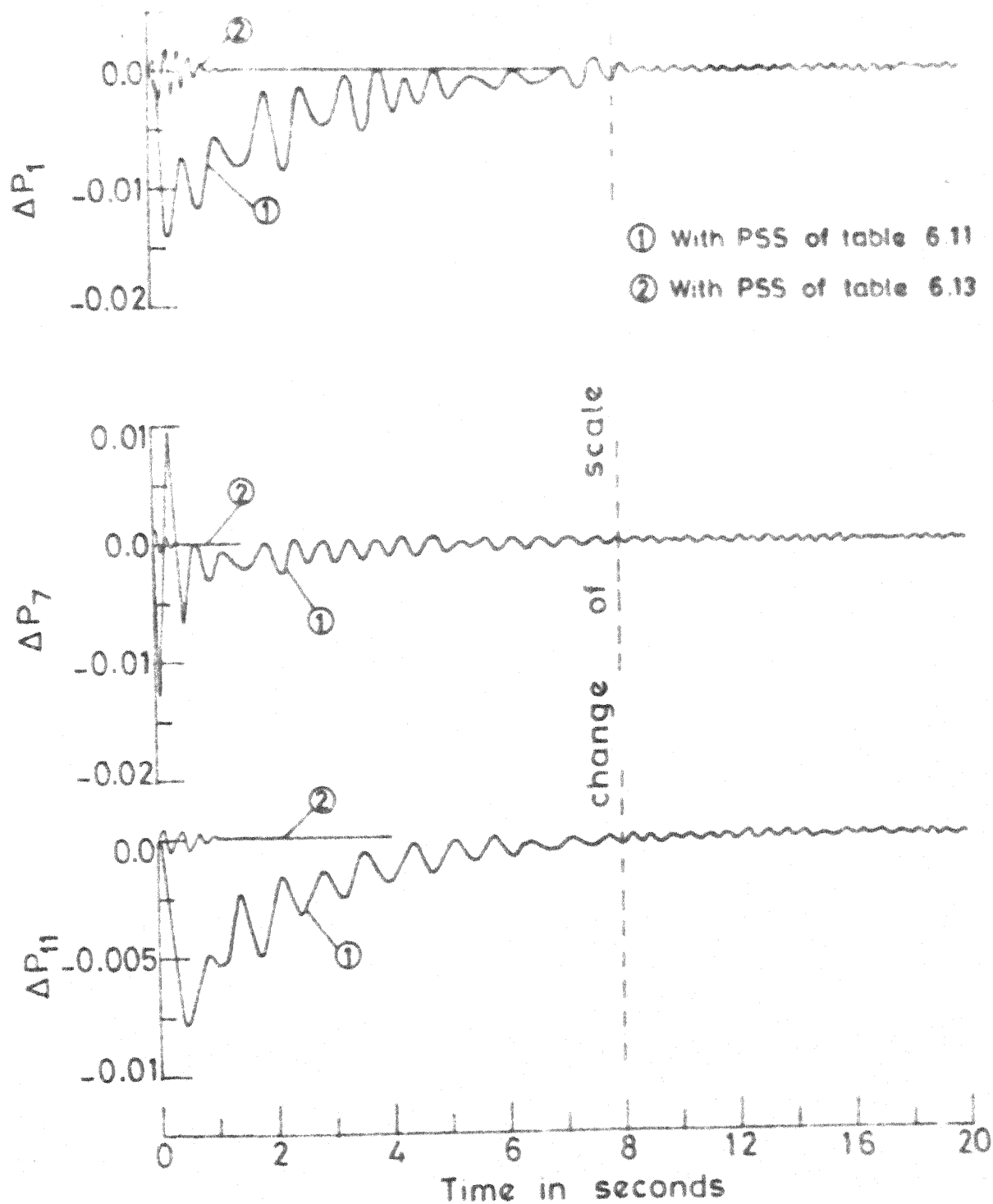


FIG.6.10 FLUCTUATION IN POWER OUTPUT OF GENERATOR IN p.u.

Case 2: for $\Delta V_{ref} = 1.0$ pu of machine 7.

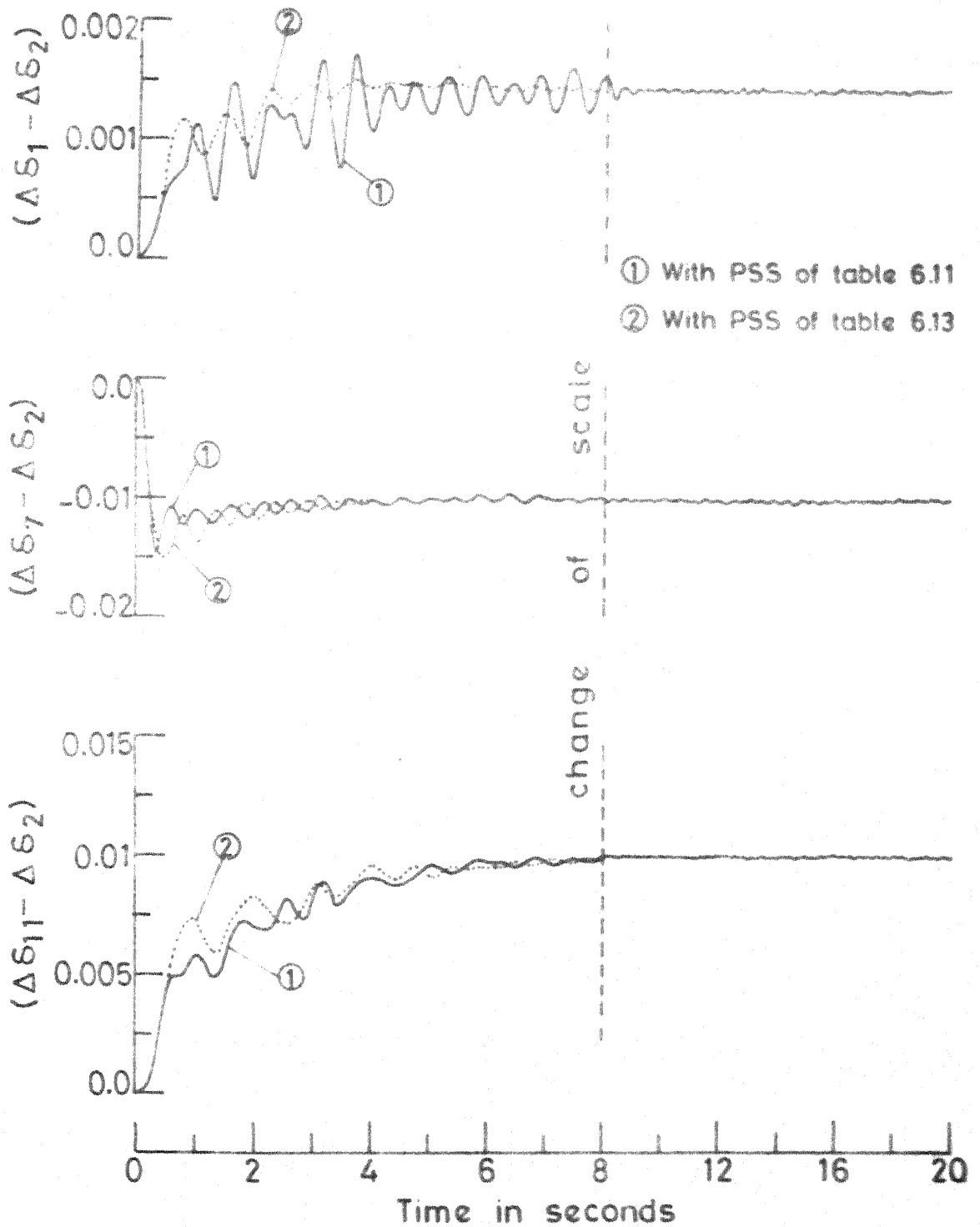


FIG.6.11 RESPONSE OF RELATIVE ROTOR ANGLE OF GENERATORS IN RADIAN.

Case 2: for $\Delta V_{ref} = 1.0$ pu of machine 7.

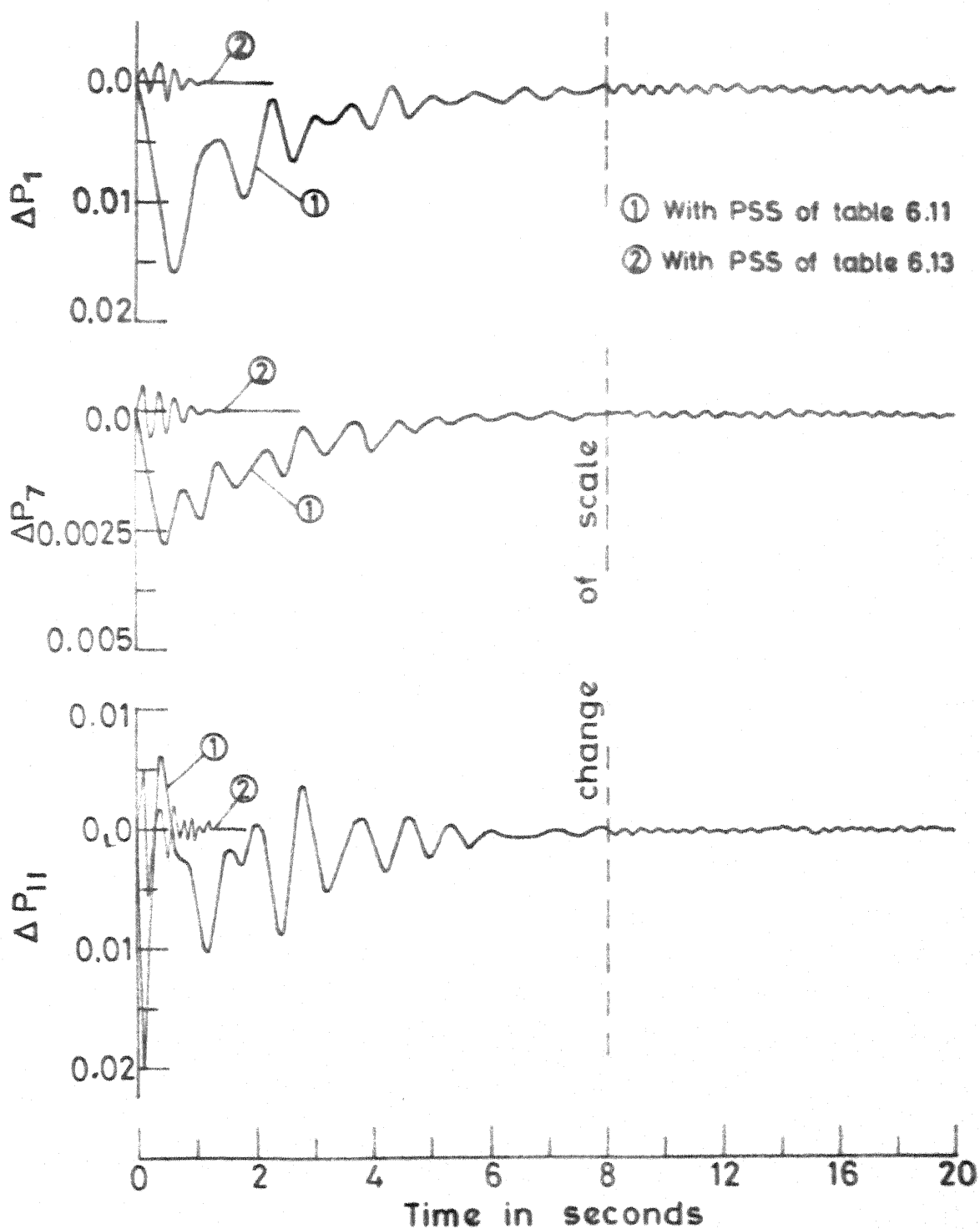


FIG.6.12 FLUCTUATION IN POWER OUTPUT OF GENERATORS IN p.u.

Case 3: for $\Delta V_{ref} = 1.0$ pu of machine 11.

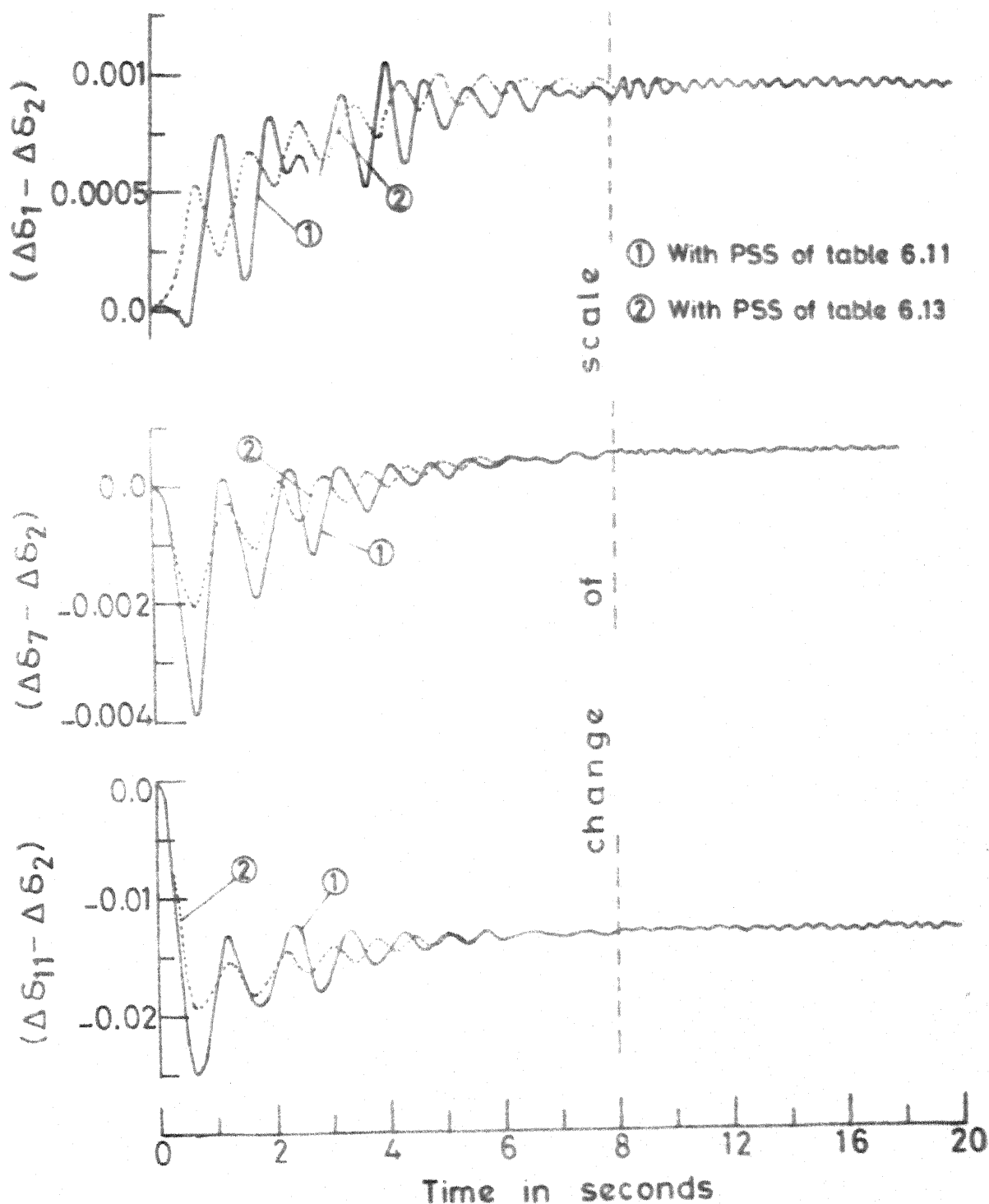


FIG.6.13 RESPONSE OF RELATIVE ROTOR ANGLE OF GENERATORS IN RADIAN.

Case 3: For $\Delta V_{ref} = 1.0$ pu of machine 11.

index (the fluctuations in the power outputs of the selected generators) gives excellent results. The approach based on eigenvalue assignment (utilizing the algorithm given in [77]) is not so satisfactory in comparison, particularly for the 13-machine system.

An n machine power system, without an infinite bus, has $(n-1)$ modes of rotor oscillations. For large systems many of these modes are quite close. This can be seen from the results of Table 5.1. The objectives of the stabilizers in a system are primarily to damp certain modes of rotor oscillations which can be troublesome. Analytically this can be found from the inspection of the open-loop eigenvalues, utilizing suitable system model. However, most often the problems are encountered during the system operation under various conditions where oscillations of power in transmission lines are experienced. It can be quite difficult to identify the particular modes that give rise to these oscillations in a large system.

Even if the problem of identification of unstable modes can be solved analytically, it is difficult to associate a particular mode with a particular machine in all the cases. This is more so in a large system as demonstrated for the 13-machine system in Chapter 5. Because of this problem, it is difficult to specify the eigenvalues when the interconnections are neglected (as required in the first stage

of the algorithm of [77])). This problem is aggravated if PSS is to be provided on all the machines as one (reference) machine will be left out which has no rotor mode associated with it in the absence of interconnections (see the 3-machine example given above). Ref. [48] considers a 3-machine example with an infinite bus which has three modes; the inclusion of infinite bus, however, is not satisfactory in general.

The above discussion shows that there is a problem associated with the design approach based on the algorithm given in [77]. Moreover, additional problems crop up in the second stage of the algorithm where the controller parameters are modified. These are (1) inadequacy of limited controller parameters in influencing all the dominant eigenvalues and (2) numerical problems caused by the drift of eigenvalues which make it impossible to distinguish between different eigenvalues when they are quite close.

As the power system stabilizers are designed to overcome the problem of low frequency power oscillations, it is convenient to choose the objective of minimizing the power fluctuations. Although, the number of examples considered are not extensive, the results based on this approach are excellent. However, the parameter optimization technique requires large computational effort in comparison with eigenvalue assignment method. The minimization of performance index is an iterative procedure which requires the solution of two Liapunov equations

in each iteration. The solution of Liapunov equation itself is obtained through an iterative technique [80]. This increases the computational effort of this method in comparison with the method based on eigenvalue assignment. The computational effort of parameter optimization technique is about six to ten times, in terms of computer time, than required in the eigenvalue assignment technique. Since the design is done off-line, the computational burden involved does not pose a serious limitation.

6.5 CONCLUSIONS

The detailed investigation into the design of PSS in a large multimachine system using decentralized control is presented in this chapter. A comparative study of the two approaches, one based on eigenvalue assignment using the algorithm given in [77], the second based on minimization of performance index is carried out using two numerical examples. The case study of a 13-machine system presented here is typical of a large power system where PSS are designed on selected machines.

The results of the case study indicate the superiority of the design technique based on parameter optimization with the objective of minimizing the fluctuations in the power output of generators. Although the computational burden is greater in this method, the results justify its adoption for large scale systems. The inherent weaknesses of the algorithm given in [77] for the design of PSS make it unattractive for its application in large systems.

CHAPTER 7

CONCLUSIONS

7.1 GENERAL

This thesis has dealt with several aspects in design of power system stabilizers, namely, (i) choice of design objectives and algorithms for PSS design as dynamic compensators, (ii) study of adequacy of system models and effectiveness of control signals and (iii) selection of the location and design of PSS in large multimachine power systems using decentralized control theory. Specific contributions of the thesis are reviewed below.

7.2 OBJECTIVES AND TECHNIQUES FOR PSS DESIGN

The design of PSS in power industry has been based on the objective of improving the damping torque. The design techniques are derived from classical control theory and utilize frequency domain techniques. The drawbacks in this approach are (i) design freedom is not fully utilized and (ii) it is difficult to extend it to multimachine system model. With this in view, design techniques have been developed in Chapter 2 based on the objectives of pole assignment and minimization of a performance index.

Pole assignment is a natural objective in power system stabilization. It has been shown [44] that the improvement of damping torque is related to the shifting of eigenvalues corresponding to the rotor oscillations to the left in the complex plane. While this idea has been used in the previously published papers, practical constraints of utilizing dynamic output feedback have not been considered in detail. The design of PSS as a dynamic compensator of a specified order has also not been reported. Chapter 2 presents two techniques for the design of dynamic output feedback compensator. In the first one, modal control theory has been used. The only restriction in this method is that, the zeros of PSS transfer functions are to be specified. The second method, which is based on the algorithm given by Munro and Hirbod [66], is more general where all the parameters of the PSS are obtained directly in terms of specified closed-loop poles. Thus, full design freedom can be utilized. The examples given for the illustration show that, the transfer function of PSS in many instances is of non-minimum phase type or the poles and zeros are complex.

While the design examples given have considered only second order compensators (as is commonly used in practice), the methods are general enough to design compensator of any arbitrary order. The algorithms are computationally efficient and require only the solution of algebraic equations to determine the PSS parameters.

Assignment of closed-loop poles anywhere in a sector in the left half of the complex plane guarantees stabilization of the system with a prescribed degree of damping. However, the design algorithms require exact specification of the closed-loop poles. This, in general, is difficult and arbitrary location of poles may not result always in a satisfactory performance. These drawbacks can be eliminated by selecting an alternate design objective, namely, that of minimising the fluctuations in power output of generators. It is to be noted that the need for PSS was recognised because of oscillations in the power in transmission lines which in turn are related to the oscillations in the power output of generators. This objective can be stated in terms of minimizing a performance index in the framework of optimal control theory. While there has been some work on the application of optimal control for power system stabilization in the past, this has neglected the practical constraints of using dynamic output feedback. Also, no attempts were made earlier, to relate the performance index to an objective related to the damping of oscillations used by power engineers. The work reported in Chapter 2 overcomes both those limitations and is novel in terms of PSS design. Although, computational requirement is more in this case, the system response following a disturbance is better than with other designs. This has been shown by examples given in Chapters 2 and 6.

7.3 CHOICE OF MACHINE MODEL AND EFFECTIVENESS OF CONTROL SIGNALS

The simplified model of synchronous machine (neglecting the effect of amortisseur windings) has been extensively used for the design of PSS, however, its adequacy has not been analysed. The adequacy of the simplified machine model for PSS design has been analysed in Chapter 3. A detailed representation of synchronous machine with three amortisseur windings was considered. PSS designed using pole assignment and the simplified representation of machine was analysed using the detailed machine representation. Eigenvalue and time-domain analyses have been carried out to judge the effectiveness of the PSS. From the results, it is shown that the simplified representation of machine is adequate for PSS design.

Control signals derived from rotor speed, bus frequency or electrical power have been used. The relative merits of these signals have not been analysed in detail, although, Larsen and Swann [26] have given some rules for the tuning of PSS utilizing these signals. It was mentioned that PSS using speed and power signals should be tuned for strong systems (smaller value of external reactance) and PSS using frequency signal should be tuned for weak systems. These conclusions are related to the design objective of providing damping torque.

Chapter 4 has presented a comparative study of the control signals for the design of PSS with the objective of pole assignment. All the three different PSS for the three different signals were designed with the same objective and their relative merits are studied by plotting the stability boundaries in the P-Q domain. The PSS designed at different values of system strength were also compared in terms of their effectiveness at different operating values of system strength. The results show that the power signal in all cases results in largest stability domains while the speed signal gives smallest. Also, it is found that PSS designed at different system strength with power signal are uniformly effective whereas PSS designed for weak systems with speed signal is more effective than PSS designed for strong systems. Similar conclusions can also be drawn for frequency signal. While those results are at variance with what is given in [26], it is to be noted, that design objective here is different.

The effectiveness of control signals when applied to a generating plant with two units has been considered in Chapter 4. Results show that the use of average speed instead of individual speed signal is distinctly superior. This observation tallies with what is given in [25]. In [25], it is mentioned that the use of individual speed, limits the usable gain of PSS because the local mode

(corresponding to the mode of oscillations between the two machines) is negatively damped as the gain is increased. It was experimentally observed that the use of average speed did not have such limitations, however, no explanation is given in [25] to explain this phenomena. It is shown in Appendix F that for identical machines and with identical loading, the local mode is not controllable when average speed is used. Thus, it is not surprising that increase in PSS gain has no effect on local mode and hence the undamping of local mode is not a factor in limiting the gain.

7.4 PSS DESIGN IN MULTIMACHINE SYSTEM

Coordinated design of PSS in multimachine system has gained much attention recently. Design of PSS in multimachine systems is not straightforward because of the complexities associated with large systems. Some work has been reported in the past for the selection of effective PSS locations and subsequent tuning of PSS parameters. However, a detailed investigation, particularly for large systems is not available. A fast technique based on eigenvalue sensitivities has been presented in Chapter 5 for the selection of effective location of PSS in multimachine system and their efficacy has been tested for a large power system. Results indicate that it is sufficient to equip relatively few machines with PSS for adequate system damping.

Design of PSS in multimachine system has been taken up in Chapter 6 with the objective of pole assignment and

minimization of the performance index. Decentralized control theory has been used for the design of stabilizers. Two examples, a 3 machine and a 13 machine systems have been considered. In case stabilizers are designed for limited number of machines, it is found that the pole assignment technique given in [77] is not effective. The design method based on the minimization of the performance index (related to the minimization of power fluctuations) is found to be superior as it gives well damped responses with little overshoot.

7.5 SUGGESTIONS FOR FURTHER WORK

Methods presented in this thesis for the design of PSS are based on deterministic system model of power systems. But the realistic system models are stochastic in nature because of noise in measurement and random nature of load variations. Design of PSS based on stochastic system model is an open area for further work.

Operating condition in a power system are not constant but keep changing. Thus, PSS designed for a particular operating condition may not be suitable for others and there is a need for adaptive PSS. Design of such PSS is another area for further work.

REFERENCES

- [1] H.M. Ellis, J.E. Hardy, A.L. Blythe and J.W. Scooglund, 'Dynamic Stability of the Peace River Transmission Systems', IEEE Trans. Power App. Sys., Vol. PAS-85, pp 586-600, June 1966.
- [2] O.W. Hanson, C.J. Goodwin and P.L. Dandeno, 'Influence of Excitation and Speed Control Parameters in Stabilizing Intersystem Oscillations', IEEE Trans. Power App. Sys., Vol. PAS-87, pp 1306-1313, May 1968.
- [3] R.T. Byerly, F.W. Keay and J.W. Scooglund, 'Damping of Power Oscillations in Salient Pole Machines with Static Exciters', IEEE Trans. Power App. Sys., Vol. PAS-89, pp 1009-1021, July/Aug. 1970.
- [4] W. Watson and G. Manchur, 'Experience with Supplementary Damping Signals for Generator Static Excitation Systems', IEEE Trans. Power App. Sys., Vol. PAS-92, pp 199-203, Jan/Feb. 1973.
- [5] P.A. Rusche, D.L. Hackett, D.H. Baker, G.E. Gareis and P.C. Krause, 'Investigation of the Dynamic Oscillations of the Ludington Pump Storage Plant', IEEE Trans. Power App. Sys., Vol. PAS-95, pp 1854-1862, Nov./Dec. 1976.
- [6] F.P. de Mello and C. Concordia, 'Concepts of Synchronous Machine Stability as Affected by Excitation Control', IEEE Trans. Power App. Sys., Vol. PAS-88, pp 316-329, April 1969.
- [7] W.G. Heffron and R.A. Phillips, 'Effect of Modern Amplidyne Voltage Regulators on Underexcited Operation of Large Turbine Generators', AIEE Trans. Power App. Sys., Vol. PAS-71, pp 692-697, Aug. 1952.
- [8] D.H. Baker, P.C. Krause and P.A. Rusche, 'An Investigation of Excitation System Interaction', IEEE Trans. Power App. Sys., Vol. PAS-94, pp 705-715, May/June 1975.
- [9] IEEE Committee Report, 'Computer Representation of Excitation Systems', IEEE Trans. Power App. Sys., Vol. PAS-87, pp 1460-1464, June 1968.

- [10] M.A. Laughton, 'Matrix Analysis of Dynamic Stability in Synchronous Multimachine Systems', Proc. IEE, Vol. 113, No.1, pp 325-336, 1966.
- [11] J.E. Van Ness and F.N. Goddard, 'Formation of the Coefficient Matrix of a Large Dynamical System', IEEE Trans. Power App. Sys., Vol. PAS-87, pp 80-83, 1968.
- [12] J.M. Undrill, 'Dynamic Stability Calculations for an Arbitrary Number of Interconnected Synchronous Machines', IEEE Trans. Power App. Sys., Vol. PAS-87, pp 835-844, 1968.
- [13] K.R. Padiyar and R.S. Ramshaw, 'Dynamic Analysis of Multimachine Power Systems', IEEE Trans. Power App. Sys., Vol. PAS-91, pp 526-535, 1972.
- [14] P.L. Dandeno and P. Kundur, 'Practical Application of Eigenvalue Techniques in the Analysis of Power System Dynamic Stability Problems', Canadian Elec. Eng. Journal, Vol. 1, No.1, pp 35-46, 1976.
- [15] M.A. Pai and P.S. Shetty, 'An Algorithm for the Formation of System Matrix of a Multimachine Power System', IEEE Paper No. A77 162-1, PES Winter Meeting, New York, Feb. 1977.
- [16] K.R. Padiyar, M.A. Pai and C. Radhakrishna, 'A Versatile System Model for the Dynamic Stability Analysis of Power Systems Including HVDC Links', IEEE Trans. Power App. Sys., Vol. PAS-100, pp 1871-1880, April 1981.
- [17] F.P. de Mello, P.J. Nolan, T.F. Laskowski and J.M. Undrill, 'Coordinated Application of Stabilizers in Multimachine Power Systems', IEEE Trans. Power App. Sys., Vol. PAS-99, pp 892-901, May/June 1980.
- [18] C. Radhakrishna, 'Stability Studies of AC/DC Power Systems', Ph.D. Thesis, IIT Kanpur, 1980.
- [19] M.A. Pai, K.R. Padiyar and C. Radhakrishna, 'Synthesis of Damping Action in Power Systems Using Eigenvalue Sensitivities', JIE (India), Vol. 65, Pt. EL4, pp 127-131, Feb. 1985.
- [20] O.H. Abdalla, S.A. Hassan and N.T. Twoig, 'Coordinated Stabilization of a Multimachine Power System', IEEE Trans. Power App. Sys., Vol. PAS-103, pp 483-494, March 1984.

- [21] P.L. Dandeno, A.N. Karas, K.R. Mc Clymont and W. Watson, 'Effect of High Speed Rectifier Excitation Systems on Generator Stability Limit', IEEE Trans. Power App. Sys., Vol. PAS-87, pp 190-200, Jan. 1968.
- [22] W. Watson and M.E. Clouts, 'Static Exciter Stabilizing Signals on Large Generators-Mechanical Problems', IEEE Trans. Power App. Sys., Vol. PAS-92, pp 205-212, Jan. 1973.
- [23] J.P. Bayne, D.C. Lee and W. Watson, 'A Power System Stabilizer Stabilizing Signal for Thermal Units Based on Derivation of Accelerating Power', IEEE Trans. Power App. Sys., Vol. PAS-96, pp 1777-1783, Nov./Dec. 1977.
- [24] F.P. de Mello, L.N. Hanell and J.M. Undrill, 'Practical Approaches to Supplementary Stabilizing from Accelerating Power', IEEE Trans. Power App. Sys., Vol. PAS-97, pp 1515-1522, Sep./Oct. 1978.
- [25] F.R. Schlieff, R.K. Feeley, W.H. Phillips and R.W. Torluemke, 'A Power System Stabilizer Application with Local Mode Cancellation', IEEE Trans. Power App. Sys., Vol. PAS-98, pp 1054-1060, May/June 1979.
- [26] E.V. Larsen and D.A. Swann, 'Applying Power System Stabilizers; Part I : General Concepts; Part II : Performance Objectives and Tuning Concepts; Part III : Practical Considerations', IEEE Trans. Power App. Sys., Vol. PAS-100, pp 3017-3046, June 1981.
- [27] D.C. Lee, R.E. Beaulieu and J.R.R. Service, 'A Power System Stabilizer Using Speed and Electrical Power Inputs - Design and Field Experience', IEEE Trans. Power App. Sys., Vol. PAS-100, pp 4151-4155, Sep. 1981.
- [28] K.E. Bollinger, A. Laha, R. Hamilton and T. Harras, 'Power System Stabilizer Design Using Root-Locus Methods', IEEE Trans. Power App. Sys., Vol. PAS-94, pp 1484-1488, Sep./Oct. 1975.
- [29] A.M.A. Hamdan and F.M. Hughes, 'Analysis and Design of Power System Stabilizers', Int. Journal of Control, Vol. 26, No.5, pp 769-782, Nov. 1977.
- [30] R.T.H. Alden and A.A. Shaltout, 'Analysis of Damping and Synchronizing Torques; Part I : A General Calculation Method; Part II : Effect of Operating Conditions and Machine Parameters', IEEE Trans. Power App. Sys., Vol. PAS-98, pp 1696-1708, Sep./Oct. 1979.

- [31] M.L. Crenshaw, J.M. Cutler, G.F. Wright and W.J. Reid, 'Power System Stabilizer Application in a Two-Unit Plant Analytical Studies and Field Tests', IEEE Trans. Power App. Sys., Vol. PAS-102, pp 267-274, Feb. 1983.
- [32] H. Rudnick, F.M. Hughes and A. Brameller, 'Steady State Stability: Simplified Studies in Multimachine Power Systems', IEEE Trans. Power App. Sys., Vol. PAS-102, pp 3859-3867, Dec. 1983.
- [33] H.B. Gooi, E.F. Hill, M.A. Mobarak, D.H. Throne and T.H. Lee, 'Coordinated Multimachine Stabilizer Setting Without Eigenvalue Drift', IEEE Trans. Power App. Sys., Vol. PAS-100, pp 3879-3898, Aug. 1981.
- [34] Y.N. Yu, K. Vongsuriya and L.N. Wedman, 'Application of an Optimal Control Theory to a Power System', IEEE Trans. Power App. Sys., Vol. PAS-89, pp 55-62, Jan. 1970.
- [35] J.H. Anderson, 'The Control of a Synchronous Machine Using Optimal Control Theory', Proc. IEEE, Vol. 59, pp 25-35, Jan. 1971.
- [36] H.A.M. Moussa and Y.N. Yu, 'Optimal Power System Stabilization through Excitation and/or Governor Control', IEEE Trans. Power App. Sys., Vol. PAS-91, pp 1166-1174, May/June 1972.
- [37] Y.N. Yu and H.A.M. Moussa, 'Optimal Stabilization of a Multimachine System', *ibid.*, pp 1174-1184.
- [38] A.B.R. Kumar and E.F. Richards, 'An Optimal Control Law by Eigenvalue Assignment for Improved Dynamic Stability in Power Systems', IEEE Trans. Power App. Sys., Vol. PAS-101, pp 1570-1577, June 1982.
- [39] Y.N. Yu and C. Siggers, 'Stabilization and Optimal Control Signals for a Power System', IEEE Trans. Power App. Sys., Vol. PAS-90, pp 1469-1481, July/Aug. 1971.
- [40] E.J. Davison and N.S. Rau, 'Optimal Output Feedback Control of a Synchronous Machine', IEEE Trans. Power App. Sys., Vol. PAS-90, pp 2123-2134, Sep./Oct. 1971.

- [41] De Sarkar and N. Dharma Rao, 'Stabilization of a Synchronous Machine through Output Feedback Control', IEEE Trans. Power App. Sys., Vol. PAS-92, pp 159-160, Jan./Feb. 1973.
- [42] V.N. Rajurkar, K.E. Hole and K.R. Padiyar, 'Design of Power System Stabilizers Using Kalman Filter', Proceedings of National System Conference (NSC-84), pp 470-477, IIT Bombay, 26-28 Dec. 1984.
- [43] R. Doraiswami, A.M. Sharaf and J.C. Castro, 'A Novel Excitation Control Design for Multimachine Power Systems', IEEE Trans. Power App. Sys., Vol. PAS-103, pp 1052-1058, May 1984.
- [44] K. Gomathi, 'Pole Assignment Techniques for Power System Stabilization', Ph.D. Thesis, I.I.T. Kanpur, 1979.
- [45] K.R. Padiyar, S.S. Prabhu, M.A. Pai and K. Gomathi, 'Design of Stabilizers by Pole Assignment with Output Feedback', Electrical Power and Energy System, Vol. 2, pp 140-146, July 1980.
- [46] V. Arcidiacono, E. Ferrari, R. Marconato, J. Dos Ghali and D. Grandy, 'Evaluation and Improvement of Electromechanical Oscillation Damping by means of Eigenvalue - Eigenvector Analysis, Practical Results in the Central Power System', IEEE Trans. Power App. Sys., Vol. PAS-99, pp 769-778, March/April 1980.
- [47] R.J. Fleming, M.A. Mohan and K. Parvatisam, 'Selection of Parameters of Stabilizers in Multimachine Power Systems', IEEE Trans. Power App. Sys., Vol. PAS-100, pp 2329-2333, May 1981.
- [48] S. Lefebvre, 'Tuning of Stabilizers in Multimachine Power Systems', IEEE Trans. Power App. Sys., Vol. PAS-102, pp 290-299, Feb. 1983.
- [49] S. Abe and A. Doi, 'A New Power System Stabilizer Synthesis in Multimachine Power Systems', IEEE Trans. Power App. Sys., Vol. PAS-102, pp 3910-3918, Dec. 1983.
- [50] A. Doi and S. Abe, 'Coordinated Synthesis of Power System Stabilizers in Multimachine Power Systems', IEEE Trans. Power App. Sys., Vol. PAS-103, pp 1473-1479, June 1984.

- [51] J. Kannaiiah, O.P. Malik and G.S. Hope, 'Excitation Control of Synchronous Generators using Adaptive Regulators; Part I : Theory and Simulation Results; Part II : Implementation and Test Results', IEEE Trans. Power App. Sys., Vol. PAS-103, pp 897-910, May 1984.
- [52] A. Ghosh, G. Ledwich, O.P. Malik and G.S. Hope, 'Power System Stabilizer Based on Adaptive Control Techniques', IEEE Trans. Power App. Sys., Vol. PAS-103, pp 1983-1989, Aug. 1984.
- [53] W.S. Levine and M. Athans, 'On the Determination of the Optimal Constant Output Feedback Gains for Linear Multivariable Systems', IEEE Trans. Automatic Control, Vol. AC-15, pp 44-48, Feb. 1970.
- [54] K.E. Hole, 'Algorithms for the Design of Controller for Output Feedback Systems', Fourth Iranian Conference on Electrical Engineering, Shiraz, Iran, Paper No. B6-1, 1974.
- [55] H.P. Horisberger and P.R. Belanger, 'Solution of the Optimal Constant Output Feedback Problem by Conjugate Gradients', IEEE Trans. Automatic Control, Vol. AC-19, pp 434-435, Aug. 1974.
- [56] B. Porter and R. Crossley, 'Modal Control Theory and Applications', Taylor and Francis, 1972.
- [57] E.J. Davison, 'On Pole Assignment of Linear Systems with Incomplete State Feedback', IEEE Trans. Automatic Control, Vol. AC-15, pp 348-351, June 1970.
- [58] F. Fallside and H. Seraji, 'Controller Design with Output Feedback', Proc. IEE, Vol. 118, pp 1648-1654, 1971.
- [59] H. Kimura, 'Pole Assignment by Gain Output Feedback', IEEE Trans. Automatic Control, Vol. AC-20, pp 509-516, Aug. 1975.
- [60] S.H. Wang and E.J. Davison, 'On Pole Assignment in Linear Multivariable System Using Output Feedback', IEEE Trans. Automatic Control, Vol. AC-20, pp 516-518, Aug. 1975.

- [61] F.M. Brasch and J.B. Pearson, 'Pole Placement Using Dynamic Compensator', IEEE Trans. Automatic Control, Vol. AC-15, pp 34-43, Feb. 1970.
- [62] R. Ahmari and A.G. Vacroux, 'On the Pole Assignment of Linear Systems with Fixed Order Compensators', Int. Journal of Control, Vol. 17, pp 397-404, 1973.
- [63] C.T. Chen and C.H. Hsu, 'Design of Dynamic Compensators for Multivariable Systems', Proc. Joint Automatic Control Conference, pp 893-900, 1971.
- [64] H. Kimura, 'On Pole Assignment by Output Feedback', Int. Journal of Control, Vol. 28, pp 11-22, 1978.
- [65] J. Belletruti, 'Control Systems Centre Report No.207', UMIST, Manchester, England, 1973.
- [66] N. Munro and S.N. Hirbod, 'Pole Assignment using Full Rank Output Feedback Compensators', Int. Journal of System Science, Vol. 10, pp 285-306, 1979.
- [67] D.C. Youla, J.J. Bongiorno and C.N. Lu, 'Single Loop Feedback Stabilization of Linear Multivariable Dynamical Plants', Automatica, Vol. 10, pp 159-173, 1974.
- [68] S.H. Wang and E.J. Davison, 'On the Stabilization of Decentralized Control Systems', IEEE Trans. Automatic Control, Vol. AC-18, pp 473-478, Oct. 1973.
- [69] J.P. Corfmat and A.S. Morse, 'Decentralized Control of Linear Multivariable Systems', Automatica, Vol. 12, pp 479-495, Sept. 1976.
- [70] R. Saeks, 'On the Decentralized Control of Interconnected Dynamical Systems', IEEE Trans. Automatic Control, Vol. AC-24, pp 269-271, April 1979.
- [71] N.R. Sandell, P. Varaiya, M. Athans and M.G. Safonov, 'Survey of Decentralized Control Methods for Large Scale Systems', IEEE Trans. Automatic Control, Vol. AC-23, pp 108-128, April 1978.
- [72] S.H. Wang and E.J. Davison, 'Minimization of Transmission Cost in Decentralized Control Systems', Int. J. Control, Vol. 26, pp 889-896, 1978.
- [73] M.E. Sezer and O. Husayin, 'On Decentralized Stabilization of Interconnected Systems', Automatica, Vol. 16, pp 205-208, March 1980.

APPENDIX A

COMPENSATOR TRANSFER FUNCTION

A.1 COMPENSATOR OF SECTION 2.3.1

Consider the single input linear dynamical system

$$p \underline{x} = [A] \underline{x} + \underline{b} u \quad (\text{A.1})$$

where $\underline{x} \in R^n$ and $u \in R^1$. Let \underline{x}' be the vector of accessible states. Then

$$\underline{x}' = [C] \underline{x} \quad (\text{A.2})$$

where $\underline{x}' \in R^r$, $r \leq n$ and C is an $r \times n$ matrix which can be expressed as

$$C = [0 | I_r]$$

I_r being an $r \times r$ identity matrix and 0 an $r \times (n-r)$ null matrix.

Consider a second order dynamic compensator

$$p \underline{z} = [D] \underline{z} + \underline{e} u \quad (\text{A.3})$$

where D is a diagonal matrix and \underline{e} is a vector with each element of unity. Combining eqns. (A.1) and (A.3), we get

$$p \hat{\underline{x}} = [\hat{A}] \hat{\underline{x}} + \hat{\underline{b}} u \quad (\text{A.4})$$

where

$$\hat{\underline{x}} = [\underline{x}^t \quad \underline{z}^t]^t$$

$$[\hat{A}] = \begin{bmatrix} A & 0 \\ 0 & D \end{bmatrix} \quad \text{and} \quad \hat{\underline{b}} = \begin{bmatrix} \underline{b} \\ \underline{e} \end{bmatrix}$$

Eqn. (A.4) represents the augmented system. For the control law

$$u = \underline{K}_1^t \underline{x}' + \underline{K}_2^t \underline{z} \quad (\text{A.5})$$

the closed-loop system is

$$p \hat{\underline{x}} = (\hat{A} + \hat{\underline{b}} \underline{K}^t) \hat{\underline{x}} \quad (\text{A.6})$$

where

$$\underline{K}^t = [\underline{K}_1^t C] : \underline{K}_2^t$$

The compensator transfer function can be obtained as follows. From eqns. (A.3) and (A.5) the state variables of compensator can be obtained as

$$\underline{z} = (sI - P)^{-1} \underline{e} \underline{K}_1^t \underline{x}'(s) \quad (\text{A.7})$$

where

$$[P] = [D + \underline{e} \underline{K}_2^t]$$

Substituting the value of \underline{z} from eqn. (A.7) into (A.5), we get

$$U(s) = [1 + K_2^t(sI - P)^{-1} e] K_1^t x'(s) \quad (A.8)$$

For a second-order compensator

$$D = \begin{bmatrix} d_1 & 0 \\ 0 & d_2 \end{bmatrix}; \quad e = \begin{bmatrix} 1 \\ 1 \end{bmatrix} \quad \text{and} \quad K_2^t = [K_{21} \quad K_{22}]$$

Substituting the values of D , e and K_2^t in eqn. (A.8), we get

$$F(s) = \frac{1}{\Delta_c(s)} (s-d_1) (s-d_2) K_1^t$$

where

$$U(s) = F(s) x'(s)$$

and

$$\Delta_c(s) = s^2 - (d_1 + d_2 + K_{21} + K_{22})s + (d_1 d_2 + d_1 K_{22} + d_2 K_{21}) \quad (A.9)$$

Thus, zeros of $F(s)$, the compensator transfer function, are eigenvalues of D . Similarly, for higher order dynamic compensators also, it can be shown that zeros of the compensator are the eigenvalues of D .

A.2 COMPENSATOR OF SECTION 2.3.2

The transfer function of a single input K th order dynamic compensator as given in Sec. 2.3.2 is

$$F(s) = \frac{\theta_0 s^k + \theta_1 s^{k-1} + \dots + \theta_k}{s^k + \gamma_1 s^{k-1} + \dots + \gamma_k} \quad (\text{A.10})$$

Dynamical equation and control law of the compensator represented by eqn. (A.10) can be given as [81]

$$p \underline{z} = [S] \underline{z} + R y \quad (\text{A.11})$$

$$u = [Q] \underline{z} + K y \quad (\text{A.12})$$

where y and u are input and output of the compensator and

$$S = \begin{bmatrix} 0 & 1 & 0 & \dots & 0 \\ 0 & 0 & 1 & 0 & \dots & 0 \\ \vdots & & & & \vdots \\ 0 & & & 0 & 1 \\ -\gamma_k & -\gamma_{k-1} & \dots & -\gamma_1 & 0 \end{bmatrix} \quad R = \begin{bmatrix} 0 \\ 0 \\ \vdots \\ 0 \\ 1 \end{bmatrix}$$

$$Q = [\theta'_k \ \theta'_{k-1} \ \dots \ \theta'_1] \quad \text{and} \quad K = \theta_0$$

and

$$\theta'_i = \theta_i - \theta_0 \gamma_i \quad (i = 1, \dots, k)$$

consider the single input single output linear system as

$$p \underline{x} = [A] \underline{x} + \underline{b} u \quad (\text{A.13})$$

$$y = [C] \underline{x} \quad (\text{A.14})$$

Combining eqns. (A.11) to (A.14), the dynamical equation and control law of the augmented system (system and compensator) can be given as

$$p \hat{\underline{x}} = [\hat{A}] \hat{\underline{x}} + [\hat{B}] \hat{\underline{u}} \quad (\text{A.15})$$

$$\hat{\underline{y}} = [\hat{C}] \hat{\underline{x}} \quad (\text{A.16})$$

and

$$\hat{\underline{u}} = [\hat{K}] \hat{\underline{y}} \quad (\text{A.17})$$

where

$$\hat{\underline{x}} = [x^t \quad z^t]^t \quad ; \quad \hat{\underline{y}} = [y \quad z^t]^t$$

$$[\hat{A}] = \begin{bmatrix} A & 0 \\ 0 & 0 \end{bmatrix} \quad ; \quad [\hat{B}] = \begin{bmatrix} b & 0 \\ 0 & I \end{bmatrix}$$

$$[\hat{C}] = \begin{bmatrix} C & 0 \\ 0 & I \end{bmatrix} \quad \text{and} \quad [\hat{K}] = \begin{bmatrix} K & Q \\ R & S \end{bmatrix}$$

\hat{K} is the gain output feedback matrix of the augmented systems given by eqns. (A.15) to (A.17). For a second order compensator, matrix \hat{K} will take the form

$$[\hat{K}] = \begin{bmatrix} \theta_0 & \theta_2' & \theta_1' \\ 0 & 0 & 1 \\ 1 & -\gamma_2 & -\gamma_1 \end{bmatrix}$$

APPENDIX B

POLE ASSIGNMENT WITH OUTPUT FEEDBACK [66]

The technique given here is based on the work of Munro and Hirbod [66]. The method presented in [66] provides a technique for the design of full-rank compensators for multivariable linear systems. Here the technique is restricted to single input linear systems

$$\dot{x} = [A] x + b u \quad (B.1)$$

and

$$y = [C] x \quad (B.2)$$

where, $x \in R^n$, $u \in R^1$ and $y \in R^r$ are respectively vectors of state, input and output variables. The $r \times 1$ open-loop transfer function matrix $G(s)$ is

$$G(s) = C(sI - A)^{-1} b = \frac{1}{\Delta_o(s)} \begin{bmatrix} N_1(s) \\ \vdots \\ N_r(s) \end{bmatrix} \quad (B.3)$$

where

$$\Delta_o(s) = s^n + \alpha_1 s^{n-1} + \dots + \alpha_n \quad (B.4)$$

and

$$N_i(s) = \beta_{i1} s^{n-1} + \beta_{i2} s^{n-2} + \dots + \beta_{in} \quad (B.5)$$

$\Delta_o(s)$ is the characteristic polynomial of $G(s)$. Consider the output feedback law

$$u(s) = u_r(s) - F(s) \cdot y(s) \quad (B.6)$$

where $u_r \in R^1$ represents the reference input.

The problem can be defined as the determination of $1 \times r$ dynamic feedback compensator, $F(s)$, such that the closed-loop system

$$H(s) = [I + G(s) F(s)]^{-1} G(s) \quad (B.7)$$

has a desired set of eigenvalues. The k th order compensator $F(s)$ has the form

$$F(s) = \frac{1}{\Delta_c(s)} [M_1(s), M_2(s), \dots, M_r(s)] \quad (B.8)$$

where

$$\Delta_c(s) = s^k + \gamma_1 s^{k-1} + \gamma_2 s^{k-2} + \dots + \gamma_k \quad (B.9)$$

and

$$M_i(s) = \theta_{i0} s^k + \theta_{i1} s^{k-1} + \dots + \theta_{ik} \quad (B.10)$$

$\Delta_c(s)$ is the characteristic polynomial of compensator transfer function $F(s)$.

The resulting closed-loop system characteristic polynomial $\Delta_d(s)$, defined as :

$$\Delta_d(s) = s^{n+k} + d_1 s^{n+k-1} + \dots + d_{n+k} \quad (B.11)$$

can be written as [66]

$$\Delta_d(s) = \Delta_o(s) \cdot \Delta_c(s) + \sum_{i=1}^r N_i(s) \cdot M_i(s) \quad (B.12)$$

B.1 COMPLETE POLE ASSIGNMENT

The problem of pole assignment can be defined as : given $\Delta_0(s)$, $N_1(s)$, ..., $N_r(s)$ and a desired set of closed-loop poles, find $\Delta_c(s)$, $M_1(s)$, ..., $M_r(s)$ of lowest degree which satisfy eqn. (B.12). Equating coefficients of like powers of s in eqn. (B.12), we get

$$[X_k] p_k = \underline{\delta}_k \quad (3.13)$$

where

$$[X_k] = \left[\begin{array}{cccc|cccc|cccc} 1 & 0 & \dots & 0 & \beta_{11} & \dots & 0 & \cdot & \beta_{r1} & \dots & 0 \\ \alpha_1 & 1 & \dots & \cdot & \beta_{12} & \dots & 0 & \cdot & \beta_{r2} & & 0 \\ \alpha_2 & \alpha_1 & & & \cdot & \dots & \cdot & & & & \\ \vdots & \alpha_2 & & 1 & & & \beta_{11} & \cdot & & & \beta_{r1} \\ \cdot & \cdot & & \alpha_1 & \beta_{1n} & & \beta_{12} & \cdot & \beta_{rn} & & \beta_{r2} \\ \cdot & \cdot & & \alpha_2 & 0 & & & & 0 & & \\ \alpha_n & \cdot & & & 0 & & & & 0 & & \\ 0 & \alpha_n & & & 0 & & & & 0 & & \\ 0 & 0 & & & & & & & & & \\ \vdots & & & & & & & & & & \vdots \\ 0 & 0 & & \alpha_n & 0 & & \beta_{1n} & & 0 & & \beta_{rn} \end{array} \right]$$

k columns
k+1 columns
k+1 columns

$$p_k = [\gamma_1 \ \gamma_2 \ \dots \ \gamma_k \mid \theta_{10} \ \dots \ \theta_{1k} \mid \dots \mid \theta_{r0} \ \dots \ \theta_{rk}]^t$$

and

$$\delta_k = [(d_1 - \alpha_1) \mid (d_2 - \alpha_2) \mid \dots \mid (d_n - \alpha_n) \mid d_{n+1} \dots d_{n+k}]^t$$

Equation (B.13) is a set of $(n+k)$ equations in $[(k+1)r+k]$ unknown parameters of $F(s)$. The difference vector δ_k contains the coefficients of the polynomial

$$\Delta_d'(s) = \Delta_d(s) - \Delta_0(s) \cdot s^k \quad (\text{B.14})$$

A necessary and sufficient condition for the existence of solution of eqn. (B.13) is

$$\text{Rank } [X_k] = \text{Rank } [X_k, \delta_k] \quad (\text{B.15})$$

and a solution of eqn. (B.13) is

$$p_k = [X_k^{g1}] \delta_k \quad (\text{B.16})$$

where X_k^{g1} is the generalized inverse of X_k such that

$$[X_k] [X_k^{g1}] [X_k] = [X_k]$$

B.2 PARTIAL POLE ASSIGNMENT

Consider the case when q poles are to be assigned, $t = (n + k - q)$ poles are allowed to assume arbitrary locations. For this case the closed-loop system characteristic polynomial $\Delta_d(s)$ has the form

$$p_k = [\gamma_1 \ \gamma_2 \ \dots \ \gamma_k] \begin{bmatrix} \theta_{10} & \dots & \theta_{1k} \\ \dots & \dots & \dots \\ \theta_{r0} & \dots & \theta_{rk} \end{bmatrix}^t$$

and

$$\delta_k = [(d_1 - \alpha_1) \ \vdots \ (d_2 - \alpha_2) \ \vdots \ \dots \ \vdots \ (d_n - \alpha_n) \ \vdots \ d_{n+1} \dots d_{n+k}]^t$$

Equation (B.13) is a set of $(n+k)$ equations in $[(k+1)r+k]$ unknown parameters of $F(s)$. The difference vector δ_k contains the coefficients of the polynomial

$$\Delta_d'(s) = \Delta_d(s) - \Delta_o(s) \cdot s^k \quad (\text{B.14})$$

A necessary and sufficient condition for the existence of solution of eqn. (B.13) is

$$\text{Rank } [X_k] = \text{Rank } [X_k, \delta_k] \quad (\text{B.15})$$

and a solution of eqn. (B.13) is

$$p_k = [X_k^{gl}] \delta_k \quad (\text{B.16})$$

where X_k^{gl} is the generalized inverse of X_k such that

$$[X_k] [X_k^{gl}] [X_k] = [X_k]$$

B.2 PARTIAL POLE ASSIGNMENT

Consider the case when q poles are to be assigned, $t = (n + k - q)$ poles are allowed to assume arbitrary locations, For this case the closed-loop system characteristic polynomial $\Delta_d(s)$ has the form

$$\Delta_d(s) = (s^q + d_1 s^{q-1} + \dots + d_q) (s^t + e_1 s^{t-1} + \dots + e_t) \quad (\text{B.17})$$

where d_1, d_2, \dots, d_q are specified and e_1, e_2, \dots, e_t are to be determined. Here the difference vector δ_k can be obtained by equating the coefficients of like powers of s in (B.17) and (B.12) as

$$\delta_{-k} = \delta'_{-k} + e_1 \delta_{-1} + \dots + e_t \delta_{-t} \quad (\text{B.18})$$

where the vectors δ'_k and δ_i , ($i = 1, \dots, t$) contain respectively the coefficients of the polynomials

$$\Delta_d''(s) = \Delta_q(s) \cdot s^t - \Delta_0(s) \cdot s^k \quad (\text{B.19})$$

and

$$\Delta_1'(s) = \Delta_q(s) \cdot s^{t-i}, \quad (i = 1, \dots, t) \quad (\text{B.20})$$

Eqn. (B.13) in this case will take the form

$$[X_k] p_k = \delta'_{-k} + [D] \underline{e} \quad (\text{B.21})$$

where

$$[D] = [\delta_1, \delta_2, \dots, \delta_t]$$

and

$$\underline{e} = [e_1, e_2, \dots, e_t]^t$$

Eqn. (B.21) can be rearranged as

$$[X'_k] \underline{p}'_k = \underline{\delta}'_k \quad (\text{B.22})$$

where

$$[X'_k] = [X_k, -D]$$

and

$$\underline{p}'_k = [p_k^t, e^t]^t \quad (\text{B.23})$$

Eqn. (B.22) is a set of $(n+k)$ simultaneous algebraic equations in $[r(k+1) + k + t]$ unknowns. Vector \underline{p}'_k contains parameters of $F(s)$ and the coefficients of polynomial of unassigned closed-loop poles. The necessary and sufficient condition for the existence of solution of eqn. (B.22) is given in eqn. (B.15) with X_k , p_k and δ_k replaced by X'_k , \underline{p}'_k and $\underline{\delta}'_k$ respectively.

APPENDIX C

DESIGN OF OPTIMAL CONTROLLER FOR OUTPUT FEEDBACK SYSTEMS [53,54]

Consider the linear, time invariant, completely controllable and observable system

$$p \underline{x} = [A] \underline{x} + [B] \underline{u} \quad (C.1)$$

$$\underline{y} = [C] \underline{x} \quad (C.2)$$

where $\underline{x} \in R^n$, $\underline{u} \in R^m$ and $\underline{y} \in R^r$ are respectively the state, control and output variables. The problem is to design a controller using output feedback to minimize the quadratic cost function

$$J = \int_0^{\infty} (\underline{x}^t Q \underline{x} + \underline{u}^t R \underline{u}) dt \quad (C.3)$$

where Q is a constant $n \times n$ positive semidefinite matrix and R is a constant $m \times m$ positive definite matrix. The control law is

$$\underline{u} = -[K] \underline{y} \quad (C.4)$$

The closed-loop system with the control law of eqn. (C.4) can be given as

$$p \underline{x} = [A_c] \underline{x} \quad (C.5)$$

where

$$A_c = A - BKC$$

From eqns. (C.1), (C.2), (C.3) and (C.4), we get

$$J = \int_0^{\infty} \underline{x}^t (Q + C^t K^t R K C) \underline{x} dt \quad (C.6)$$

As the solution of eqn. (C.5) depends upon initial state $x(o)$, the cost J given by eqn. (C.6) will be a function of $x(o)$. For the completely controllable and observable system of eqns. (C.1) and (C.2), the cost J is given from (C.5) and (C.6) by [53]

$$J = \underline{x}^t(o) S \underline{x}(o) \quad (C.7)$$

where the cost matrix S is given as

$$S = \int_0^{\infty} e^{A_c^t} (Q + C^t K^t R K C) e^{A_c} dt \quad (C.8)$$

S can be obtained as the unique positive definite solution of the Liapunov equation [53]

$$A_c^t S + S A_c + (Q + C^t K^t R K C) = 0 \quad (C.9)$$

If the initial state $x(o)$ is assumed to be a random variable uniformly distributed over an n -dimensional unit sphere, the average cost can be seen to be [53]

$$J = \text{trace } [S] \quad (C.10)$$

Forming the Hamiltonian corresponding to eqns. (C.9) and (C.10), we get

$$H = \text{trace}[S] + \text{trace}[P^t(A_c^t S + S A_c + Q + C^t K^t R K C)] \quad (\text{C.11})$$

where P is an $n \times n$ matrix of Langrange multipliers. The necessary conditions for minimum J [54] are

$$\frac{\partial H}{\partial P} = 0 \quad ; \quad \frac{\partial H}{\partial S} = 0 \quad \text{and} \quad \frac{\partial H}{\partial K} = 0 \quad (\text{C.12})$$

The first condition in (C.12) gives eqn. (C.9). The second condition in (C.12) gives

$$P A_c^t + A_c P + I = 0 \quad (\text{C.13})$$

where I is an $n \times n$ identity matrix. The third condition in eqn. (C.12) gives

$$\frac{\partial H}{\partial K} = 2(R K C P C^t - B^t S P C^t) = 0 \quad (\text{C.14})$$

The gradient obtained from eqn. (C.14) is utilized in applying steepest descent method for updating the feedback matrix K . Following are the steps in getting the optimum value of K .

Step 1 : Start with initial guess $K^{(0)}$ of K such that

$$A - B K^{(0)} C \text{ is stable.}$$

Step 2 : Compute S by solving Liapunov eqn. (C.9)

- Step 3 : Compute P by solving Liapunov eqn. (C.13)
- Step 4 : Compute gradient $\frac{\partial H}{\partial K}$ from eqn. (C.14)
- Step 5 : Update K according to

$$K^{(i+1)} = K^{(i)} - \alpha \left. \frac{\partial H}{\partial K} \right|_{K=K^{(i)}}$$

where $0 < \alpha < 1$

- Step 6 : Go to step 2 until $\left| \frac{\partial H}{\partial K} \right|$ is close to zero or difference in the values of J obtained in two successive iteration is less than a prespecified value.

APPENDIX D

SYNCHRONOUS MACHINE EQUATIONS AND EXCITATION SYSTEM

D.1 SYNCHRONOUS MACHINE

D.1.1 Higher Order Model

Machine armature is represented by a single-phase equivalent circuit [78] shown in Fig. D.1. The equivalent circuit consists of a dependent current source in conjunction with a constant impedance. The magnitude and phase angle of the dependent current source are determined from the knowledge of the rotor flux linkages and the rotor angle. The model can take into account any number of circuits in the d and q axes of the rotor depending upon the details required and the availability of the machine data. However, a synchronous machine with two rotor circuits in each axis is considered as shown in Fig. D.2. The subscripts f and h refer to the field circuit and the damper circuit in the d-axis respectively. The subscripts g and k refer to the damper circuits in the q-axis. All variables and parameters are expressed in per unit of the machine rating. Unlike in the Ref. [78], the generator convention is used. Also, the convention of q-axis leading the d-axis is followed here.

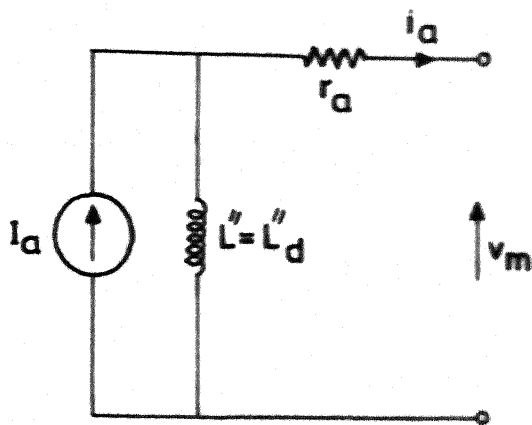


FIG. D.1 CIRCUIT MODEL OF THE SYNCHRONOUS MACHINE.

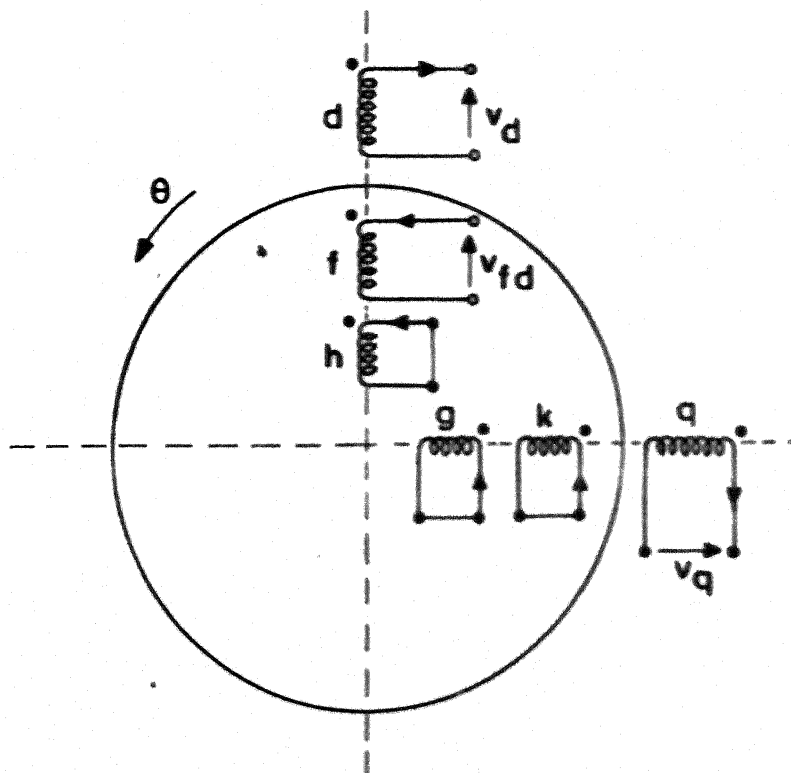


FIG. D.2 SYNCHRONOUS MACHINE WITH THREE DAMPER WINDINGS.

Rotor Circuit Equations

Park's equations for rotor circuit are given by

$$\underline{v}_r = [R_r] \underline{i}_r + \frac{1}{\omega_0} p \underline{\psi}_r \quad (D.1)$$

where

$$\underline{v}_r = [v_{fd} \ 0 \ 0 \ 0]^t$$

$$\underline{i}_r = [\underline{i}_{rd}^t \ \underline{i}_{rq}^t]^t$$

$$\underline{\psi}_r = [\underline{\psi}_{rd}^t \ \underline{\psi}_{rq}^t]^t$$

$$R_r = \text{Block diag} [\{R_{rd}\}, \{R_{rq}\}]$$

$$\underline{i}_{rd} = [i_f \ i_h]^t ; \quad \underline{i}_{rq} = [i_k \ i_g]^t$$

$$\underline{\psi}_{rd} = [\psi_f \ \psi_h]^t ; \quad \underline{\psi}_{rq} = [\psi_k \ \psi_g]^t$$

$$\text{and } [R_{rd}] = \text{Diag} [R_f, R_h] ; \quad [R_{rq}] = \text{Diag} [R_k, R_g]$$

The flux linkages in the machine are defined by :

$$\begin{bmatrix} \underline{\psi}_s \\ \underline{\psi}_r \end{bmatrix} = \begin{bmatrix} [L_s] & [M] \\ [M]^t & [L_r] \end{bmatrix} \begin{bmatrix} \underline{i}_s \\ \underline{i}_r \end{bmatrix} \quad (D.2)$$

where

$$\underline{\psi}_s = [\psi_d \ \psi_q]^t$$

$$\underline{i}_s = [-i_d \ -i_q]^t$$

$$[L_s] = \text{Diag} [L_d, L_q]$$

$$[M] = \text{Block diag. } [\underline{M}_d, \underline{M}_q]$$

$$[L_r] = \text{Block diag. } [\{L_{rd}\}, \{L_{rq}\}]$$

$$\underline{M}_d = [\underline{M}_{df} \quad \underline{M}_{dh}]$$

$$\underline{M}_q = [\underline{M}_{qk} \quad \underline{M}_{qg}]$$

$$[L_{rd}] = \begin{bmatrix} L_f & L_{fh} \\ L_{fh} & L_h \end{bmatrix}$$

and

$$[L_{rq}] = \begin{bmatrix} L_k & L_{kg} \\ L_{kg} & L_g \end{bmatrix}$$

The rotor flux linkages are more important than the rotor currents as explained in [78]. Therefore, eliminating \underline{i}_{rd} and \underline{i}_{rq} from eqns. (D.1) and (D.2), we get

$$\begin{aligned} p \underline{\Psi}_{rd} &= \omega_o [v_{fd} \quad 0]^t - \omega_o [R_{rd}] [L_{rd}]^{-1} \underline{\Psi}_{rd} \\ &\quad - \omega_o [R_{rd}] [L_{rd}]^{-1} \underline{M}_d^t i_d \end{aligned} \quad (D.3)$$

$$p \underline{\Psi}_{rq} = -\omega_o [R_{rq}] [L_{rq}]^{-1} [\underline{\Psi}_{rq} + \underline{M}_q^t i_q] \quad (D.4)$$

Stator Equations

Park's equations for the stator are given by :

$$\begin{bmatrix} v_d \\ v_q \end{bmatrix} = \begin{bmatrix} r_a & 0 \\ 0 & r_a \end{bmatrix} \begin{bmatrix} -i_d \\ -i_q \end{bmatrix} + \frac{1}{\omega_o} \begin{bmatrix} p \underline{\Psi}_d \\ p \underline{\Psi}_q \end{bmatrix} + \frac{\omega_o}{\omega_o} \begin{bmatrix} 0 & -1 \\ 1 & 0 \end{bmatrix} \begin{bmatrix} \underline{\Psi}_d \\ \underline{\Psi}_q \end{bmatrix} \quad (D.5)$$

The armature transients are ignored by neglecting $p \Psi_d$ and $p \Psi_q$ terms in Park's eqn. (D.5). This is normally justified since these terms are small compared to the speed terms and also their exclusion makes the armature equations algebraic which is consistent with the steady-state representation of the network to which the machine armature circuits are connected. This results in the reduction of the order of the machine by two. By setting $p \Psi_d$ and $p \Psi_q$ equal to zero and $\omega = \omega_0$ in eqn. (D.5), the stator equations are reduced to a pair of algebraic equations given by :

$$\begin{bmatrix} v_d \\ v_q \end{bmatrix} = \begin{bmatrix} r_a & 0 \\ 0 & r_a \end{bmatrix} \begin{bmatrix} -i_d \\ -i_q \end{bmatrix} + \begin{bmatrix} 0 & -1 \\ 1 & 0 \end{bmatrix} \begin{bmatrix} \Psi_d \\ \Psi_q \end{bmatrix} \quad (D.6)$$

Substituting the values of Ψ_d and Ψ_q from eqn. (D.2) into eqn. (D.6), we get :

$$\begin{bmatrix} v_d \\ v_q \end{bmatrix} = \begin{bmatrix} -r_a & L_q'' \\ -L_d'' & -r_a \end{bmatrix} \begin{bmatrix} i_d \\ i_q \end{bmatrix} + \begin{bmatrix} 0 & -L_q'' \\ L_d'' & 0 \end{bmatrix} \begin{bmatrix} I_d \\ I_q' \end{bmatrix} \quad (D.7)$$

where

$$L_d'' \triangleq L_d - \underline{M}_d [L_{rd}]^{-1} \underline{M}_d^t$$

$$L_q'' \triangleq L_q - \underline{M}_q [L_{rq}]^{-1} \underline{M}_q^t$$

$$I_d \triangleq \frac{1}{L_d''} \underline{M}_d [L_{rd}]^{-1} \underline{\Psi}_{rd}$$

$$I_q' \triangleq \frac{1}{L_q''} \underline{M}_q [L_{rq}]^{-1} \underline{\Psi}_{rq}$$

Subtransient Saliency

Although L_d'' and L_q'' are not equal, in general, introduction of dummy coils can make the new values equal. Following the general procedure outlined in Ref. [78], the effect of the subtransient saliency is taken into account and we get

$$I_q' = I_q + \xi i_q \quad (D.8)$$

where

$$I_q = \frac{1}{L_d''} [L_{rq}]^{-1} \Psi_{rq}$$

and

$$\xi \triangleq 1 - \frac{L_q''}{L_d''}$$

The second term in eqn. (D.8) represents subtransient saliency. L_d'' and L_q'' are the conventional subtransient inductances.

Equations of Mechanical Motion

The rotor mechanical motion is represented by

$$p\omega = \frac{1}{M} (P_m - P_e) - \frac{K_D}{M} (\omega - \omega_o) \quad (D.9)$$

and

$$p\delta = \omega - \omega_o \quad (D.10)$$

where

$$M = \frac{2H}{\omega_o}$$

P_m - is the mechanical power input

and

P_e - is the electrical power output.

State Equations

Unlike Ref. [78], the variables I_d and I_q are directly utilized as state variables. Thus, replacing Ψ_h and Ψ_g in eqns. (D.3) and (D.4) by I_d and I_q respectively, the dynamical equations of the generator are given as :

$$pI_d = C_1 I_d + C_3 \Psi_f + C_{11} i_d + C_9 \bar{e}_{fd} \quad (D.11)$$

$$pI_q = C_2 I_q + C_4 \Psi_k + C_{12} i_q \quad (D.12)$$

$$p\Psi_f = C_5 I_d + C_7 \Psi_f + C_{13} i_d + C_{10} \bar{e}_{fd} \quad (D.13)$$

$$p\Psi_k = C_6 I_q + C_8 \Psi_k + C_{14} i_q \quad (D.14)$$

where

$$C_1 = \frac{\omega_0}{a_1} (d_1 R_f L_{fh} d_2^{-1} - d_2 R_h L_f d_2^{-1})$$

$$C_2 = \frac{\omega_0}{a_2} (d_3 R_k L_{kg} d_4^{-1} - d_4 R_g L_k d_4^{-1})$$

$$C_3 = \frac{\omega_0}{a_1} [d_2 R_h (L_{fh} + L_f d_2^{-1} d_1) - d_1 R_f (L_h + L_{fh} d_2^{-1} d_1)]$$

$$C_4 = \frac{\omega_0}{a_2} [d_4 R_g (L_{kg} + L_k d_4^{-1} d_3) - d_3 R_k (L_g + L_{kg} d_4^{-1} d_3)]$$

$$C_5 = \frac{\omega_0}{a_1} R_f L_{fh} d_2^{-1}$$

$$C_6 = \frac{\omega_0}{a_2} R_k L_{kg} d_4^{-1}$$

$$C_7 = -\frac{\omega_0}{a_1} R_f (L_h + L_{fh} d_2^{-1} d_1)$$

$$C_8 = -\frac{\omega_0}{a_2} R_k (L_g + L_{kg} d_4^{-1} d_3)$$

$$C_9 = \omega_0 d_1 \frac{R_f}{M_{df}}$$

$$C_{10} = \omega_0 \frac{R_f}{M_{df}}$$

$$C_{11} = -\frac{\omega_0}{a_1} [d_1 R_f (L_h M_{df} - L_{fh} M_{dh}) + d_2 R_h (-L_{fh} M_{df} + L_f M_{dh})]$$

$$C_{12} = -\frac{\omega_0}{a_2} [d_3 R_k (L_g M_{qk} - L_{kg} M_{qg}) + d_4 R_g (-L_{kg} M_{qk} + L_k M_{qg})]$$

$$C_{13} = -\frac{\omega_0}{a_1} R_f (L_h M_{df} - L_{fh} M_{dh})$$

$$C_{14} = -\frac{\omega_0}{a_2} R_k (L_g M_{qk} - L_{kg} M_{qg})$$

$$a_1 = L_f L_h - L_{fh}^2$$

$$a_2 = L_k L_g - L_{kg}^2$$

$$d_1 = \frac{1}{a_1 L_d''} (M_{df} L_h - M_{dh} L_{fh})$$

$$d_2 = \frac{1}{a_1 L_d''} (M_{dh} L_f - M_{df} L_{fh})$$

$$d_3 = \frac{1}{a_2 L_d''} (M_{qk} L_g - M_{qg} L_{kg})$$

$$d_4 = \frac{1}{a_2 L_d''} (M_{qg} L_g - M_{qk} L_{kg})$$

and

$$E_{fd} = \frac{M_{df}}{R_f} v_{fd}$$

Linearized state-space equation of the generator can be obtained by linearizing eqns. (D.9) to (D.14) as :

$$p \underline{x}_m = [A'_m] \underline{x}_m + \underline{b}_{me} \Delta E_{fd} + \underline{b}_{mg} (\Delta P_m - \Delta P_e) + [B_{al}] \Delta \underline{i}_m \quad (D.15)$$

where

$$\underline{x}_m = [\Delta \omega \quad \Delta \delta \quad \Delta I_d \quad \Delta I'_q \quad \Delta \Psi_f \quad \Delta \Psi_k]^t$$

$$\Delta \underline{i}_m = [\Delta i_d \quad \Delta i_q]^t$$

$$[A'_m] = \begin{bmatrix} -K_D/M & 0 & 0 & 0 & 0 & 0 \\ 1 & 0 & 0 & 0 & 0 & 0 \\ 0 & 0 & C_1 & 0 & C_3 & 0 \\ 0 & 0 & 0 & C_2 & 0 & C_4 \\ 0 & 0 & C_5 & 0 & C_7 & 0 \\ 0 & 0 & 0 & C_6 & 0 & C_8 \end{bmatrix}$$

$$\underline{b}_{me} = [0 \quad 0 \quad C_9 \quad 0 \quad C_{10} \quad 0]^t$$

$$\underline{b}_{mg} = [1/M \quad 0 \quad 0 \quad 0 \quad 0 \quad 0]^t$$

and

$$[B_{al}] = \begin{bmatrix} 0 & 0 & C_{11} & 0 & C_{13} & 0 \\ 0 & 0 & 0 & C_{12} & 0 & C_{14} \end{bmatrix}^t$$

Steady State Representation

In the steady state representation

$$f_a = f_d \cos(\omega_0 t + \delta) - f_q \sin(\omega_0 t + \delta)$$

where f_{qr} is the current or voltage variable and subscript 'o' denotes the reference frame. $\omega_r (= \omega_o + \dot{\delta})$ is the rotor speed and δ is the relative angle. Park's components f_d and f_q can be used to denote the magnitude of the phasors representing f_a . The phasor diagram is shown in Fig. D.3. The usual convention is to denote δ as the angle between the quadrature axis and the reference frame. Thus, the phasor \bar{f}_a can be written as

$$\bar{f}_a = (f_q - jf_d) e^{j\delta} \quad (D.16)$$

Hence, in steady-state the single phase equivalent circuit of the machine can be represented as shown in Fig. D.4, when all the phasors are referred to the reference frame.

Expression for $\Delta \underline{i}_m$

As the network is represented by its Jacobian matrix from which $\Delta \underline{S}_g$ is directly available, $\Delta \underline{i}_m$ can be expressed in terms of $\Delta \underline{S}_g$ and \underline{x}_m as follows. Generator power output is given by

$$P_g + jQ_g = \hat{v}_m \hat{i}_m^* \quad (D.17)$$

where

$$\hat{v}_m = jX_d''(\hat{I}_a - \hat{i}_m)$$

Linearizing Eqn. (D.16), we get

$$\Delta \underline{i}_m = [w_{a1}] \Delta \underline{S}_g + [w_{a2}] \underline{x}_m \quad (D.18)$$

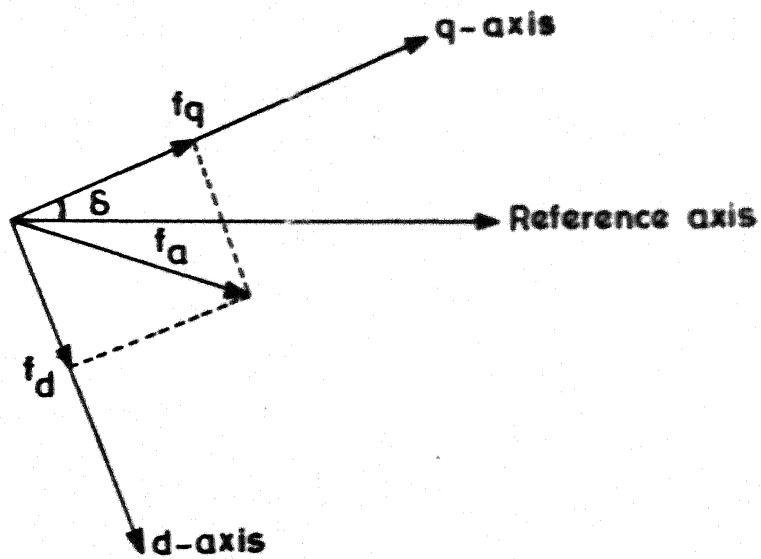


FIG. D.3 PHASOR DIAGRAM .

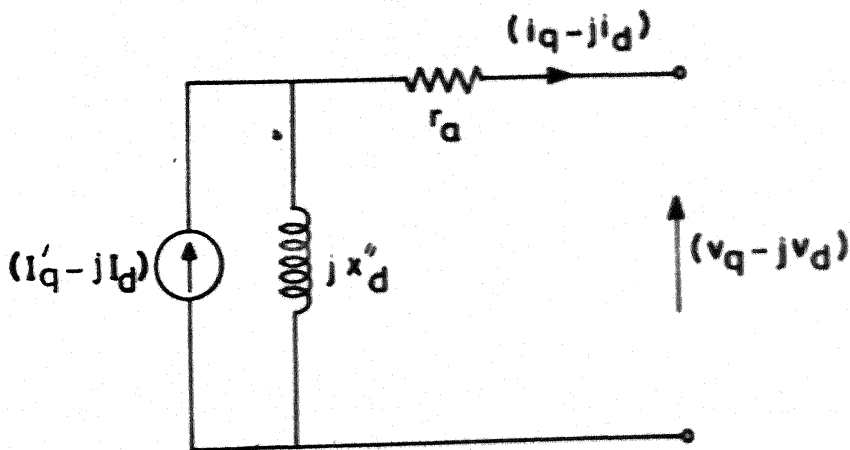


FIG. D.4 STEADY STATE EQUIVALENT CIRCUIT FOR ARMATURE .

where

$$[W_{a1}] = \frac{1}{a_3 X_d''} \begin{bmatrix} I_{qo} + 2(\xi - 1)i_{qo} & -(I_{do} - \xi i_{do}) \\ -(I_{do} - 2i_{do}) & -(I_{qo} + \xi i_{qo}) \end{bmatrix}$$

$$[W_{a2}] = X_d'' [W_{a1}] \begin{bmatrix} -i_{qo} & i_{do} \\ -i_{do} & -i_{qo} \end{bmatrix} \begin{bmatrix} 0 & 0 & 1 & 0 & 0 & 0 \\ 0 & 0 & 0 & 1 & 0 & 0 \end{bmatrix}$$

and

$$a_3 = -(I_{qo} + \xi i_{qo}) [I_{qo} + 2(\xi - 1)i_{qo}] - (I_{do} - 2i_{do})(I_{do} - \xi i_{do})$$

Expression for Generator Terminal Voltage

The magnitude and phase angle of generator terminal voltage can be obtained from Fig. D.5 as :

$$V_t = (v_d^2 + v_q^2)^{1/2} \quad (D.19)$$

$$\theta = \delta - \tan^{-1} \left(\frac{v_d}{v_q} \right) \quad (D.20)$$

Linearizing eqns. (D.19) and (D.20), we get

$$\Delta V_t = \frac{1}{V_{to}} [v_{do} \quad v_{qo}] \Delta \underline{v}_m \quad (D.21)$$

and

$$\Delta \theta = \Delta \delta - \frac{1}{v_{to}^2} [v_{qo} \quad -v_{do}] \Delta \underline{v}_m \quad (D.22)$$

where

$$\Delta \underline{v}_m = [\Delta v_d \quad \Delta v_q]^t = [W_{a3}] \Delta \underline{s}_g + [W_{a4}] \underline{x}_m \quad (D.23)$$

$$[W_{a3}] = X_d'' \begin{bmatrix} 0 & (1 - \xi) \\ -1 & 0 \end{bmatrix} [W_{a1}]$$

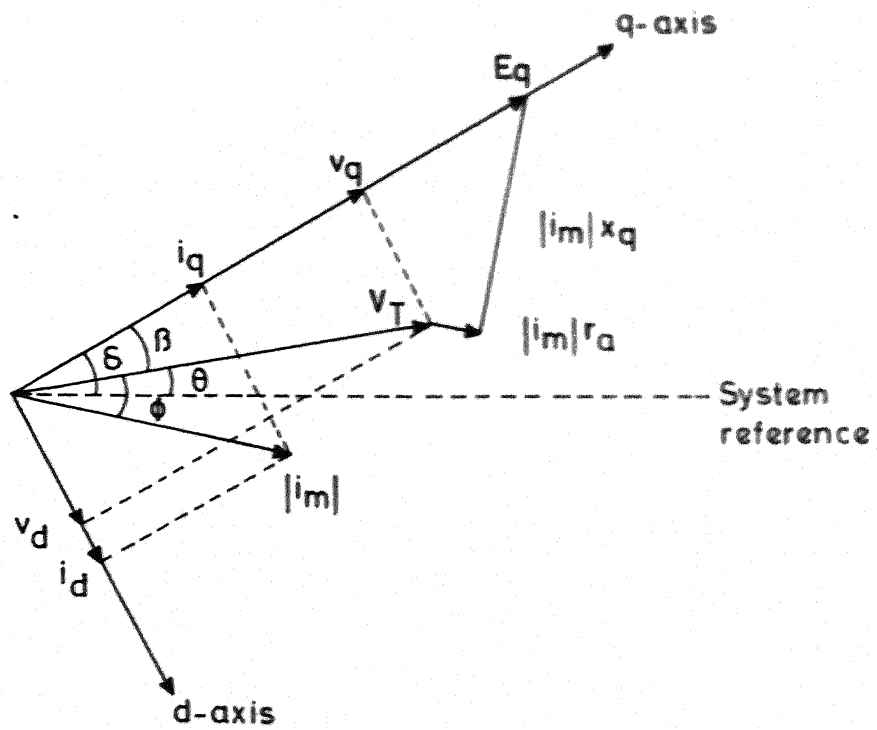


FIG. D.5 PHASOR DIAGRAM OF SYNCHRONOUS MACHINE.

and

$$[w_{a4}] = x_d'' \begin{bmatrix} 0 & (1-\xi) \\ -1 & 0 \end{bmatrix} [w_{a2}] + \begin{bmatrix} 0 & 0 & 0 & -1 & 0 & 0 \\ 0 & 0 & 1 & 0 & 0 & 0 \end{bmatrix}$$

Substituting Eqns. (D.23) in (D.21) and (D.22), we get

$$\Delta \underline{z}_g = \begin{bmatrix} \Delta \theta \\ \Delta V_t \end{bmatrix} = [D_p] \Delta s_g + [D_s] x_m \quad (D.24)$$

where

$$[D_p] = \frac{1}{V_{to}} \begin{bmatrix} -v_{qo}/V_{to} & v_{do}/V_{to} \\ v_{do} & v_{qo} \end{bmatrix} [w_{a3}]$$

$$[D_s] = \begin{bmatrix} 0 & 1 & 0 & 0 & 0 & 0 \\ 0 & 0 & 0 & 0 & 0 & 0 \end{bmatrix} + \frac{1}{V_{to}} \begin{bmatrix} -v_{qo}/V_{to} & v_{do}/V_{to} \\ v_{do} & v_{qo} \end{bmatrix} [w_{a4}]$$

Substituting the value of Δi_m from eqn. (D.18) into eqn. (D.15), we get

$$p x_m = [A_m] x_m + [B_{ap}] \Delta s_g + b_{me} \Delta E_{fd} + b_{mg} \Delta P_m \quad (D.25)$$

where

$$[A_m] = [A_m'] + [B_{a1}] [w_{a2}]$$

$$[B_{ap}] = -b_{mg} + [B_{a1}] [w_{a1}]$$

D.1.2 Lower Order Model

In lower order representation of a synchronous m/c only the effect of field flux decay is considered and the effect of amortisseur windings is neglected. This results in a three

winding model of the synchronous machine - d and q windings in the stator and the field winding f in the d-axis of the rotor. Thus, L_d'' in Fig. D.1 will be replaced by L_d' and there will be no h, g and k windings in Fig. D.2. eqns. (D.1) and (D.2) will be reduced to

$$v_{fd} = R_f i_f + \frac{1}{\omega_o} p \Psi_f \quad (D.26)$$

and

$$\begin{bmatrix} \Psi_s \\ \Psi_f \end{bmatrix} = \begin{bmatrix} [L_s] & \underline{M} \\ \underline{M}^t & L_f \end{bmatrix} \begin{bmatrix} i_s \\ i_f \end{bmatrix} \quad (D.27)$$

where

$$\underline{M} = [M_{df} \ 0]^t$$

Eliminating i_f from (D.26) and (D.27), we get

$$p \Psi_f = \omega_o v_{fd} - \omega_o \frac{R_f}{L_f} \Psi_f - \omega_o \frac{R_f}{L_f} M_{df} i_d \quad (D.28)$$

The stator equations for lower order machine model will take the form :

$$\begin{bmatrix} v_d \\ v_q \end{bmatrix} = \begin{bmatrix} -r_a & L_d' \\ -L_d' & -r_a \end{bmatrix} \begin{bmatrix} i_d \\ i_q \end{bmatrix} + \begin{bmatrix} 0 & -L_d' \\ L_d' & 0 \end{bmatrix} \begin{bmatrix} I_d \\ I_q \end{bmatrix} \quad (D.29)$$

where

$$L_d' \triangleq L_d - \frac{1}{L_f} M_{df}^2$$

$$I_d \triangleq \frac{1}{L'_d} \frac{M_{df}}{L_f} \Psi_f \quad (D.30)$$

and

$$I_q \triangleq \xi i_q$$

$$\xi = 1 - \frac{L_q}{L'_d}$$

Eliminating Ψ_f from eqns. (D.28) and (D.30) we get

$$pI_d = \frac{1}{T'_{do}} \left[-I_d + \frac{1}{L'_d} E_{fd} - \left(\frac{L_d - L'_d}{L'_d} \right) i_d \right] \quad (D.31)$$

where

$$T'_{do} \triangleq \frac{L_f}{R_f}$$

and

$$E_{fd} \triangleq \frac{M_{df}}{R_f} v_{fd}$$

The dynamical equation of the machine will be same as given in eqn. (D.15) with state variables as $\Delta\omega, \Delta\delta$ and ΔI_d . Various matrices in eqn. (D.15) will take the form :

$$[A'_m] = \begin{bmatrix} -K_D/M & 0 & 0 \\ 1 & 0 & 0 \\ 0 & 0 & -1/T'_{do} \end{bmatrix}$$

$$\underline{b}_{me} = [0 \quad 0 \quad 1/(L'_d \quad T'_{do})]$$

$$\underline{b}_{mg} = [1/M \quad 0 \quad 0]$$

$$[B_{al}] = \begin{bmatrix} 0 & 0 & [-\frac{1}{T'_{do}} \left(\frac{L_d - L'_d}{L'_d} \right)] \\ 0 & 0 & 0 \end{bmatrix}$$

Expression for Δi_m : Matrices W_{a1} and W_{a2} in eqn. (D.17) will take the form :

$$[W_{a1}] = \frac{1}{a_4 x'_d} \begin{bmatrix} 2(\xi - 1) i_{qo} & -(I_{do} - \xi i_{do}) \\ -(I_{do} - 2i_{do}) & -\xi i_{qo} \end{bmatrix}$$

$$[W_{a2}] = x'_d [W_{a1}] \begin{bmatrix} 0 & 0 & -i_{qo} \\ 0 & 0 & -i_{do} \end{bmatrix}$$

where

$$a_4 = -2\xi (\xi - 1) i_{qo}^2 - (I_{do} - \xi i_{do})(I_{do} - 2i_{do})$$

Expression for Δv_m

Matrices W_{a3} and W_{a4} in eqn. (D.23) will take the form :

$$[W_{a3}] = x'_d \begin{bmatrix} 0 & (1 - \xi) \\ -1 & 0 \end{bmatrix} [W_{a1}]$$

$$[W_{a4}] = x'_d \begin{bmatrix} 0 & (1 - \xi) \\ -1 & 0 \end{bmatrix} [W_{a2}] + \begin{bmatrix} 0 & 0 & 0 \\ 0 & 0 & 1 \end{bmatrix}$$

Expression for ΔZ_g

Matrices $[D_p]$ and $[D_s]$ in eqn. (D.24) will take the form

$$[D_p] = \frac{1}{V_{to}} \begin{bmatrix} -v_{qo}/V_{to} & v_{do}/V_{to} \\ v_{do} & v_{qo} \end{bmatrix} [W_{a3}]$$

$$[D_s] = \begin{bmatrix} 0 & 1 & 0 \\ 0 & 0 & 0 \end{bmatrix} + \frac{1}{V_{to}} \begin{bmatrix} -v_{qo}/V_{to} & v_{do}/V_{to} \\ v_{do} & v_{qo} \end{bmatrix} [W_{a4}]$$

D.1.3 Calculation of Operating Condition

The values of Park's components of voltage and current at the given operating point of the system are calculated from the results of a load-flow analysis. Let P_o and Q_o be respectively the active and reactive power supplied by the generator at the terminal bus and V_{to} and θ_o represent the magnitude and phase angle of the terminal bus voltage. The power factor angle and the stator current are, respectively.

$$\varphi_o = \tan^{-1} (Q_o/P_o)$$

$$i_{mo} = P_o / (V_{to} \cos \varphi_o)$$

From the phasor diagram shown in Fig. D.5, the angle between the q-axis and the axis of bus voltage V_{to} is given by

$$\beta_o = \tan^{-1} \left[\frac{i_{mo}(x_q \cos \varphi_o - r_a \sin \varphi_o)}{V_{to} + i_{mo}(x_q \sin \varphi_o + r_a \cos \varphi_o)} \right]$$

Angle of lead of machine reference, q-axis, from the system reference is given as

$$\delta_o = \beta_o + \theta_o$$

$$v_{do} = V_{to} \sin \beta_o$$

$$v_{qo} = V_{to} \cos \beta_o$$

$$i_{do} = i_{mo} \sin(\beta_o + \varphi_o)$$

and

$$i_{qo} = i_{mo} \cos(\beta_o + \varphi_o)$$

D.2 EXCITATION SYSTEM [9]

D.2.1 Continuously Acting Regulator and Exciter (IEEE Type 1)

IEEE type 1 excitation system is shown in Fig. D.6. The linearized equations for the excitation system can be written

$$p \underline{x}_e = [A_c] \underline{x}_e + \underline{b}_{ev} \Delta V_t + \underline{b}_{eu} (u + \Delta V_{ref})$$

$$\Delta E_{fd} = [C_e] \underline{x}_e \quad (D.32)$$

where

$$\underline{x}_e = [\Delta E_{fd} \quad \Delta V_R \quad \Delta V_2]^t$$

$$[A_e] = \begin{bmatrix} -\frac{(K_E + S_E)}{T_E} & \frac{1}{T_E} & 0 \\ 0 & -1/T_R & -K_R/T_R \\ \frac{-K_S(K_E + S_E)}{T_E T_S} & \frac{K_S}{T_E T_S} & -1/T_S \end{bmatrix}$$

$$\underline{b}_{ev} = [0 \quad -\frac{K_R}{T_R} \quad 0]^t$$

$$\underline{b}_{eu} = [0 \quad \frac{K_R}{T_R} \quad 0]^t$$

D.2.2 Single Time Constant Excitation System (IEEE Type 1G)

A special case of type 1 is a system employing an excitation source from terminal voltage with controlled rectifiers only. In general, the constants for this type of system are such that $K_E = 1$, $T_E = 0$ and $S_E = 0$ [9]. The

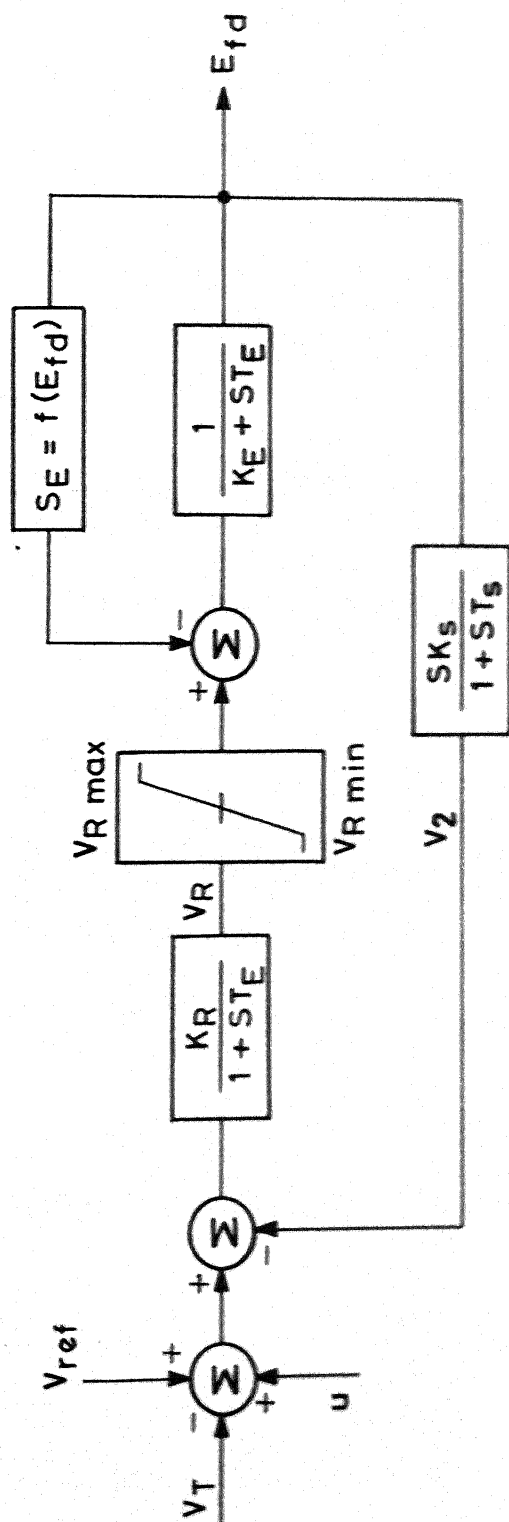


FIG. D.6 IEEE TYPE 1 EXCITATION SYSTEM.

linearized equation for this excitation system will be same as given in eqn. (D.32), where

$$x_e = \Delta E_{fd} ; \quad A_e = -1/T_R ; \quad b_{ev} = -K_R/T_R ; \quad b_{eu} = K_R/T_R$$

Combined dynamical equation of machine and excitation system can be obtained from eqns. (D.25) and (D.32) as :

$$p \underline{x} = [A] \underline{x} + [B_p] \Delta \underline{S}_g + \underline{b}_g \Delta P_m + \underline{b} (u + \Delta V_{ref}) \quad (D.33)$$

where

$$\underline{x} = [x_m^t \quad x_e^t]^t$$

$$[A] = \begin{bmatrix} A_m & \underline{b}_{me} & C_e \\ \underline{b}_{ev} & W_{a6} & A_e \end{bmatrix}$$

$$[B_p] = \begin{bmatrix} B_{ap} \\ \underline{b}_{ev} & W_{a5} \end{bmatrix}$$

$$\underline{b}_g = [\underline{b}_{mg}^t \quad 0]^t$$

$$\underline{b} = [0 \quad b_{eu}^t]^t$$

W_{a5} and W_{a6} are obtained from matrices D_p and D_s respectively of eqn. (D.24) as ΔV_t is one of the entries in ΔZ_g .

APPENDIX E

PSS DESIGN BASED ON CLASSICAL CONTROL

E.1 DESIGN PROCEDURE

The design of PSS using classical control theory given here is based on the work reported in [26]. As discussed in Chapter 2, the design of PSS using the guide lines given in [26] requires the determination of K_s , n_t and T_1 of the PSS transfer function

$$PSS(s) = \frac{K_s(1 + sT_1)^2}{(1 + sT_1/n_t)^2}$$

The method suggested in [26] utilizes the following terms.

Plant Transfer Function : GEP (s)

This is defined as the transfer function from the stabilizer output to the component of electrical torque which can be modulated through excitation control. The stabilizer operates through GEP and therefore PSS should compensate for the gain and phase characteristic of GEP which is strongly influenced by the voltage regulator gain, generator power level and ac system strength.

Compensated Phase Lag : $\phi_p(\omega)$

This represents the phase angle of the complete stabilizer path, i.e., phase angle from the input signal (usually speed)

to the electrical torque. This can be obtained as

$$\begin{aligned}\angle P(j\omega) &= \angle GEP(j\omega) + \angle PSS(j\omega) \\ &= \varphi_p(\omega)\end{aligned}$$

The procedure for the design of PSS consists of two basic steps [26].

- (1) Adjustment of parameters n_t and T_1 such that
 - (a) Maximum frequency at which the compensated phase lag passes through 90° should be in the range of 3 to 3.5 Hz.
 - (b) Compensated phase lag at local mode frequency should be between 0° and 45° , preferably near 20° .
- (2) Adjustment of gain K_s based upon the determination of gain which causes instability (say K_s^*) in the stabilizer loop. Gain should be adjusted at

$$K_s \approx \frac{1}{3} K_s^*$$

E.2 EXPRESSION FOR GEP(s)

From eqn. (2.4), electrical torque in per unit is

$$T_e = x_d' (I_d - \xi i_d) i_q \quad (E.2)$$

Linearizing eqn. (E.2) and substituting the values of Δi_q and Δi_d from eqn. (2.10), we get

$$\Delta T_e = K_5 \Delta I_d + K_6 \Delta \delta \quad (E.3)$$

$$K_5 = x'_d [K_1(I_{d0} - \xi i_{d0}) + (1 - \xi K_3) i_{q0}]$$

and

$$K_6 = x'_d [K_2(I_{d0} - \xi i_{d0}) - K_4 \xi i_{q0}]$$

Taking the Laplace transform of the state equations given in eqn. (2.11), we get :

$$s \Delta \omega = a_{11} \Delta \omega + a_{12} \Delta \delta + a_{13} \Delta I_d \quad (E.4)$$

$$s \Delta \delta = \Delta \omega \quad (E.5)$$

$$s \Delta I_d = a_{32} \Delta \delta + a_{33} \Delta I_d + a_{34} \Delta E_{fd} \quad (E.6)$$

and

$$s \Delta E_{fd} = a_{42} \Delta \delta + a_{43} \Delta I_d + a_{44} \Delta E_{fd} + b_4 u \quad (E.7)$$

From eqns. (E.3) to (E.6), ΔI_d can be expressed as :

$$\Delta I_d = \left[\frac{a_{32}(s-a_{44}) + a_{34}a_{42}}{(s-a_{33})(s-a_{44}) - a_{34}a_{43}} \right] \Delta \delta + \left[\frac{a_{34}b_4}{(s-a_{33})(s-a_{44}) - a_{34}a_{43}} \right] u \quad (E.8)$$

Substituting the value of ΔI_d from (E.8) into eqn. (E.3), we get

$$\Delta T_e = G_1(s) \Delta \delta + G_2(s) u \quad (E.9)$$

where

$$G_1(s) = K_6 + K_5 \left[\frac{a_{32}(s-a_{44}) + a_{34}a_{42}}{(s-a_{33})(s-a_{44}) - a_{34}a_{43}} \right]$$

$$G_2(s) = GEP(s) = \frac{K_5 a_{34} b_4}{(s-a_{33})(s-a_{44}) - a_{34}a_{43}} \quad (E.10)$$

Block diagram of the system giving relationship of electrical torque with speed and angular displacement is given in Fig. E.1.

E.3 DESIGN OF PSS

Speed signal is utilized for the PSS design by classical control. As recommended in [26], PSS utilizing speed signal should be designed for strong ac system and at full load conditions. Thus, the value of X_T considered is equal to 0.2 p.u. for the system given in Chapter 2. Fig. E.2 shows the phase versus frequency plot of phase angle of GEP and compensated phase given by eqn. (E.1), for different values of the parameters n_t and T_1 . It is found that curve 'a' of Fig. E.2 with $n_t = 3$ and $T_1 = 0.5$ sec. fulfills the design criteria given in Sec. E.1.

Fig. E.3 shows the loci of closed-loop eigenvalues for variation in the PSS gain K_s . It is found that the value of K_s which causes instability of the system is equal to 0.165. Thus, as per the criteria given in [26], a gain of 0.05 ($\approx \frac{1}{3} K_s^*$) is selected for the PSS.

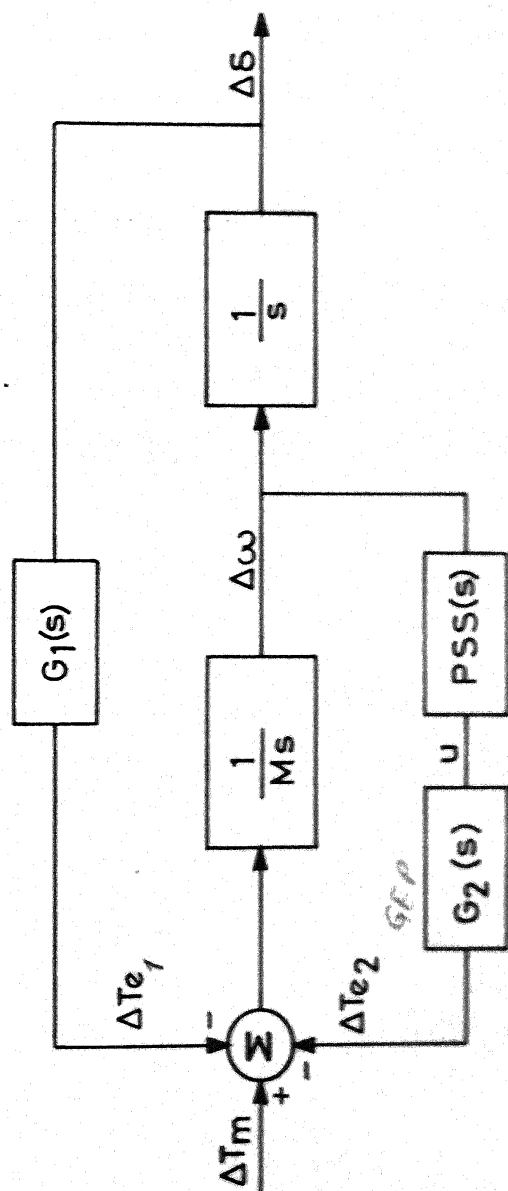


FIG. E.1 SYSTEM BLOCK DIAGRAM WITH PSS.

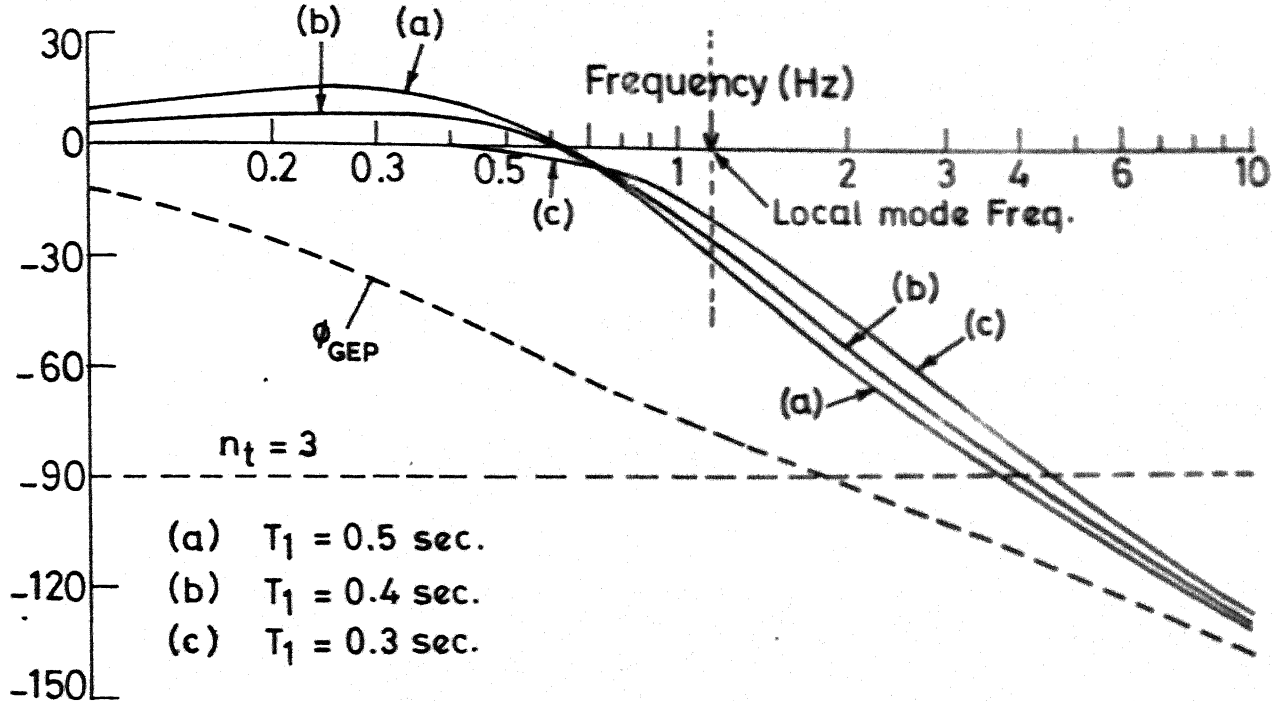


FIG.E.2 COMPENSATED PHASE FOR VARIOUS LEAD/LAG SETTINGS.

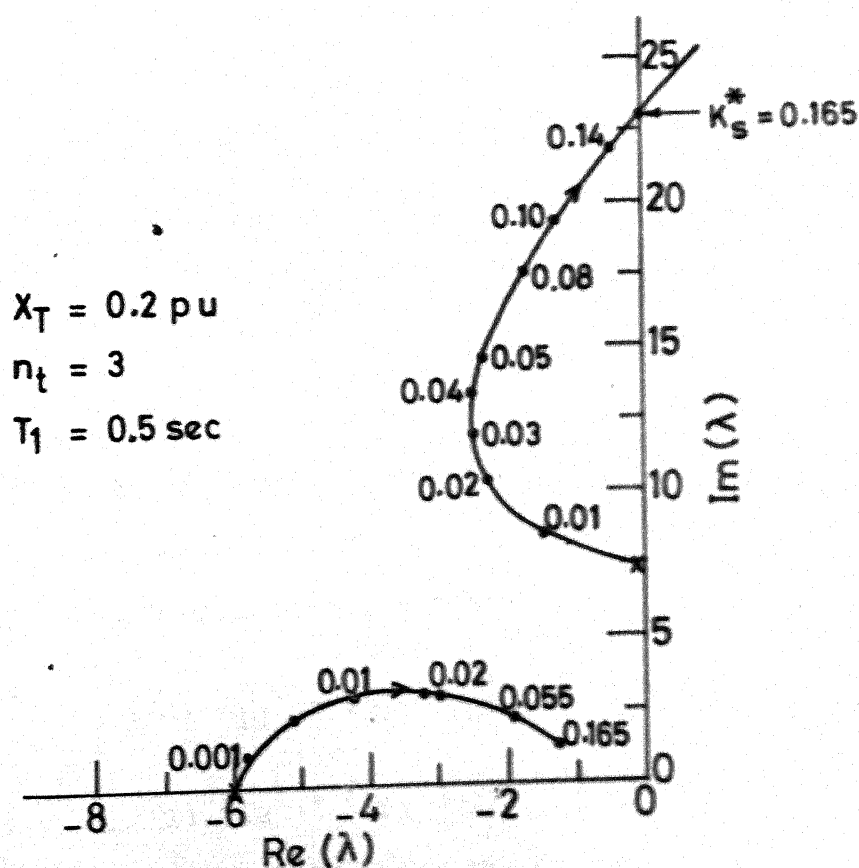


FIG.E.3 LOCI OF CLOSED-LOOP EIGENVALUES FOR VARIATION IN PSS GAIN K_s .

APPENDIX F

ANALYSIS OF RESULT OF CHAPTER 4

The state-space equation (4.26) for the two machine system can be expressed as

$$p \begin{bmatrix} x_1 \\ x_2 \end{bmatrix} = \begin{bmatrix} A_{11} & A_{12} \\ A_{21} & A_{22} \end{bmatrix} \begin{bmatrix} x_1 \\ x_2 \end{bmatrix} + \begin{bmatrix} b_1 & 0 \\ 0 & b_2 \end{bmatrix} \begin{bmatrix} u_1 \\ u_2 \end{bmatrix} \quad (F.1)$$

Defining new state variables

$$z_1 \triangleq x_1 - x_2$$

$$z_2 \triangleq x_1 + x_2$$

we get the transformation as

$$\begin{bmatrix} x_1 \\ x_2 \end{bmatrix} = \frac{1}{2} \begin{bmatrix} I & I \\ -I & I \end{bmatrix} \begin{bmatrix} z_1 \\ z_2 \end{bmatrix} \quad (F.2)$$

where I is an identity matrix. With the defined transformation, eqn. (F.1) will take the form

$$p \begin{bmatrix} z_1 \\ z_2 \end{bmatrix} = \frac{1}{2} \begin{bmatrix} (A_{11}-A_{12}) - (A_{21}-A_{22}) & (A_{11}+A_{12}) - (A_{21}+A_{22}) \\ (A_{11}-A_{12}) + (A_{21}-A_{22}) & (A_{11}+A_{12}) + (A_{21}+A_{22}) \end{bmatrix} \begin{bmatrix} z_1 \\ z_2 \end{bmatrix} + \begin{bmatrix} b_1 & -b_2 \\ b_1 & b_2 \end{bmatrix} \begin{bmatrix} u_1 \\ u_2 \end{bmatrix} \quad (F.3)$$

For identical machines and with equal loading, we have

$$A_{22} = A_{11} (= A_s)$$

$$A_{21} = A_{12} (= A_m)$$

$$b_2 = b_1 (= b)$$

and thus eqn. (F.3) will be reduced to a pair of decoupled state equations as

$$p \begin{bmatrix} z_1 \\ z_2 \end{bmatrix} = \begin{bmatrix} (A_s - A_m) & 0 \\ 0 & (A_s + A_m) \end{bmatrix} \begin{bmatrix} z_1 \\ z_2 \end{bmatrix} + \begin{bmatrix} b & 0 \\ 0 & b \end{bmatrix} \begin{bmatrix} u_1' \\ u_2' \end{bmatrix} \quad (F.4)$$

where $u_1' = u_1 - u_2$ and $u_2' = u_1 + u_2$. For plant signals, that is, average speed, average power and bus frequency and with identical PSS on each machine u_2 will be equal to u_1 and thus,

$$u_1' = 0. \quad (F.5)$$

and eqn. (F.4) can be expressed as

$$p \begin{bmatrix} z_1 \\ z_2 \end{bmatrix} = \begin{bmatrix} (A_s - A_m) & 0 \\ 0 & (A_s + A_m) \end{bmatrix} \begin{bmatrix} z_1 \\ z_2 \end{bmatrix} + \begin{bmatrix} 0 \\ b \end{bmatrix} u_2' \quad (F.6)$$

which proves that the system is not completely controllable.

APPENDIX G

NETWORK REPRESENTATION

The network can be represented by its Jacobian matrix in the polar form. For an 'N' bus power system network, the Jacobian matrix is of (2N x 2N) dimension. By representing the network by its Jacobian the identity of all the buses is retained. The elements of the Jacobian matrix of the network can be obtained by one of the following ways :

The Jacobian of the network, excluding the slack bus, is available from the load-flow analysis using Newton's method in polar form. The elements of Jacobian corresponding to the slack bus are obtained using the load-flow results as described in the alternative method given here. Thus, the Jacobian available from the load-flow analysis can be conveniently utilized in obtaining the full Jacobian of the network.

Alternatively, if the Jacobian is not available from the load-flow analysis, the Jacobian for the complete network can be constructed using load-flow results as follows :

Eqn. (5.1) can also be expressed as

$$\Delta \underline{S}_i = [J_{ii}] \Delta \underline{Z}_i + \sum_{\substack{j=1 \\ j \neq i}}^N [J_{ij}] \Delta \underline{Z}_j \quad (G.1)$$

where

$$\Delta \underline{S}_i = [\Delta P_i \quad \Delta Q_i]^t$$

$$\Delta \underline{Z}_i = [\Delta \theta_i \quad \Delta V_i]^t$$

J_{ii} - is a 2x2 matrix representing the diagonal block of $[J]$ corresponding to i th bus in eqn. (5.1)

J_{ij} - is a 2x2 matrix representing the off-diagonal blocks of $[J]$ corresponding to i th bus in eqn. (5.1).

$$[J_{ij}] = \begin{bmatrix} -(Q_{io} + B_{ii} V_{io}^2) & (P_{io} + G_{ii} V_{io}^2)/V_{io} \\ (P_{io} - G_{ii} V_{io}^2) & (Q_{io} - B_{ii} V_{io}^2)/V_{io} \end{bmatrix};$$

$$[J_{ij}] = \begin{bmatrix} V_{io} V_{jo} D_{ij} & V_{io} C_{ij} \\ -V_{io} V_{jo} C_{ij} & V_{io} D_{ij} \end{bmatrix}$$

where

$$C_{ij} = G_{ij} \cos(\theta_{io} - \theta_{jo}) + B_{ij} \sin(\theta_{io} - \theta_{jo})$$

$$D_{ij} = G_{ij} \sin(\theta_{io} - \theta_{jo}) - B_{ij} \cos(\theta_{io} - \theta_{jo})$$

$$Y_{ij} \stackrel{\Delta}{=} G_{ij} + jB_{ij} \text{ } -ij\text{th element of bus admittance matrix.}$$

P_{io} , Q_{io} , V_{io} and θ_{io} are respectively active power, reactive power, voltage magnitude and voltage angle at the i th bus obtained from load-flow results.

APPENDIX H

JUSTIFICATION OF CRITERIA USED FOR CHOICE OF PSS LOCATION

The linear mathematical model of a multimachine power system used for the selection of PSS location can be expressed as

$$p \underline{X} = [A] \underline{X} + [B] \underline{U} \quad (H.1)$$

$$\underline{Y} = [C] \underline{X} \quad (H.2)$$

and the PSS structure can be expressed as

$$u_i = F_i Y_i \quad (H.3)$$

Derivation of these equations are given in Chapter 5. When the i th machine is chosen for PSS, eqns. (H.1) and (H.2) will take this form

$$p \underline{X} = [A] \underline{X} + \underline{b}_i u_i \quad (H.4)$$

$$\text{and} \quad y_i = \underline{C}_i \underline{X} \quad (H.5)$$

where \underline{C}_i is a row vector, i th row of matrix C in eqn. (5.21).

Justification of First Method in Sec. 5.3

Consider the transformation

$$\underline{X} = [T] \underline{Z} \quad (H.6)$$

which reduces the system of equation (H.4) to

$$\begin{aligned} p \underline{Z} &= [T^{-1} A T] \underline{Z} + T^{-1} b_i u_i \\ &= [\Lambda] \underline{Z} + \underline{b}'_i u_i \end{aligned} \quad (\text{H.7})$$

where Λ is a diagonal matrix (assuming distinct eigenvalues) whose elements are the eigenvalues of the A matrix. The row in eqn. (H.7) corresponding to the critical eigenvalue λ_j , can be expressed as

$$p z_j = \lambda_j z_j + b'_{ji} u_i \quad (\text{H.8})$$

where b'_{ji} is the j th element of b'_i . Assuming that the control law for u_i is going to be selected in order to shift the eigenvalue λ_j to the left in complex plane, it can be observed that the control effort would be small if the magnitude of element b'_{ji} is large. It is to be noted that b'_{ji} is the scalar product of the eigenvector w_j of the matrix A^t corresponding to λ_j and the vector b_i , or

$$b'_{ji} = \langle w_j, b_i \rangle$$

Justification of Second Method in Sec. 5.3

From eqns. (H.3), (H.4) and (H.5), the closed-loop system can be represented as

$$p \underline{X} = (A + \underline{b}_i F_i C_i) \underline{X} \quad (\text{H.9})$$

The value of the feedback gain, F_i , is so chosen as to shift the critical eigenvalue λ_j to the left in complex plane. This is to be achieved with smallest possible value of gain. The closed-loop eigenvalue λ_j^c is given by

$$\lambda_j^c = \lambda_j + \frac{\partial \lambda_j}{\partial F_i} \Delta F_i + \text{Higher order terms} \quad (\text{H.10})$$

If higher order terms are neglected, the best control is determined by maximizing the absolute value of $\text{Re}(\frac{\partial \lambda_j}{\partial F_i})$. The eigenvalue sensitivity is given by

$$S_{ji} = \frac{\partial \lambda_j}{\partial F_i} = \frac{\langle \underline{b}_i \underline{C}_i \underline{V}_j, \underline{W}_j \rangle}{\langle \underline{V}_j, \underline{W}_j \rangle} \quad (\text{H.11})$$

where \underline{V}_j and \underline{W}_j are respectively the eigenvectors of A and A^t corresponding to λ_j .

APPENDIX I

13-MACHINE 71-BUS POWER SYSTEM

The single line diagram of a 13-machine, 71-bus power system is shown in Fig. I.1. Table I.1 shows the bus data and load-flow results. Generator, line and shunt capacitor data are given respectively in Tables I.2, I.3 and I.4 in per unit on 200 MVA base.

Table I.1 Bus Data and Load Flow Result

Bus No.	Generation		Load Power		Bus Voltage	
	(MW)	(MVAR)	(MW)	(MVAR)	Mag.	Ang. (Deg.)
1	2	3	4	5	6	7
1	630.667	169.722	0.0	0.0	1.030	0.0
2	0.0	0.0	0.0	0.0	1.057	-5.931
3	506.0	149.492	0.0	0.0	1.025	-1.406
4	0.0	0.0	0.0	0.0	1.054	-6.061
5	0.0	0.0	0.0	0.0	1.047	-5.064
6	98.0	31.986	0.0	0.0	1.025	0.397
7	0.0	0.0	12.8	8.3	1.045	-3.723
8	297.0	124.227	0.0	0.0	1.025	-0.204
9	0.0	0.0	185.0	130.0	1.0433	-4.976
10	0.0	0.0	80.0	50.0	1.026	-7.413

1	2	3	4	5	6	7
11	0.0	0.0	155.0	96.0	1.023	-11.762
12	0.0	0.0	0.0	0.0	1.003	-10.057
13	0.0	0.0	100.0	62.0	1.007	-13.839
14	0.0	0.0	0.0	0.0	1.004	-11.934
15	184.08	114.0	0.0	0.0	1.005	-9.413
16	0.0	0.0	73.0	45.5	1.024	-16.682
17	0.0	0.0	36.0	22.4	1.005	-14.460
18	0.0	0.0	16.0	9.9	1.009	-17.881
19	0.0	0.0	32.0	19.8	0.981	-19.786
20	0.0	0.0	27.0	16.8	1.003	-21.838
21	0.0	0.0	32.0	19.8	1.016	-21.376
22	0.0	0.0	0.0	0.0	1.008	-17.625
23	0.0	0.0	75.0	46.6	1.036	-19.815
24	0.0	0.0	0.0	0.0	0.985	-16.193
25	0.0	0.0	133.0	82.5	1.039	-17.441
26	0.0	0.0	0.0	0.0	1.016	-14.382
27	304.0	76.287	0.0	0.0	1.025	-5.453
28	0.0	0.0	30.0	20.0	1.055	-12.342
29	261.0	70.506	0.0	0.0	1.025	-15.519
30	0.0	0.0	120.0	74.5	1.057	-19.947
31	0.0	0.0	160.0	99.4	1.014	-22.817
32	0.0	0.0	0.0	0.0	1.025	-15.936
33	0.0	0.0	0.0	0.0	0.998	-25.515

1	2	3	4	5	6	7
34	0.0	0.0	112.0	69.5	1.306	-29.639
35	0.0	0.0	0.0	0.0	0.966	-21.803
36	0.0	0.0	50.0	32.0	0.994	-34.030
37	0.0	0.0	147.0	92.0	0.967	-37.982
38	0.0	0.0	93.5	88.0	0.972	-37.638
39	25.0	30.383	0.0	0.0	1.025	-34.166
40	0.0	0.0	0.0	0.0	1.018	-36.913
41	0.0	0.0	255.0	123.0	1.007	-34.778
42	0.0	0.0	0.0	0.0	0.979	-31.484
43	0.0	0.0	0.0	0.0	0.946	-27.835
44	180.0	55.037	0.0	0.0	1.025	-24.448
45	0.0	0.0	0.0	0.0	1.048	-30.514
46	0.0	0.0	78.0	38.6	1.020	-32.678
47	0.0	0.0	234.0	145.0	0.989	-29.053
48	341.0	256.0	0.0	0.0	1.005	-25.781
49	0.0	0.0	295.0	183.0	0.997	-30.500
50	0.0	0.0	40.0	24.6	0.977	-32.056
51	0.0	0.0	227.0	142.0	1.005	-35.309
52	0.0	0.0	0.0	0.0	0.957	-26.552
53	0.0	0.0	0.0	0.0	0.972	-32.845
54	0.0	0.0	108.0	68.0	1.004	-35.318

1	2	3	4	5	6	7
55	0.0	0.0	25.5	48.0	0.985	-31.313
56	0.0	0.0	0.0	0.0	1.013	-29.253
57	0.0	0.0	55.6	35.6	1.016	-29.967
58	0.0	0.0	42.0	27.0	1.018	-30.261
59	0.0	0.0	57.0	27.4	1.013	-30.715
60	0.0	0.0	0.0	0.0	1.008	-29.974
61	0.0	0.0	0.0	0.0	1.019	-27.874
62	0.0	0.0	40.0	27.0	1.044	-28.940
63	0.0	0.0	33.2	20.6	1.042	-27.695
64	300.0	72.882	0.0	0.0	1.025	-19.401
65	0.0	0.0	0.0	0.0	1.057	-24.662
66	96.0	25.636	0.0	0.0	1.025	-20.610
67	0.0	0.0	14.0	6.5	1.055	-25.641
68	89.0	26.689	0.0	0.0	1.025	-19.829
69	0.0	0.0	0.0	0.0	1.050	-25.363
70	0.0	0.0	11.4	7.0	0.998	-34.790
71	0.0	0.0	0.0	0.0	0.927	-35.329

Table I.2 Generator Data

Gen. No.	Bus No.	Rated MVA	Inertia Constant H secs.	Open Circuit Field Time Constant T'_{do} sec.	Direct Axis Reactance x_d p.u.	Direct Axis Transient Reactance x'_d p.u.
1	1	1175.0	12.900	7.0	0.36	0.0488
2	3	665.0	9.000	6.5	0.535	0.069
3	6	110.0	1.923	6.0	1.638	0.5278
4	8	335.0	6.648	6.0	0.567	0.201
5	15	275.0	2.590	6.0	0.6	0.244
6	27	400.0	2.550	6.0	0.9	0.1455
7	29	300.0	2.700	6.0	1.578	0.1355
8	39	51.75	1.035	6.0	2.705	1.082
9	44	220.0	5.430	6.0	0.9118	0.227
10	48	500.0	7.800	6.0	0.74	0.0595
11	64	376.0	7.140	6.0	0.532	0.13
12	66	127.8	2.176	6.0	1.405	0.486
13	68	103.5	1.473	6.0	2.28	0.599

Table I.3 Line and Transformer Data

Line No.	From Bus	To Bus	Series R	Impedance X	$\frac{1}{2}$ Y charge	Turns Ratio
1	2	3	4	5	6	7
1	9	8	0.0	0.0570		1.05
2	9	7	0.0320	0.0780	0.0090	
3	9	5	0.0660	0.1600	0.0047	
4	9	10	0.0520	0.1270	0.0140	
5	10	11	0.0660	0.1610	0.0180	
6	7	10	0.0270	0.0700	0.0070	
7	12	11	0.0	0.0530		0.95
8	11	13	0.0600	0.1480	0.0360	
9	14	13	0.0	0.0800		1.00
10	13	16	0.0970	0.2380	0.270	
11	17	15	0.0	0.0920		1.05
12	7	6	0.0	0.2220		1.05
13	6	4	0.0	0.0800		1.00
14	4	3	0.0	0.0330		1.05
15	4	5	0.0	0.1600		1.00
16	4	12	0.0160	0.0790	0.0710	
17	12	14	0.0160	0.0790	0.0710	
18	17	16	0.0	0.0800		0.95
19	2	4	0.0	0.0620		1.00
20	4	26	0.0190	0.0950	0.1930	
21	2	1	0.0	0.0340		1.05
22	31	26	0.0340	0.1670	0.1500	

1	2	3	4	5	6	7
23	26	25	0.0	0.0800		0.95
24	25	23	0.2040	0.5200	0.0130	
25	22	23	0.0	0.0800		0.95
26	24	22	0.0	0.0840		0.95
27	22	17	0.0480	0.2500	0.0505	
28	2	24	0.0100	0.0200	0.3353	
29	23	21	0.0366	0.1412	0.0140	
30	21	20	0.0720	0.1860	0.0050	
31	20	19	0.1460	0.3740	0.0100	
32	19	18	0.0590	0.1500	0.0040	
33	18	16	0.0300	0.0755	0.0080	
34	28	27	0.0	0.0810		1.05
35	30	29	0.0	0.0610		1.05
36	32	31	0.0	0.0930		0.95
37	31	30	0.0	0.0800		0.95
38	28	32	0.005	0.0510	0.6706	
39	31	33	0.0130	0.0640	0.0580	
40	31	47	0.0100	0.0790	0.1770	
41	2	32	0.0158	0.1570	0.5100	
42	33	34	0.0	0.0800		0.95
43	35	33	0.0	0.0840		0.95
44	35	24	0.0062	0.0612	0.2012	
45	34	36	0.0790	0.2010	0.0220	
46	36	37	0.1690	0.4310	0.0110	

1	2	3	4	5	6	7
47	37	38	0.0840	0.1880	0.0210	
48	40	39	0.0	0.3800		1.05
49	40	38	0.0890	0.2170	0.0250	
50	38	41	0.1090	0.1960	0.0220	
51	41	51	0.2350	0.6000	0.0160	
52	42	41	0.0	0.0530		0.95
53	43	42	0.0	0.0840		0.95
54	47	49	0.0210	0.1030	0.0920	
55	49	48	0.0	0.0460		1.05
56	49	50	0.0170	0.0840	0.0760	
57	49	42	0.0370	0.1950	0.0390	
58	50	51	0.0	0.0530		0.95
59	52	50	0.0	0.0840		0.95
60	50	55	0.0290	0.1520	0.0300	
61	50	53	0.0100	0.0520	0.0390	
62	53	54	0.0	0.0800		0.95
63	51	54	0.0220	0.0540	0.0060	
64	55	56	0.0160	0.0850	0.0170	
65	56	57	0.0	0.0800		1.00
66	57	59	0.0280	0.0720	0.0070	
67	59	58	0.0480	0.1240	0.0120	
68	60	59	0.0	0.0800		1.00
69	53	60	0.0360	0.1840	0.0370	
70	45	44	0.0	0.1200		1.05

1	2	3	4	5	6	7
71	45	46	0.0370	0.0900	0.0100	
72	46	41	0.0830	0.1540	0.0170	
73	46	59	0.1070	0.1970	0.0210	
74	60	61	0.0160	0.0830	0.0160	
75	61	62	0.0	0.0800		0.95
76	58	62	0.0420	0.1080	0.0020	
77	62	63	0.0350	0.0890	0.0090	
78	69	68	0.0	0.2220		1.05
79	69	61	0.0230	0.1160	0.1040	
80	67	66	0.0	0.1880		1.05
81	65	64	0.0	0.0630		1.05
82	65	56	0.0280	0.1440	0.0290	
83	65	61	0.0230	0.1140	0.0240	
84	65	67	0.0240	0.0600	0.0950	
85	67	63	0.0390	0.0990	0.0100	
86	61	42	0.0230	0.2293	0.0695	
87	57	67	0.0550	0.2910	0.0070	
88	45	70	0.1840	0.4680	0.0120	
89	70	38	0.1650	0.4220	0.0110	
90	33	71	0.0570	0.2960	0.0590	
91	71	37	0.0	0.0800		0.95
92	45	41	0.1530	0.3880	0.0100	
93	35	43	0.0131	0.1306	0.4293	
94	32	52	0.0164	0.1632	0.5360	

Table I.4 Shunt Capacitor Data

S.No.	Bus No.	Shunt Load	Admittance
1	2	0.0	-0.4275
2	13	0.0	0.1500
3	20	0.0	0.0800
4	24	0.0	-0.2700
5	28	0.0	-0.3375
6	31	0.0	0.2000
7	32	0.0	-0.8700
8	34	0.0	0.2250
9	35	0.0	-0.3220
10	36	0.0	0.1000
11	37	0.0	0.3500
12	38	0.0	0.2000
13	41	0.0	0.2000
14	43	0.0	-0.2170
15	46	0.0	0.1000
16	47	0.0	0.3000
17	50	0.0	0.1000
18	51	0.0	0.1750
19	52	0.0	-0.2700
20	54	0.0	0.1500
21	57	0.0	0.1000
22	59	0.0	0.0750
23	21	0.0	0.0500

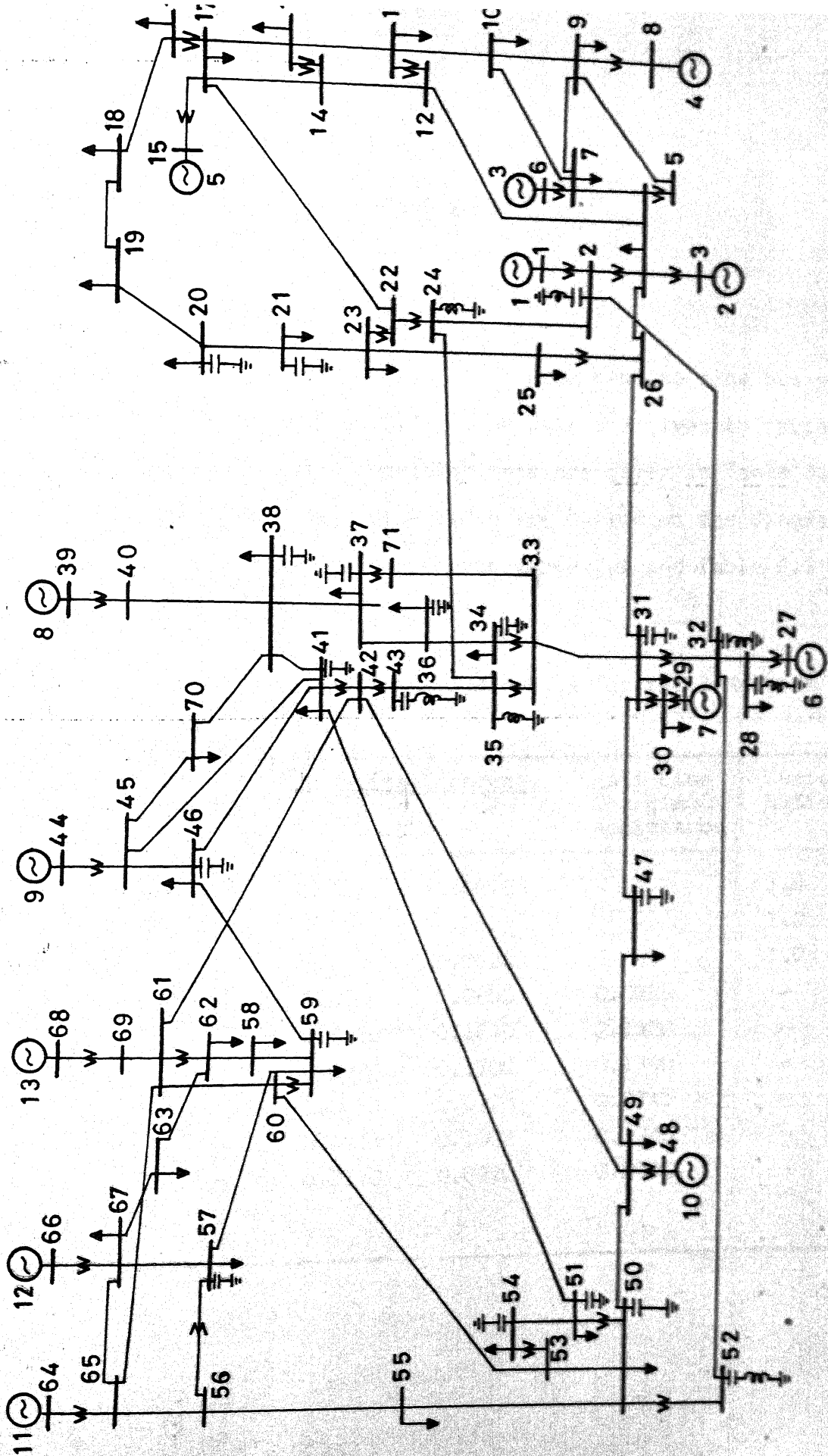


FIG. I . 1 SINGLE LINE DIAGRAM OF 13-MACHINE SYSTEM .

APPENDIX J

3-MACHINE 9-BUS POWER SYSTEM

The single-line diagram of a three machine nine bus power system is shown in Fig. J.1. Line data are given in Table J.1. Generator and Voltage Regulator data are given in Table J.2. Load-flow results with line flows are marked on the diagram given in Fig. J.2. Data given in Table J.1 and Table J.2 are in per unit on 100 MVA base.

Table J.1 Line and Transformer Data for the 3-Machine System

Line No.	From Bus	To Bus	Series Impedance		Half Line Charging Admittance	Turns Ratio
			R	X		
1	1	4	0.0	0.0576	-	1.0
2	2	7	0.0	0.0625	-	1.0
3	3	9	0.0	0.0586	-	1.0
4	4	5	0.0100	0.0850	0.0880	-
5	5	7	0.0320	0.1610	0.1530	-
6	6	9	0.0390	0.1700	0.1790	-
7	7	8	0.0085	0.0720	0.0745	-
8	8	9	0.0119	0.1008	0.1045	-
9	4	6	0.0170	0.0920	0.0790	-

Table J.2 Generator Data for the 3-Machine System

Generator	1	2	3
Rated MVA	245.5	192.0	128.0
KV	16.5	18.0	13.8
Power Factor	1.0	0.85	0.85
Type	Hydro	Steam	Steam
Speed (rpm)	180	3600	3600
x_d (p.u.)	0.1460	0.8958	1.3125
x'_d (p.u.)	0.0608	0.1198	0.1813
x_q (p.u.)	0.0969	0.8645	1.2578
x'_q (p.u.)	0.0969	0.1969	0.2500
x_l leakage (p.u.)	0.0336	0.0521	0.0742
T'_{do} sec	8.96	6.00	5.89
T'_{qo} sec	0	0.535	0.600
H (MWS/100 MVA) sec	23.64	6.40	3.01
VR Gain	50.0	50.0	50.0
T_R sec	0.020	0.020	0.020

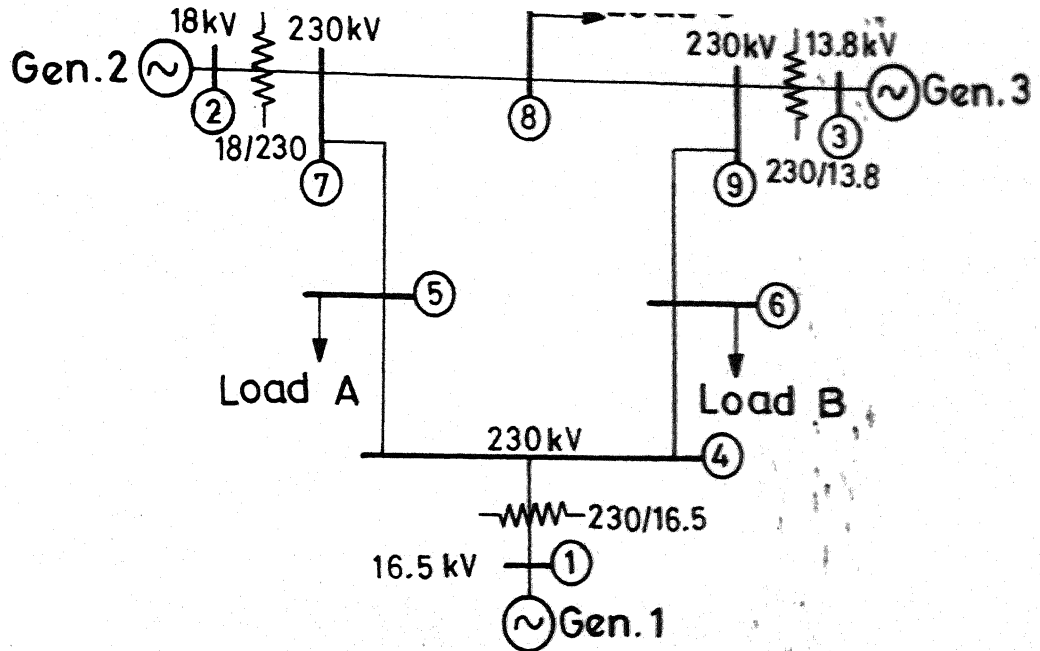


FIG. J . 1 SINGLE LINE DIAGRAM OF NINE-BUS, THREE-MACHINE POWER SYSTEM.

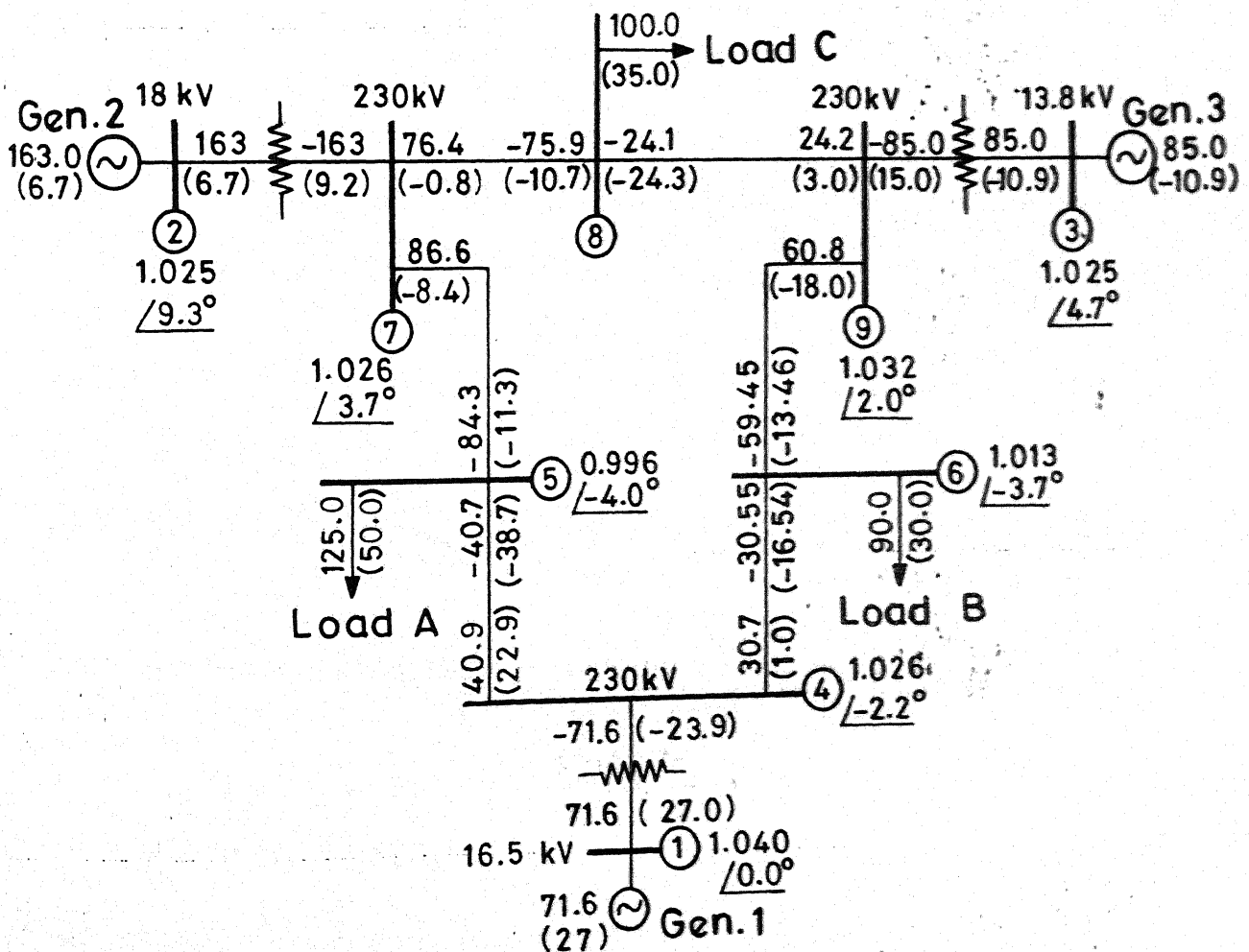


FIG. J . 2 LOAD FLOW DIAGRAM OF THE NINE-BUS THREE-MACHINE SYSTEM.

CURRICULUM VITAE

1. Candidates' Name ANWARUDDIN ANWAR

2. Academic Background :

<u>Degree</u>	<u>Specialization</u>	<u>Institution</u>	<u>Year</u>
B.Sc.Engg.	Electrical Engineering	AMU, Aligarh	1971
M.Sc.Engg.	System Engineering	AMU, Aligarh	1974

3. Publications :

- (i) 'Short Circuit Studies with Particular Reference to Large Power Systems' (with K.P. Basu), JIE (India), Vol. 56, pt.EL6, pp 280-286, June 1976.
- (ii) 'Very Low Speed Drive with Doubly-fed Induction Motor' (with K.P. Basu and B. Singh), IEEE Trans. Industrial Electronics and Control Instrumentation, Vol. IECI-24, pp 220-222, May 1977.
- (iii) 'Step Operation of Polyphase Wound-Rotor Induction Motor' (with K.P. Basu and A.K. Gupta), IEEE Trans. Industrial Electronics and Control Instrumentation, Vol. IECI-27, pp 122-124, May 1980.
- (iv) 'Simple Algorithm for Calculating Unbalances of Untransposed Transmission Lines' (with K.P. Basu), All India Seminar on Digital Computer Applications to the Control and Protection of EHV AC-HVDC Power Systems, Paper No. 6/2, REC Rourkela, Sept. 18-20, 1979.
- * (v) 'Decentralized Stabilization in Multimachine Power Systems' (with K.R. Padiyar and S.S. Prabhu), National System Conference, NSC-83, Trivandrum, 1983.
- * (vi) 'Application of Decentralized Control for the Design of PSS in Multimachine Power Systems' (with K.R. Padiyar and S.S. Prabhu), (communicated).

*Pertaining to the thesis